CLIMATE EXTREMES AND PRECIPITATION TRENDS IN KELANI RIVER BASIN, SRI LANKA AND IMPACT ON STREAMFLOW VARIABILITY UNDER CLIMATE CHANGE

K. D .C. R. Dissanayaka

(158554 K)

Degree of Master of Science

Department of Civil Engineering

University of Moratuwa

Sri Lanka

February 2017

CLIMATE EXTREMES AND PRECIPITATION TRENDS IN KELANI RIVER BASIN, SRI LANKA AND IMPACT ON STREAMFLOW VARIABILITY UNDER CLIMATE CHANGE

K. D. C. R. Dissanayaka

(158554 K)

Thesis submitted in partial fulfilment of the requirements for the degree of Master of Science in Water Resources Engineering and Management

Supervised by
Dr. R. L. H. L Rajapakse

Department of Civil Engineering
UNESCO Madanjeet Singh Centre for South Asia Water Management (UMCSAWM)

University of Moratuwa
Sri Lanka

February 2017

DECLARATION

I declare that this is my own work and this thesis does not incorporate without acknowledgement any material previously submitted for a Degree or Diploma in any other University or institute of higher learning and to the best of knowledge and belief it does not contain any material previously published or written by another person except where the acknowledgement is made in text.

Also I hereby grant to University of Moratuwa the non-exclusive right to reproduce and distribute my thesis, in whole or in part in print, electronic or other medium. I retain the right to use this content in whole or part in future works (Such as articles or books).

Signature: Date:

The above candidate has carried out research for the Master's thesis under my supervision.

Name of the supervisor:

Signature of the supervisor: Date:

ACKNOWLEDGEMENT

I would like to express my sincere gratitude to my research supervisor, Dr. R.L.H.L Rajapakse for the continuous support extended for this research and case study, for his patience, motivation and guidance. Without his dedicated supervision and continued guidance, this thesis would not have been a success. I am really grateful to him for spending his valuable time with me towards completing this research.

I wish to convey my sincere gratitude to the Centre Chairman, Senior Professor N.T.S. Wijesekera for extending all necessary help to achieve success in the program. His kindness to provide me all the guidance, help and support amidst his busy schedule and sincere and consistent encouragement are greatly appreciated.

I would also like to thank Late Shri Madanjeet Singh, the Founder of SAF-Madanjeet Singh Scholarship Scheme, the South Asia Foundation (SAF) and the University of Moratuwa for enabling me to join this study towards a Master Degree of Water Resource Engineering and Management, at UNESCO Madanjeet Singh Centre for South Asia Water Management (UMCSAWM),, Department of Civil Engineering, University of Moratuwa, Sri Lanka.

My gratitude is also extended to Mr. Wajira Kumarasinghe, Mr. Samantha Ranaweera and all Centre staff who gave me support to do the studies successfully within the university and there encouragement are greatly appreciated.

I also like to thank Mr. Ajith Wijemanna (Deputy Director, Department of Meteorology), Mr. Lalith Liyanarachchi (Director General, Department of Meteorology) and Eng. Mrs. Prema Hettiarachchi (Director Hydrology, Department of Irrigation) who gave me enormous support to acquire meteorological data and hydrological data for this research work.

I wish to thank again to Dr. Shaeb-ul Hasson (University of Hamberg, Germany) and Professor Robert L. Wilby (Loughborough University, United Kingdom) who were of tremendous support for me to understand about GCM modelling and the team of South Asia CORDEX and CanESM2 who granted the permission to enter to their central data base to acquire GCM/RCM data related to research work.

Finally, I would like to express my very profound gratitude to my parents and my friends for providing unfailing support and continuous encouragement throughout this research work.

Climate Extremes and Precipitation Trends in Kelani River Basin, Sri Lanka and Impact on Streamflow Variability under Climate Change

ABSTRACT

The study region comprises a major river basin in the West of Sri Lanka namely Kelani River basin. The hydrological regime of this river differs significantly from that of the others because the basin features great geographical and climatic diversities over its latitudinal and longitudinal extent. Kelani River is the second largest river in Sri Lanka that originates from the central hills and flows to the west coast through Colombo city. The river basin is bound by northern latitudes from 6°47' to 7°05' and eastern longitudes from 79°52' to 80°13'. The river originates approximately 2,250 m above mean sea level and passes 192 km to reach the Indian Ocean. The river basin experiences an annual average rainfall of about 3,450 mm corresponding to a volume of about 7,860 MCM out of 43% discharges into the sea. However, changes in precipitation and temperature due to the climate change can cause more frequent extremes with extended droughts and floods with further impact to the reservoir storage resulting a significant threat to water resources. Therefore, the present study focuses on climate extremes with reference to the past, present and future behavior of rainfall, temperature and streamflow at watershed scale to identify climate change impact on the spatial and temporal variations of streamflow in the Kelani River Basin.

For this research, basin-wide future hydrology is simulated by using downscaled temperature and precipitation outputs according to RCP Scenarios of the Canadian Earth System Model - version 2 (CanESM2), Statistical Downscaling Model (SDSM) and the Hydrologic Engineering Centre's Hydrologic Modeling System (HEC-HMS). The case study further evaluates the long-term behaviour and trends of the climate extremes based on the observed historical temperature and precipitation data. The findings suggest that the temperature and precipitation extremes are on the rise while the annual average precipitation in the river basin is declining. It is also predicted with the application of statistical downscaling that temperature may rise annually for representative concentration pathways of RCP2.6, RCP4.5 and RCP8.5. The mean explained variance are 67, 86 and 13% for temperature maximum, temperature minimum and precipitation respectively, for calibration with NCEP predictors. During calibration, the R^2 value of the monthly and seasonal sub-model of RCP 2.6, RCP 4.5 and RCP 8.5 scenarios are lies between 80.1% and 99.4% for both maximum and minimum temperature and 50 to 90% for precipitation. During validation, R^2 value for both monthly seasonal sub-model followed by bias correction was between 76.9% and 99.2% for both maximum and minimum temperature, and 55% to 95.2% for precipitation. A detailed modelling approach is incorporated to Hanwella sub-watershed (1799.67 km2) of the Kelani River basin, to study the subsequent water resource management options with the varying streamflow of the Kelani River basin under the effect of the future (2020's, 2050's and 2080's) rainfall and temperature as impending climate change impacts for RCP scenarios. The paper reviews the current state of the catchment as well as the suitability of applying the GCM's rather than RCM's to Sri Lanka to assess this river basin, according to monthly, seasonal and annual variations of the climatology. Apart from the water resources management, a quantitative analysis was conduct to assess the change in the amount of surface water within the selected river basin as a function of the expected variations in precipitation and temperature. This study will set the baseline for commencing and continuing quantitative studies incorporating the behaviour of the basin-wide climatology and streamflow variability with the use of general circulation models

Key words: - Climate Change, GCM, RCP Scenarios, Statistical Downscaling, Water Resources Management

TABLE OF CONTENTS

LIST OF ABBREVIATIONS

ANN	-	Artificial Neural Networks
AR4	-	Assessment Report 04
AVGPRCP	-	Annual Average Precipitation
BC	-	Bias Correction
CanESM2	-	Canadian Earth System Model Version 02
CCCMA	-	Canadian Centre for Climate Modelling and Analysis
CDD	-	Consecutive Dry Days (Maximum number of consecutive days with rainfall < 1 mm)
CE	-	Coefficient of Efficiency
CGCM3	-	Coupled Global Climate Change Model Version 03
CMIP	-	Coupled Model Intercomparison Project
CORDEX	-	Coordinated Regional Climate Downscaling Experiment
CWD	-	Consecutive Wet Days (Maximum number of consecutive days with rainfall > 1 mm)
DS	-	Dual Simplex
DTR	-	Diurnal Temperature Range (Annual mean difference between TX and TN)
E	-	Explained Variance
ENSO	-	El Nino Southern Oscillation
ETR	-	Extreme Temperature Range (Annual difference between highest TX and lowest TN)
GCM	-	General Circulation Model
HadCM3	-	Hadley Centre Climate Model version 03
HEC-HMS	-	Hydrologic Engineering Centre - Hydrologic Modeling System
IDW	-	Inverse Distance Weightage Method
IPCC	-	Inter-governmental Panel for Climate Change
MCL	-	Maximum Conservation Level
MCM	-	Million Cubic Meters
MRAE	-	Mean Ratio of Absolute Error
NAO	-	North Atlantic Oscillations
NASA	-	National Aeronautics and Space Administration
NCEP	-	National Centre for Environmental Predictions
NCEP-M	-	National Centre for Environmental Predictions - Monthly Model
NCEP-S	-	National Centre for Environmental Predictions - Seasonal Model
NCER	-	National Centre for Environmental Research
OLS	-	Ordinary Least Squares
P_{CONT}	-	Control Period Temperature
P_{deb}	-	De-biased Precipitation
PEP	-	Percent Error in Peak
PEV	-	Percentage Error Volume
P_{obs}	-	Observed Precipitation
PRCPTOT	-	Annual Total Wet Say Precipitation
PRP	-	Percentage Reduction of Partial Correlation
P_{SCEN}	-	Scenario Period Precipitation
R10	-	Number of Heavy Precipitation Days (Daily Rainfall ≥ 10 mm)
R^2	-	Goodness of Fit
R20	-	Number of Very Heavy Precipitation Days (Daily Rainfall ≥ 20 mm)
R95p	-	Very Wet Days (Annual Total PRCP when daily rainfall > 95^{th} percentile)
R99p	-	Extremely Wet Days (Annual Total PRCP when daily rainfall > 99^{th} percentile)

RAEM	-	Ratio of Absolute Error to Mean Error
RCM	-	Regional Climate Model
RCP	-	Representative Concentration Pathways
RE_μ	-	Relative Error of Mean
RE_σ	-	Relative Error of Standard Deviation
RMSE	-	Root Mean Square Error
RR	-	Rainfall Record
RX-1day	-	Maximum 1-day precipitation (Annual maximum 1-day precipitation)
RX-5day	-	Maximum 5-day precipitation (Annual maximum consecutive 5-day precipitation)
SAR	-	Sum of Absolute Residuals
SDSM-M	-	Statistical Downscaling Model - Monthly Model
SDSM-S	-	Statistical Downscaling Model - Seasonal Model
SE	-	Standard Error
SRES	-	Special Report on Emission Scenarios
SSR	-	Sum of Squared Residuals
SU25	-	Summer Days (Annual count when daily maximum temperature > 25°C)
T_{CONT}	-	Control Period Temperature
T_{deb}	-	De-biased Temperature
T_{max}	-	Maximum Temperature
T_{min}	-	Minimum Temperature
TN10p	-	Cool Nights (Percentage of days when Temperature Minimum < 10^{th} percentile)
TN90p	-	Warm Nights (Percentage of days when Temperature Minimum > 90^{th} percentile)
TN_n	-	Minimum of Temperature Minimum (Annual minimum value of daily minimum temperature)
TN_x	-	Maximum of Temperature Minimum (Annual maximum value of daily minimum temperature)
T_{obs}	-	Observed Temperature
TR20	-	Tropical Nights (Annual count when daily minimum temperature > 20°C)
T_{SCEN}	-	Scenario Period Temperature
TX10p	-	Cool Days (Percentage of days when Temperature Maximum < 10^{th} percentile)
TX90p	-	Warm Days (Percentage of days when Temperature Maximum > 90^{th} percentile)
TX_n	-	Minimum of Temperature Maximum (Annual minimum value of daily maximum temperature)
TX_x	-	Maximum of Temperature Maximum (Annual maximum value of daily maximum temperature)
UNEP	-	United Nations Environment Program
UNESCO	-	United Nations Educational, Scientific and Cultural Organization
UNFCCC	-	United Nations Framework Convention on Climate Change
WMO	-	World Meteorological Organization
μ	-	Mean
σ	-	Standard Deviation

LIST OF FIGURES

LIST OF TABLES

1 INTRODUCTION

1.1 General

One of the most relevant and debated aspects of the climate change is dealing with its impacts on the hydrological cycle and in particular on the statistical properties and seasonality changes of the precipitation, evaporation, change of runoff and consequently on the discharge of the river (Hasson, Lucarini & Pascale, 2013). Due to the changes of climate, at the present, the agriculture-based economies of most of the countries in South and South East Asia facing the effect of challenges in the food security and economies due to their large dependencies on the variable supplies of freshwater and inadequate integrated water resources management (Lal et al., 2011). As an example, considering the future water availability under the warmer climate while planning new water reservoirs can be long-sighted, keeping in mind the vast investment is comparable to the timescale over which significant changes in hydro-climatology of the region will manifest themselves clearly (Krol et al., 2000).

Considering the climate change, South and South East Asia became as hot spots of climate change and it is anticipated that the changes in the hydrological cycle will be quite severe in this region in terms of public policy, the water resource management problems with the potentially severe impacts for its socio-economical processes (IPCC, 2007).

1.2 Background

This case study is carried out to investigate the change in climate and impacts due to the environment in the river basin scale. The selected river basin for the case study is the Kelani River basin in Sri Lanka. Kelani River is the second largest river in Sri Lanka that originates from the central hills and flows to the west coast through Colombo City. The river basin is bounded by northern latitudes from 6o47' to 7o05' and eastern longitudes from 79o52' to 80o13'. The river originates approximately at 2,250 m above from mean sea level and passes 192km distance through four districts namely Nuwara-Eliya, Kegalle, Gampaha and Colombo before it reaches to the Indian Ocean. The river basin area is approximately about 2,230 km^2. Topographically Kelani River basin area distinctly characterized as upper and lower basins; a mountainous

upper basin, with an area of approximately 1,740 km^2 that lies upstream of the Hanwella River gauging station and a lower basin with an area of 500 km^2 and that is on flat terrain which lies downstream of Hanwella.

The river basin experiences an annual average rainfall of about 3,450 mm corresponding to a volume of about 7,860 MCMs out of which nearly 43% discharges into the Indian Ocean. For the period from 1949 to 1993, the streamflow at Glencourse has an average of 4565 MCM and a standard deviation of 895 MCM with a minimum of 2655 MCM in 1984 and a maximum of 6,556 MCM in 1976 (Zubair, 2003).

Since 1953, two reservoirs and five power stations (aggregated capacity of 335 MW) have been built to harness hydroelectricity. The Kelani hydropower plants provide 38% of the hydroelectricity that generates in Sri Lanka. Two hundred MCM of river water is tapped annually for municipal water supply for the Colombo metropolitan area. Also, heavy rains resulting in a rapid rise in Kelani streamflow poses a frequent flood hazard (e.g., May 2016) for Colombo. Hence streamflow variations have profound impacts, and skilful streamflow predictions would be useful for energy planning, flood preparedness, and municipal water budgeting.

1.3 Climate of Sri Lanka

Sri Lanka is an island which is in the Indian Ocean and located in the south of Indian Subcontinent. It lies within the 6° N – 10° N of north latitude and 80° E – 82° E of east longitude. The average yearly temperature in Sri Lanka as a whole range from 28 ℃ to 32 ℃. The mean temperature varies from a 16 ℃ in Nuwara Eliya in the central highlands of the island to high of 32 ℃ in Trincomalee on the northeast coast.

Sri Lanka is lying close to the equatorial and in the tropical zone. Therefore, Sri Lanka is influenced by the monsoons, allowing into four distinct seasons. The difference of the elevation also affects temperature variation. It is always hot in the lowland and getting to cooler when reaching to the higher altitudes of the island. For the monsoons of Sri Lanka, northeast monsoon brings rain in the northern and eastern regions in December and January. The western, southern and central areas of the island get rain from May to July by the south-west monsoon (Department of Meteorology, 2009).

By the receiving rainfall on the island, the island is divided into two climatic zones namely the wet zone and the dry zone. Where the west zone is comprising by the South West area covering about the quarter of the island, receive rainfall by South West monsoon. The wet-zone gets 2400 mm rainfall as an average annual within its two rainy seasons. Another part of the island is comprising of the North East area and covering by the North East Monsoon. The dry zone receives 1400 mm rainfall as an annual average. Also, Sri Lanka has multiple origins of rains such that Monsoonal, Convectional and Expressional rain accounts for the significant share of the annual precipitation to the island. The volume of water annually received for the island by rains is estimated as 188,015 MCMs (Jayatillake et al., 2005).

Regarding the climate change Wijesekera (2010) quoting on Jayatillake et al. (2005) about the increasing trend of air temperature, mainly from few decades of duration by after analysing the long-term temperature variations data and the variation of annual average rainfall has reached below the average for the entire period of study. Also, Wijesekera (2010) has quoted on Sri Lankan Centre for Climate Change Studies for the National level modelling and stated that the temperature decreases during the South-West monsoon season are anticipated to be 2.5 ℃ whereas the North-East monsoon season is expected to have a temperature increase of 2.9 ℃. The change of precipitation to be more significant from the south-west monsoon than the north-east monsoon. Therefore, that might be a significant challenge when planning water resources and as well as the performance of the associated structure for the efficient management of water resources in the country.

1.4 Impact of Climate Change on Weather and Hydrology of Sri Lanka

The analysis of the climate data for Sri Lanka clearly indicates that the changes in precipitation and temperature throughout the country. As climate change is expected to change the pattern and quantity of rainfall, evapotranspiration, surface runoff and soil moisture storage, changes in the water availability for irrigated agriculture and public use could be anticipated.

Sri Lanka is frequently subjected to several kinds of natural hazards mainly floods, landslides, coastal erosion and droughts. The cyclone is less felt within the island than

in the Indian subcontinent as Sri Lanka is situated outside of the cyclone belt, although the impacts of several severe storms have been experienced periodically. Where the frequency and intensity of these kinds of hazards are expected to increase with the outcomes of the changes of climate, such as changes in rainfall regimes and the rise in ambient temperature. These factors of variation of rainfall and temperature expected to be exacerbated by various anthropogenic factors that already threaten freshwater resources in the island and have resulted in many problems related to socio-economic and environmental. The following are the results of climate change on weather in Sri Lanka (Department of Meteorology, 2009).

1. Precipitation Variability

   i. The precipitation patterns have changed, but the conclusive trends are difficult to establish well.
   ii. A trend for precipitation decrease has been observed historically over the past 30 to 40-years, but that is not significant in statistical basis.
   iii. Also there is a trend for the increase of extreme rainfall events in daily basis.
   iv. An increase in the frequency of extreme rainfall events is anticipated, which would be lead to more floods.

2. Increasing Temperature
   i. A0.64 ℃ increase in air temperature has been recorded in Sri Lanka during over the past 40-years and 0.97 ℃ over during the last 72 years of the period, which is revealed a trend for an increase of 0.14 ℃ of temperature for a decade (Giorgi et al., 2012). However, the assessment of a more recent time band of 22-years has shown a 0.45 ℃ increase of the period of last 22-years, which is suggesting a rate of 0.2 ℃ increase per decade (Giorgi et al., 2012).
   ii. Consecutive dry days are increasing in the Dry and Intermediate Zones.
   iii. The ambient temperature of both minimum and maximum has increased during past few years.
   iv. The number of warm days and warm nights have both increased, while the number of cold days and cold nights both are decreasing.

v. The general warming trend is expected to increase the frequency of extreme hot days.

Climate is defined as the general weather conditions over a specified period and a particular area. According to the United Nations Framework on Convention on Climate Change (UNFCCC, 1992), climate change refers only to the anthropogenic changes over comparable time periods. However, in Intergovernmental Panel on Climate Change (IPCC) usage, climate change consists of both natural variability and human-induced change, even though most of the observed increase in global average temperature since the mid of 20th century is mostly related to the anthropogenic activities. Therefore, in a broad sense, climate change is defined as a statistically significant variation in mean or variability persisting for an extended period.

A variety of the potential impacts resulting from climate change have been hypothesised (Gleick, 1989; Houghton, Jenkins & Ephraums, 1990). Some of the possible climate change on hydrology that has been identifying include changes in the availability of water supply (Revelle & Waggoner, 1983; Gleick, 1987), changes in runoff production (Gleick, 1986; Lettenmaier & Gan, 1990) and changes in the timing of hydrologic events (Lettenmaier & Gan, 1990; Kite & Linton, 1993; Burn, 1994).

Therefore, as a result of potential hydrologic impacts of climate change, there are also likely to be many water resource systems that are affected by the changing climate. The World Climate Program informs this, initiated by the World Meteorological Organization, documented the need for research in this regard. Nemec and Schaake, (1982) raised the issue of "whether the sensitivity of the water resource system to climate variations is so small, that it can include in the modelling error, and the water system so robust that it will not even feel it, so is it large enough to be taken in to account (Burn & Simonovic, 1996).

In the hydrological cycle, water moves continuously between oceans and the atmospheric regions through different processes such as evaporation, percolation and precipitation over various temporal and spatial scales. Hence under natural conditions, climate variations are already considered to be one of the major causes of hydrological change and have significant social and economic implications for water resources and

flood risk. Therefore, according to the anthropogenic climate change affects the energy and mass balance of fundamental hydrological processes as well as hydraulic processes, the water cycle is expected to be intensified, and hydrological patterns are very likely to be different under different climate scenarios. Also, there are distinctions between natural variability and anthropogenic climate abnormality, both human activity and natural climate influences are interconnected with the current climate events, and the changes in climate are to be expected to affect the balance of water distribution and living organisms on the earth.

1.5 Historical Background of Climate Change

Climate change and development are closely intertwined. Poor people in developing countries will feel the impacts first and worst because of vulnerable geography and lesser ability to cope with damages from severe weather and rising sea levels (IPCC, 2007). Historically, the responsibility for climate change, though, rested with the rich countries that emitted greenhouse gases unimpeded from the industrial revolution on and become rich by doing so. Presently, some of the most quickly developing countries have become significant emitter themselves just as all states are compelled by the common good to reduce greenhouse gas emissions. Therefore, a considerable challenge of reaching a global deal on climate change was to find a way for developing countries to continue growing under the planetary carbon limits that wealthy nations already pushed too far (UNFCCC, 1992).

The current warming trend is of particular significance because most of it is very likely human-induced and proceeding at a rate that is unprecedented in the past 1,300-years. Earth-orbiting satellites and other technological advances have enabled scientists to see the big picture, collecting many different types of information about our planet and its climate on a global scale. This body of data, received over many years, reveals the signals of changing the environment to the world.

Also, the heat-trapping nature of carbon dioxide and other gasses was demonstrating in the middle of the 19th century. Their ability to affect to the transfer of infrared energy through the atmosphere is the scientific basis of many instruments flown by NASA. No question increased levels of greenhouse gases that must cause the earth to warm in

response. Ice cores are drawing from Greenland, Antarctica, and Tropical Mountain glaciers show that the Earth's climate responds to the changes of heat regarding the greenhouse gas levels increase. They also explained that in the past, significant changes in climate had happened very quickly, geologically speaking, in tens of years not in millions or even thousands of millions. The evidences for the rapid climate change is compelling with (IPCC, 2007);

- Global temperature rises
- Warming of oceans/seas
- Shrinking of ice sheets
- Declining the Arctic sea ice
- Glacial retreat
- Extreme weather events
- Acidifications of oceans and decreased the snow cover

1.6 The Importance of Study of Climate Change

Rainfall is of primary importance to both the physical and cultural landscape of any region (IPCC, 2007). Of all the standard parameters of climate, rain is the most vulnerable parameter in time and space (Manawadu, 2008). Rainfall received across Sri Lanka varies dramatically from year to year, ranging from dry periods that can persist for months, to periods of intense downpours, storms and flooding (Manawadu, 2008).

Scenes of flooding and storms show us just how much weather and climate can affect our lives. Understanding and predicting what the coming weather might bring, or be predicting how climate will change over the next century is of vital importance both for our economy and society (Hasson, Lucarini & Pascale, 2013). Also climate can be a thought of as the average or typical weather conditions we experience. Scientists know that climate varies naturally on many time scales and they know that people are affecting climate particularly through emission of gases (UNFCCC, 1992).

The reason for climate affected situation is flooding of Colombo city by the flow of Kelani River. Therefore, predicting the changes in weather would be very important to identify the hazardous conditions in future regarding the previous extreme events.

If there is one thing that the paleoclimate record shows, it is that the Earth's climate is always changing. Climatic variability, including changes in the frequency of extreme events like droughts, floods and storms have ever had a tremendous impact on humans (IPCC, 2013). A particularly severe El-Nino or relatively short drought can cost billions of dollars. Due to this reason, scientists study about the past climatic variability on various time scales to gain clues that will help society plan for future climate changes (Burt & Weerasinghe, 2014).

Unfortunately, records of past climate change from satellites and other relevant human measurements generally covers less than about 150 years. These are too short to examine the full range of climatic variability on the globe. Due to this reason, it is critical to investigate the climate change going back to hundreds and thousands of years using paleoclimate records from the trees, corals, sediments, glaciers and other natural sources. Also, the study of past climate change also helps us to understand how humans influence on the Earth's climate systems. According to the paleoclimate method, over the last thousand years clearly shows that the global temperature increased significantly in the 20th century and that this warming was likely to have been unprecedented in the previous 1,200-years (Indian Climatology Institute, 2014).

Otherwise, the state of the art of climate prediction is accomplished using large, sophisticated computer models of the climate system. A great deal of research has focused on ensuring that these models can simulate most aspects of the modern present-day climate. It is also important to know how these models affect climate change.

1.7 The Importance of Climate Change Predictions

As mentioned in the Fifth Assessment Report of the IPCC, the current Global average surface temperature warmed by 0.85 ℃ from 1880 to 2012, and the beginning of the 21st century has been the warmest on record (IPCC, 2013). The increase in global temperature has caused higher evapotranspiration rates leading to changes in precipitation worldwide (Urrutia & Vuille, 2009; Paparrizos et al., 2016) and significantly impacted hydrological processes and the occurrences of the frequency of hydrological events that is extreme floods and droughts have changed. As a result,

complex meteorological situations are effects streamflow regimes, especially at the basin scale, which is the focus of the present study.

The term “prediction” has often avoided within the global change debate because non-experts can easily misinterpret it due to its use in numerical weather predictions. In fact, climate prediction aims at forecasting about how specific weather patterns are evolving at time scales of the order of days based on the knowledge of the state of the atmosphere at a particular time (Lorenz, 1975). Therefore, climate change prediction is of an entirely different nature, and it is essential that the end users of the climate change information understand this difference and are aware of the uncertainties and limitations underlying current predictions of climate change.

In the late 1960s and the mid of 1970s, the chaotic nature is the climate system was first recognised. In this regard (Lorenz, 1969) defined two types of predictability problems of climate;

i. Predictability of the first kind, which is mostly the prediction of the evolution of the atmosphere, or more generally the climate system, given some knowledge of its initial state. Predictability of the first kind is therefore primarily an initial value problem, and numerical weather prediction is a typical example of it (Giorgi, 2006).
ii. Then the predictability of the second kind, in which the objective is to predict the evolution of the statistical properties of the climate system in response to changes in external forcing. Therefore, the predictability of the second kind is thus primarily a boundary value problem (Giorgi, 2006).

In a predictability problem, the predictability is defining as the time over which we can expect a prediction to be skilful. That depends on the temporal scale of the phenomenon under consideration. In general, the shorter the characteristic time scale of an event, the quicker the predictability (Lorenz, 1969).

1.7.1 Regional vs. Global Climate Change Predictions

Changes in globally averaged climate primarily determined by the radiative budget of the coupled atmosphere-ocean-land system, modulated by internal nonlinear feedbacks and modes of variability. Hence, a positive global radiative forcing like due to GHG

generally results in global warming and an increase of global precipitation in response to increased evaporation from the warmer land and ocean surfaces (Allen & Ingram, 2002). That is implementing by all global model simulations (Cubasch & Meehl, 2001).

As the scale of interest, several factors make climate change prediction in to more difficult. Those are changes in circulation features, even relatively minor, can have profound regional impacts (Giorgi, 2006). As an example, the horizontal displacements of storm tracks due to differential horizontal heating do not affect much on the global precipitation change, but they may cause significant increases in precipitation over some regions and corresponding decreases over other areas (Giorgi, 2006). Hence can be identified that it is necessary to predict the details of changes in atmospheric circulations.

Regional climate is affected by the fine scale forcing and processes, such as due to the complex of the topography of the regions, coastline and land use features, atmospheric aerosols and another kind of pollutants (Giorgi et al., 1998). But in many situations, these forcing and processes do not adequately represent in climate models (Giorgi & Shields, 1999). Also on the other hand, in some regions, stationary forcing, such as due to the changes of topography, may increase the predictability by locking the local response to large-scale changes in circulations. (Lambert & Boer, 2000; Giorgi, 2006).

Also, the effects of the circulation regimes and the internal modes of the variability are most important at the regional scale. In particular, often the climate of a region is affected by processes occurring in the remote areas through teleconnection patterns involving the interaction of local energy sources with the large-scale circulations. The aerosol forcing over specific regions can also have a substantial climatic impact over remote areas (Giorgi, 2006).

1.8 Problem Statement

It is evident that global temperature profile has significantly been modified due to the climate change effects or impacts, which would subsequently have a major impact on the component of the hydrologic cycle, essentially the precipitation patterns. This will lead to higher variability in local and regional rainfall intensities producing more

frequent extreme events with sharp rainfall intensities while on the other hand leading to the extended droughts since the global mean annual precipitation value remain unchanged with only a minimum increment in most of the parts in the world.

1.9 Main Objective

To study the climate extremes and precipitation trends as affected by the climate change impact and subsequent influences on the streamflow on watershed scale to manage water resources more efficiently.

1.10 Specific Objectives

Review of the variation of the precipitation and temperature anomalies with respect to inputs to the model of rainfall runoff, objective functions, optimization criteria and the future forecast.

1 Identify the natural climatic extremes and precipitation trends based on historical data in the basin.
2 Identification of GCM climate model and their applicability for the region.
3 Selection of suitable climate scenario for the region, from developed scenarios and downscaling to required resolution.
4 Compute stream flow estimates by HEC-HMS model.
5 Comparison of the model performance with respect to the measured streamflow of catchments.
6 Evaluation of future climate (Precipitation and Temperature changes) and its impact on streamflow
7 Derive and develop recommendations and guidelines targeting mitigatory measures

1.11 Scope and Limitations

The scope of the present study is to evaluate the future changes of the precipitation, temperature including temperature maximum, temperature minimum and temperature average and the streamflow variability concerning the climate change. The limitations of the study are the applicability of the General Circulation Model for regional/local scale and issues associated with downscaling.

Global Climate Models (GCMs) continue to yield important scientific insights into the dynamics and evolution of the climate system on time scales ranging from months to centuries. Outputs from GCMs have also played a key role in informing various assessments of the impact of large-scale climate variation and change on natural resources, human health, infrastructure and commerce. Raw GCM output, however, is not always adequate to address the inter-disciplinary questions of interest to stakeholders. Two primary impediments to impacts studies are the spatial scales represented by the GCM may not be as excellent as the end-use application requires, and the GCM raw output is deemed to contain biases relative to the observational data, which preclude its direct use in downstream applications.

Over time, high-resolution GCMs and advances in the model formulation will reduce these impediments, but the myriad of climate impacts, the question makes it unlikely that even these improved models will be able to address all scales and applications of interest adequately. A variety of downscaling methods may be used to process and refine GCM output with the aim of producing output more suitable for impacts studies. The refined production aims to address the limitations of coarse resolution and regional biases in the GCM output. Following are the restrictions listed out.

- Properties inherent in models make dynamic predictability impossible. Without dynamic predictability, other techniques must be used to simulate climate. Such methods introduce biases of varying magnitude into model projections.
- To have any validity regarding future predictions, GCMs must incorporate not only the many physical processes involved in determining climate but also all critical chemical and biological processes that influence climate over long time periods. Several of these vital processes are either missing or inadequately represented in today's state-of-the-art climate models.
- Limitations in computing power frequently result in the inability of models to resolve essential climate processes. Low-resolution models fail to capture many important phenomena of regional and lesser scales, such as clouds; downscaling to higher-resolution models introduces boundary interactions that can contaminate the modelling area and propagate error.
- Although some improvements have noted in performance between the CMIP3 set of models used in AR4 and the newer CMIP5 models utilised in AR5, many researchers report finding little or no improvement in the CMIP5 model output for several vital parameters and features of Earth's climate.

2 LITERATURE REVIEW

2.1 General

For the literature review, a study was carried out on observed climate change over the region, observed trends of the climate of Sri Lanka, climate variations and a data requirement for study. Also studied about the future climate change of Asia, climate change impacts in South Asia, impacts by increased temperature, impacts of precipitation variability and water resources in South Asia and consequences of increased frequency of extreme climate events and natural disasters. For future climate change prediction studied about General Circulation Models (GCMs), Regional Climate Models (RCMs), climate change scenarios, reliability of the climate models, verifications and validations of the climate datasets (GCMs), methods of downscaling, bias correction and hydrological modelling of Sri Lanka including hydrological model calibration and validation.

2.2 Observed Climate Change over the Region

At the time of the Third Assessment Report of IPCC, scientists could say that the abundances of all the well-mixed greenhouse gases during the 1900s were higher than at any time during the last half million years and this record now extends back nearly one million years (IPCC, 2007). In 2005 the concentration of carbon dioxide exceeded the natural range that has existed over 650,000 years. Evidence from observations of the climate system show an increase of 0.74±0.18 ℃ in global average surface temperature during the 100-years period from 1906 to 2005 and even more significant warming trend over the 50-year period from 1956 to 2005 than over the entire 100-years period, i.e. 0.13±0.03 ℃ vs 0.07±0.02 ℃ per decade (IPCC, 2007). Eleven of the 12-years period between 1995 and 2006 are among the 12 warmest years since the instrumental record of global surface temperature was started in 1850 (IPCC, 2007). Land regions have warmed at a faster rate than the oceans. Warming has occurred in both land and ocean domains, and in both sea surface temperature (SST) and night-time marine air temperature over the oceans. However, for the globe as a whole, surface air temperatures over land have risen at about double the ocean rate after 1979 (more than 0.27 ℃ per decade vs. 0.13 ℃ per decade).

The following information on the observed climate change in South Asia was summarised from the report of the Working Group II chapter on Asia (Cruz et al., 2007) of IPCC. In general, past and present climate trends and variability in Asia can be characterised by increasing air temperatures which are more pronounced during winter than in summer. During recent decades, the observed increase in some parts of Asia has ranged from less than 1.0-3.0 ℃ per century. Across all of Asia, inter-seasonal, inter-annual and spatial variability in rainfall trend has observed during the past few decades. Table 3.1 provides a detailed list of perceived characteristics in surface air temperature and rainfall for the countries in South Asia under an Indian Continent (Cruz et al., 2007).

As for extreme climate events, there has been new evidence on recent trends, particularly on the increasing tendency in the intensity and frequency of these events in South Asia over the last century. There have been significantly longer heat waves in many countries of South Asia with several cases of seven heat waves. The IPCC AR4 report noted that, in general, the frequency of more intense rainfall events in many parts of Asia has increased, causing severe floods, landslides and debris/mudflows. It is interesting that at the same time, the number of rainy days and the total annual amount of precipitation has decreased. Therefore, the total amount of rainfall has decreased, but the rain has concentrated in a few days. Analysis of rainfall data for India highlights the increase in the frequency of severe rainstorms over the last 50-years. The number of storms with more than 100 mm of rainfall in a day is reported to have increased by 10% per decade (UNEP, 2007).

An example of this can be demonstrated by the extreme rainfall event which occurred in Mumbai, India on 26 and 27 July 2005. In a matter of 18h duration, 944 mm of rain recorded and which was the highest rainfall ever recorded in the last 100 years in India. Mumbai and adjacent areas of Maharashtra experienced one of their worst floods in history (Government of Maharashtra, 2014). Also in Sri Lanka, in 15, 16 and 17 of May 2016 for Kelani River Basin, the extreme rainfall is recorded, that is an over 200 mm of rains of each day as a daily rainfall. Table 2.1 represents the current trend of observed temperature and precipitation of countries in an Indian Continent.

Table 2-1 Summary of Observed Trends of Temperature and Precipitation of Countries in an Indian Continent

Country	Change in Temperature	Change in Precipitation
Bangladesh	Increasing trend of about 1.0°C of in May and 0.5°C in November from 1985 to 1998	Decadal rain anomalies above long-term averages since 1960s
India	A 0.68°C increase per century with increasing trends in annual mean temperature and warming more pronounced during post-monsoon and winter	Increase in extreme rains in north-west region during summer monsoon in recent decades and lower number of rainy days along the east coast
Nepal	A 0.09°C increase per year in the Himalayas and 0.04°C in Terai region with more winter	No distinct long-term trends in precipitation records for 1948-1994
Pakistan	A 0.6-1.0°C increase in mean temperature in coastal areas since the early 1900s	10-15% decrease in the coastal belt and hyper arid plains and increase in summer and winter precipitation over the last 40 years in northern Pakistan
Sri Lanka	A 0.016°C has increased per year between 1961 to 90 over an entire country and 0.02°C increase per year in central highlands	An increasing trend in February and decrease trend in June

(Source: Sanjay et al., 2013)

In many parts of South Asia, there have been an increasing frequency and intensity of droughts. The linear trends of rainfall decrease for 1900-2005 were 7.5% in South Asia (Significant at < 1.0%). Droughts have become a more common problem, especially in the tropics and subtropics, since the 1970s (IPCC, 2007). Observed marked increases in droughts in the past three decades arise from more intense and more prolonged droughts over more extensive areas, as a critical threshold for delineating drought that exceeded over increasingly broad regions. Decreased land precipitation and increased temperatures that enhance evapotranspiration and drying are essential factors that have contributed to more areas experiencing droughts, as measured by the Palmer Drought Severity Index. Also, there has been a noted decrease in the number of cyclones originating from the Bay of Bengal and the Arabian Sea since 1970 but the

intensity of these storms has increased, and the damage caused by the intense hurricanes have risen significantly in India and the Tibetan Plateau. Table 2.2 gives a detailed summary of observed changes in extreme events and severe climate anomalies in South Asia.

Table 2-2 Summary of Observed Changes in Extreme Events and Severe Climate Anomalies in South Asia

Climate event	**Observed change**
Heat waves	The frequency of hot days and multiple-day wave has increased in past century in India with an increase of deaths due to heat stress in recent years.
Intense rains and floods	Severe and recurrent floods in Bangladesh, Nepal and north-east states of India during 2002, 2003, and 2004; floods in Surat, Barmer and Srinagar of India during summer monsoon season of 2006; 17 May 2003 floods in the southern province of Sri Lanka were triggered by 730 mm rain.
Droughts	A 505 of droughts have associated with El Nino; consecutive droughts between 1999 and 2000 in Pakistan and Northwest of India led to sharp decline in water tables; consecutive droughts between 2000 and 2002 caused crop failures, mass starvation and affected – 11 million people in Orissa, India; droughts in Northeast India during summer monsoon of 2006.
Cyclones/typhoons	The frequency of the monsoon depressions and cyclones formation in the Bay of Bengal and the Arabian Sea on the declining trend since 1970 but the intensity is increasing causing severe floods concerning damages to life and property.

(Source: Sanjay et al., 2013)

During the twentieth century, the changes in temperature and precipitation described above caused necessary changes in hydrology over large areas. One difference was a decline in spring snow cover, and less snow generally translates to lower reservoir levels. The earlier onset of spring snowmelt exacerbates this problem. Snowmelt started 2-3 weeks earlier in 2000 than it was in 1948 (Stewart et al., 2004). Mainly, worrisome is the reduction of the mass balance in the glaciers, and this has severe implications for the availability of water for over 500 million people in South Asia (Shivakumar & Stefanski, 2011).

Another manifestation of the changes in the climate system is a warming trend in the world's oceans. The global ocean temperature rose by 0.10 °C from the surface to 700 m depth from 1961 to 2003 (IPCC, 2013). Warming trend causes seawater to expand and thus contributes to sea level rise. This factor referred to as thermal expansion that is committed of 1.6 ± 0.5 mm per year to a global average sea level over the last decade (1993–2003). Other factors are contributing to sea level rise over the previous decade include of decline in mountain glaciers and ice caps of 0.77 ± 0.22 mm per year (IPCC, 2014). In the coastal areas of Asia, the current rate of sea-level rise is reported to be between 1.0 and 3.0 mm/year which is slightly higher than the global average. The amount of sea-level rise of 3.1 mm/year has observed over the past decade compared to 1.7–2.4 mm/year over the twentieth century, which suggests that the rate of sea level rise has accelerated relative to the long-term average.

The coastlines of South Asia are highly prone to cyclones, and the combination of extreme climatic and non-climatic events have caused coastal flooding, resulting in substantial economic losses and fatalities. In the major river deltas of the region, wetlands have significantly altered in recent years due to massive scale sedimentation, land-use conversion, logging and human settlements. Also, salt water is reported to have penetrated to 100 km or more inland along secondary channels of the Bay of Bengal during the dry season. Along the South Asian coastlines, a significant portion of the mangroves, which help prevent salt-water intrusion have reportedly lost during the last 50-years primarily due to human activities.

Chapter 10 of the IPCC Working Group II report, also summarised the impacts of observed changes in climate. For agriculture, the report noted that the production of rice, maize and wheat over recent decades has declining trend in many parts of Asia due to increasing water stress partly due to increasing temperature, increasing frequency of El Niño's and a lower number of rainy days. The chapter summarises a study by the International Rice Research Institute which observed a 10% decrease in rice yield for every 1.0 °C increase in growing-season minimum temperature (Peng et al., 2007). For water resources, there is concern about melting glaciers, since they account for over 10% of freshwater supplies the drier parts of Asia.

There have been observations of Asian glaciers melting faster than in the past, especially in Central Asia, Western Mongolia and North-West China. However, studies in northern Pakistan indicates that glaciers in the Indus Valley region may be expanding, due to increases in winter precipitation over the western Himalayas during the past 40-years. In India, Pakistan, Nepal and Bangladesh, water shortages have been attributing to rapid urban growth, industrialisation, population growth and inefficient water use, which are exacerbated by a changing climate and its negative impacts on water demand, supply and quality.

2.2.1 Climate Extremes over the South Asia

The Inter-governmental Panel on Climate Change (IPCC) projected in its Third Assessment Report (TAR 2001) that over the period of 1990 to 2100; the average global temperature would increase by 1.4 to 5.8 °C and would be subject to increase in frequency and intensity of extreme climate events (massive precipitation events, floods, droughts, extreme temperature, etc.). Later a study; "Extreme Weather on the rise" released by World Meteorological Organization (WMO) in 2003 said that the world was experiencing record number of extreme events such as droughts and tornadoes. Laying the blame firmly at the feet of global warming, the agency warned that the number of extreme events could continue to increase. The South Asia region was a no exception to that and witnessed too a good amount of weather extremes in the recent past. A catastrophic cyclonic storm in Bangladesh left 100,000 people dead in 1991. Pakistan faced the previous century's worst flood in Jhelum River in 1992. There was a severe urban storm flooding in Lahore, the Capital city of Punjab Province, during August 1996, the wettest month on record with 437 mm of rainfall occurring during a 3-day period from 23-25 August. Dokriani glacier in the Himalayas, India retreated at a record pace of 66 feet in 1998 despite a severe winter in that year. In 1999, a severe cyclonic storm hit the coastal areas of Pakistan and India and brought in its wake, massive devastation to the coastal regions of both the countries. Pakistan faced the history's worst drought during the period 1998-2001. A record level of 620 mm of rainfall felt in Islamabad, Pakistan one in just 10 hours brought in its wake substantial urban storm flooding in the famous Lai Nullah flowing through the two cities of Rawalpindi and Islamabad caused catastrophic losses to life and property. A

pre-monsoon heat wave that hit India in 2003 created the peak temperatures to reach 45 to 49 °C and killed more than 1400 people. In Sri Lanka, heavy rains from the Tropical Cyclone 01B during May, 2003 exacerbated the already wet conditions, caused flooding and landslides and resulted in more than 300 fatalities. In the year 2004, Pakistan received very low monsoon rains leaving Tarbela Dam on Indus River some 60 feet below its Maximum Conservation Level (MCL) of 1550 SPD (Survey of Pakistan Datum) which previously had not come across such a situation. Starting on July 15, 2004, Bangladesh faced the worst ever flood in its history, and broke the record of flooding in 1988. Two third of the country went out under water. The attached Table A1-1 and Table A1-2 in Appendix 01 which are shows the indices used to identify the climate extremes and the results of trends of extremes of climate over the South Asian region for the period of 1971-2000 for daily temperature and 1961-2000 for the daily precipitation.

An increase in the warmest day temperature of the year (TXx) was seeing at most stations across India, Nepal and Sri Lanka, whereas the changes are more mixed over Pakistan and Bangladesh. The percentages of stations showing an increase are around 56%, 73%, 90%, 52%, and 99% respectively for Pakistan, India, Nepal, Bangladesh and Sri Lanka. Many of the warming trends over Nepal are significant, compared to non-significant changes in the upper Himalayan parts of Pakistan. Southern and central parts of India below about 18.0 °C have stronger increases in TXx relative to other components. The northwestern parts of India and adjoining northeastern part of Pakistan (the monsoon-dominated region) show decreasing trends at most stations. The coldest night temperature of the year (TNn) also indicates increasing trends at most stations over India, Nepal, Pakistan and Sri Lanka but mixed trends were seeing over Bangladesh. The Greater Himalayan region of Pakistan shows a decreasing trend though non-significant at most stations, whereas, over Nepal, a non-significant increasing trend is most common. The annual count of days when the daily maximum temperature exceeds 25.0 °C (SU25) is seen to have increased at most stations across the region. The percentage of stations showing positive trends over Nepal (85%) is higher than Pakistan and India both around 65%. Around 92% and 82% of stations show warming trends over Bangladesh and Sri Lanka respectively (Revadekar &

Kulkarni, 2008). Nepal has increasing trends for 19 stations, with eight significant, whereas Pakistan has rising trends over 20 stations, with five significant. The Greater Himalayan region has a significant decreasing trend at three stations and only one with a significant positive trend. The southern tip of India and Sri Lanka show strong, increasing trends at most stations. The regional average of SU25 has grown significantly over the whole period of analysis (1971-2000).

The consecutive dry days (CDD) index has generally decreased across the region except in Sri Lanka. The decrease is stronger over Nepal and Bangladesh with around 76% and 89% of stations showing a decline. In contrast, consecutive wet days (CWD) have increased over most of India and Pakistan, but changes are more mixed than for CDD (Revadekar & Kulkarni, 2008). Sri Lanka shows significant increases in CDD along the west coast. Similar trends in CDD are seen for the islands of the Aegean Sea and Cyprus (Kostopoulou & Jones, 2005), indicating that southern Mediterranean areas, and especially the islands, are becoming more prone to drought and desertification (Brandit & Thornes, 1996). The annual count of days with daily precipitation greater than 10mm (R10mm) has increased in many parts of the world (Alexander et al., 2006). There are mixed changes in R10mm across South Asia, but some sub-regional consistencies are evident. Stations in Pakistan and northwestern India mostly show an increase in the number of heavy precipitation days, as do stations in Bangladesh and on India's east coast. However, southern India and Sri Lanka show consistent patterns of decline. Similar results obtained for the R20mm index. Regionally-averaged, the trend is positive for both indices. The number of heavy precipitation days is seen usually decreased during El Niño years and increased during La Niña years (Revadekar & Kulkarni, 2008).

2.2.2 Observed Trends of Climate in Sri Lanka

Comprehensive reviews of hydrological trends are widely available. In most of the countries, surveyed historical hydrological trends related to climate change and flood risk (Wijesekera, 1998). Also (Manawadu, 2008) quoted regard to the number of rainy days received in each season, the Northeast Monsoon Season has witnessed a negative trend in all the meteorological stations subjected for the study of Climate Changes in Sri Lanka.

Considering the change of rainfall of Sri Lanka over the last century identified that, a long-term increasing trend at the 95% confidence level observed at Colombo with a rate of 3.15 mm/year. Decreasing long-term trends were found at two locations, Nuwara Eliya at a rate of 4.87 mm/year and Kandy at a rate of 2.88 mm/year. No consistent increase or decrease in trends was observing for stations in the wet or the dry zones during the last century. However, a recent study has indicated a significant decline in rainfall in several stations (nearby) on the western slopes of the highlands (Jayawardena et al., 2005).

Climate change challenges the traditional stationary analysis and assumptions in hydrology. Experience will not be very likely to provide an excellent guide to future conditions under changing the climate (UNFCCC, 1992). Therefore, understanding observed and projected change in hydrological processes is essential to future water resources management, flood risk management as well as ecosystems. In hydrology, different hydrological processes are related to each other and are under the rule of conservation of mass. Therefore, the trends of one hydrological process are likely to be related to that of other operations. Precipitation, evaporation, temperature, change in storage and runoff are the most fundamental processes in water balance equation based on the rule of conservation of mass where quantifying their time-variant characteristics under the driving of climate change is one of the foremost focal points in current hydrological studies.

2.2.3 Climate Variations

Climate, although very slowly, keeps evolving. There are many causes behind the variations of climate. Climate variations can be categorised into two broad contexts (IPCC, 2014).

1 Natural Climate Variations

Several natural causes force climate to change across time and scale. It can be further drilled down into the following categories.

A. Natural Forcing of the Climate System

- The sun and the global energy balance
- Radioactive forcing

- Greenhouse effect

B. Natural Variability of the Climate

- Externally and internally induced climate variability
- Feedback
- Global and hemispherical variability
- Regional variability

2 Human induced Climate Variation

Human activities also influence the climate. The major human-induced causes include changes in greenhouse gas concentrations, changes in aerosol levels and the changes in land use and land cover.

A. Enhanced Greenhouse Effect

Most human activities influence the climate by bringing about an increase in the concentration of greenhouse gases in the atmosphere. An increase of the concentration of greenhouse gases leads to an increase in the magnitude of the greenhouse effect. This is known as enhanced effect of greenhouse.

The enhanced effect of greenhouse is the direct result of human activities through the processes, such as burning of fossil fuels, industrial operations and forest clearing which lead to releasing of tons of carbon dioxide, nitrous oxide and methane to the atmosphere. Chlorofluorocarbons or CFCs, are also potent greenhouse gases, and as an added danger (IPCC, 2014).

2.2.4 Data Requirement for Study

In the study on detection of hydrologic trends and variability on 248 watersheds in Canada, states that the selection of stations in a climate change research is substantial at the initial step and that a minimum record length of 25-years ensures the validity of the result of the trends statistically (Burn & Elnur, 2002). While carrying out the study on the trends and variability in Mackenzie River basin in northern Canada using hydrologic data of 54 hydrological and 10 meteorological stations, states that considering more extended periods of analysis increase the power of the trend test and therefore increase the likelihood identifying trends that exist in data (Aziz & Burn, 2006). In the streamflow trend analysis in Turkey considering monthly data of 31-years period in 26 watersheds states that hydro climatologists are concerned with

analysing time series by concentrating on differences in 30-year normal along the whole period of records (Kahaya & Kalayci, 2004). Hence, the period of 30-years is assumed to be long enough for a valid mean statistic.

Climate change studies could be carried out using either daily or monthly data. Therefore, literature suggested that in temperature, rainfall and streamflow can be computed using daily and monthly data. However, Training Manual on Drought Risk Reduction (UNDP, 2015) by United Nations Development Program (UNDP) states that since rainfall is very intermittent, a particular day cannot compare to that specific day in previous years.

2.3 Future Climate Change of Asia

Looking ahead, IPCC, 2007 projects increases in global mean surface air temperature continuing over the twenty-first century, driven mainly by increases in anthropogenic greenhouse gas concentrations, with the warming proportional to the associated radiative forcing. An expert assessment based on the combination of available constraints from observations and the strength of known feedbacks simulated in the models used to produce the climate change projections indicates that the equilibrium global mean surface air temperature warming for a doubling of atmospheric CO_2. The 'equilibrium climate sensitivity', is likely to lie in the range of 2.0-4.5 ℃, with a most likely value of about 3.0 ℃ (IPCC, 2007). Warming in the twenty-first century is expected to be greatest over land and at the highest northern latitudes. It is very likely that heat waves will be more intense, more frequent and longer lasting in a future warmer climate.

Increasingly reliable regional climate projections are now available due to advances in modelling and understanding of the physical processes of the climate system. IPCC, (2007) projections show that drier subtropical regions are warming more than the moisture tropics. Warming is likely to be above the global mean temperature in South Asia. The temperature projections for South Asia for the twenty-first century suggest a significant acceleration of warming over that observed in the twentieth century. The increase in temperature is least rapid, similar to the mean global warming, in South-East Asia, more substantial over South Asia and East Asia and most significant in the

continental Asia (Central, West and North Asia). Also, in general, the projected warming over Asia is higher during northern hemisphere winter than during summer for all time periods. Recent modelling experiments indicate that the warming would be significant in Himalayan Highlands including the Tibetan Plateau and arid regions of Asia.

Mean winter precipitation will very likely increase in Northern Asia and the Tibetan Plateau and likely increase in West, Central, South-East and East Asia. Summer precipitation will likely increase in North, South, South-East and East Asia but decrease in West and Central Asia in future. Droughts associated with summer drying could result in regional vegetation die-offs (Breshears et al., 2009) and contribute to an increase of the percentage of land area experiencing drought at any one time, for example, extreme drought increasing from 1% of present-day land area to 30% by the end of the century (Burke et al., 2015).

Climate extremes encompass both extreme weather, with durations of minutes to days (the synoptic timescale), and extreme events of climate with durations of months, in the case of periods of wet weather, or years, in the case of drought (McGregor, 2005). In all cases, the frequency of extreme events may be affected by seasonal to inter-annual fluctuations of large-scale climate variations such as El Niño/Southern Oscillation (ENSO) and the North Atlantic Oscillation (NAO) (Schwierz et al., 2006).

The frequency of occurrence of climate extremes is expected to change during the next century, with an increase of the incidence of heat waves and massive precipitation events, and decreases in the frequency of frost days, as a consequence of anthropogenically-forced climate change (Easterling et al., 2000). An increase in the occurrence of extreme weather events including heat wave and intense precipitation events is projected in South Asia (Lal, 2003) along with an increase in the interannual variability of daily precipitation in the Asian summer monsoon (Giorgi & Bi, 2005; Lal et al., 2011). For tropical cyclones, there is a projected increase of 10–20% in the intensity of storms with an increase in sea-surface temperature of 2.0–4.0 ℃ relative to the current temperatures in East Asia, South-East Asia and South Asia. An increase in heights of storm-surges could result from the occurrence of stronger winds, increases in sea-surface temperatures and low pressures associated with tropical

cyclones occurring in an enhanced risk of coastal disasters along the coastal regions of the countries of East, South and South-East Asia.

Annual average river runoff and water availability projected to decreasing trend by 10–30% over some dry regions at mid-latitudes as well as in the dry tropics. The areas suitable for rain-fed agriculture are expected to significantly decrease affecting adversely land productivity potential of the continent (Fischer et al., 2002).

2.4 Climate Change Impacts in South Asia

Climate Change projections are indicating that climate variations in South Asia will be varied and heterogeneous, with some regions experiencing more intense precipitation and increased flood risks, while others encounter sparser rainfall and prolonged droughts. The impacts will vary across sectors, locations and populations. Temperature rise will negatively impact rice and wheat yields in tropical parts of South Asia where these crops have already grown close to their temperature tolerance threshold. While direct impacts associated with the rise in temperatures of the region, indirect effects due to the water availability, changing soil moisture status, pest and disease become as incidence are likely to be felt. The most significant impact was expected to be borne by smallholder rainfed farmers who can constitute the majority of the farmers in this region and possess low financial and technical capacity to adapt to climate variability and change over the area (Shivakumar & Stefanski, 2011). The following classifications are a summary of the expected impacts of climate change across this diverse region.

2.4.1 Impacts by Increased Temperature

The increased temperatures may also reduce the effects of CO_2 indirectly, by increasing water demand. Rain-fed wheat grown at 450 ppm CO_2 demonstrated yield increases with temperature increases of up to 0.8 ℃, but declines with temperature increases beyond 1.5 ℃; additional irrigation was needed to counterbalance these adverse effects (Xiao et al., 2005; Shivakumar & Stefanski, 2011).

Temperature rises may negatively impact on the yields of rice and wheat in tropical parts of South Asia where these crops have already grown close to their temperature tolerance threshold (Kelkar & Bhadwal, 2007). Kumar & Parikh (2001), show that

even after accounting for farm level adaptation, a 2.0 ℃ rise in the mean temperature and a 7% increase in mean precipitation will cause to reduce the net revenues by 8.4% in an India. Wheat yields are predicted to decline trend by an amount of 6–9% in sub-humid, semiarid, and arid areas with 1.0 ℃ increase in temperature (Sultana et al., 2009), while even a 0.3 ℃ decadal rise could be a severe impact on essential cash crops like cotton, mango, and sugarcane.

In Sri Lanka, half a degree temperature rise is predicted to reduce rice output by 6%, and increased dryness will adversely affect yields of critical products like tea, rubber, and Ministry of Environment and Natural Resources stated coconut in 2000. In the hot climate of Pakistan, cereal crops are already at the margin of stress. An increase of 2.5 ℃ in average temperature would translate into a much higher ambient temperature of the wheat planting and growing stages. Higher temperatures are more likely to result in the decline in yields, mainly due to the shortening of the crop life cycle especially the grain filling period. The National Communication highlighted that crops like wheat, cotton, mango, and sugarcane would be more sensitive to increase in temperatures compared to rice.

Dry lands and mountain regions more likely to be vulnerable than others areas (Gitay et al., 2001) and also the degradation of the ecosystem are significant in these regions (Hassan et al., 2005). Climate change more likely to cause additional inequities, as its impacts are unevenly distributed over space and time and disproportionately affect the poor (Tol, 2001; Stem, 2007).

2.4.2 Impacts of Precipitation Variability and Water Resources in South Asia

The current vulnerabilities to the climate are strongly correlated with climate variability, in particular, precipitation variability. These vulnerabilities of the climate change most significant in the semi-arid and arid low-income countries with large tracts of dry lands, where precipitation and streamflow concentrated over a few months, and where year-to-year variations are high (Lenton, 2004). In such regions, the major problem is lack of deep groundwater wells or reservoirs which leads to a high level of vulnerability to the climate variability, and to the climate changes that are likely to increase the variability of climate in future further.

Water resources are inextricably linked with the climate, so the prospect of the global change of climate has severe implications for water resources and regional development (Riebsame et al., 1995). Tendencies of increase in intense rainfall with the potential for massive rainfall events spread over few days are likely to impact water recharge rates and soil moisture conditions. A warmer climate, with its increased climate variability, will increase the risk of both floods and droughts (Wetherald & Manabe, 2002).

South Asia is endowed with great rivers, which are the lifelines of the regional economy. The ice mass covering the Himalayan-Hindu Kush mountain range is the source of the nine largest rivers of Asia, including the Ganges, Brahmaputra, and Indus. These rivers provide water to a more than half of the world's population. Many people in Asia are dependent on glacial melted water during the dry season. Accelerated glacial melt questions the very perennial nature of many of the Himalayan flowing rivers. This is likely to have enormous implications for those dependent on the resource affecting water availability for agricultural purposes (Kelkar & Bhadwal, 2007). In Nepal and Bhutan, melting glaciers are filling glacial lakes beyond their capacities contributing to Glacial Lake Outburst Floods (GLOFs) (UNEP, 2007). Of 2,323 glacial lakes in Nepal, 20 have been found to be potentially dangerous concerning GLOFs. The most significant such an event was encountered in 1985 when a glacial lake outburst flood caused a 10–15 m high surge of water and debris to flood down the Bhote Koshi and Dudh Koshi rivers for 90 km, destroying the Namche Small Hydro Project (Raut, 2006).

Agricultural irrigation demand in the arid and semi-arid regions of Asia is estimated to increase by at least 10% for an increase in temperature of 1.0 °C (Fischer et al., 2002; Liu, 2002). Efforts to offset declining surface water availability due to increasing precipitation variability will hamper by the fact that groundwater recharge will decrease considerably in some already water-stressed regions, where the vulnerability is often exacerbated by the rapid increase of world population and the water demand.

The most significant impact will continue to be felt by the poor, who have the most limited access to water resources. Rapid depletion of water resource is already a cause for concern in many countries in South Asia. About 2.5 billion people will be affected

by water stress and scarcity by the year 2050 in South Asia. In the dry lands, farmers and pastoralists also have to contend with other extreme natural resource challenges and constraints such as reduced soil fertility, pests, crop diseases, and a lack of access to inputs and improved seeds. These challenges are usually aggravated by periods of prolonged droughts and floods and are often particularly severe during El Nino events (Vogel, 2005; Stige et al., 2006). The impact of changes in the precipitation and evaporation could have profound effects in some lakes and reservoirs.

2.4.3 Impacts of Increased Frequency of Extreme Climate Events and Natural Disasters

Comparing with other regions, South Asia suffers an exceptionally high number of natural disasters. Between 1990 and 2008 period, more than 750 million people – 50% of the region's population were affected by a natural disaster, leaving almost 60,000 dead and resulting in about $45 billion in damages.

Several case studies showed that generally, the frequency of occurrence of more intense rainfall events in many parts of South Asia has increased, causing severe floods, landslides, debris and mudflows, while the number of rainy days and total annual precipitation has decreased (Mirza, 2002; Lal, 2003). Increasing frequency and intensity of severe droughts in many parts of South Asia are attributed mostly to a rise in temperature, particularly during the summer and usually drier months, and during ENSO events (Lal, 2003). An increase of the frequency of severe droughts and extreme rainfall events could be a result of a decline of tea yield, which would be the greatest in regions below 600 m (Wijeratne, 1996). With the tea industry of Sri Lanka being a significant source of foreign exchange and a significant source of income of labourers the impacts are likely to be grave. On an average basis from 1962 through 1988, Bangladesh lost about 0.5 million tonnes of rice annually as a result of floods that accounts for nearly 30% of the country's average annual food grain imports (Paul & Rashid, 1993).

Short-term natural extremes, such as cyclones and floods, inter-annual and decadal variations of climate, as well as large-scale circulation changes, such as the El Niño Southern Oscillation (ENSO), all have significant effects on crop yield, pasture and

forest production (Tubiello, 2005). Increased climate extremes may promote plant disease and pest outbreaks (Gan, 2004).

There is growing evidence that the frequency and extent of drought have increased as a result of global warming. A comprehensive analysis has shown that abrupt changes in rainfall are more likely to occur in the arid and semi-arid regions and that this susceptibility is possibly linked to strong positive feedbacks between vegetation and climate interactions (Narisma et al., 2007). The socio-economic impacts of droughts may arise from the interaction between natural conditions and human factors, such as changes in land use and land cover, water demand and use. Excessive water withdrawals can exacerbate the impact of drought. Differences in the frequencies of extreme events will have an impact on land degradation processes such as floods and mass movements, soil erosion by both water and wind, and on soil salinisation.

2.5 IPCC Climate Change Scenarios

In 1996, the IPCC started the development of a new set of emissions scenarios, effectively to update and replace the well-known IS92 scenarios. The approved new set of scenarios described in the IPCC Special Report on Emission Scenarios (SRES). Four different narrative storylines were developed to describe consistently the relationships between the forces driving emissions and their evolutions and to add context for the scenario quantifications. The resulting set of 40 number of scenarios (35 of which contain data on the full range of gases required to force climate models) covers a wide range of the main demographic, economic, and technological driving forces of the future greenhouse gas and sulphur emissions. Each scenario represents a specific quantification of one of the four storylines (IPCC, 2007). All the scenarios based on the same storyline constitute a scenario family. The SRES scenarios do not include additional climate initiatives, which means that no scenarios included that explicitly assume implementation of the United Nations Framework Convention on Climate Change or UNFCCC and the emissions targets of the Kyoto Protocol.

However, greenhouse gas emissions are directly affected by non-climate change policies designed for a wide range of other purposes. Furthermore, government policies can, to varying degrees, influence the greenhouse gas emission drivers, such

as demographic change, social and economic development, technological change, resource use, and pollution management. The storylines and resulting scenarios broadly reflect this influence.

The following are the RCP (Representation Concentration Pathways) Scenarios of the Special Report on AR5, IPCC (IPCC, 2014).

RCP 2.6 (low emission): - This RCP is developed by the PBL Netherlands Environmental Assessment Agency. Here radiative forcing reaches 3.1 W/m^2 before it returns to 2.6 W/m^2 by 2100. To achieve such forcing levels, ambitious greenhouse gas emissions reductions would be required over time.

RCP 4.5 (intermediate emission): - This scenario was developed by the Pacific Northwest National Laboratory in the US. Here radiative forcing is stabilised shortly after the year 2100, consistent with a future with relatively ambitious between reductions and comparable SRES scenario is B1.

RCP 8.5 (high emission): - This RCP is consistent with a future with no policy changes to reduce emissions. It is a development of the International Institute for Applied System Analysis in Austria and characterised by increasing greenhouse gas emissions that lead to high greenhouse gas concentrations over time, and comparable SRES scenario is A1F1.

2.6 Available Climate Models

The general circulation model (GCM) is a type of climate model which mathematically represents the general circulation of a planetary atmosphere or ocean (Li et al., 2017). The impact of climate change has been widely studied using GCMs, which are considered one of the most useful tools for exploring the process of physical changes in the earth's surface atmospheric system. Also, GCMs can provide very credible

information in regards to the events of historical, current and future change of climate (Gonzalez et al., 2010; Li et al., 2017).

There is considerable confidence, where that the climate models provide credible quantitative estimates of the future climate change, particularly at continental scales and an above. This confidence becomes from the foundation of the models within the accepted physical principles and its ability to reproduce the observed features of current and past changes of the climate circulations (Li et al., 2017). Confidence in the model estimates is higher for some climate variables than for others. Over several decades of development, models have been consistently provided with a robust and unambiguous picture if significant climate warming in response to increasing greenhouse effects.

The available general circulation models (GCMs) and their resolutions gave in the following attached Table A1-1 in Appendix 01 (Climate Models and Their Evaluations). These GCMs are limited to regional studies, however, because their spatial resolution is too coarse to be compatible with hydrological models necessary to simulate the sub-grid or basin scale hydrological processes. Therefore, for regional studies, Regional Climate Models (RCMs) are developed based on the GCMs. For the South Asian region, most reliable RCM is the model name as CORDEX CCCR South Asia climate analysis model. The process called downscaling is the bridge, connecting these two different scales of climate predictions coarser to finer scales (Hidalgo et al., 2013).

2.6.1 Reliability of the Climate Models

What does the accuracy of the climate model simulation of past or contemporary climate say about the accuracy of the output or predictions of climate change? There is some different observationally based metrics have been used to weight the reliability of contributing models when making probabilistic projections (Randall et al., 2007). For any parameter, it is essential to assess how far of good a test of model results for making projections of future change of the climate, which is not predictable directly since there are no observed periods with forcing modifications precisely analogous to those expected over the 21st century. Hence, the relationship between observable

metrics and the predicted quantity of interest such as the sensitivity of the climate model can be explored across model ensembles (Randall et al., 2007).

Randall et al. (2007) correlated a measure of the fidelity of the simulated surface temperature in the 20th century with simulated 21st-century temperature changes in a multi-model ensemble. From this, they have found that the models with smallest 20th-century error produced relatively large surface temperature increases in the 21st century. Also, Knutti et al. (2006), used a different and perturbed physics ensemble showed that the model with a strong relationship of the seasonal cycle in surface temperature tended to have more critical climate sensitivity. By the way, more complex metrics have also been developed based multiple observables in present-day climate, and have been shown to have the potential to narrow the uncertainty in climate sensitivity across a given model ensemble (Murphy et al., 2004). Hence the reliability of the climate model which is the sensitivity for the real situation of climate variations concerning the model value.

2.7 Methods of Downscaling

The GCMs are valuable predictive tools, but they cannot account for finer scale heterogeneity of the climate variability and changes due to their low resolution. Also, some landscape features cannot be predictive, such as mountains, water bodies, infrastructure, land cover characteristics and components of the climate system including convective clouds and coastal breezes, have scales that are much finer than 100-500 kilometres. Such heterogeneities are essential for decision makers who require the information on potential impacts on crop production, hydrology, species distribution, etc. at scales of 10-50 kilometres.

The derivation of the fine-scale climate information based on the assumptions that the local climate conditioned by interactions between large-scale atmospheric characteristics (circulation, temperature, moisture, etc.) and local features (water bodies, mountain ranges, land surface properties, etc.). It is possible to model these interactions and to establish relationships between the present day local climate and atmospheric conditions through the downscaling processes. It is essential to understand the downscaling method adds information to the coarse GCM output so that

information is more realistic at a finer scale, capturing sub-grid scale contrasts and in-homogeneities (Hidalgo et al., 2013).

The downscaling process can be performed on the spatial and temporal aspects of climate projections. Spatial downscaling is a method used to derive finer resolution spatial climate information from coarser resolution GCM output. Temporal downscaling refers to the derivation of finer scale temporal information from coarser scale temporal GCM output. There are two methods of downscaling the GCM data to the required resolution to the required locations. Those are Dynamical Downscaling and Statistical Downscaling.

Dynamical downscaling relies on the use of a regional climate model (RCM), similar to the GCM in its principles but with high resolution. RCMs take large-scale atmospheric information supplied by GCM output at the lateral boundaries and incorporate more complex topography, the land-sea contrast, surface heterogeneities and detailed descriptions of physical processes to generate realistic climate information at a spatial resolution of approximately 20-50 kilometres (Fujihara et al., 2008). Table 2.3 shows the summary of the comparison and aspects of the dynamical and statistical downscaling approaches.

Since the RCM is nested to a GCM, the overall quality of the dynamically downscaled RCM output is tied up to the accuracy of the large-scale forcing of the GCM and its biases. Despite recovering critical regional-scale features that are underestimated in coarse resolution GCMs, RCM outputs are still subject to systematic errors and therefore often require a bias correction as well as further downscaling to a higher resolution. Figure 2.1 shows the method of downscaling of projections general circulation models to an identified location.

The statistical downscaling involves the establishment of empirical relationships between historical and current large-scale atmospheric variable with local climate variables. Once a relationship is determined and validated, future atmospheric variables that GCMs project are used to predict future local climate variables. Statistical downscaling can produce site-specific climate projections, which RCMs

cannot provide since they are computationally limited to a 20–50 kilometres spatial resolution (Sachindra, 2014).

However, this approach relies on the critical assumption that the relationship between present large-scale circulation and local climate remains valid under different forcing conditions of possible future climates. It is unknown whether present-day statistical relationships between large-scale and regional scale variables will be upheld in the future climate system (Zhang et al., 2015).

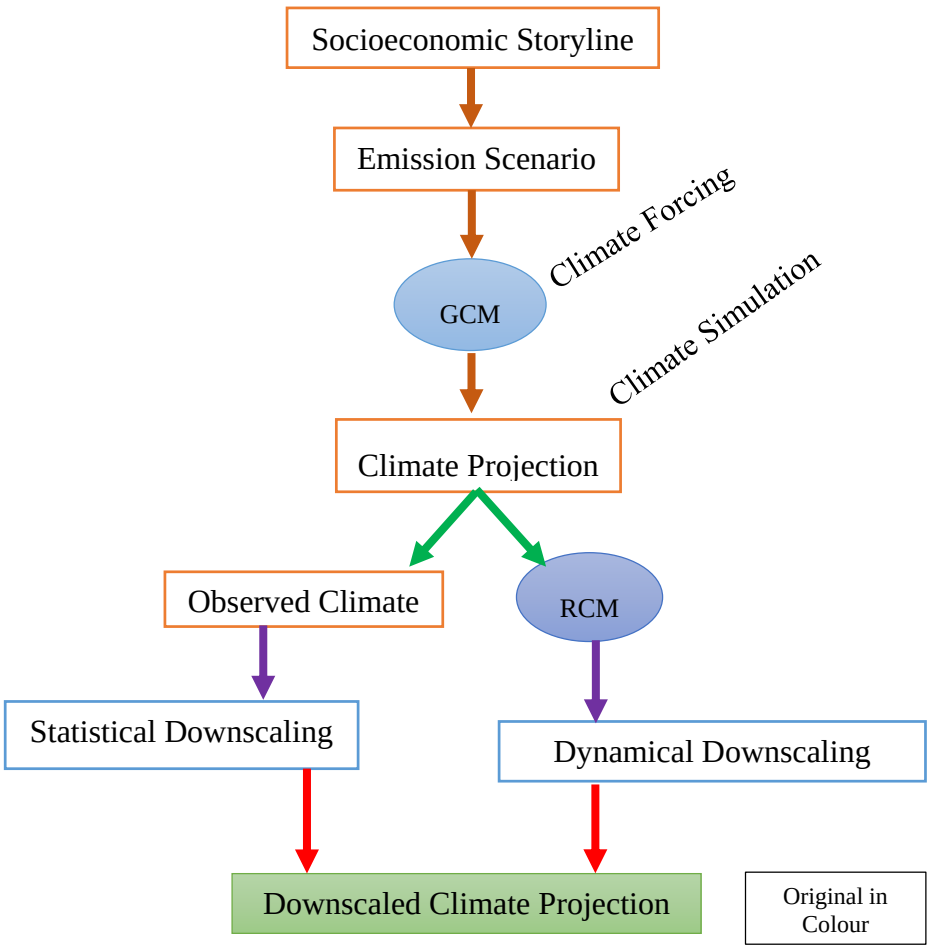

Figure 2-1 Illustration of the Components Involved in Developing Global and Regional Climate Projections

Table 2-3 Advantages, Disadvantages, Outputs, Requirements and Applications of Dynamical and Statistical Downscaling

	Dynamical Downscaling	**Statistical Downscaling**
Provides	• 20-50 km grid cell information • Information at sites with no observational data • Daily time series • Monthly time series • Scenarios for extreme events	• Any scale down to station level information • Daily time series • Monthly time series • Scenarios for extreme events • Scenarios for any consistently observed variables
Requires	• High computational resources and expertise • High volume of data inputs • Reliable GCM simulations	• Medium/low computational resources • Medium/low volume of data inputs • Reliable GCM simulations
Advantages	• Based on consistent, physical mechanism • Resolves atmospheric and surface processes occurring at sub-GCM grid scale • Not constrained by historical record so that novel scenarios can be simulated • Experiments involving and ensemble of RCMs are becoming available for uncertainty analysis	• Computationally inexpensive and efficient, which allows for many different emissions scenarios and GCM pairings • Methods range from simple to elaborate and are flexible enough to tailor for specific purposes • The same method can be applied across regions or the entire globe, which facilitates comparison across different case studies • Relies on the observed climate as a basis for driving future projections • Can provide point scale climatic variables for GCM scale output • Tools are freely available and easy to implement and interpret; some methods can capture extreme events
Disadvantages	• Computationally intensive • Due to computational demands, RCMs are typically driven by only one or two GCM/emission scenario simulations • Limited number of RCMs available and no more results for many parts of the globe • May require further downscaling and bias correction of RCM outputs • Results depend on RCM assumptions; different RCMs will give different results • Affected by bias of driving GCM	• High quality observed data may be unavailable for many areas or variables • Assumes that relationships between large and local-scale processes will remain the same in the future • The simplest methods may only provide projections at a monthly resolution

2.8 Verifications and Validations of Climate Data Sets (GCMs)

Method of verification and validation of the climate datasets is chosen depending upon the selected GCM and RCM. That is the most validated data sets should be selected to verify the RCM chosen for the study. Because of that, RCMs are generated using application of downscaling for the GCM datasets to the required resolution and the selected regions (Sachindra & Perera, 2016).

Although climate models should aid understanding the processes which control and perturb the climate system, the confidence placed in such models should always be questioned. It should be remembered that all the climate models are representing a simplification of the climate system, a system which indeed may ultimately prove to be too complicated to model (Zhang et al., 2015).

Given that many processes which are modelled occur over time scales so long that it is possible to test model results against real-world observations, it is also argued that climate modelling is, in some respects and philosophically suspect. Model performance is verified through many simulations of shorter time scale processes, but short-term performance may not necessarily reflect long range accuracy. Climate models must therefore be used with care, and their results may interpret with due caution. Margins of the uncertainty should be attached to the model projection. Uncertainty margins can be derived by the comparison of the effects of different model experiments or through sensitivity studies, in which fundamental assumptions are altered to determine the role they play in influencing the final climate response (Mishra & Lilhare, 2016).

Validation of the climate models provides the only objective test of model performance. As far as GCMs are concerned, validation exercise has revealed many deficiencies in their simulations of present-day conditions;

- Modelled stratospheric temperatures tend to be lower than equivalent instrumental observations,
- Modelled mid-latitude westerlies tend to be too strong; easterlies are too weak,
- The modelled sub-polar low-pressure system in winter tend to be too broad and displace east, and
- Day to day variability is lower than in the real world.

Finally, it has been observed that some models suffer from climate drift and the background climate shifts as the simulation proceeds, despite the absence of any climate forcing.

2.9 Methods of Statistical Downscaling

According to the techniques for application, statistical downscaling methods can be classified into three categories. Such as regression methods (Linear Methods), weather pattern based approaches and stochastic weather generators (Sachindra, 2014) or mixed methods of these three techniques. No matter whether the process is simple or complex, it is always based on the kind of a regression relationship. Regression methods depend on linear or non-linear relationships between predictands and predictors used for the analysis.

The method of the downscaling technique used for the large-scale data to small-scale data there should be a data checking to identify the errors of downscaling, a variation of the data for the selected scenarios and distribution of error within the downscaled datasets (Wilby & Wigley, 2000; Hashimi et al., 2009). Most probably data checking is doing for the statistically downscaled datasets. Because of that dynamic downscaling is doing by supercomputers and various computer programs, where there can find out the errors within the data sets automatically. But for the statistical downscaling process is different, because of whole work based on empirical relationships. Therefore, data checking is a must.

2.9.1 Linear Methods

Linear downscaling methods are applied when the relationship between the predictor and the variable being predicted, termed as the predictand, can be approximated by linear equations

2.9.1.1 Delta Method

One of the simplest ways to statistically downscale GCM projections is to use the data or change factor method. The change factor method is the ratio between the GCM simulation and the current climate and is used as a multiplicative factor to obtain future regional conditions. For example, to determine future regional temperature (T_f), the following steps are involved for it.

1. The ratio (∂) between future (T_F) and current (T_C) GCM-simulated temperature is computed.
2. This ratio is multiplied by the currently observed regional scale temperature (T_c)

$$T_f = \partial \times T_c; \; \partial = T_F/T_C \qquad \ldots\ldots\ldots\ldots\ldots\ldots\ldots (1)$$

The predictor is the currently observed temperature, and the GCM output is used to define the change factor by which to multiply the current observed temperature to obtain future values. More generally, the predictor and the predictand need to be the same variable. Since the ratio between GCM simulation of future and the current climate is used to obtain future regional climate, this method assumes that GCMs more reliably simulate relative change rather than absolute real values (Wilby et al., 2006).

2.9.1.2 Simple and Multiple Linear Regression

A simple linear regression is widely used method that establishes a direct relationship between one large-scale atmospheric predictor, e.g., GCM-simulated temperature, and one local predictand, e.g., local scale temperature, represented in the equation below as x and y, respectively. This relationship is generated by analysing observational local-scale and correlating it with GCM simulations, once a connection is established, it can be applied to derive projected local conditions using GCM simulations of the future climate as input as follows.

$$y = \alpha + \beta x \qquad \ldots\ldots\ldots\ldots\ldots\ldots\ldots (2)$$

When there are two or more predictor variables, e.g., large-scale rainfall and temperature, which influences the regional climate, a multiple regression equation can be built. To establish a multiple regression equation, a procedure known as forward selection method is most commonly used in which the predictor variable that explains the most variance is first identified (X_1). The rest of the variables are then searched, and the one that most reduces the remaining unexplained variance is selected (X_2). The procedure is repeated until no further improvement is obtained (Hay & Clark, 2003).

$$y = \beta_0 + \beta_1 X_1 + \beta_2 X_2 + \ldots + \beta_k X_k \qquad \ldots\ldots\ldots\ldots\ldots\ldots\ldots (3)$$

An assumption implicit in the linear regression method is that the variables are normally distributed, i.e. symmetrically distributed around the mean of a bell-shaped

curve and skewed towards higher or lower values. Large-scale atmospheric circulation data is usually normally distributed but some variables, such as daily precipitation, deviate vigorously form normality (Zorita & von Storch, 1999). Thus linear regression is not suitable for the analysis of daily rainfall and other highly skewed distributions (Hay & Clark, 2003).

2.9.2 Weather Classification

Methods described in this category can be applied to variables that have normal as well non-normal distributions. In weather classification schemes, the local variable is predicted based on a limited number of large scale atmospheric states. The states can be identifiable synoptic weather patterns or hidden, complex systems. The future atmospheric state, simulated by a GCM, is matched with its most similar observed atmospheric state. To that historic state there corresponds a value, or a class of values, of that local variable, which are then replicated under the future atmospheric state.

This class of method is particularly well suited for downscaling non-normal distributions, such as daily rainfall or frequencies of occurrence; however, a large amount of observational daily data, e.g. 30-years of daily data for the region of interest, is required in order to evaluate all the possible weather conditions. Also, daily data for both historical and future large scale atmospheric states need to be analysed, which is computationally demanding.

2.9.2.1 Analog Method

The analogue method is a relatively simple statistical weather classification method. The large-scale atmospheric circulation simulated by a GCM is compared to historical observations, and the most similar is chosen as its analogue. The simultaneously observed local weather is then associated with the projected large-scale pattern. To find an appropriate analogue, a sufficiently long record of observations is required (Zorita & von Storch, 1999). Assessment of the performance of the analogue method for predicting normally and non-normally distributed variables determined that the analogue approach is most appropriate for non-normal distributions, such as daily rainfall. However, this method is incapable of predicting new values that are outside the range of the historical records. Thus new record-breaking precipitation values,

which are likely to become more frequent in the future, cannot be forecasted (Benestad, 2010).

2.9.2.2 Cluster Analysis

Cluster analysis is a data reduction method that aggregates values within a dataset into a limited number of groups or classes (Schoof & Pryor, 2001). By searching for natural groupings or types, complex relationships can be identified, and additional information about large scale to local scale relationships can be understood (Xiaofeng & Richman, 1995).

Cluster analysis can be applied to any data, binary, discrete and continuous (Xiaofeng & Richman, 1995). Through cluster analysis, daily weather can be grouped into synoptic types, weather regimes can be identified from upper airflow patterns, and members of ensemble forecasts can also be consolidated. As in the analogue method, to estimate future values of local predictand, the output from a GCM is compared to the large-scale observations over the historical period. Once a large-scale simulation is aggregated to a cluster, a random observation from the batch of data associated with this cluster is chosen as the local scale prediction (Benestad, 2010).

2.9.2.3 Artificial Neural Network (ANN)

An artificial neural network (ANN) can be described as an algorithm that transforms input data into an output data using stepwise nonlinear functions (Benestad et al., 2008). An ANN can represent any arbitrary nonlinear function given sufficient training and can be generalised to a relationship from a small subset of data. The topology of the network involves many interconnected nodes arranged into three layers: input, hidden and output. The input and output layers represent large scale and local climate information, respectively. The ANN must first be calibrated based on historical data. Various weights and biases are applied to each neuron and adjusted during the training period to match the network and actual outputs (Wilby et al., 2002). Once the system is appropriately trained, high-resolution local climate data can be obtained from large-scale circulation information.

2.9.3 Weather Generators

A weather generator is a statistical model used to generate sequences of daily variables, e.g. daily precipitation, maximum and minimum temperature, humidity etc., from monthly GCM output. This method is used for impact models that require local spatial data at a daily timescale. Weather generators produce multiple daily weather series, which is natural and logically consistent because any number of small-scale weather sequences may associate with a given set of larger scale values. In other words, for a particular monthly rainfall projection in the future, the weather generator will produce numerous possible daily rainfall sequences that have the same statistical characteristics that occurred in the past with the same monthly average (Wilby & Dessai, 2010). Also, weather generators are data intensive, require several years of daily data, and they are sensitive to the missing or erroneous data in the calibration set (Wilby & Dessai, 2010). Similarly, when multiple variables are predicted, it is often crucial to account for the coherency between them.

2.9.4 Mixed Methods and Tools

Frequently, multiple methods are used subsequently for statistical downscaling of GCM data. As an example, if the goal is to obtain localised daily precipitation, spatial downscaling may first be applied followed by a weather generator. The use of the following method in SDSM is used to downscale large-scale GCM data for local scale data for this research.

2.9.4.1 Statistical Downscaling Model (SDSM)

To date, many statistical models have been developed and are available. SDSM is widely used throughout the world (Huang & Zhang, 2011) to downscale the most critical climate variables such as temperature, precipitation and evaporation etc. for assessing hydrologic responses in climate change scenarios. This SDSM model is developed through a combination of multiple linear regression and the stochastic weather generator (Wilby et al., 2002; Diaz-Nieto & Wilby, 2005; Gebremeskel & Li, 2005; Gangon-Lebrun & Agrawala, 2006).

The SDSM provides climate information at specific locations for which there is daily data adequate to calibrate the model, as well as archived GCM output (Wilby et al.,

2002). The key inputs include quality observed daily data for both local scale and large-scale climate variables as well as daily GCM outputs for large-scale variables for future climate (UNFCCC, 2013). Also, the outputs can be applied over a range of climate impact sectors and include site-specific daily scenarios for maximum and minimum temperatures, precipitation and humidity as well. A variety of statistical parameters such as variance, frequencies of extremes, and spell lengths also produced by the model (UNFCCC, 2013). Based on the review of the literature and as far as authors are aware, it was found that not a single study has been reported that uses SDSM in watersheds in Sri Lanka, or even throughout South Asia. The SDSM model has been proven to be skilful and is widely used for downscaling of precipitation and temperature elsewhere in the world (Liu et al., 2011).

In SDSM, some suitable predictors from the atmospheric predictors are selected through a multiple linear regression model, utilising the combination of the correlation matrix, partial correlation, P value, histograms and scatter plots. Multiple co-linearity must be considered during the selection of predictors. There are two kinds of optimisation methods. Such as;

1. Ordinary least square (OLS)
2. Dual simplex (DS)

The OLS produces comparable results with DS and is also faster than DS (Huang et al., 2010). There is three kind of submodels- monthly, seasonal and annual – that comprise the statistical/empirical relationship between the regional-scale variables (temperature and precipitation), and large-scale atmospheric variables. Also, yearly sub-models drive the same kind of regression parameters for 12 months, and the monthly sub-model represents 12 regression equations, giving different calibrated parameters for each of the 12 months. There are also two kinds of sub-models, conditional and unconditional; any of them can be used according to the local scale variables. The unconditional sub-model is used for independent or unconditional variables such as temperature (Mahmood & Babel, 2012).

The conditional sub-model is used for variables such as precipitation and evaporation (Wilby et al., 2002; Chu & Steinman, 2009). Most of the time, precipitation data does

not distribute normally. The SDSM can transform the data to make it regular before using the data in regression equations (Sultana et al., 2009). Two kinds of daily time series, namely daily historical site data and NCEP daily predictors are used to develop SDSM, the output of this model are daily time series, which can be produced by forcing the NCEP predictors (Huang et al., 2010). The mathematical details (Wilby & Wigley, 2000) are presented in Chapter 04.

2.9.4.2 Selection of Predictors

To date, the primary tools to predict the variability and changes in climate variables on global and continental levels, are Global Climate Models that are also called General Circulation Models (GCMs). These advanced and numerical-based coupled models interpret global systems such as sea-ice, the oceans, and atmosphere (Fowler et al., 2007). Although these models are beneficial in the investigation and prediction regarding future changes in climate, the outputs of these model are based on a large grid scale (Gebremeskel & Li, 2005). Because of their coarse resolution, the outputs cannot be used successfully to investigate the environmental and hydrological impacts of change of climate on a regional scale (Wilby & Wigley, 2000).

The 26 predictors of NCEP/NCAR and CanESM2 (RCP scenarios) obtained from a Canadian website: "http://ccds-dscc.ec.gc.ca/index.php?page=dst-sdi", for the periods of 1961-2005 and 2006-2100, respectively. The RCP 2.6, RCP 4.5 and RCP 8.5 are respectively the IPCC emission scenarios of CanESM2. These predictors are designed for the SDSM model. The NCEP predictors (2.5° x 2.5°) are first interpolated to CanESM2 grid resolution (2.8125° x 2.8125°) to eliminate spatial differences. Subsequently, the NCEP/NCAR and CanESM2 predictors are normalised by utilising long-term mean and standard deviations of 1961-1990.

2.9.4.3 Bias Correction

The bias correction approach is used to eliminate the biases from the daily time series of downscaled data (Salzmann et al., 2007). In this method, the biases are obtained by subtracting (in the case of temperature) the long-term monthly mean (30-years) of observed data, from the mean monthly simulated control data (downscaled data by the SDSM for the period of 2001-2005), and dividing (in the case of precipitation) the

long-term observed monthly mean data with simulated control data. The biases are then adjusted with the future downscaled daily time series according to their respective months. Following two equations (4) and (5) are used to the de-biased daily temperature and precipitation data as follows.

$$T_{deb} = T_{SCEN} - (\overline{T_{CONT}} - \overline{T_{obs}}) \quad \text{..... (4)}$$

$$P_{deb} = P_{SCEN} \times (\overline{P_{obs}} / \overline{P_{CONT}}) \quad \text{..... (5)}$$

where T_{deb} and P_{deb} are the de-biased (corrected) daily time series of temperature and precipitation respectively for future periods. SCEN represents the scenario data downscaled by SDSM for future periods (eg. 2006-2100), and CONT represents downscaled data by SDSM for the present period (e.g., 1970-2000). T_{SCEN} and P_{SCEN} are the daily time series of temperature and precipitation generated by the SDSM for future periods respectively. T_{CONT} and P_{CONT} are the long-term mean monthly values for temperature and precipitation respectively for the control period simulated by the SDSM. T_{obs} and P_{obs} represent the long-term mean monthly observed values for temperature and precipitation. The bar on T and P shows the long-term average. The frequency and intensity of precipitation are the two main factors affecting precipitation variability (Eisner et al., 2013). The application of this method of study is to correct the precipitation amount and not the frequency, and also to remove any systematic errors belonging to SDSM during downscaling. Also it is assumed that the frequency is accurately simulated by SDSM especially for precipitation.

2.10 Use of Hydrological Models for Kelani River Basin

The use of hydrological models is very important for a wide range of applications, which are including the water resources planning, development and management of watersheds, flood prediction analysis and also for the design and couple's system model analysis. Also, the use of mathematical models for hydrologic computations in water resources planning and forecasting has become increasingly popular in Sri Lanka for few years.

Therefore, to evaluate the streamflow through river basin, there should be a mathematical model to calculate how much of stream flow generated by the precipitation for the river basin. Then the computed value can be compared with one

of the uppermost streamflow gauging stations to diminish the accuracy of the selected mathematical model. Therefore, for the Kelani river basin model output can be compared with the stream flow values recorded at Kithulgala gauging station where considering their catchment and with mathematical model selected.

Therefore, the suggested mathematical model to evaluate streamflow is the HEC-HMS model. This kind of model is done for the Kelani River basin previously. This is useful to assess the future stream flow by the forecasted data of precipitation and evaporation obtained by the climatic analysis (Chu & Steinman, 2009).

2.10.1 Objectives of Using of Hydrological Models

Hydrological applications of mathematical models have a variety of the objectives which depend on the problem that needs to be identified and should be investigated. Hence the objectives of the hydrological modelling and model applications are extrapolation of point measurements in both spatial and temporal, improving the fundamental understanding of existing hydrological systems and assessing the impact of changes due to climate and land use on water resources, developing new models or improving existing models for management decisions on current and future catchment hydrology such as irrigation water management, flood forecasting and management, streamflow restoration, water quality evaluations and wetland restorations etc.

2.10.2 Hydrological Modelling in Sri Lanka

The hydrological models used in hydrologic studies in Sri Lanka in different categories. In this regard (Dharmasena, 1999) has reviewed five types of hydrological models and one was hydrodynamic model with use of case study applications to selected river basins in Sri Lanka and results of the case study stated that while using hydrological models for representing head basins, and hydrodynamic models are interfaced for represent the lower part of the selected river basins. Also, the application of the hydrological model is indicated that a wide variety of models can be successfully applied to the river basins of Sri Lanka, instead of particular models. Furthermore, the author was suggested that the conceptual models would provide superior results especially five rivers subject to prolonged droughts.

Using of HEC-HMS lumped conceptual model, De Silva et al. (2014) developed an event based continuous model for the upper catchment of Kelani River by using HEC-HMS. The results of the case study of De Silva et al. (2014) showed that the suitability of the HEC-HMS software in the modelling of the Kelani river basin. In this study Kelani River basin divided into two sub-basins and within that two sub-basins again divided the model into sub-watersheds. This model was calibrated by using historical flood events of 2005 and validated for the flood happened in 2008 and 2010. Also, the results of HEC-HMS output showed that there was no impact of the number of sub-basins considered in the modelling of the river basin for the prediction of flood events. But the associated problem is study was mainly focused on high flows and model performance only in the high flows were discussed whereas the representativeness of the model low and medium flow did not analyse.

Wijesekera & Musiake (1990) carried out a streamflow modelling for two selected catchments in Sri Lanka namely Mahaweli River basin at Peradeniya and Kalu Ganga river basin at Putupaula. This was a simple tank model with four tanks and the tanks were used to simulate the streamflow and the power search technique considering the spatial variability of rainfall was incorporated to optimise the model parameters. Also in this study, rain gauge weights considered as parameters were optimised. Data from 1969-1973 were used to calibrate the model and data from 1976-1980 were used for the verification of the model. Results of the Mahaweli basin showed that the average annual water balance values provided better results than the yearly values which implied that the evaporation values were not critical in the model outputs. The model was used for both basins, and the inclusion of non-uniformity of rainfall improved the model predictions very marginally. The authors concluded that the optimised parameters were acceptable with the rainfall distribution and the location of the rainfall stations.

2.10.3 Objective Function

The objective function is the function used to match the model results with the reality. The objective function depends on the modelling objectives such as modelling for flood control, water resources planning and management etc. The objective function used has differed from researcher to researcher even with the same purpose.

This objective function selection measures the degree of matching the relevant component of computed and observed hydrographs. The calibration process can find the optimal parameters which minimise the objective function. Further, the calibration process estimates some model parameters, which cannot be evaluated by observation or measurement or have no direct physical meaning. Calibration may be either manual or automated where manual calibration relies on user's knowledge of basin physical properties and expertise in hydrologic modelling (Chunderlik & Simonovic, 2004).

Green & Stephenson, (2009) discussed 21 objective functions and stated that the method of assigning an objective function for a model depends on the objective of modelling. As an example, if the modeller is interested only in peak flows, there is a little point in investigating low flows or even the hydrograph shape. Also, if routing effects are concerned, it is said that the rising and falling limbs of the hydrographs are important. Authors recommended that to use a percent error in peak, percent error in volume and sum of squares/ sum of absolute residuals objective functions in single event modelling. When more general dimensionless ordinate independent measures of fit are required to assess the performance of a model over many different events and authors suggested using the coefficient of efficiency or Nash Sutcliff objective function as it is a reasonable choice. The objective functions recommended by the Green & Stephenson (2009) are listed below.

i. Percent Error in Volume (PEV)

$$PEV = \frac{Vo-Vc}{Vo}\ x\ 100 \qquad \text{..... (6)}$$

ii. Percent Error in Peak (PEP)

$$PEP = \frac{Qop-Qcp}{Qop}\ x\ 100 \qquad \text{..... (7)}$$

iii. Sum of Squared Residuals (SSR)

$$SSR = \sum(Qobs - Qcal)^2 \qquad \text{..... (8)}$$

iv. Sum of Absolute Residuals (SAR)

$$SAR = \sum\ ABS(Qobs - Qcal) \qquad \text{..... (9)}$$

v. Coefficient Efficiency of CE or Nash-Sutcliff

$$CE = 1 - \frac{\Sigma(Qobs-Qcal)^2}{\Sigma(Qobs-Qcal)^2} \quad \ldots\ldots\ldots\ldots\ldots\ldots\ldots (10)$$

World Meteorological Organization (WMO) in 1975 in its publication compares conceptual models used for operational hydrological forecasting and recommends several objective functions. One of them are Ratio of Absolute Error to Mean Error (RAME) which is given by following equation.

$$RAEM = \frac{\Sigma\,|Qobs-Qcal|}{n.Qobs} \quad \ldots\ldots\ldots\ldots\ldots\ldots\ldots (11)$$

In this objective functions too, Q_{obs} is the observed streamflow, and Q_{cal} is the calculated streamflow and n is the number of observations used for comparisons.

This objective function that is RAEM compares the errors with respect to each observed flow. Therefore, this gives better representation when contrasting data are present in the observed data set. When there are significant and small peaks of the modelled flow, the error values may not enable for the easy comparison and mean of observed flow does not reflect the real mean of the series of flow.

Further, Wijesekera & Abeynayake (2003) defined that Mean Ratio of Absolute Error (MRAE) is the difference between the calculated and observed flow with respect to that particular observation. This can be defined as

$$MRAE = \frac{1}{n}\Sigma\frac{|Qobs-Qcal|}{Qobs} \quad \ldots\ldots\ldots\ldots\ldots\ldots\ldots (12)$$

This MRAE function compares the errors with respect to each observed flow for modelled flow. Therefore, this gives a better representation when contrasting data are present in the observed data set of flow.

2.10.4 HEC-HMS for Event and Continuous Based Hydrological Modelling

Hydrologic models are simplified conceptual representations of a part of the hydrologic cycle. Hydrological models are primarily used for hydrologic prediction and for understanding the hydrologic processes. Watershed hydrological modelling and associated calibration and validation processes require a broad set of spatial and temporal data. In practice, the availability and quality of these data are often an issue

to cope with the model. Sometimes, the modellers have to compromise on the overall modelling quality because of insufficient high-resolution data for developing, calibrating and validating models (Patel et al., 2014). Event process models are designed to simulate individual events, and it emphasises only on infiltration and surface runoff. It gives peak discharge and volume only. Continuous-process models are developed for long-term simulations, and it focuses on all hydrologic processes. It simulates drought and water balance.

Paper presented by De Silva et al. (2014) describes a modelling of the event and continuous flow hydrographs with the HEC-HMS with a case study in the Kelani River Basin Sri Lanka. In this study, an extremely high rainfall event in November 2005 was used for calibration of model parameters and extremely high rainfall events in April-May 2008, May-June 2008, and May 2010 were used for validation of the event model. Two consecutive extreme flood events have occurred during April to June 2008 were selected for the model calibration under continuous simulations. The time series data from January 2005 to December 2007 and January 2009 to December 2010 were used for the model validation. The calibrated. Direct runoff and baseflow parameters were then used in the continuous hydrologic model. In this study, for event modelling Recession baseflow as baseflow parameters, Green and Ampt method as loss parameters and Clark Unit hydrograph as runoff transform parameters were selected. Also for continuous modelling Recession baseflow as baseflow parameters, Soil Moisture accounting as loss parameters and Clark Unit hydrograph as runoff transform parameters were chosen.

The use of the HEC-HMS model for an experimental watershed under even based simulation is given in the paper presented by Reshma et al. (2010). In this case study, the HEC-HMS model used to simulate the runoff process in Walnut Gulch watershed located in Arizona, USA. Estimation of the proper runoff for a given rainfall event is a difficult task due to various influencing factors. In this model has been applied for seven nos. of rainfall events of sub watershed of Walnut Gulch watershed. The model has been calibrated for four rainfall events and validated for three rainfall events.

The case study done for Mona Lake watershed by Xuefeng et al. (2009) describes the use of HEC-HMS hydrologic model for event base and continuous base hydrologic modelling. In this study joint even and continuous hydrologic modelling with the HEC-

HMS is discussed, and an application to the Mona Lake watershed in Michigan is presented. Primarily, four rainfall events were selected for calibrating to verifying the event model and identifying the model parameters. The calibrated settings are then used in the continuous hydrologic model. The Soil Conservation Service curve number and soil moisture accounting methods in HEC-HMS were used for simulating surface runoff in the event, and continuous models, respectively, and the relationship between the two rainfall-runoff models were analysed. The simulations provided hydrologic details about the quantity, variability, and sources of runoff in the watershed. The model output suggests that the fine-scale (5 min time step) event hydrologic modelling, supported by intensive field data, is useful for improving the coarse-scale (hourly time step) continuous modelling by providing more accurate and well-calibrated parameters.

2.10.5 Sensitivity Analysis

Sensitivity analysis is a method to determine which parameters of the model have the most significant impact on the model results. It ranks models parameters based on their contribution to overall error in model predictions. Sensitivity analysis can be local and global. In the local sensitivity analysis, the effect of each input parameter is determined separately by keeping other model parameters constant. The result is a set of sensitivity functions, one for each model parameter. In the global sensitivity analysis, all model inputs are allowed to vary over their ranges at the same time. Global sensitivity is based on the use of probabilistic characteristics of the random input variables. Three types of coefficients can be used in local and global sensitivity analysis. The Absolute Sensitivity coefficient, SA is defined as;

$$SA = \frac{\partial O}{\partial P} \qquad \text{..... (13)}$$

where O is the model output and P represents a particular input parameter. The absolute sensitivity coefficients are affected by units of output and input and therefore cannot be used for the comparison of parametric sensitivities. The Relative Sensitivity, SR, is defined as;

$$SA = \frac{\partial O}{\partial P} . \frac{P}{O} \qquad \text{..... (14)}$$

The relative sensitivity coefficients are dimensionless and thus can be compared across parameters. Finally, the deviation sensitivity, SD is quantified as the change in the output ΔO;

$$SD = \Delta O = \frac{\partial O}{\partial P}.\Delta P \qquad \text{..... (15)}$$

The deviation sensitivity has the same units as the variables *O*.

3 MATERIALS AND METHODS

3.1 Methodology Flow Chart

The methodology adopted in the present study is illustrated using Figure 3-1 below.

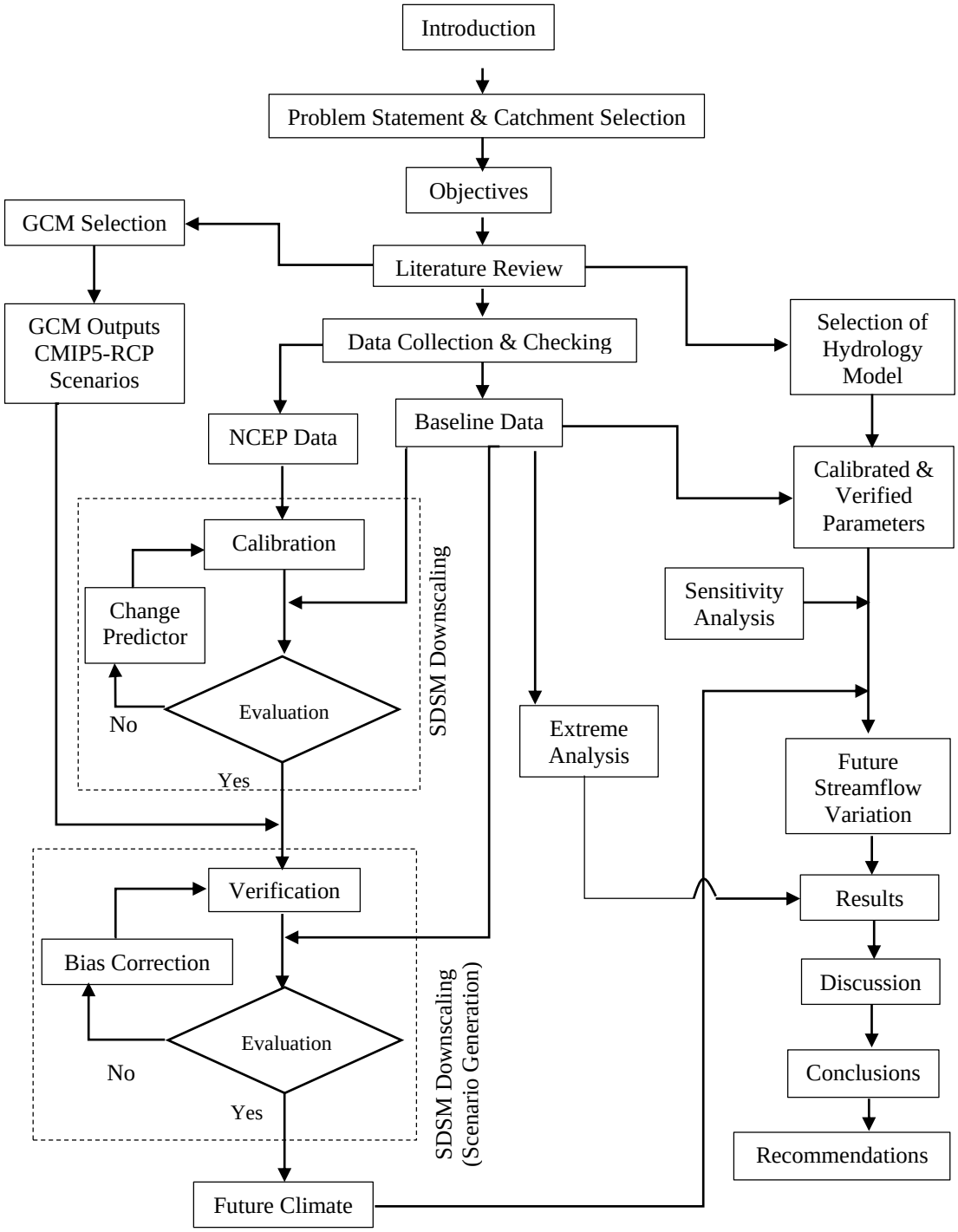

Figure 3-1 Methodology Flow Chart

3.1.1 Methodology

Figure 3.1, represents the methodology followed for this case study. After identifying the main objective and specific objectives, the literature survey was carried out to determine the commonly used GCM models and their applicability and variety of their uses for climate studies within the region. After reviewing various model applications applied to different river basins, with considering the model flexibility and availability the HEC-HMS model was selected for the Kelani River basin. The lower catchment of the Kelani river basin was chosen for evaluation of the model performance. For the downscaling of the GCM data to the required resolution, the statistical downscaling model (SDSM) is used as it is the flexible software freely available and which is having a graphical user interface. Also, this SDSM model is selected by after reviewing research publications done for different regions and its applicability and reliability of the outputs. The graphical representations of the accuracy of the downscaled GCM data (precipitation, temperature) for RCP scenarios implemented in the Chapter 5.0 Analysis and Results. The model performance evaluated of the hydrologic model by the minimum value of Mean Ratio of Absolute Error (MRAE) as the objective function. Besides, percent error in volume (also referred as mass balance error) and Nash-Sutcliff values also checked for the observations.

3.1.2 Screening of Predictors in SDSM

The screening of predictors is central to all statistical downscaling (Wilby et al., 2002; Huang et al., 2010;). To select the first and most suitable large-scale variable is relatively easy, but the selection of the second, third, fourth and so on is much subjective. Therefore, a more quantitative procedure was applied for screening large-scale variables for each local-scale variable at each of the climate station (Mahmood & Babel, 2012). The following steps described the entire procedure along with the example how predictors were selected for the modelling of precipitation at the climate stations chosen for the study. Prediction of the modelled rainfall of Colombo climate station described in below.

1. First, the correlation matrix between 26 NCEP predictors and the predictand was made, and then the predictors of high correlation coefficient maximum of 12 are selected out of the 26 and arranged in descending order. The first ranked predictor, having the highest correlation coefficient among all predictors, is selected and defined as a super predictor. The correlation between them was determined as the super correlation coefficients.
2. Following above, the absolute correlation coefficient between the predictor and the predictand, the absolute correlation coefficient between individual predictors, absolute partial correlation and P value were obtained by regressing the remaining highly correlated predictors individually in the presence of super predictor.
3. Then the predictors which have a P value greater than α are removed to render the results statistically significant, and the predictors which are highly correlated are taken out to remove any multi-co-linearity is there. The correlation coefficient up to 0.7 between the two predictors is acceptable.
4. Then the Percentage Reduction in an absolute Partial Correlation (PRP) value concerning absolute partial correlation for each predictor using the following equation is calculated.

$$PRP = \frac{p.r - R1}{R1} \qquad \ldots\ldots\ldots\ldots\ldots\ldots\ldots\ldots (13)$$

   Where PRP is the percentage reduction in partial correlation with respect to the correlation coefficient, P.r is the partial correlation coefficient and R_1 is the correlation coefficient between the predictor and the predictand.
5. The predictor which has the minimum value of PRP in partial correlation, selected as the second most suitable predictor. Then as a result of this predictor has almost no, or a very insignificant multi-co-linearity with the super predictor.
6. The third, fourth and the following predictors can be obtained according to repeating the steps 2 to 5. In the second repetition, there will be two super predictors. It is then seen that the most one to three predictors are enough to explain the predictand during the calibration and without multi-co-linearity (Mahmood & Babel, 2012).

3.1.3 Calibration and Validation of SDSM

Based on the available observed daily data, 1970~2000 data was used for the calibration of the T_{max}, T_{min} and precipitation. In this study, SDSM iwa developed with selected NCEP predictors using monthly sub-model and seasonal sub-model. The conditional sub-model was used for T_{max} and T_{min} without any transformation and unconditional sub-model for precipitation with fourth root transformation. The optimisation of the best fit iwa done according to the ordinary least square method. The explained variance and standard error were used to evaluate the performance of the SDSM (Huang et al., 2010; Mahmood & Babel, 2012).

The outputs of the SDSM were compared with the observed data by calculating the coefficient of determination (R^2), root mean square error (RMSE), mean (μ), standard deviation (σ), relative error in mean (RE_μ) and relative error in standard deviation (RE_σ) for temperature and precipitation for the periods of calibration and validation. The R^2 and RMSE values show the accuracy of the model in predicting data. Also, μ and RE_μ are used to check how well the model predicts the mean values, and σ and RE_σ are used to observe the variability of data predicted by the model.

In this case study, the method of bias correction (BC) discussed in detail in sub-chapter 2.9.4.3, was applied to the downscaled data obtained from the two SDSMs using CanESM2 predictors, to achieve a more realistic and unbiased data of future climate. Before applying it to the future downscaled data, bias-corrected results were first validated from 1970 to 2000. For this purpose, the mean monthly biases had to be adjusted for the validation period of 2001 to 2005 of 5-year duration by utilising downscaled data of SDSM and observed data at each site. The corrected downscaled data of T_{max}, T_{min} and precipitation werecompared with the observed data by calculating the above mentioned statistical indicators.

After successful, bias-correction, the observed and modelled mean was applied to the future downscaled data of T_{max}, T_{min} and precipitation. For this, more recent data set of 1970 to 2000 was used to calculate the 30-year mean monthly biases, and then these biases were adjusted to the downscaled daily time series according to their respective months. The reason for using a recent period was to justify the variability of the

observed data with respect to the model data during validation. The period from 1970-2000 was selected as the baseline period in this case study as this period has been utilised worldwide in most climate studies while some others have used the period from 1961-1990 (Huang & Zhang, 2011).

A 30-year period was considered long enough to define the local climate because it is likely to have dry, wet, cold and warm periods (Mahmood & Babel, 2012). The IPCC also recommends the length of the period of study (30 years) for use as a baseline period for climate change study (Gebremeskel & Li, 2005).

3.1.4 Sensitivity Analysis of Hydrology Model

A local sensitivity analysis was adopted to evaluate the parameters of the continuous model. The final set of the parameters of the calibrated model was considered as a baseline/nominal parameter set. The model was repeatedly run with the baseline value for each parameter multiplied, in turn, by 0.8 and 1.2, while keeping all other parameters constant at their nominal starting values. The hydrographs resulting from the scenarios of adjusted model parameters were then compared with the baseline model hydrograph. In this study using calibrated and verified HEC-HMS model for Kelani River basin by De Silva et al. (2014). The sensitivity analysis was used to justify the model performance with respect to the baseflow model.

3.2 Study Area

The study regions comprise a major river basin in the west of Sri Lanka namely Kelani River basin. The hydrological regimes of the river differ because of their basin feature significant geographical and climatic diversities within its latitudinal and longitudinal extent. As a common ground, the hydrology of this river basin depends on the moisture input from the monsoon systems. Kelani River is in the wet zone of the country.

Measured daily mean temperature, maximum temperature, minimum temperature and precipitation from the Department of Meteorology of Sri Lanka were used for the selected weather stations under the project area. The dataset period is from 1970 to 2015.

Because of that, the mean temperature precipitation and pan evaporation are the critical climate parameters. The migration of rain belts, as well as the change of tempo-spatial

distribution and intensity of rainfall has a direct influence on the total amount of water resources, while temperature and pan evaporation can indirectly affect the hydrologic trend due to the interaction with land surface processes on a longer timescale.

The data set period is 1970 to 2015 and collected from the Department of Irrigation and Department of Meteorology of Sri Lanka. The detail description of the meteorological and hydrological data selected for the Kelani River Basin tabulated in Table 3.1 and Table 3.2.

Table 3-1 Coordinates of River Gauging Stations

River Gauging Station	**Coordinates**	
	Latitudes	**Longitudes**
Hanwella	6º 54′ 35″ N	81º 04′ 54″ E

Table 3-2 Coordinates of Meteorological Stations (RF, Temp., and Evaporation.)

Rainfall Gauging Station	**Coordinates**	
	Latitudes	**Longitudes**
Annefield (CEB)	6º 52′ 12″ N	80º 37′ 48″ E
Clombo Meteo	6º 54′ 00″ N	79º 51′ 36″ E
Hanwella Group	6º 52′ 48″ N	80º 07′ 12″ E
Laxapana	6º 52′ 48″ N	80º 30′ 36″ E
Nuwara Eliya Met Station (CEB)	6º 58′ 12″ N	80º 46′ 12″ E
Pasyala	7º 09′ 00″ N	80º 07′ 48″ E
Dunedin Chesterford	7º 04′ 48″ N	80º 13′ 12″ E
Yatiyanthota (Wewaltalawa	7º 03′ 00″ N	80º 22′ 48″ E

The map in Figure 3.2 presents details about the gauging station distribution in Kelani River basin of the present study.

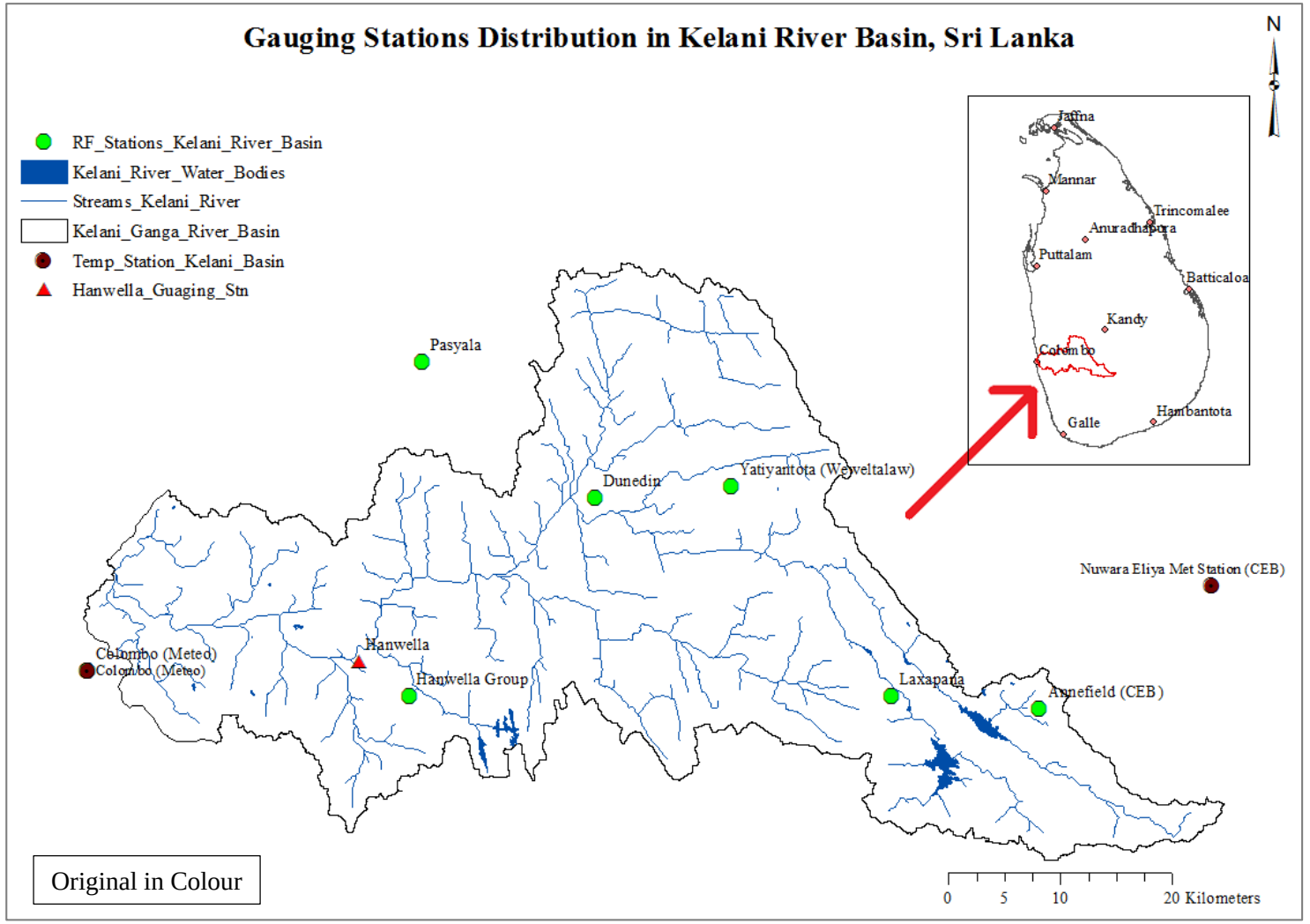

Figure 3-2 Gauging Stations of Kelani River Basin

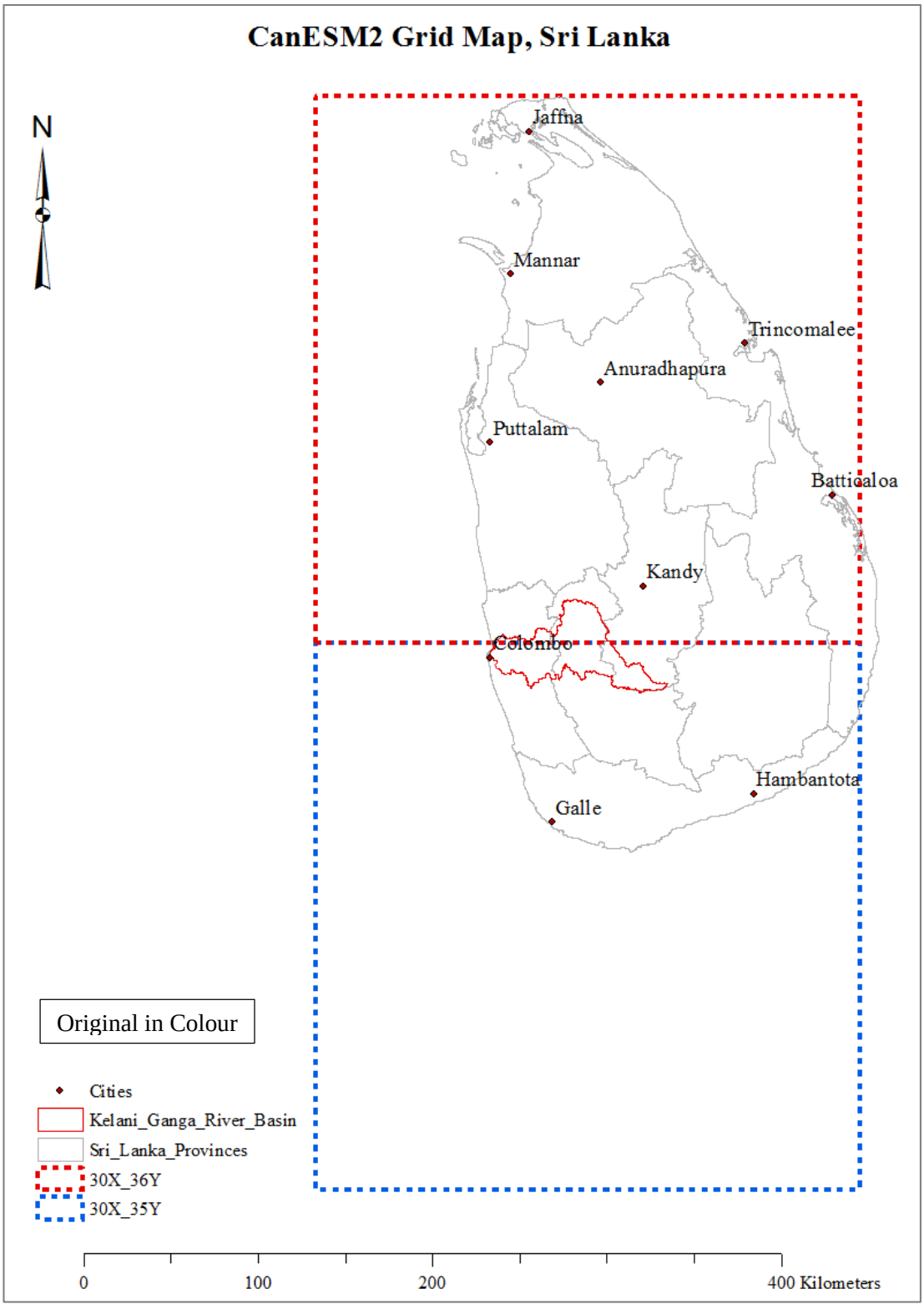

Figure 3-3 CanESM2 (Canadian Earth System Model Version 2) – GCM Grid Map of Sri Lanka

3.3 Data

3.3.1 Data Sources and Resolution

The main types of data used in the present study are Temperature, Evaporation, Rainfall and Streamflow. Data sources and data resolution are tabulated in Table 3.3. Daily minimum and maximum temperatures were used to calculate the daily average temperature.

Table 3-3 Data Sources and Availability

Data Types	Temporal Resolution	Station Name	Data Period	Data Source
Minimum Temperature Maximum Temperature	Daily	Colombo Nuwara-Eliya,	1970–2015	Department of Meteorology
Evaporation	Daily	Colombo	1985-2015	Department of Meteorology
Rainfall	Daily	Colombo Hanwella Group Pasyala Laxapana Annfield Dunedin-Chesterford Yatiyanthota-Wewalthalawa	1970–2015	Department of Meteorology
Streamflow	Daily	Hanwella	1985–2015	Department of Irrigation

3.3.2 Global Climate Data

Global climate data are the collected data of precipitation, temperature, evaporation, humidity, etc. globally. These data are available with General Circulation Models or Regional Climate Models. The global climate data obtained from the data portal of CGCM3 (Canadian General Circulation Model 3), HadCM3 (Hadley Centre for Climate Prediction and Research – Climate Model 3), CORDEX South Asia (Coordinated Regional Climate Downscaling Experiment – South Asia) and CanESM2-CMIP5 (The second generation of Earth System Model CanESM2 – Canadian Centre for Climate Modelling and Analysis CCCMA) can be used for statistical based climate change analysis except regional model CORDEX South Asia. From the above mentioned global & regional climate models, the CanESM2 model was selected for this study because for the selected region, the CanESM2 has already been used in a few case studies (Patabandige et al., 2016).

Table 3-4 GCM (General Circulation Model) Climate Data

Data	Location	Resolution	Period	Source
Precipitation	Global	Daily	1961 - 2100	CanESM2 (NCEP/NCAR, RCP2.6, RCP4.5, RCP8.5)
Temperature	Global	Daily	1961 - 2100	CanESM2 (NCEP/NCAR, RCP2.6, RCP4.5, RCP8.5)

3.4 Data Checking

Hanwella streamflow gauging station has continuous missing data for two months from 1989. The method called regression analysis was used to replace the missing data in datasets. The number of missing data of temperature, evaporation, rainfall and streamflow is tabulated in Table 3.6. Single mass curve (Figure 3.4) was plotted after evaluation of missing data of rainfall by simple linear regression method. The consistency of the rainfall data was checked by using the double mass curve analysis. The double mass curve indicated the homogeneity of annual rainfall. The double mass curve plotted is showed in Figure 3.5. Distribution of the gauging stations for entire

river basin and the sub-watershed compared with the standards of the World Meteorological Organization (WMO) were found to be within the acceptable range. Table 3.5 shows the distribution of the gauging stations selected for the case study according to WMO standards.

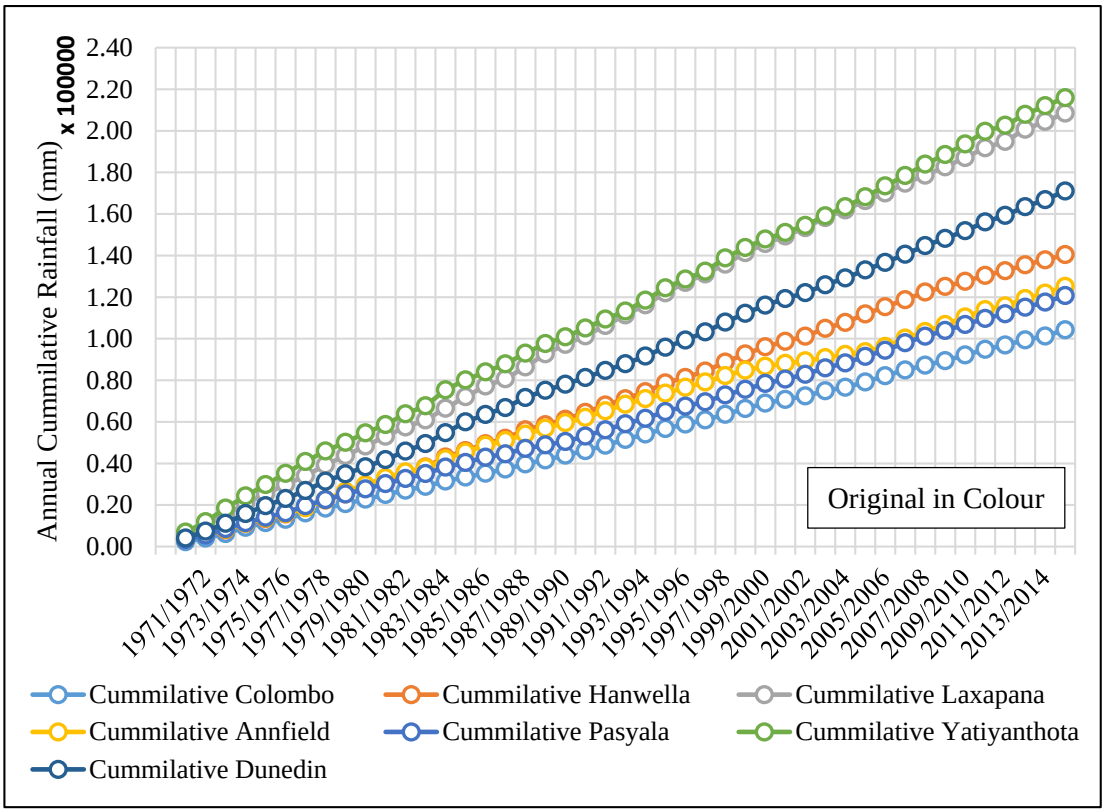

Figure 3-4 Single Mass Curve

Table 3-5 Distribution of Gauging Stations inf Entire Basin and Sub-watersheds

Basin	Gauging station	No of stations	Station Density (km^2/station)	WMO standards (km^2/station)
Kelani River Basin	Rainfall	7	330.57	575
Kelani River Basin	Streamflow	2	1157.50	1875
Hanwella Sub Watershed	Rainfall	5	359.84	575
Hanwella Sub Watershed	Streamflow	1	1799.21	1875

Table 3-6 Description of Missing Data

Data Type	Station Name	No. of Missing Data (Months)	Percentage (%)
Temperature	Colombo Nuwara-Eliya	5 4	1.39 % 1.11 %
Evaporation	Colombo	8	2.22 %
Rainfall	Colombo Hanwella Group Pasyala Laxapana Annfield Dunedin-Chesterford Yatiyanthota-Wewalthalawa	0 5 5 2 5 30 6	0 1.39 % 1.39 % 0.55 % 1.39 % 8.33 % 1.67 %
Streamflow	Hanwella	2	0.55 %

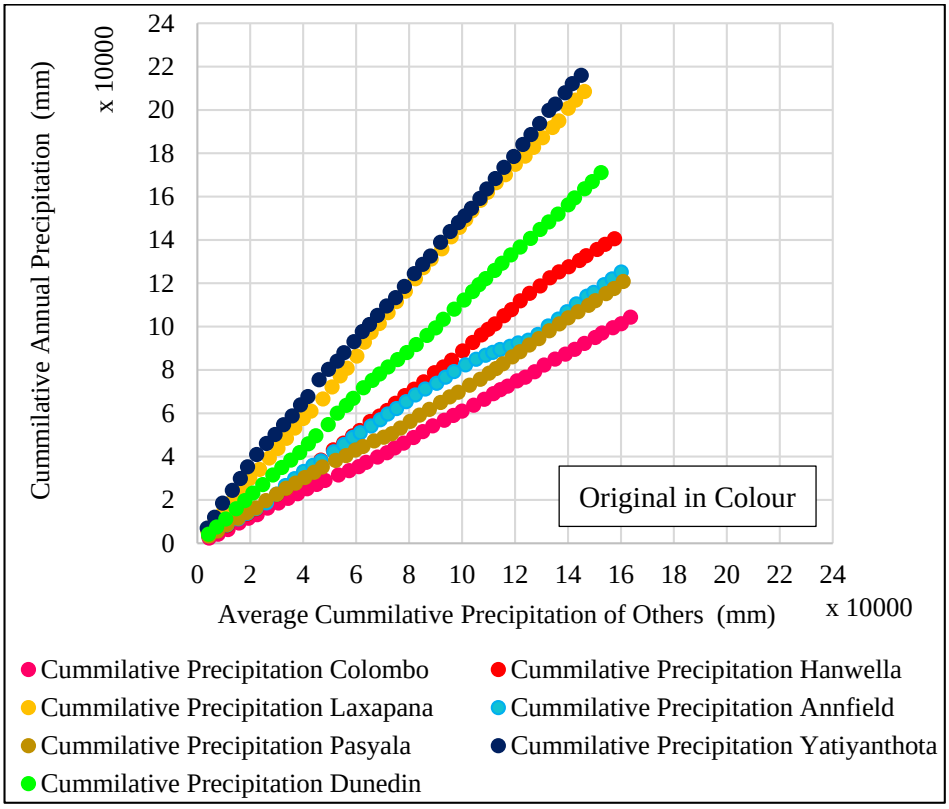

Figure 3-5 Double Mass Curve of Precipitation Stations

The double mass curve plotted for Annfield rainfall station has a slight variation with respect to the other stations. The theory of the double-mass curve is based on the fact that a graph of the cumulative value of one quantity against the cumulative value in

another quantity during the same period will plot as a straight line so long as the data are proportional; the slope of the line represents the constant of proportionality between the quantities.

A break in the slope of the double-mass curve means that a change in the constant of proportionality between the two variable has occurred or perhaps that the proportionality is not a constant value at all the rates of cumulation. If the possibility of a variable ratio between the two quantities can be ignored, a break in the slope indicates that the time at which a change occurs in the relation between the two quantities. The difference between the slopes of the adjacent lines on either side of the break in the slope indicates the degree of change in the relation. Changes in the slope of the line can be more accurately discerned if scales for the ordinate and the abscissa are chosen so that the general course of the curve is within a 45° direction angle relative to the axes.

The number of stations that can be included in a pattern is sometimes limited due to the criterion that the area in which the stations are located should be small enough to be influenced by the same general weather conditions. If less than ten stations are used in the pattern, each record should be tested for consistency by plotting it against the pattern, and those records that are inconsistent should be eliminated from the pattern.

The inherent variability in hydrologic data causes spurious breaks in the double-mass curve that should be recognised as such. Most users recognize that the year-to-year breaks are due to chance and, thus, ignore any break that persists for less than five years. Breaks that persist for longer than five years are subtler in that they may be due to chance or they may be due to a case of real change. Unless the time of the break coincides with a logical reason for the break, statistical methods should be used to evaluate the significance of the break of the pattern.

3.4.1 Visual Data Checking

Visual checks were also carried out to find whether there are inconsistencies in data. Streamflow response to rainfall was plotted for Thiessen weighted average rainfall for each year for Hanwella sub-watershed in Kelani River in Appendix 02.

3.4.2 Thiessen Average Rainfall

Thiessen polygon method (Chow et al., 1988) was used to calculate the average catchment rainfall. Thiessen polygons were developed for Hanwella sub-watersheds only. Because the calibrated HEC-HMS model used (De Silva et al., 2014) was just developed for Hanwella sub-watershed. Thiessen polygon map is shown in Figure 3.6 for Hanwella sub-watershed. Thiessen average values or weights for Hanwella sub-watershed is in Table 3.7. The streamflow responses for Thiessen average rainfall for Hanwella sub-watershed were given in Appendix-02.

Table 3-7 Thiessen Polygon area and Weight for Hanwella Watershed

Station Name	Thiessen Area (km^2)	Thiessen Weight
Hanwella	280.815	0.156
Yatiyanthota (Wewalthalawa)	434.612	0.241
Dunedin (Chesterford)	450.029	0.250
Pasyala	78.564	0.044
Laxapana	348.541	0.194
Annfield	207.100	.0115

3.5. Annual Water Balance

The annual water balance was carried out for Hanwella sub-watershed to compare the yearly volume of rainfall, streamflow, evaporation observed at Colombo and annual runoff coefficients. The average runoff coefficient of Hanwella sub-watersheds is 0.53.

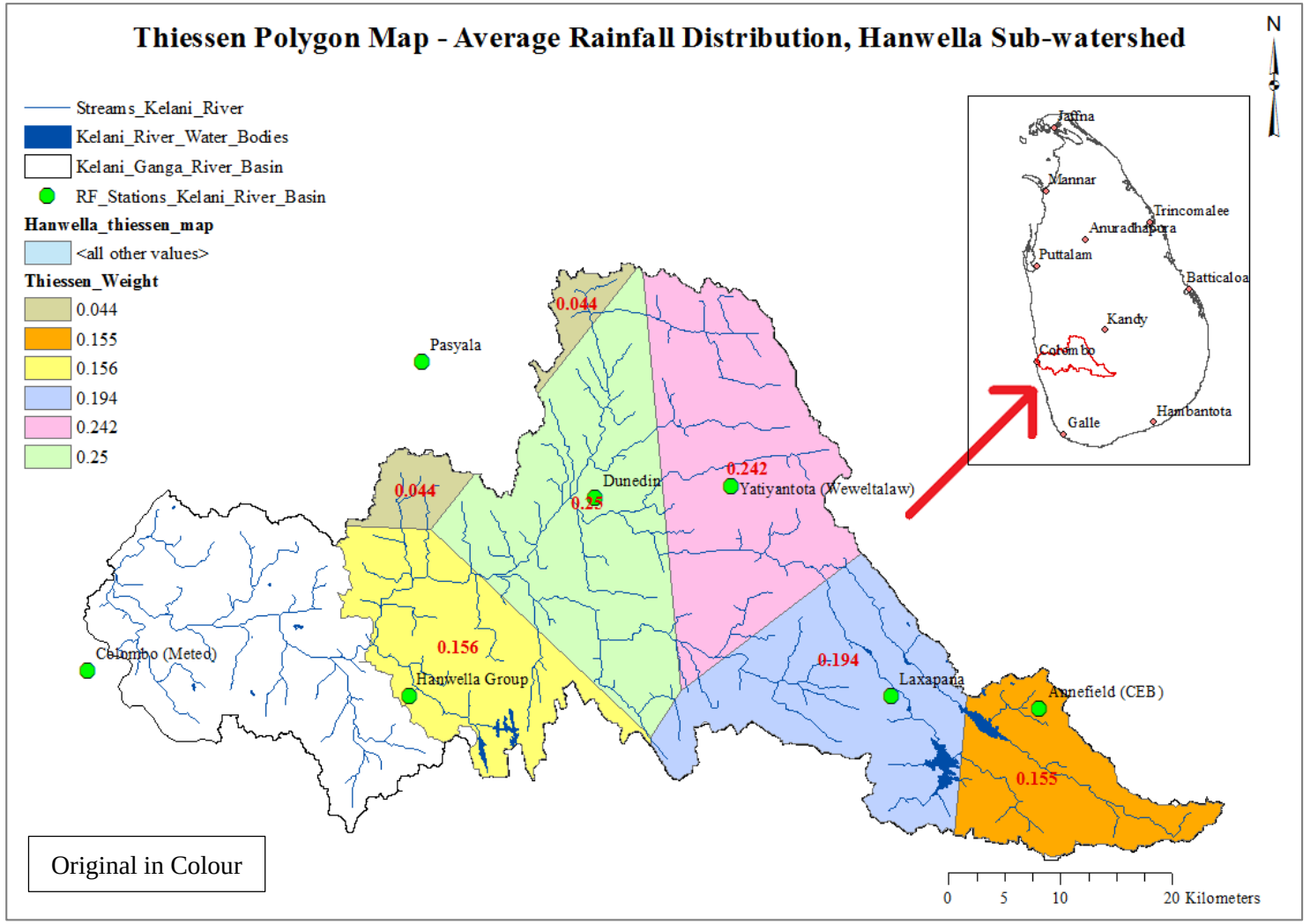

Figure 3-6 Thiessen Polygon of Hanwella Watershed

3.5.1. Variation of Annual Runoff Coefficient and Water Balance of Hanwella Watershed

Annual runoff coefficient varies from 0.26 to 0.79 during the 30 years of the period. It can be observed that in year 1994/1995, runoff coefficient is very high compared to other years whereas it is very low in the year 2011/2012 (Figure 3.7). The runoff coefficient value of the Kelani River basin was verified with the values recommended by literature. In 1996/1997, water balance also has a meagre value compared with the other years. The maximum water balance can be seen in 2008/2009. Because of that, despite the highest rainfall observed in the year of 2008/2009, the corresponding streamflow is not that much high.

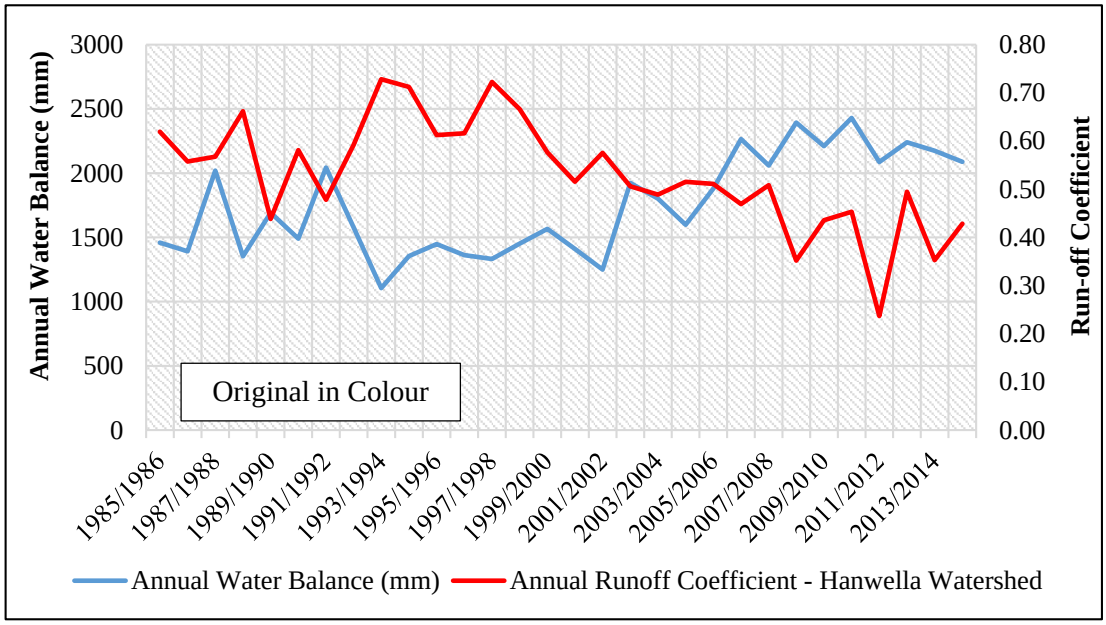

Figure 3-7 Variation of annual Water Balance and Runoff Coefficient of Hanwella Watershed

3.5.2 Variation of Annual Rainfall and Streamflow of Hanwella Watershed

The streamflow in the years of 1994/1995 and 1997/1998 are comparatively very high compared to other years. It was implemented in Figure 3.7 that although the rainfall in 2001/2002 – 2002/2003 and 2013/2014 – 2014/2015 are almost the same, in those years' streamflow has increased by more than 500 mm and this is unexpected. In contrast, the streamflow value in 2011/2012 has decreased up to 648 mm which is the

lowest streamflow during the period which shows that streamflow does not respond to rainfall. Year 2011/2012 observed as the driest year, but the streamflow is much smaller leading to a value of high evaporation and low runoff coefficient. Also, it reveals that there may be inconsistencies in streamflow data.

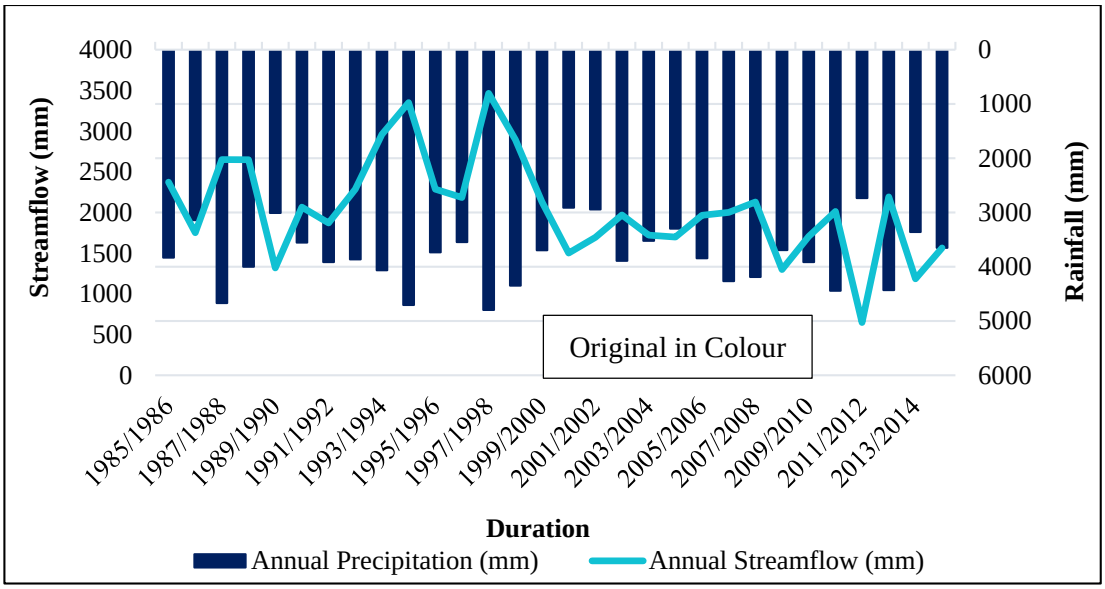

Figure 3-8 Variation of Annual Rainfall and Annual Streamflow of Hanwella Watershed

3.6 Mean Monthly Rainfall Comparison

For Hanwella sub-watershed the plotted variation of the mean monthly rainfall for the duration of 1970 to 2015 and the mean precipitation of the watershed were plotted in Figure 3.9. Also the box plot of each rainfall station for the period of 1970 to 2015 presented in Figure 3.10. The mean rainfall for the watershed was obtained by the Thiessen Weighted method. The comparison of precipitation as a monthly cumulative for each year from 1970-2015 for every rainfall station selected for Kelani River Basin was attached to the Appendix 04.

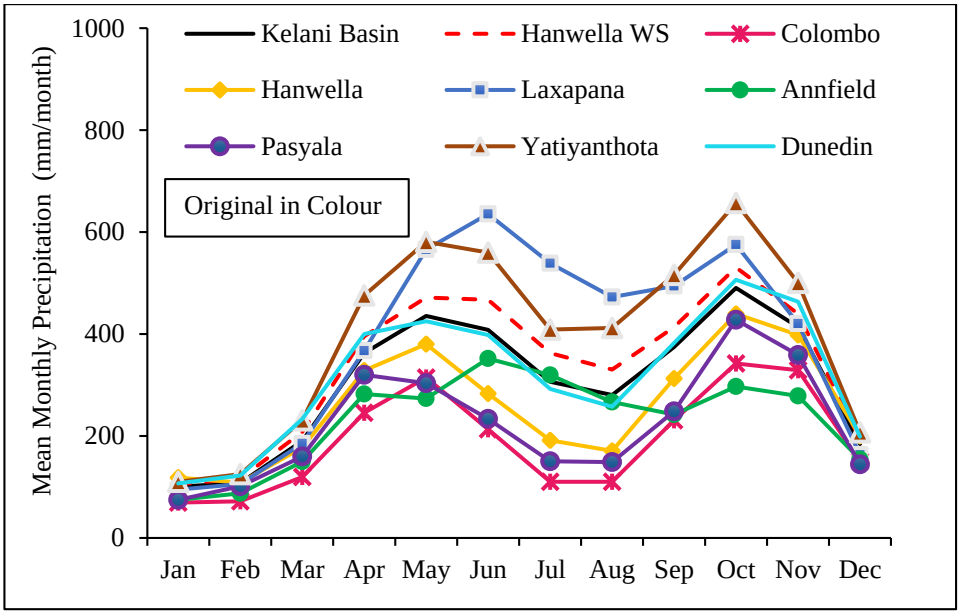

Figure 3-9 Monthly Mean Rainfall Distribution (1970-2015)

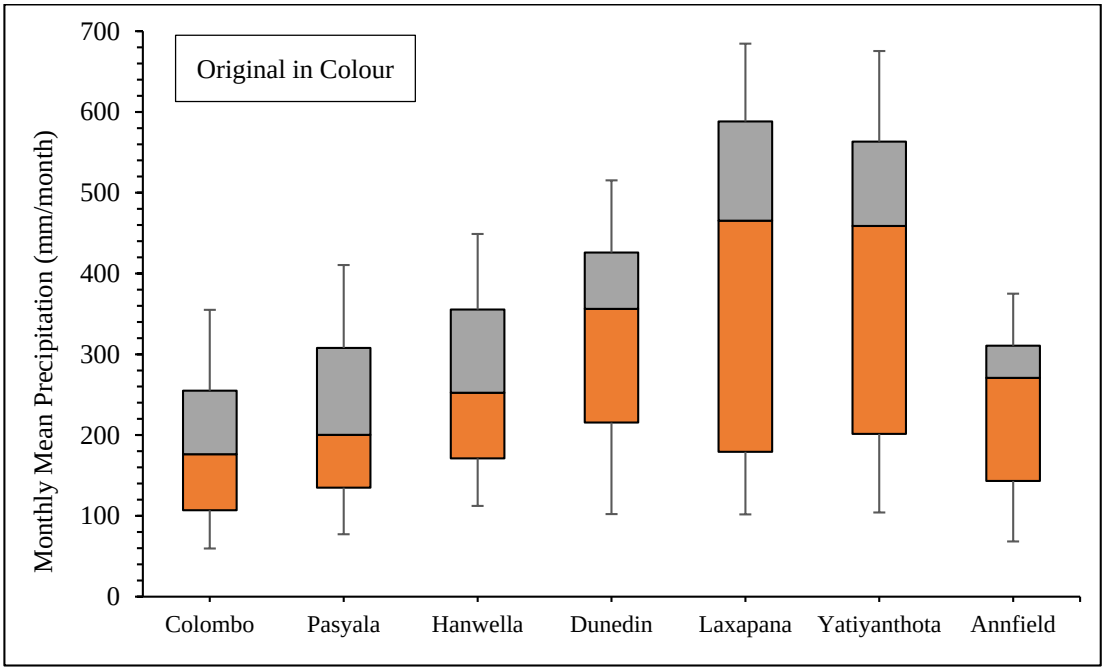

Figure 3-10 Box Plot of Observed Rainfall for the Period of 1970-2015

3.7 Variation of Average Temperature (Minimum and Maximum)

For this case study, two temperature gauging stations were selected to cover the entire watershed of the Kelani River basin. Those temperature gauging stations are namely

the Colombo Meteorology and Nuwara-Eliya Meteorology stations. The average monthly mean temperature of maximum and minimum temperature for Kelani River basin are depicted in Figures 3-11 and 3-12. The replacing of the missing data of the temperature minimum and maximum were calculated according to the linear regression method.

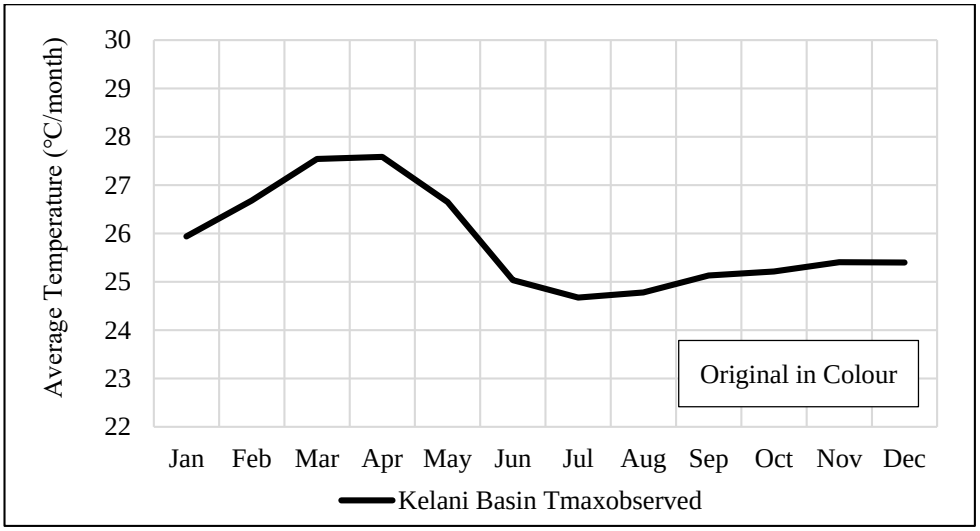

Figure 3-11 Average Temperature Maximum in Kelani River Basin

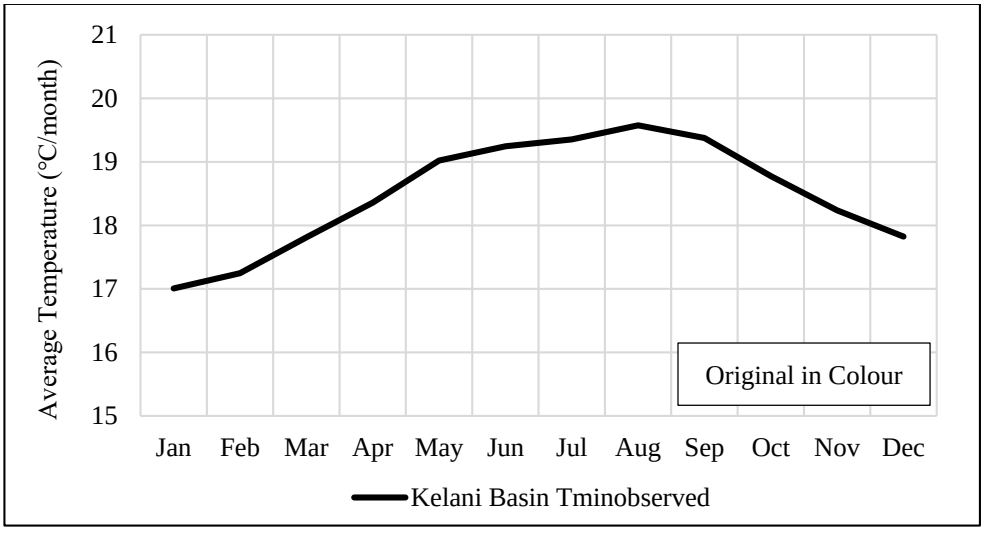

Figure 3-12 Average Temperature Minimum in Kelani River Basin

3.8 Performance Evaluation of Downscaled Output

To analyse the streamflow with the HEC-HMS hydrology model, one objective of this research is using the GCM downscaled data. The CanESM2 is the GCM used for downscaling the precipitation, temperature in maximum and minimum for the Kelani River Basin according to the statistical downscaling method. The Statistical Downscaling model was used for the downscaling process. The calibration period of the downscaling model is 01st of January 1970 to the 31st of December, 2000. For validation, NCEP was used and downscaled to get the precipitation and temperature values from 2001 to 2005. For future climate evaluation, mean of precipitation, mean of maximum temperature and mean of minimum temperature over the Kelani River basin were evaluated for the periods of the 2020s (2010-2039), 2050s (2040-2069) and 2080s (2070-2099).

Statistical downscaling models, in general, fail to capture the full range of the variance of a predictand such as precipitation (Wilby et al., 2006). This is because, in general, the difference in the observations of rainfall is much higher than the variance in the large-scale atmospheric variables obtained from the GCM or reanalysis data. When the downscaling model is run with the GCM or the reanalysis data, it tends to explain the mid-range of the variance of the observed precipitation better than the low and high extremes. Therefore, statistical downscaling models, in general, tend to reproduce the average of the precipitation better than the low and high extremes. In other words, this results in an under-estimation of large precipitation values and over-estimations of near-zero precipitation values. Tripathi et al. (2006) also commented that even a downscaling model based on support vector machine technique (complicated nonlinear regression technique) fails to accurately reproduce the extremes of precipitation though it captures the average well.

The performance of the downscaling model results during the calibration and validation phase were numerically assessed by comparing the mean, standard deviation and the coefficient of variance of the model precipitation with those of observations. Also, the model performances in calibration and validation were further quantified with the coefficient of determination (R^2), and the root mean square error (RMSE).

Table 3.8 gives the results of mean Explained Variance and Standard Error for calibration.

This situation is entirely different from the temperature. In statistical downscaling, the frequency of the temperature can be captured by the model rather than precipitation. Because of that in temperature, there is no significant variance in the rate of the observed like in precipitation and temperature variation is usually following a cyclical increasing or decreasing trend (Wilby et al., 2006).

Table 3-8 Explained Variance (E) and Standard Error (SE) during Calibration (1970-2000)

Variable	Explained Variance E (%)		Standard Error SE (℃ or mm/day)	
	Max	Min	Max	Min
Tmax	72.9	50.9	55.8	3.8
Tmin	84.3	61.7	68.1	4.6
Precipitation	35.7	9.2	15.5	0.6

4. ANALYSIS AND RESULTS

4.1 Identification of Extreme Events

In this study, precipitation and temperature were identified as the parameters to monitor climate variations. Therefore, to determine the extreme events of the precipitation and temperature, the IPCC indices (IPCC, 2007) were used. Identifying extreme precipitation and temperature events are important as these events are often associated with flood hazards, extended droughts and, ultimately, higher risk of the vector and epidemic diseases. The data period used for the present study is 1970 to 2015 of 45-year duration.

Also, the climate extremes are receiving increased attention because the impacts of climate change are felt most strongly through changes in the extremes. Global picture of changes in extremes (Frich et al., 2002) typically show large areas with sparse data coverage or not at all. One such area includes parts of the Central and South Asia where no long-term digital daily data are readily available.

4.1.2 Precipitation Indices in the Kelani River Basin

To evaluate the extremes of precipitation, the long-term trend of the indices was identified for point rainfall stations used for the present study, namely Colombo, Hanwella, Pasyala, Dunedin-Chesterford, Yatiyanthota-Wewalthalawa, Laxapana and Annfield. The Table 4-1 below shows the summary result of the trends of indices used to identify the precipitation extremes. For this study, 10 number of indices recommended by the IPCC were used.

According to the results, two out of seven stations were showing an increasing trend in ‘PRCPTOT’- total precipitation, namely in Colombo and Pasyala. Also, only Colombo was showing a rising trend of 0.297 for’ RX-5day’, the annual maximum consecutive 5-day rainfall. The result of the trend of ‘RX-1day’ of annual maximum rainfall shows four out of seven stations have an increasing trend and maximum increasing trend is given as 0.516 for Colombo, and the maximum decreasing trend is giving as -0.471 for Yatiyanthota. The maximum number of consecutive dry days, ‘CDD’ were giving decreasing trend for all the stations and the highest decrease is -

0.515 for Pasyala. Three out of seven stations have an increasing trend for the maximum number of consecutive wet days, 'CWD' index and the highest increase is 0.344 for Pasyala, and the highest decreasing trend is -0.581 for Annfield. The increasing trends of CDD and CWD have a direct link to the increase or decrease of extreme events and as well as the change of climate in future with respect to the precipitation. According to the Table 4.1, CWD has an incremental trend, which is indicating an increase of extreme events of rainfall in the Kelani River basin.

Figure 4.1 to Figure 4.10 attached in below are the results of identification of trends of indices used for Colombo precipitation station to identify how the behaviour of the extremes of climate regarding rainfall for the period of 1970 to 2015.

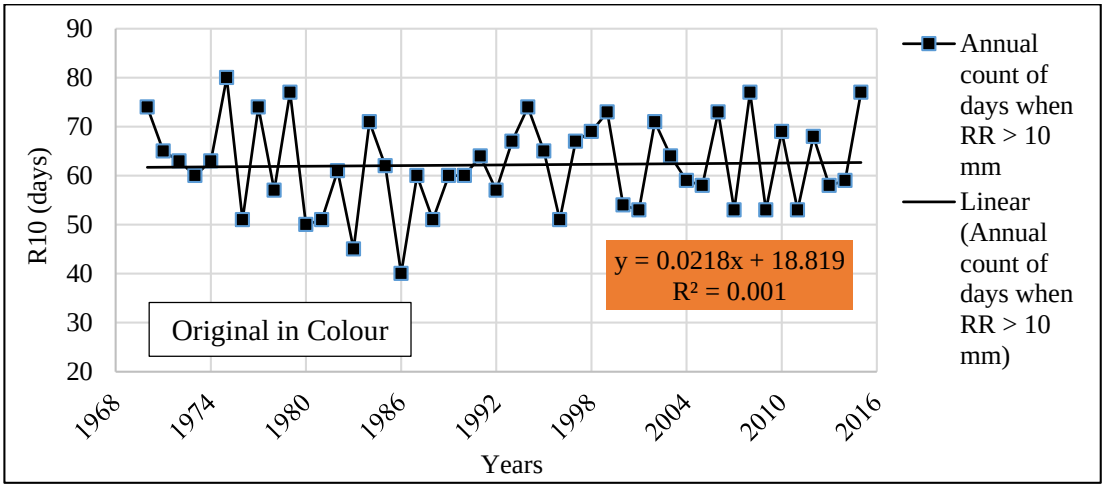

Figure 4-1 Trend of Annual Count of Days when RR > 10mm

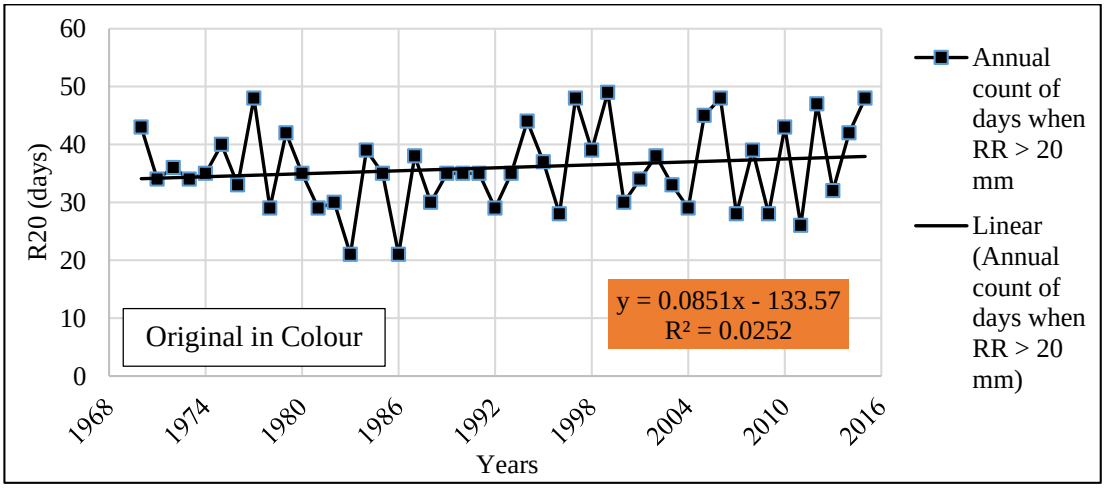

Figure 4-2 Trend of Annual Count of Days when RR > 20mm

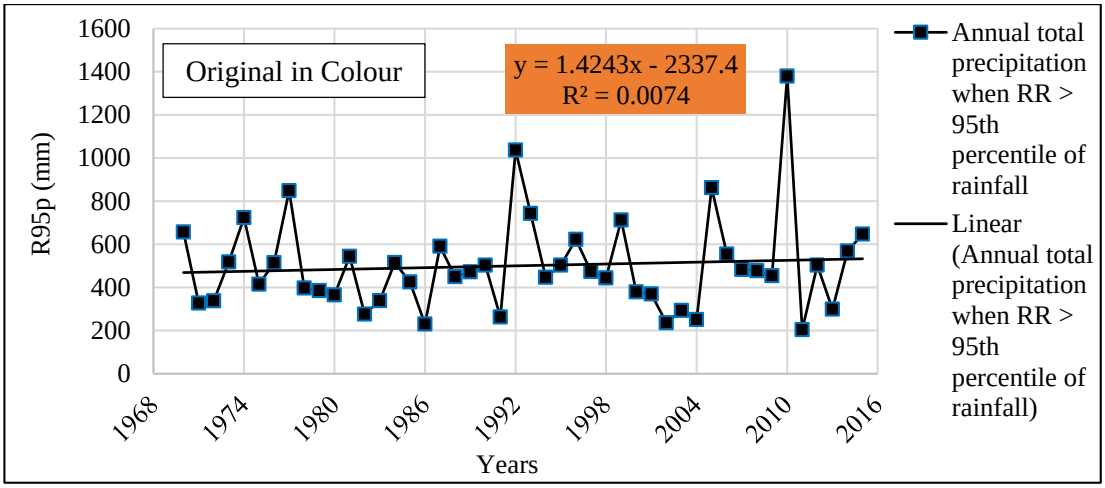

Figure 4-3 Trend of Annual Total Precipitation when RR > 95th Percentile of Daily Rainfall

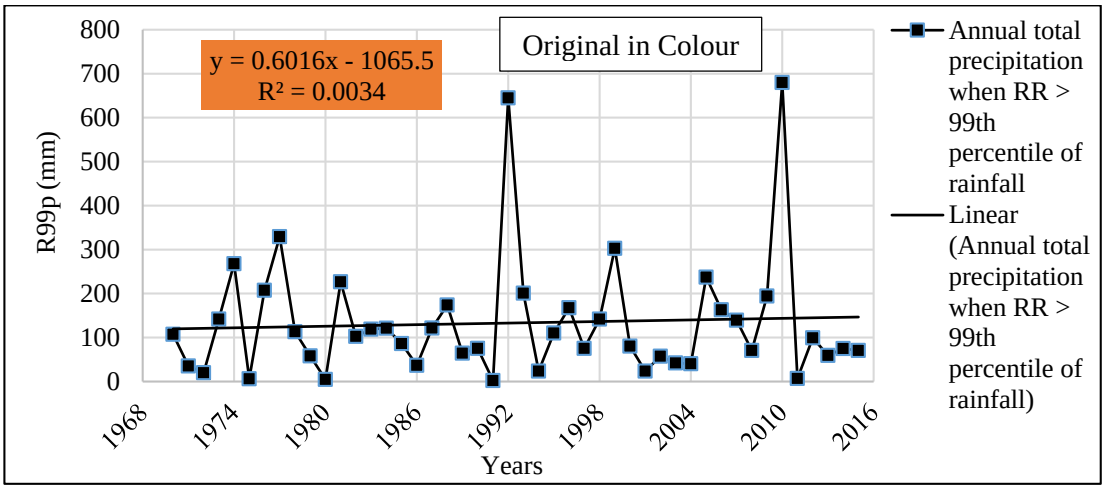

Figure 4-4 Trend of Annual Total Precipitation when RR > 99th Percentile of Daily Rainfall

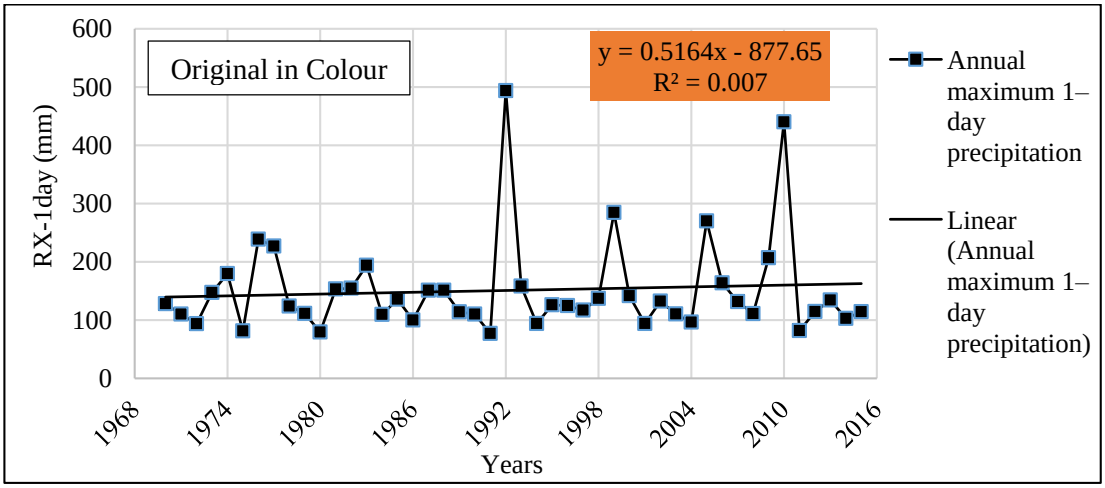

Figure 4-5 Trend of Annual Maximum 1-day Precipitation

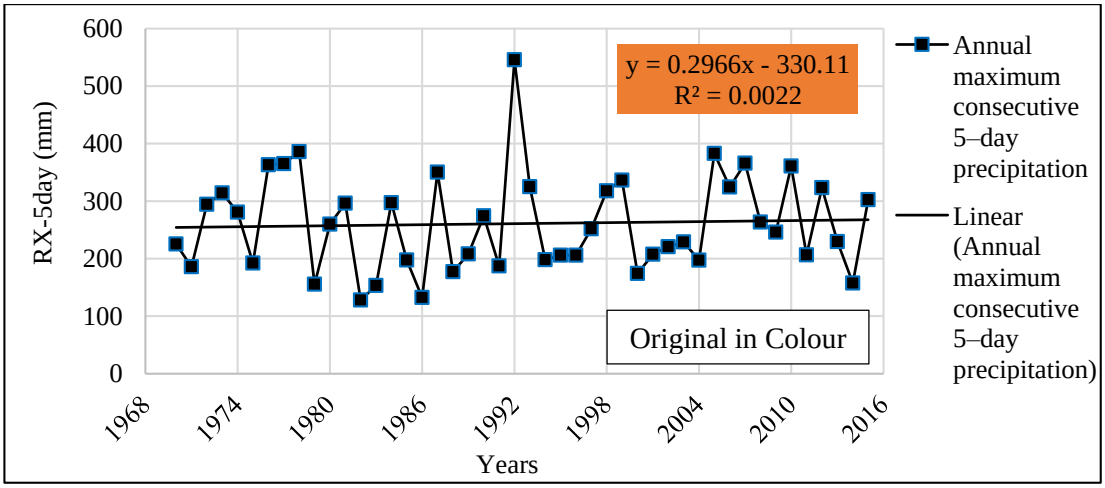

Figure 4-6 Trend of Annual Maximum Consecutive 5-day Precipitation

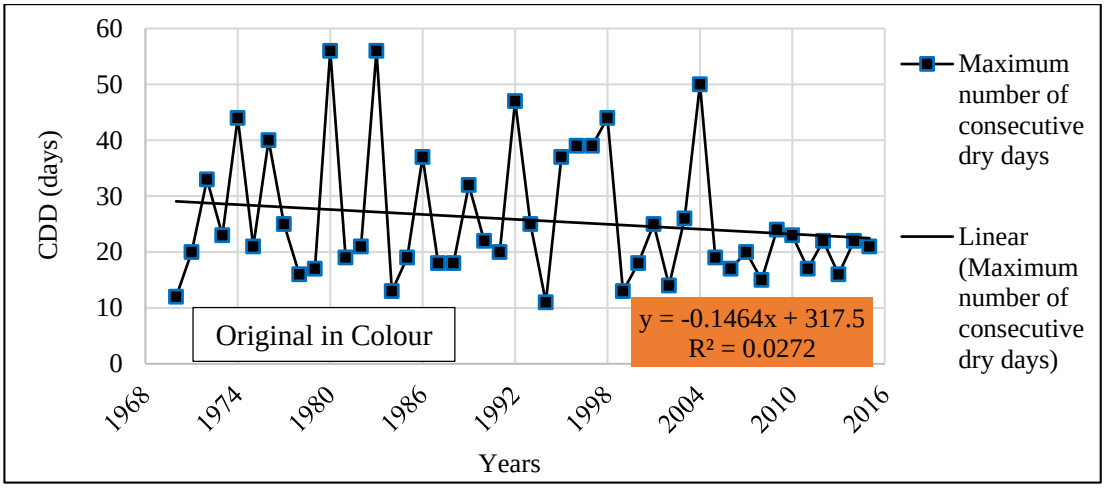

Figure 4-7 Trend of Maximum Number of Consecutive Dry Days

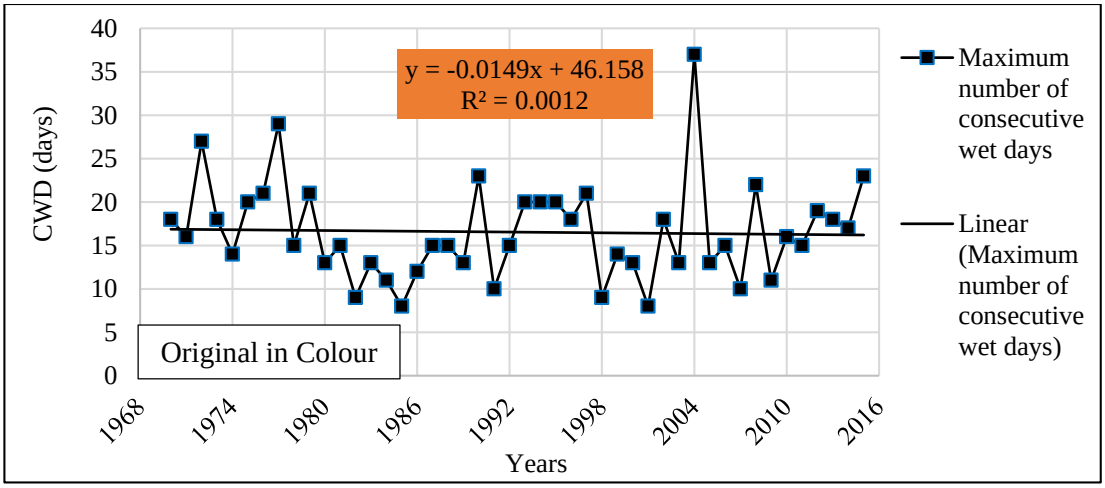

Figure 4-8 Trend of Maximum Number of Consecutive Wet Days

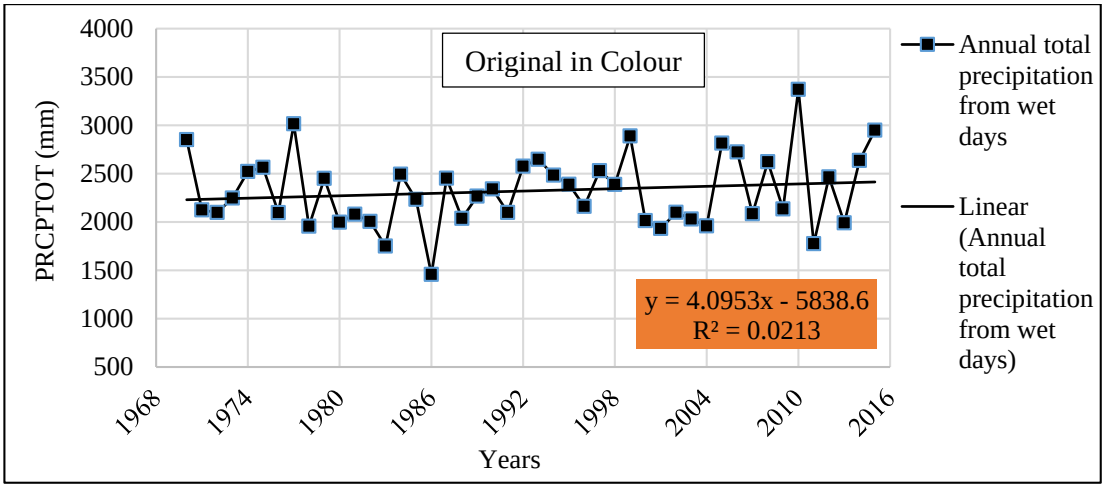

Figure 4-9 Trend of Annual Total Precipitation from Wet Days

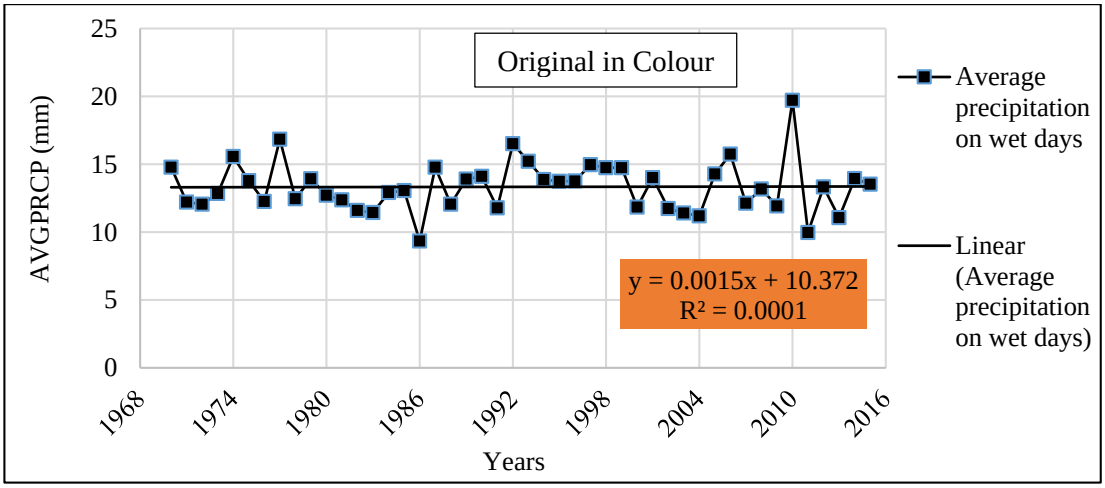

Figure 4-10 Trend of Average Precipitation on Wet Days

Table 4-1 Trends of Precipitation Extreme Indices in Point Rainfall Stations (1970-2015)

Index	Colombo	Hanwella	Laxapana	Annfield	Pasyala	Dunedin (Chesterford)	Yatiyanthota (Wewalthalawa)	Hanwella Sub-watershed	Kelani River Basin
R10	0.022	-0.185	-0.519	-0.158	0.017	-0.067	-0.492	-0.278	-0.278
R20	0.085	0.054	-0.225	-0.123	-0.002	-0.146	-0.390	-0.266	-0.244
R95p	1.424	0.183	-6.548	-3.048	-0.385	-3.485	-10.145	-4.809	-3.212
R99p	0.602	-0.439	-2.258	-0.850	-0.499	-1.136	-3.593	-1.534	-0.925
RX-1day	0.516	0.067	0.089	-0.461	0.028	-0.100	-0.471	-0.085	0.023
RX-5day	0.297	-0.534	-2.007	-0.649	-0.564	-1.113	-3.629	-1.593	-1.163
CDD	-0.146	-0.258	-0.192	-0.217	-0.515	-0.117	-0.236	-0.105	-0.140
CWD	-0.015	-0.581	-0.134	-0.024	0.287	0.344	0.068	-0.561	1.320
PRCPTOT	4.095	-4.850	-20.333	-7.514	3.623	-5.136	-24.559	-12.552	-9.567
AVGPRCP	0.002	0.018	-0.097	-0.005	-0.096	-0.051	-0.141	-0.052	-0.046

4.1.3 Temperature Indices in the Kelani river Basin

To evaluate the extremes of temperature, the long-term trend of the indices was identified for two selected temperature stations used for the present study, namely Colombo and Nuwara-Eliya. That was because, these two stations were the only stations contributed for the monitoring of temperature change in Kelani basin. For this study, 12 number of indices were used to analyse the behaviour of temperature extremes.

The Table 4-2 shows the summary result of the trends of indices used to identify the temperature extremes. According to the result, the trend of Summer Days – SU25 (annual count of days when TX > 25℃) is about 0.784 for average maximum temperature in the Kelani River basin. is the findings further indicate that the increase of the summer days for Colombo is 0.012 and the decrease in Nuwara-Eliya is -0.181. Also, the trend of Tropical Nights – TR20 has an increasing trend of 0.905 for average temperature in Kelani river basin.

The annual minimum of maximum temperature (TXn) and the annual minimum of minimum temperature (TNn) both are having increasing trends. The trend of Warm Nights (TN90p) has an increasing trend of 0.767, 1.028 and 0.819 within the Kelani River basin, Colombo and Nuwara-Eliya, respectively. The rising trend of TN90p is an indicator of the climate change. Because of that, with the shift in the climate system, warm days and warm nights may increase which is in agreement with IPCC (2007).

Figure 4.11 to Figure 4.22 are the results of the extreme temperature analysis of average temperature distribution within the Kelani River basin according to the Thiessen polygon map developed.

Table 4-2 Trends of Temperature Extreme Indices (1970-2015)

Index	Kelani Basin Average Temperature	Colombo	Nuwara-Eliya
SU25 (TX > 25℃)	0.784	0.012	-0.181
TR20 (TN > 20℃)	0.905	0.124	0.000
TXx (Annual Max of Tmax)	-0.006	0.008	-0.012
TNx (Annual Max. of Tmin	-0.003	0.011	-0.002
TXn (Annual Min of Tmax)	0.019	0.015	0.015
TNn (Annual Min of Tmin)	0.074	0.030	0.040
TN10p (Days TN < 10th percentile)	-1.366	-1.125	-0.548
TX10p (Days TX < 10th percentile)	-0.580	-0.626	-0.364
TN90p (Days TN > 90th percentile)	0.767	1.028	0.819
TX90p (Days TX > 90th percentile)	-0.076	0.168	-0.332
DTR (Annual mean TX - TN)	-0.018	-0.019	-0.017
ETR (Annual TXmax - TNmin)	-0.079	-0.023	-0.052

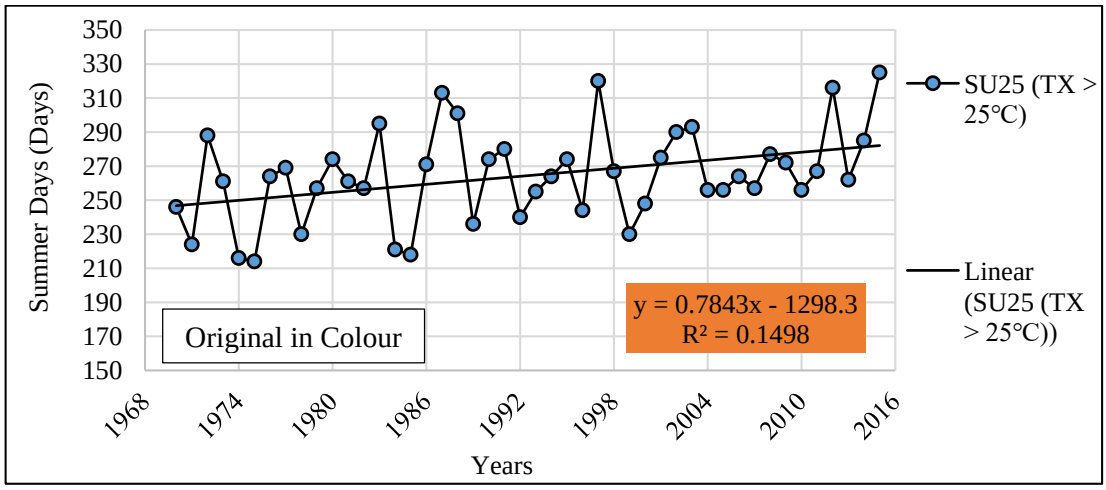

Figure 4-11 Trend of Summer Days

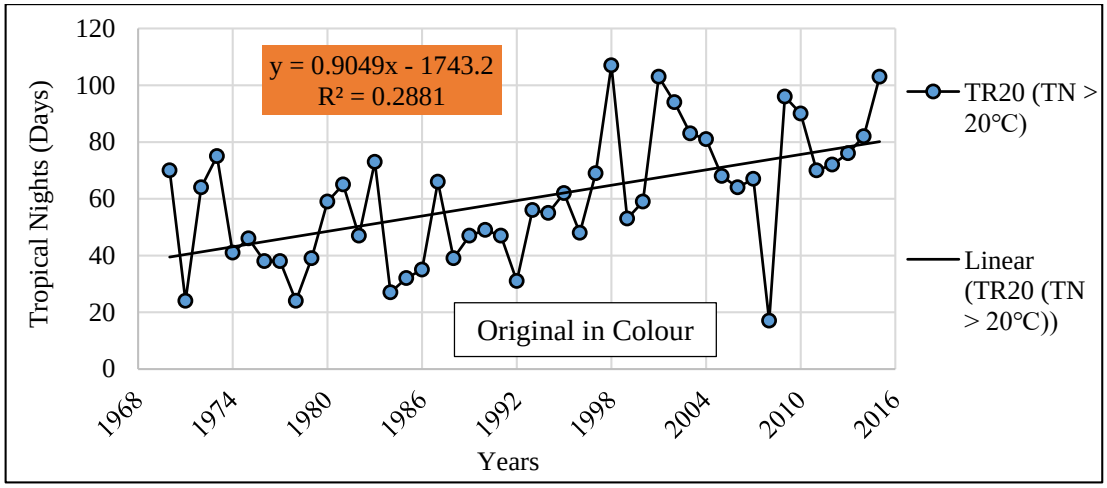

Figure 4-12 Trend of Tropical Nights

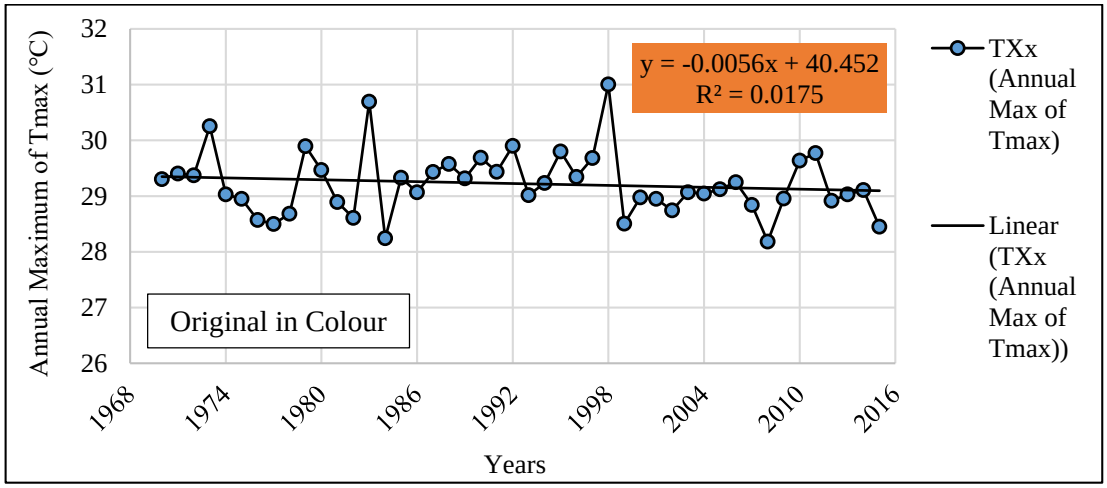

Figure 4-13 Trend of Annual Maximum of Tmax

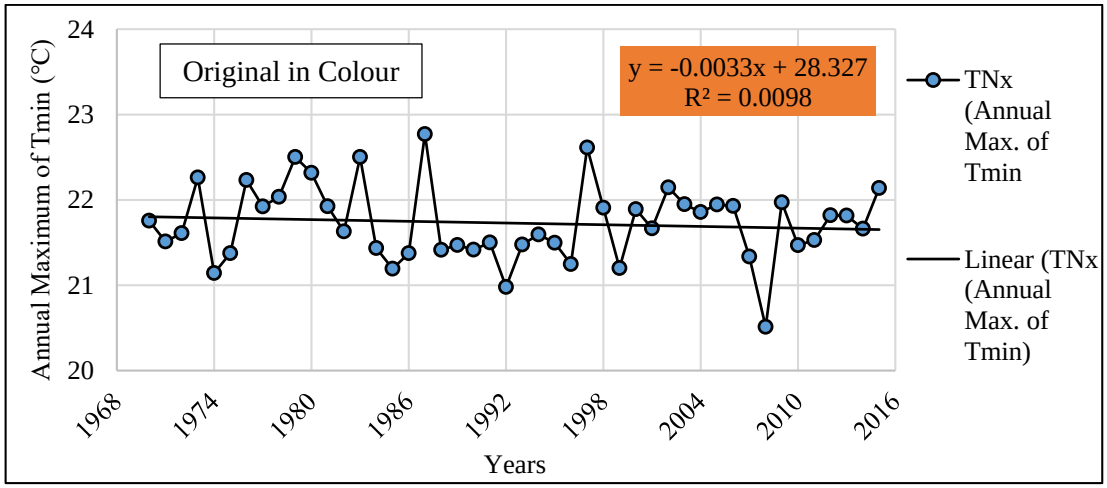

Figure 4-14 Trend of Annual Maximum of Tmin

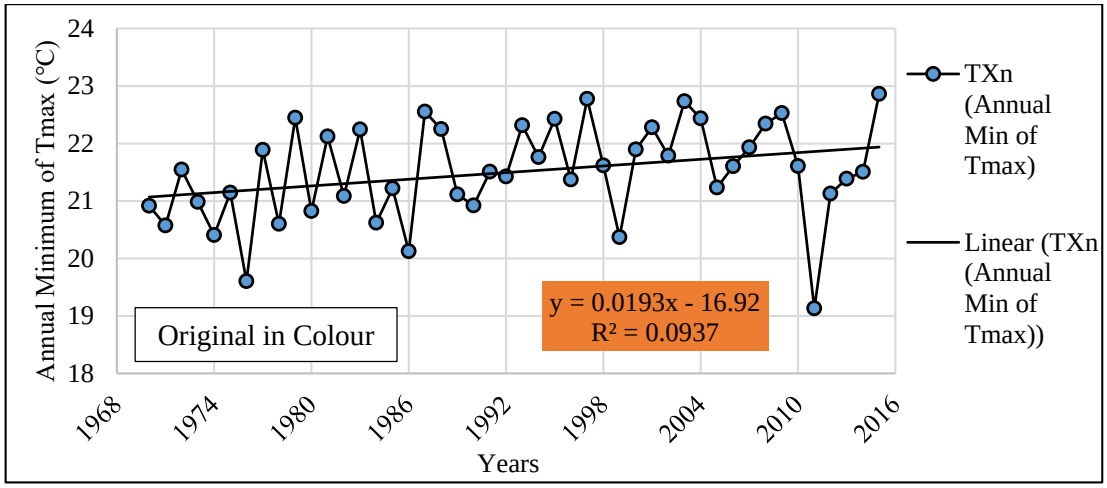

Figure 4-15 Trend of Annual Minimum of Tmax

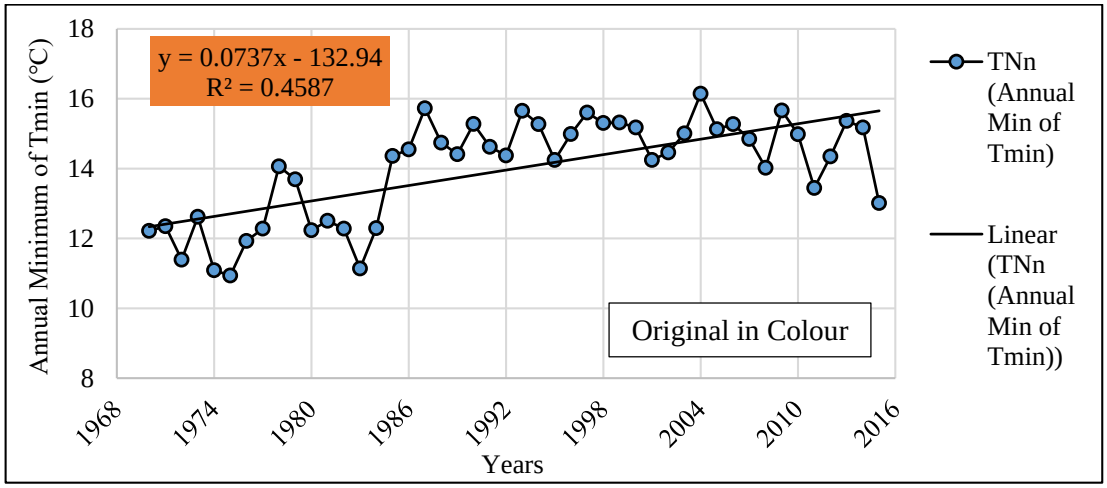

Figure 4-16 Trend of Annual Minimum of Tmin

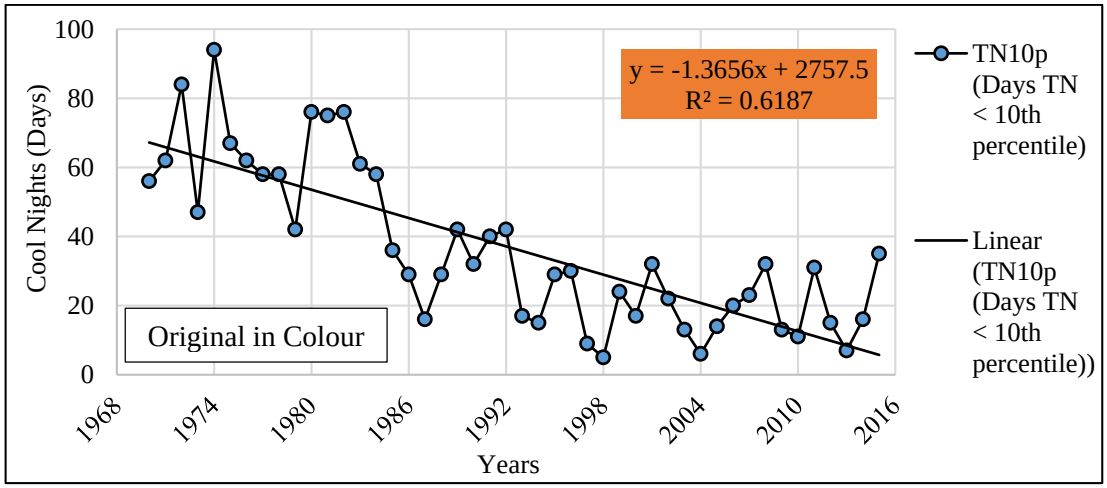

Figure 4-17 Trend of Percentage of Days Minimum Temperature <10th Percentile

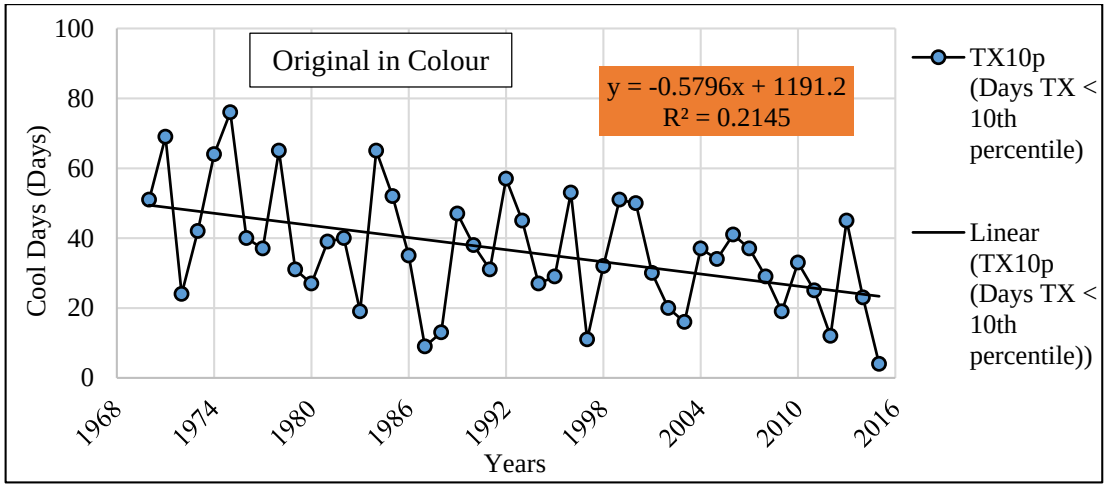

Figure 4-18 Trend of Percentage of Days Maximum Temperature <10th Percentile

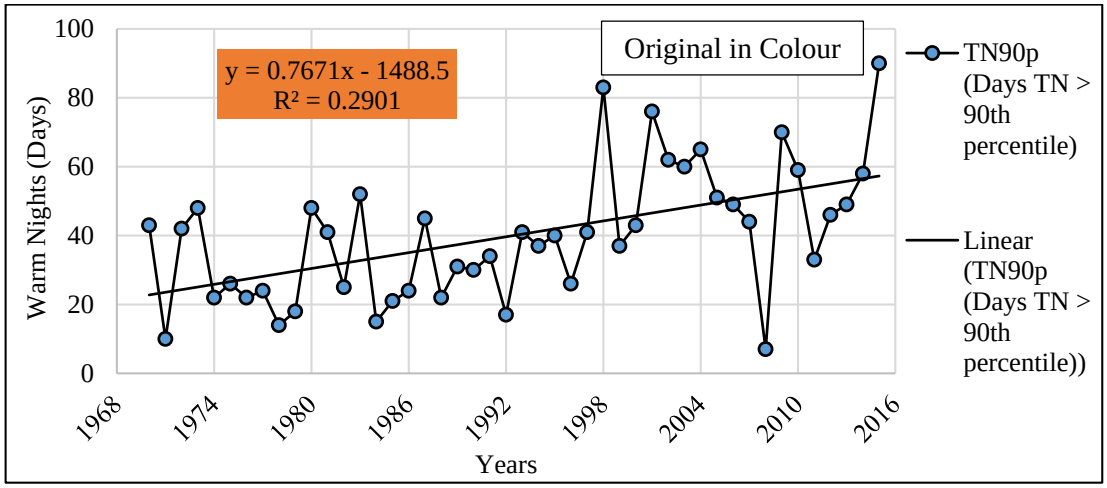

Figure 4-19 Trend of Percentage of Days Minimum Temperature >90th Percentile

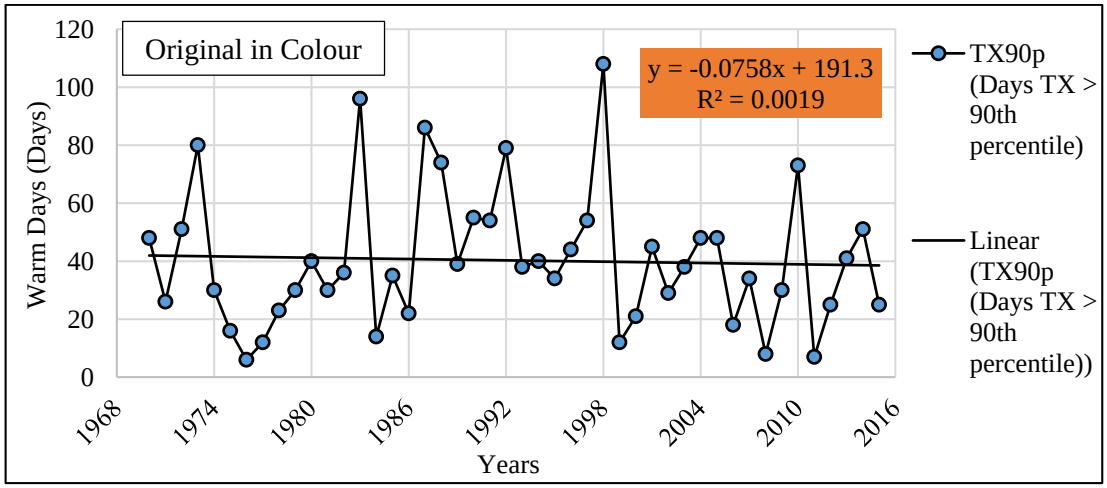

Figure 4-20 Trend of Percentage of Days Maximum Temperature >90th Percentile

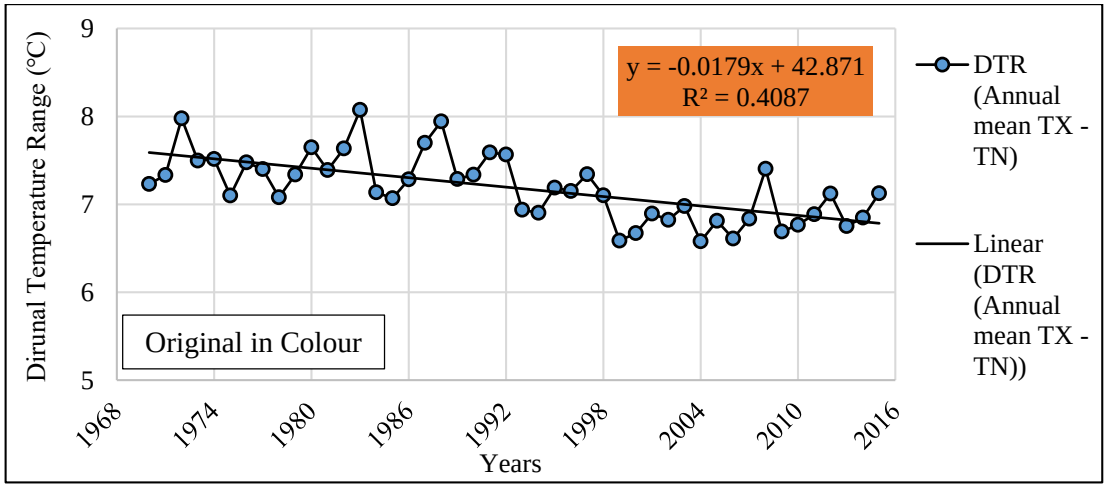

Figure 4-21 Trend of Diurnal Temperature Range (Kelani River Basin)

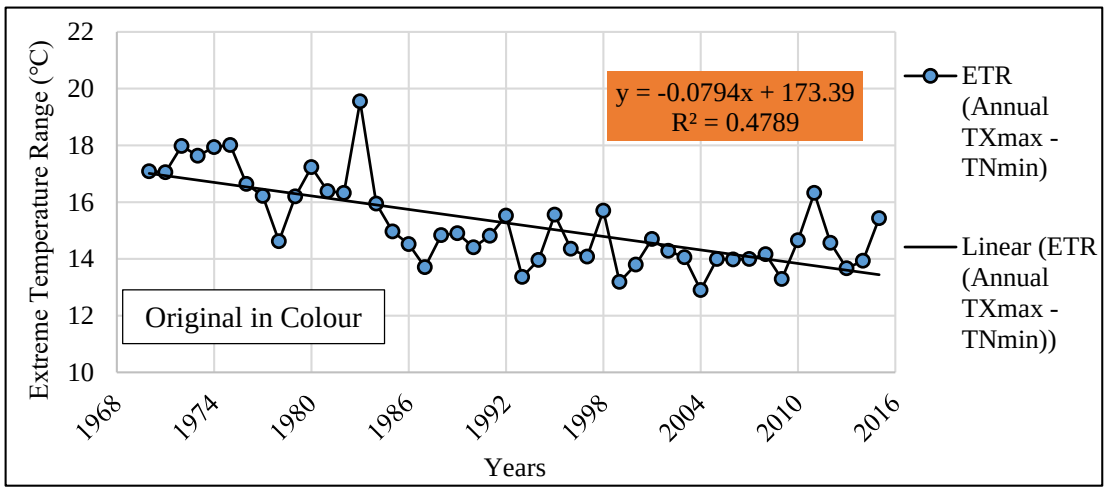

Figure 4-22 Trend of Extreme Temperature Range (Kelani River Basin)

4.2 Analysis of Trends in Precipitation and Temperature

To identify the trend of precipitation and temperature (maximum and minimum) in the Kelani River basin, the observed values were plotted in daily, monthly, seasonally and annually basis and it was recognised whether the trend is increasing or decreasing with respect to the slope of the trend line. For this trend analysis, a simple linear regression model was applied.

4.2.1 Identification of Trends in Point Rainfall

Trends in daily, monthly, seasonal and annual rainfall from 1970/71-2014/15 in gauging stations showed that there is a significant spatial variation in changes in

precipitation in the Kelani River basin. Most of the stations reveal decreasing trends in monthly, seasonal and annual time periods (Figure 4.23). Yearly rainfall showed declining trends in five stations, namely Hanwella, Laxapana, Annfield, Yatiyanthota and Dunedin. Highest reduction of -24.278 mm/year was observed in annual rainfall of the Yatiyanthota station. Other stations, i.e. Colombo and Pasyala, showed an increasing trend.

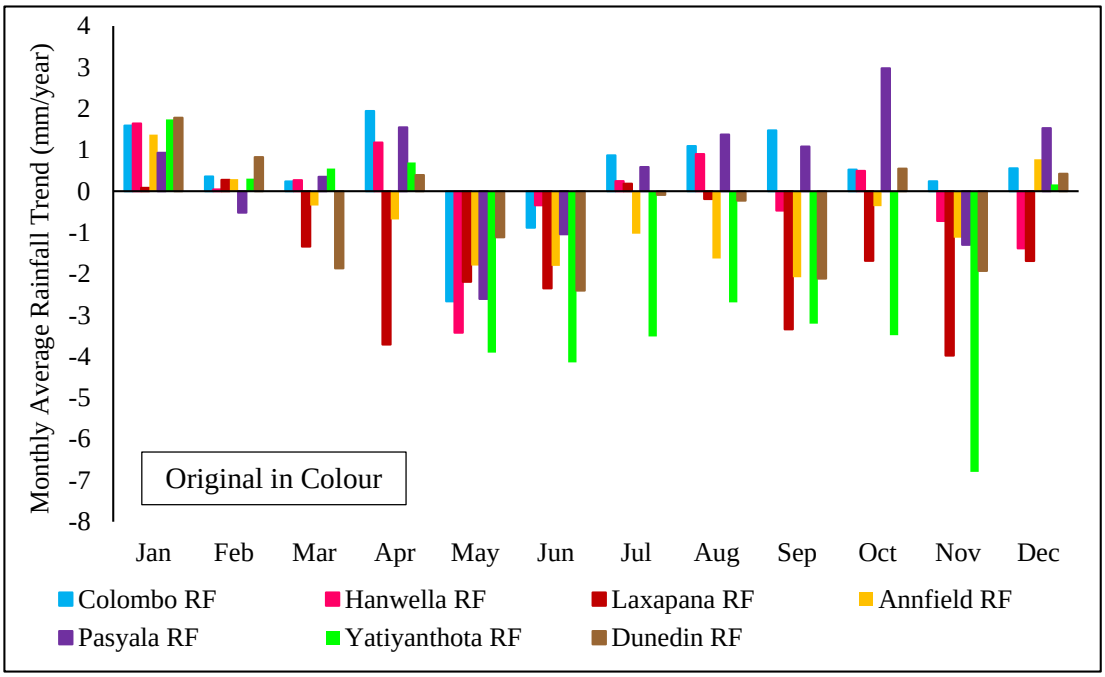

Figure 4-23 Monthly Trends in Point Rainfall

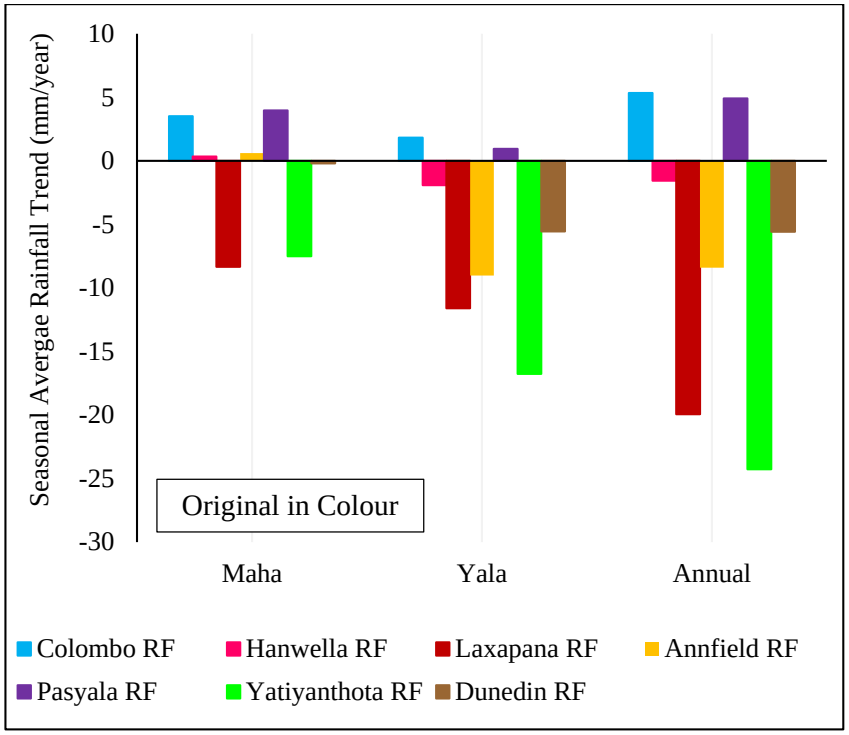

Figure 4-24 Seasonal and Annual trends in Point Rainfall

All the stations except for Colombo and Pasyala showed increasing trends in seasonal rainfall in Maha season. The highest increase of 5.35 mm/year was observed in Colombo. The highest increase of precipitation in Maha season was found as 3.98 mm/year in Pasyala. Only Colombo and Pasyala showed an increasing trend in seasonal rainfall in Yala season. All other stations showed decreasing trends where highest decreasing trend of -24.28 mm/year was observed in Yatiyanthota. In monthly rainfall, the highest decreasing trend of -6.79 mm/year was found in November at Yatiyanthota. The highest monthly increasing trend of 2.98 mm/year was found in October at Pasyala.

To identify the trends of the precipitation, the number of dry days and number of wet days were plotted for the period of 1970/1971 to 2014/2015 duration. The graphs of trend analysis are attached in the Appendix 05.

According to the plotted graphs, an increasing trend was identified for the rainfall in Colombo for the 45-year period. The increase of precipitation for the 45-year period is 5.35 mm/year. Also, the number of rainy days have an increasing trend. This also

proves the increase of rainfall for Colombo. The following tables attached are describing the trends of precipitation of each rainfall station according to the dry days and wet days (Manawadu & Fernando, 2008).

Table 4-3 Number of Rainy Days of Point Rainfall Station 1970-2015

Station Name	**m (Slope)**	**c (Intercept)**	**R^2**	**Remarks**
Colombo	0.286	166.75	0.054	Low
Hanwella	-1.433	206.66	0.123	High
Laxapana	-0.163	216.61	0.006	Low
Annfield	-0.590	206.43	0.096	Moderate
Pasyala	0.995	110.51	0.170	Moderate
Yatiyanthota-Wewalthalawa	0.140	184.55	0.002	Low
Dunedin - Chesterford	0.320	194.85	0.025	Low

Table 4-4 Number of Dry Days of Point Rainfall Station for 1970-2015

Station Name	**m (Slope)**	**c (Intercept)**	**R^2**	**Remarks**
Colombo	-0.287	198.52	0.054	Low
Hanwella	1.432	158.62	0.123	High
Laxapana	0.162	148.67	0.006	Low
Annfield	0.589	158.85	0.096	Moderate
Pasyala	-0.996	254.77	0.172	Moderate
Yatiyanthota-Wewalthalawa	-0.141	180.73	0.003	Low
Dunedin - Chesterford	-0.322	170.43	0.026	Low

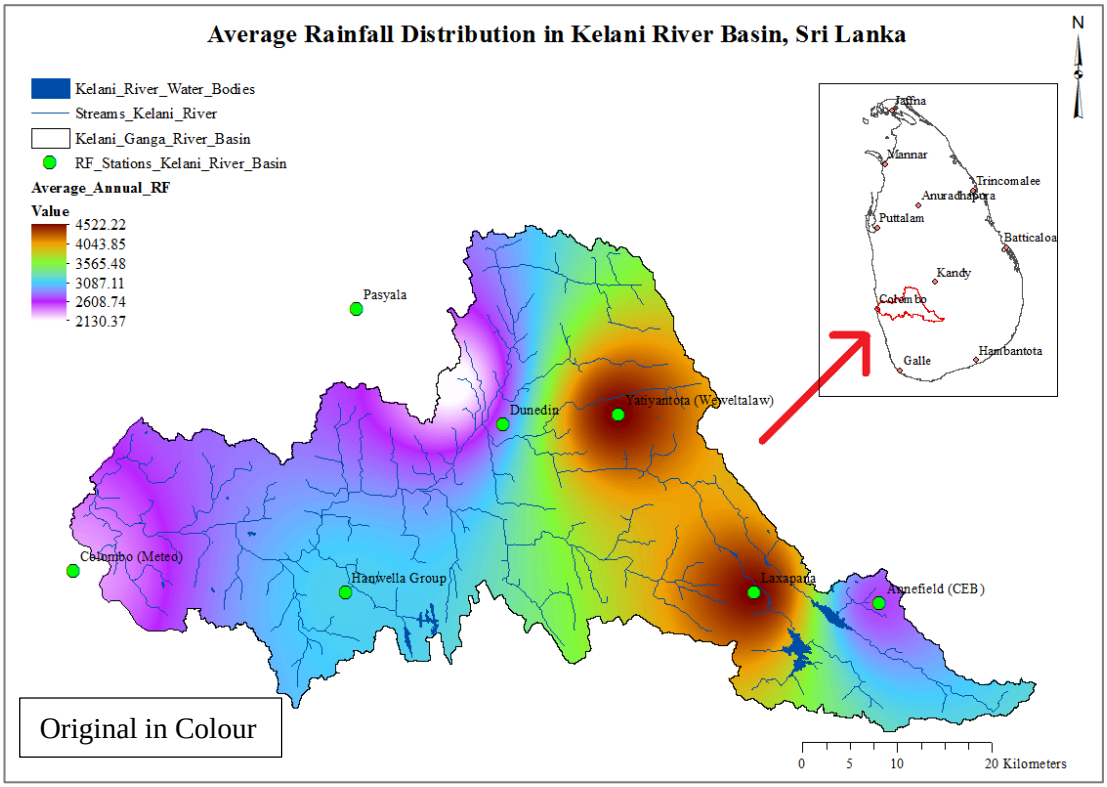

Figure 4-25 Average Annual Rainfall Distribution in Kelani River Basin

4.2.2 Identification of Trends in Catchment Rainfall

Trends in monthly, seasonal and annual rainfall from 1970/1971-2014/2015 in catchment rainfall showed that there is a spatial variation in changes of precipitation within the sub-watersheds in the Kelani River basin. Majority of the trend in Hanwella sub-watershed in monthly, seasonal and annual time scale is decreasing, and it appears that the reduction is higher in November (Figure 4.26 & Figure 4.27)

Annual rainfall shows a decreasing trend of -12.16 mm/year in Hanwella sub-watershed. Maha season showed a decreasing trend of -3.18 mm/year and Yala season showed a decreasing trend of -8.98 mm/year in Hanwella sub-watershed. All months showed decreasing trends in Hanwella sub watershed except for January and February. The highest increasing trend of 1.34 mm/year was observed in January for Hanwella sub-watershed.

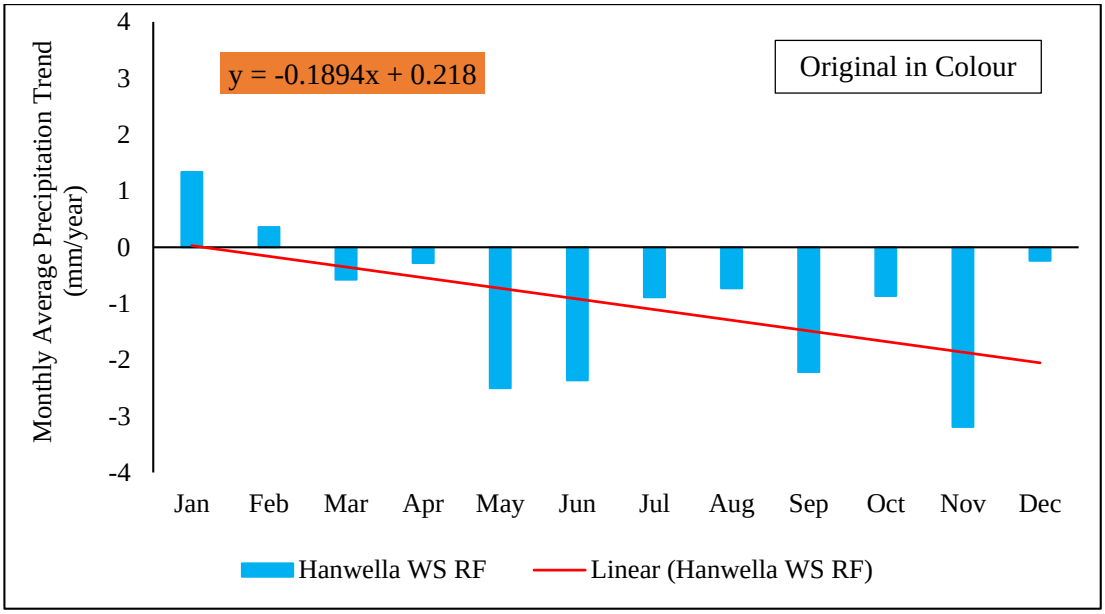

Figure 4-26 Monthly Average Trend in Catchment Rainfall (1970-2015)

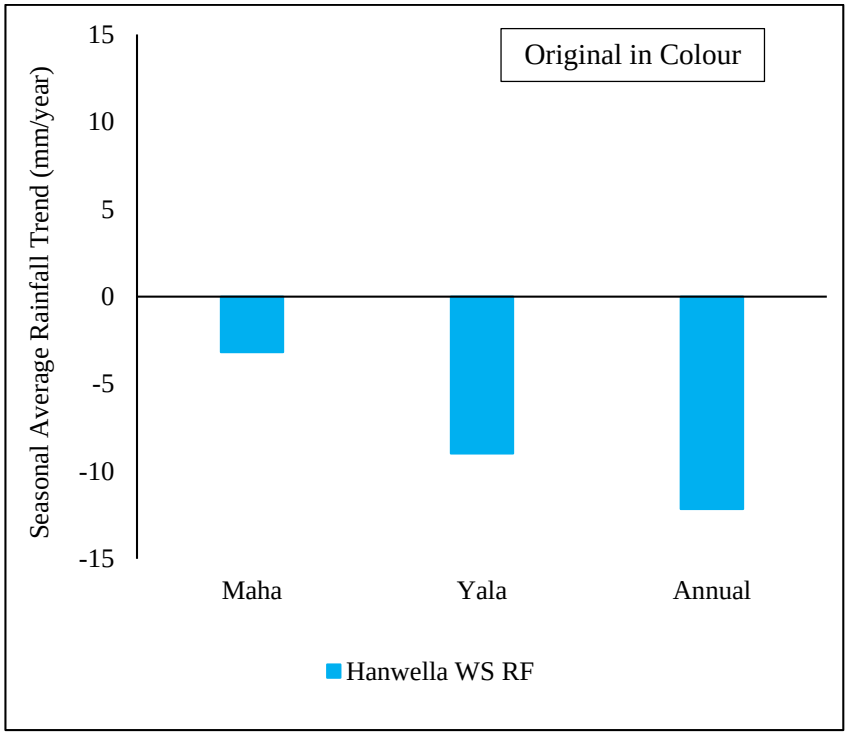

Figure 4-27 Seasonal and Annual Trends in Catchment Rainfall

4.2.3 Trends of Temperature

The selected temperature stations for the case study are Colombo and Nuwara-Eliya Meteorological stations. To identify the trends of the temperature, the maximum, minimum and average temperature were plotted in monthly, seasonal and annual basis for all two stations. The Ratnapura temperature station does not contribute to the variations according to the Thiessen polygon developed for the temperature distribution over the Kelani River basin. The overall variation of the average annual maximum temperature and average annual minimum temperature over the Kelani River basin are plotted according to the spatial distribution, using Inverse Distance Weighting (IDW) method used in ArcGIS tool. This method is recommended for spatial distribution mapping of climate change studies by IPCC (2007) (Figure 4.29 & Figure 4.30).

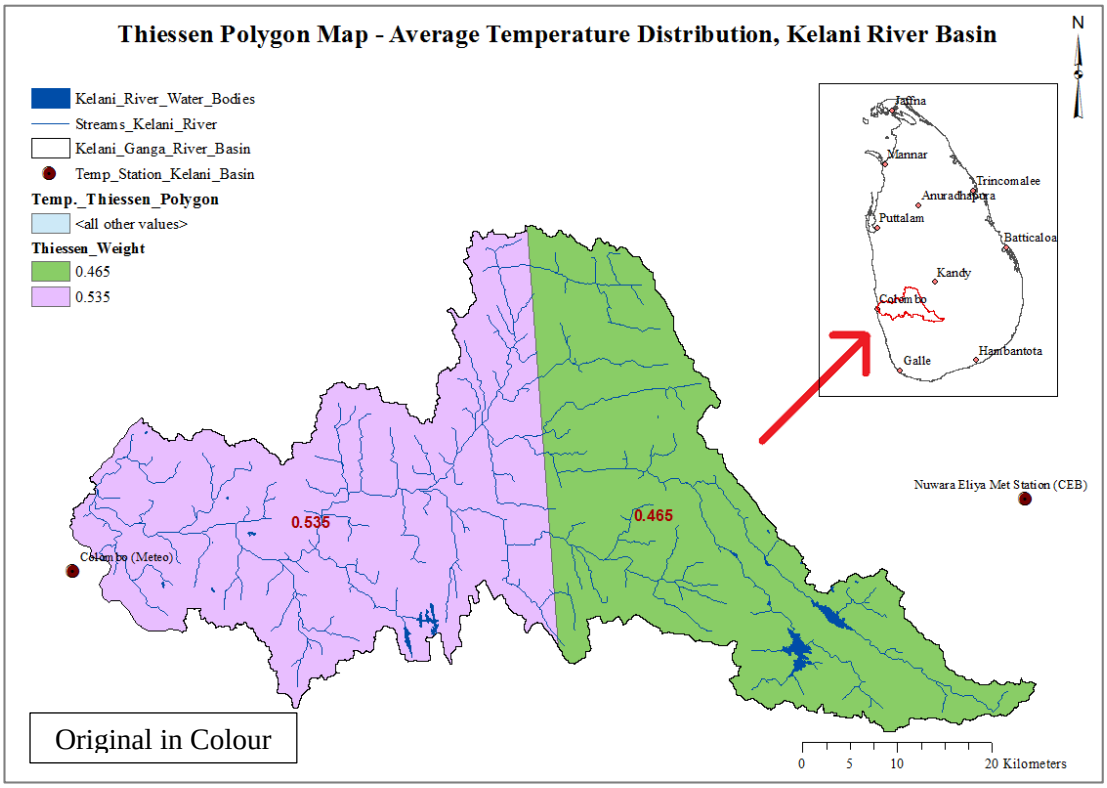

Figure 4-28 Temperature Distribution over Kelani River Basin (Thiessen Polygon Map Developed)

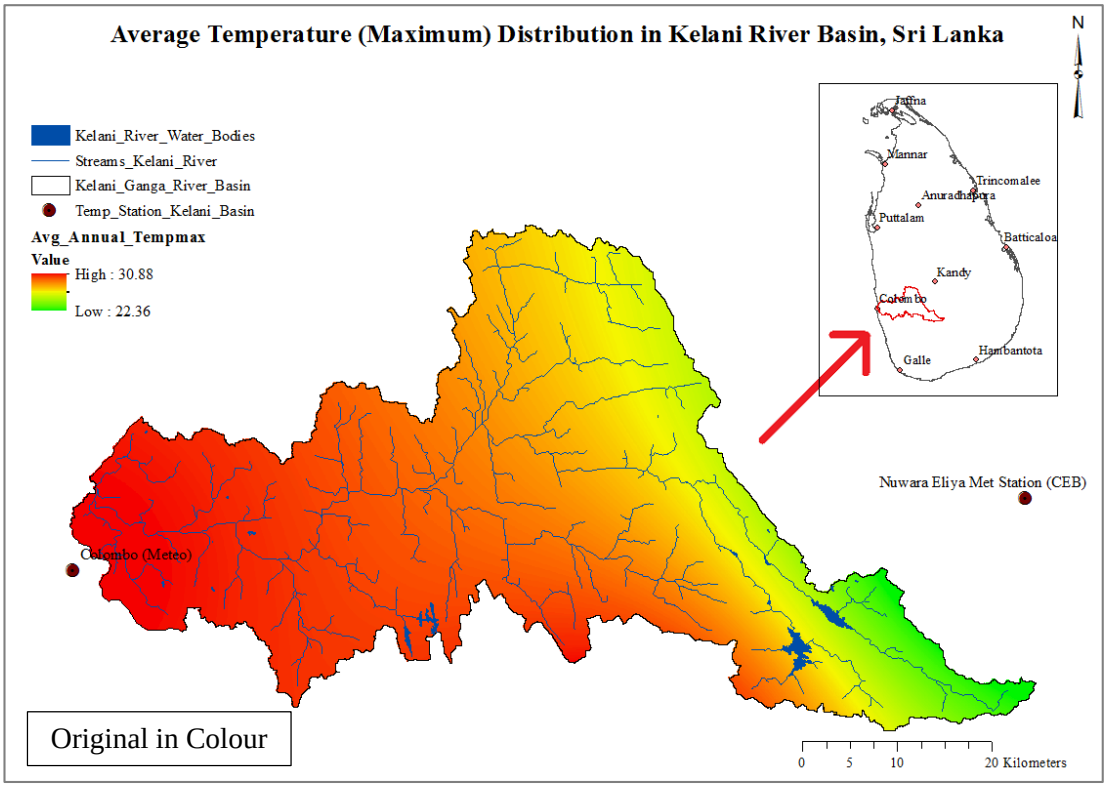

Figure 4-29 Average Annual Maximum Temperature Distribution in Kelani Basin

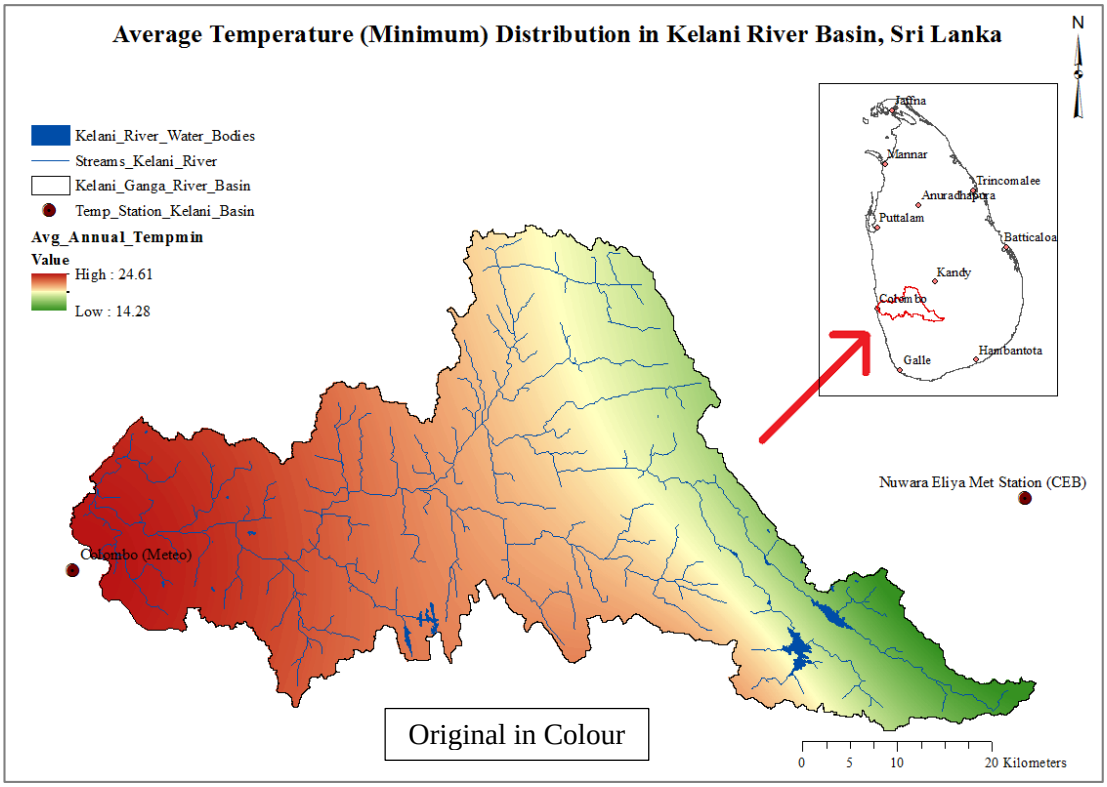

Figure 4-30 Average Annual Minimum Temperature Distribution in Kelani Basin

4.2.4 Identification of Trends of Basin Temperature (Maximum and Minimum)

Annual average temperature minimum in Kelani River basin is increasing at a rate of 0.0256℃/year from 1970/1971-2014/2015. Growing trend in temperature minimum in Maha season is 0.0459℃/year and for Yala season, it is 0.0053℃/year. Increasing trend in temperature maximum in Maha season is 0.003℃/year and for Yala season, it is 0.0191℃/year.

Temperature minimum over in Kelani River basin shows an increasing trend in monthly plots except in May and June from 1970/1971-2014/2015 and Temperature maximum was showing a rising trend in monthly data except in February, March and April. Temperature minimum was showing the highest upward trend of 0.0615℃/year in January and Temperature maximum was showing the highest upward trend of 0.0191℃/year in August.

The highest downward trend of Temperature minimum is -0.0151℃/year in June, and the highest declining trend of Temperature maximum is -0.0067℃/year in April.

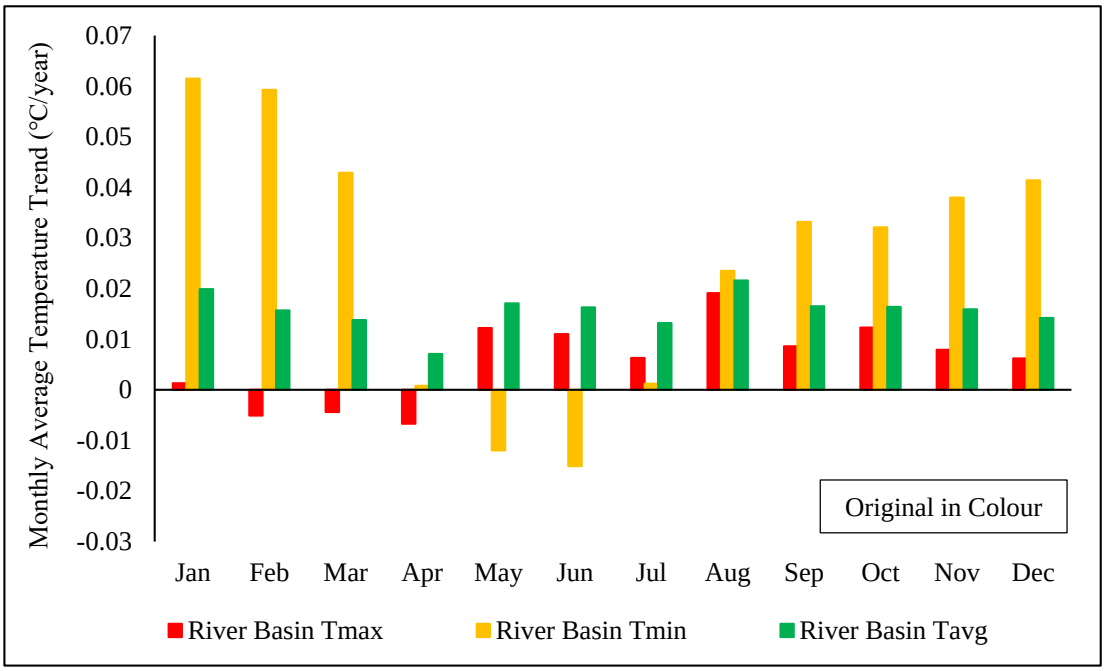

Figure 4-31 Monthly Average Temperature Trends in Kelani River Basin

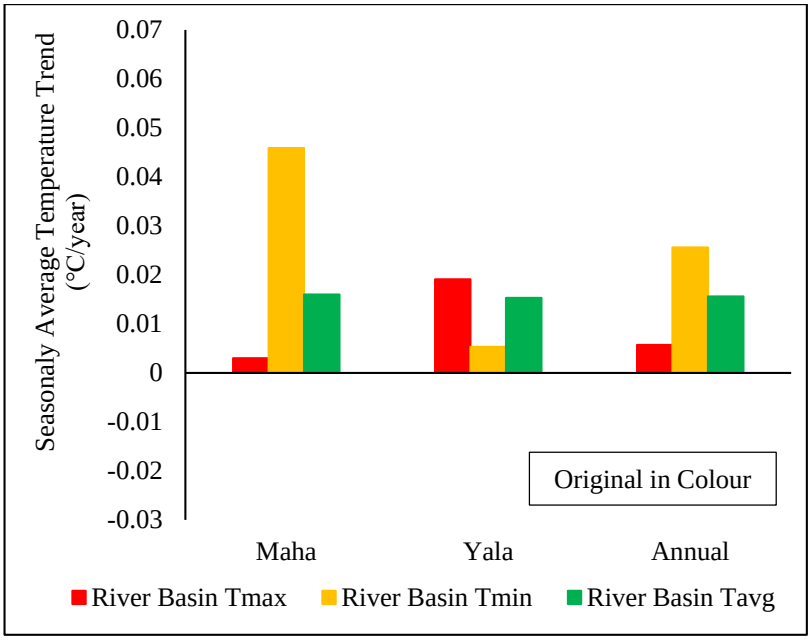

Figure 4-32 Seasonal and Annual Average Temperature Trends in Kelani River Basin

The linear trend of the temperature in the Kelani River basin can be implemented by the constructed temperature anomalies for the average temperature of Colombo, Nuwara-Eliya and Kelani River basin, respectively. The following Figure 4-33 depicts the identified temperature anomalies for the period of 1970-2015 of 45-years duration.

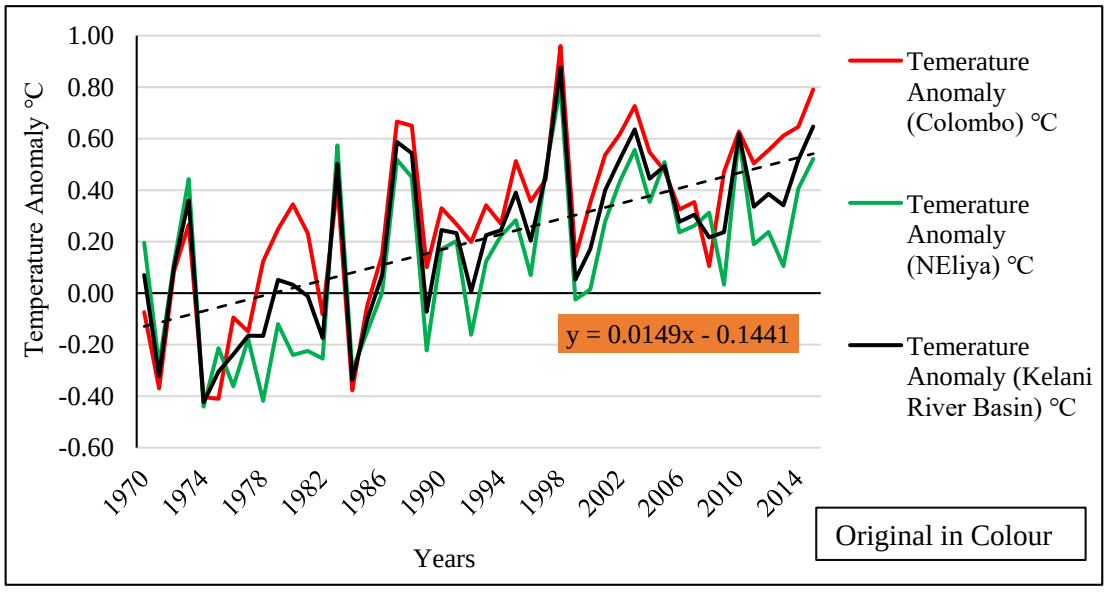

Figure 4-33 Temperature Anomaly of Colombo, Nuwara-Eliya and Kelani River Basin

According to the result of the above graph, the increment of the average temperature in the Kelani River basin is about 0.015℃/year, and the increased temperature is about 0.675℃ from 1970-2015 of 45-years duration. The expected increment of the average temperature in the Kelani River basin is about 1.27℃ to 2.00℃ at 2100 according to the observed trend.

4.3 Climate Data Downscaling

4.3.1 Calibration of Precipitation Data of GCM (NCEP/CanESM2) Model

To downscale the GCM data, SDSM model and CanESM2 (Canadian Earth System Model Version 02) climate model were used based on the multiple linear regression method. For downscaling climate data, it was first needed to calibrate the models and then validate for the observed data series. For calibration, the 1970-2000 period was selected out of the 37-year period of 1970 to 2005.

The calibration results and the summary statistics of the Hanwella sub-watershed precipitation for the period of 1970-2000 were plotted in the Figure 4-34 and tabulated in Table 4.7, respectively. For the statistical check of the downscaled results, mean (μ), standard deviation (σ), and the relative error of the mean (RE_μ), the relative error of standard deviation (RE_σ), root mean square error (RMSE) and the correlation value of R^2 were used. In the following graph, the monthly and seasonally model results are called as NCEP_M and NCEP_S respectively (Mahmood et al., 2015).

According to the summary statistics for evaluation of the future change of the climate system within the Kelani River basin, the sub-models called as monthly and seasonal models can be used.

To model the precipitation and temperature, the predictors were selected with the correlation values of Predictand and Predictors, Super Predictor to other predictors and with the PRP (%) Percentage Reduction in Partial Correlation value obtained according to the method described in Section 3.1.2. The predictors were selected from the out of 28 predictors of NCEP (National Centre for Environmental Predictions) Scenarios listed in Table 4.3 for CanESM 2 GCM.

Table 4-5 NCEP Predictors of CanESM2 GCM

No.	Predictor	Description	No.	Predictor	Description
1	nepmslpgl	Mean sea level pressure	16	ncepp8_vgl	800hPa meridional velocity
2	ncepp1_fgl	1000hPa wind speed	17	ncepp8_zgl	800hPa vorotocity
3	ncepp1_ugl	1000hPa zonal velocity	18	ncepp8thgl	800hPa wind direction
4	ncepp1_vgl	1000hPa meridional velocity	19	ncepp8zhgl	800hPa divergence
5	ncepp1_zgl	1000hPa vortocity	20	ncepp500gl	RH at 500hPa
6	ncepp1thgl	1000hPa wind direction	21	ncepp500gl_lag	Lag RH at 500hPa
7	ncepp1zhgl	1000hPa divergence	22	ncepp850gl	RH at 850hPa
8	ncepp5_fgl	500hPa wind speed	23	ncepprcpgl	Total rainfall
9	ncepp5_ugl	500hPa zonal velocity	24	nceps500gl	Specific humidity at 500hPa
10	ncepp5_vgl	500hPa meridional velocity	25	nceps850gl	Specific humidity at 850hPa
11	ncepp5_zgl	500hPa vortocity	26	ncepshumgl	Surface specific humidity
12	ncepp5thgl	500hPa wind direction	27	ncepshumgl_lag	Lag surface specific humidity
13	ncepp5zhgl	500hPa divergence	28	nceptemgl	Mean temperature at 2m height
14	ncepp8_fgl	800hPa wind speed	29	nceptempgl_lag	Lag mean temperature at 2m height
15	ncepp8_ugl	800hPa zonal velocity			

Table 4.6 represents the result of screening of predictors according to the method described by Mahmood & Babel (2012) for Colombo point rainfall station.

Table 4-6 Screening of Most Effective Predictors for Precipitation at the Colombo Climate Station

Screen No.	Predictor	R_1 (%)	R_2 (%)	P.r (%)	P value	PRP (%)
1	**ncepp1_zgl**	10.20			0.0000	
2	**ncepp1thgl**	9.60	45.73	9.69	0.0000	0.90
3	ncepshumgl_lag	9.30	19.41	17.89	0.0000	92.34
4	ncepshumgl	8.60	24.58	19.23	0.0000	100.00
5	ncepp8_zgl	7.90	74.20	12.43	0.0000	57.38
6	ncepp1_vgl	7.50	38.97	10.38	0.0182	38.33
7	**ncepp8thgl**	7.50	39.26	7.49	0.0000	0.20
8	ncepp1_ugl	6.90	46.13	5.91	0.0000	14.33
9	ncepmslpgl	6.60	35.60	9.25	0.0000	40.09
10	ncepp8_vgl	5.90	6.00	16.27	0.0000	100.00
11	**ncepp8_ugl**	4.80	33.40	4.85	0.5460	1.10
12	ncepp850gl	4.70	27.19	8.50	0.0000	80.83
13	nceps500gl	4.20	8.30	11.27	0.0000	100.00
14	ncepp8_fgl	3.90	2.97	1.84	0.0186	52.90
15	ncepp5_zgl	3.80	17.07	10.03	0.0000	100.00
16	ncepp1_fgl	3.00	5.76	5.29	0.0000	76.27
17	ncepp5_ugl	3.00	14.41	2.08	0.0000	30.70
18	ncepprcpgl	2.70	8.05	17.01	0.0000	100.00
19	**nceptempgl**	2.50	1.51	2.54	0.0000	1.44
20	nceptempgl_lag	2.10	2.59	0.45	0.0000	78.57
21	ncepp5_fgl	1.80	1.24	0.48	0.0000	73.17

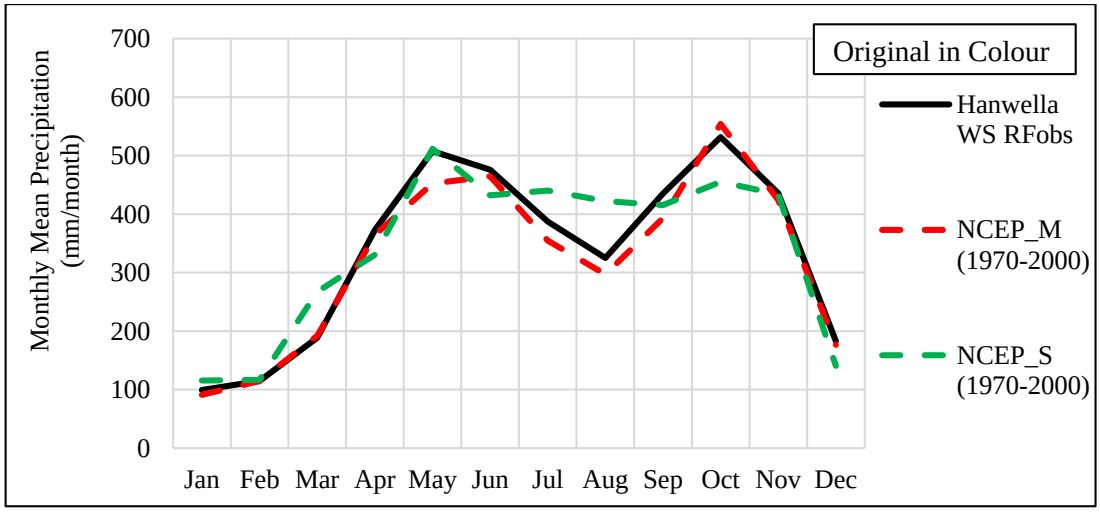

Figure 4-34 Observed and Simulated Mean Monthly Precipitation for the Calibration Period (1970-2000) in the Hanwella Sub-watershed

Table 4-7 Summary Statistics of Hanwella Sub-watershed Precipitation GCM Calibration Model Outputs

Precipitation	R^2	RMSE (mm)	μ (mm)	σ (mm)	RE_μ (%)	RE_σ (%)
Observed			11.110	16.376		
NCEP_M	0.9954	18.947	11.135	11.802	-0.221	27.925
NCEP_S	0.8719	18.954	11.119	11.407	-0.072	30.338

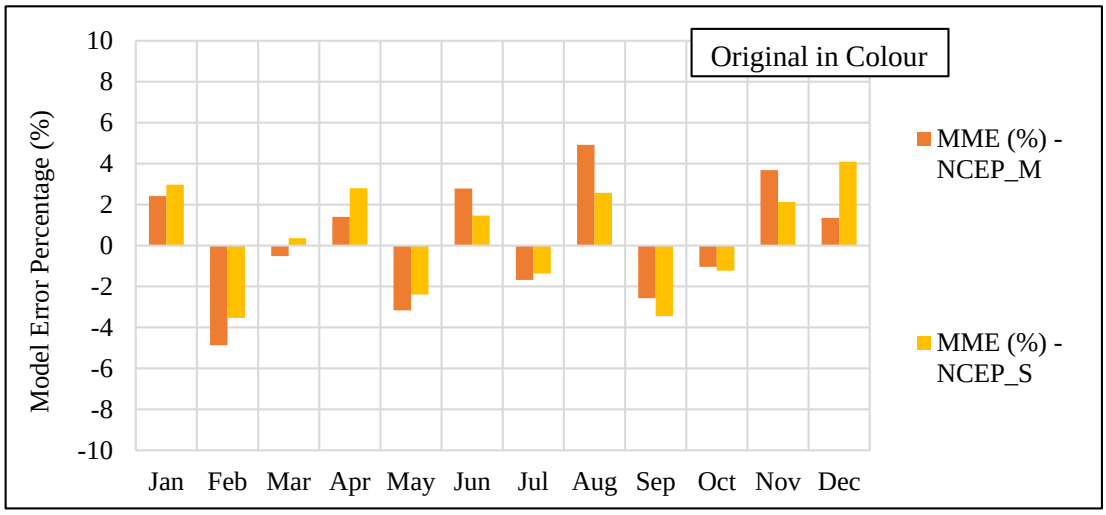

Figure 4-35 Modelled Error Percentage of Calibration of Precipitation in Hanwella Sub-watershed

Figure 4.36 depicts a detailed description about the selected predictors for precipitation modelling in the Kelani River basin.

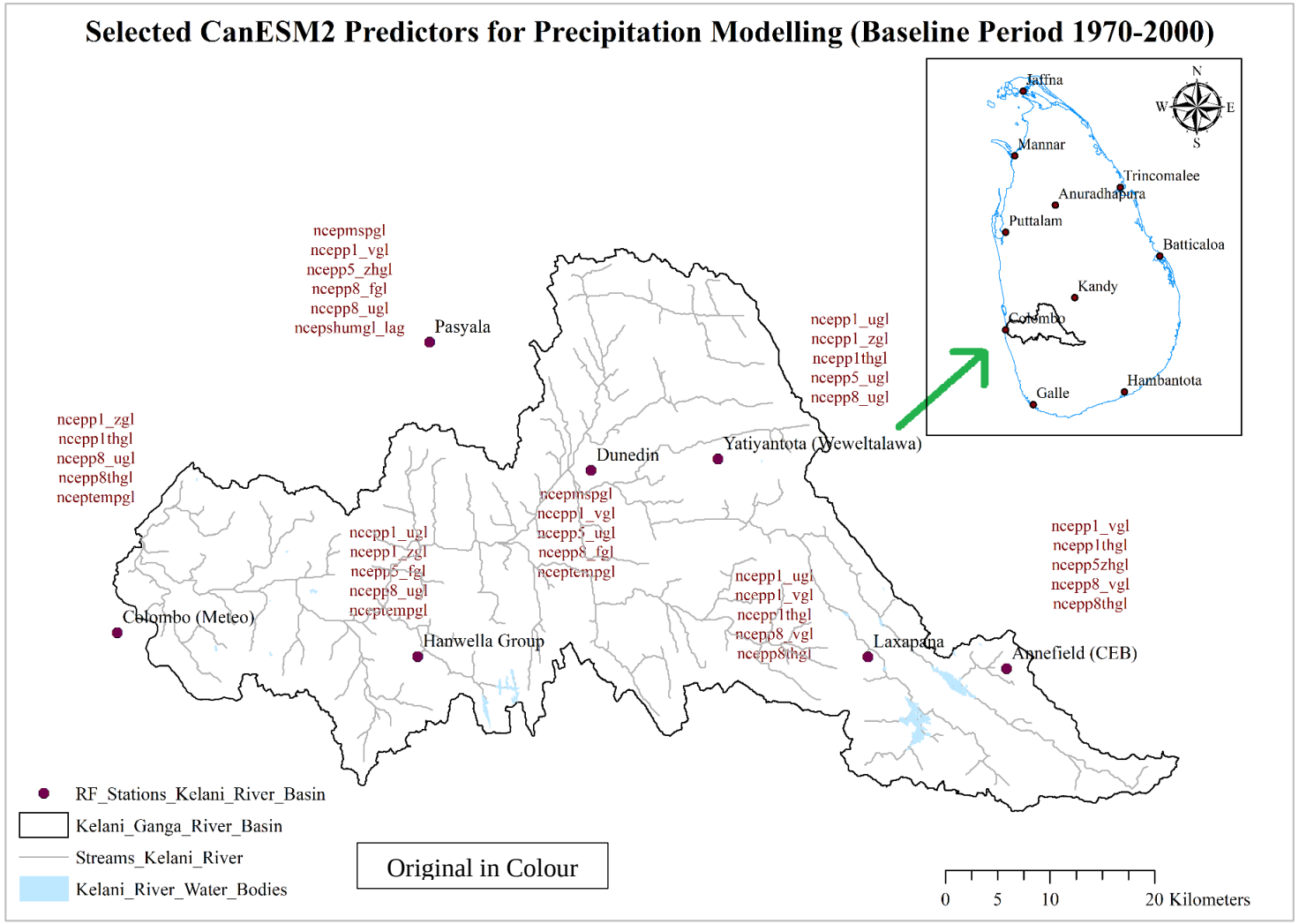

Figure 4-36 Selected Predictors for Precipitation Modelling of CanESM2 GC

4.3.2 Validation of Precipitation Data of GCM (NCEP/CanESM2) Model (without Bias Correction)

To validate the modelled rainfall, the period of 2001-2005 was selected as the validation period. The same predictors chosen previously at calibration were used to downscale the precipitation data for the validation period. In this validation, the developed NCEP scenarios were used. The standard deviation value was used to check whether the model data are within the limit with the observed mean. Figure 4-37 illustrates modelled rainfall in the Hanwella sub-watershed , for the validation period.

This model values are not bias corrected. By applying the bias correction can take the model values closer to the observed values by removing the associated biases with the GCM output results. The bias correction method is a method of shifting of means of ensembles, long-term observed and the calibrated results mean for every month to make future predictions of the precipitation as an output of NCEP, RCP2.6, RCP4.5 and RCP8.5 for present and future periods.

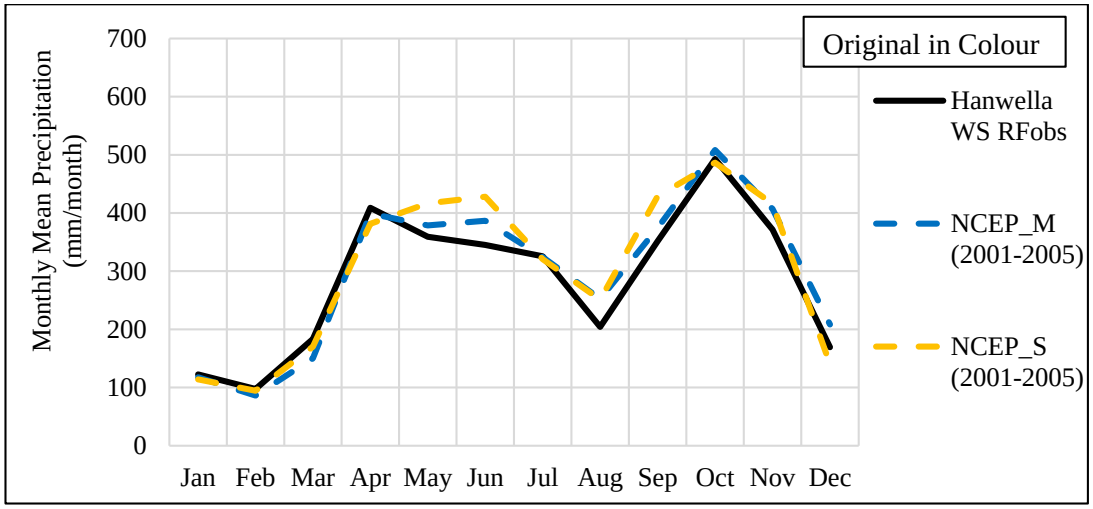

Figure 4-37 Validation of Hanwella Sub-watershed Modelled Precipitation (2001-2005) without Bias Correction

Table 4-8 Summary Statistics of Hanwella Modelled Precipitation (2001-2005) without Bias Correction

Precipitation	R^2	RMSE (mm)	μ (mm)	σ (mm)	RE_μ (%)	RE_σ (%)
Observed			9.397	12.977		
NCEP_M	0.9654	15.557	9.840	10.556	-4.675	-6.572
NCEP_S	0.9244	16.315	9.989	10.727	-6.2850	-13.599

4.3.3 Validation of Precipitation Data of GCM (NCEP/CanESM2) Model (with Bias Correction)

Bias correction effectively improves both the mean and the variance of the precipitation and temperature fields in all but a few regions of the globe. Also, bias correction has an impact on the climate change signal for specific locations and months. That is low precipitation amounts or temperature are differently corrected as high amounts due to different model bases slope of transfer function significantly differs from the effectiveness of the bias correction.

The GCM runs with the climate change signal captured and forecast it to the future. That is dependable with the functionality of the climate model. For some regions, the impact of the bias correction on the climate change signal may be more significant than the signal itself, thereby uncovering another level of uncertainty that is comparable in magnitude to the uncertainty related to the choice of the GCM or hydrology model. Note that the bias correction has only uncovered but not necessarily caused this extra level of uncertainty within the GCM – hydrology model or any other impact model within the modelling chain. Further, it is tricky to judge whether the impact of the bias correction on the climate signal leads to a more realistic signal or not. Figures 4-38 to 4-40 and Table 4-9 are indicators of the results of the bias correction for the validation of the predicted data for the present period for point rainfall.

Bias correction for the precipitation is done according to the method described in Section 2.8.4.3. Usually, bias correction is needed for precipitation only because statistical downscaling does not capture the extremes and dryness in the climate signal like dynamical downscaling.

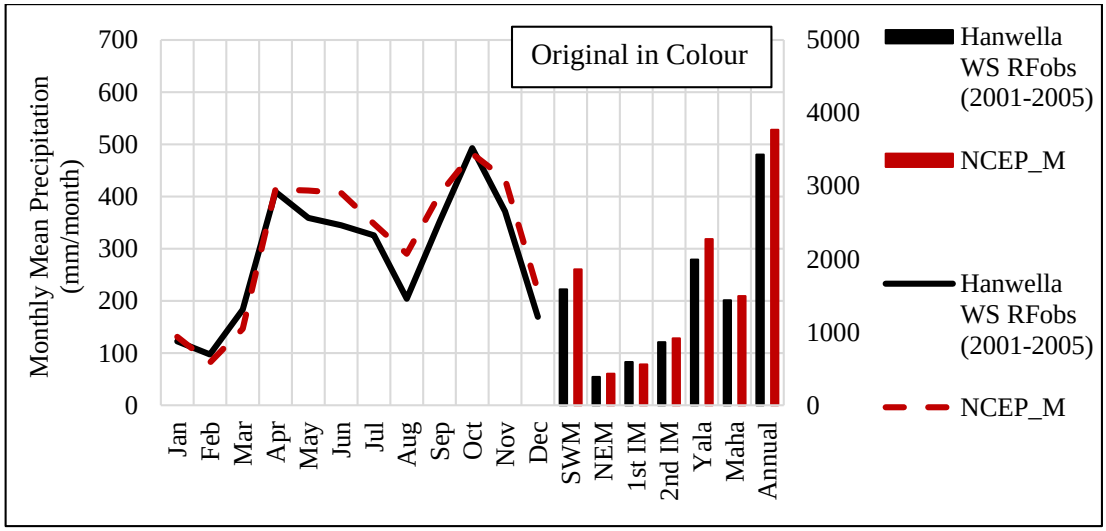

Figure 4-38 Validation of Hanwella Sub-watershed Modelled Precipitation – NCEP_M (2001-2005) with Bias Correction

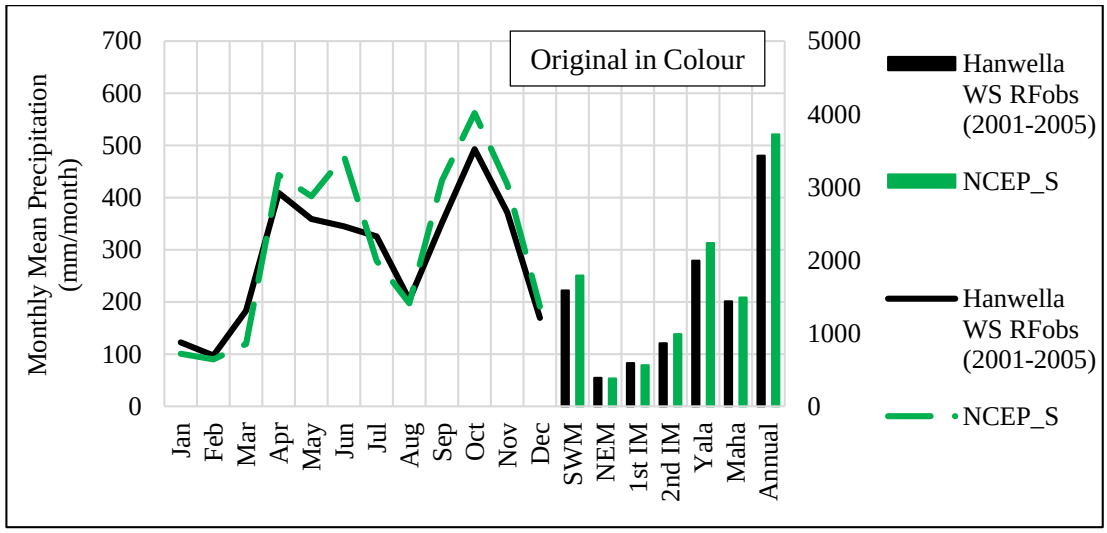

Figure 4-39 Validation of Hanwella Sub-watershed Modelled Precipitation – NCEP_S (2001-2005) with Bias Correction

Table 4-9 Summary Statistics of Hanwella Modelled Precipitation (2001-2005) with Bias Correction

Precipitation	R^2	RMSE (mm)	μ (mm)	σ (mm)	RE_μ (%)	RE_σ (%)
Observed			9.397	12.977		
NCEP_M	0.9239	15.901	10.325	11.060	-9.837	-8.774
NCEP_S	0.9250	16.315	10.196	11.464	-8.491	-32.387

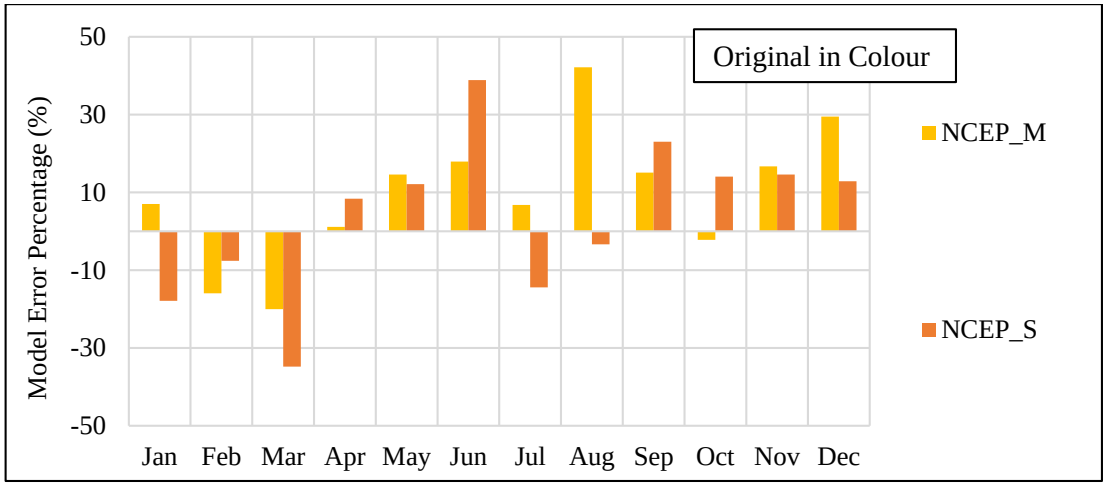

Figure 4-40 Model Error Percentage of Validation of Hanwella Sub-watershed Modelled Precipitation with Bias Correction

4.3.4 Calibration of Temperature Data of GCM (NCEP/CanESM2) Model

As in the section 4.3.1 to downscale the temperature data, the predictors which are mostly validated with the observed series by evaluating the correlation matrixes, PRP (%) values were first selected. The calibration period is also the same for precipitation from 1970-2000. Figure 4.41 and Figure 4.42 are representing the calibration of the temperature maximum and temperature minimum, respectively.

The selected predictors for the two stations of Colombo and Nuwara-Eliya are presented in the Figure 4.44. Following plotted graphs were the outputs of the model results of monthly and seasonally Temperature (max.) and Temperature (min.) of calibration of the temperature for the Kelani river basin.

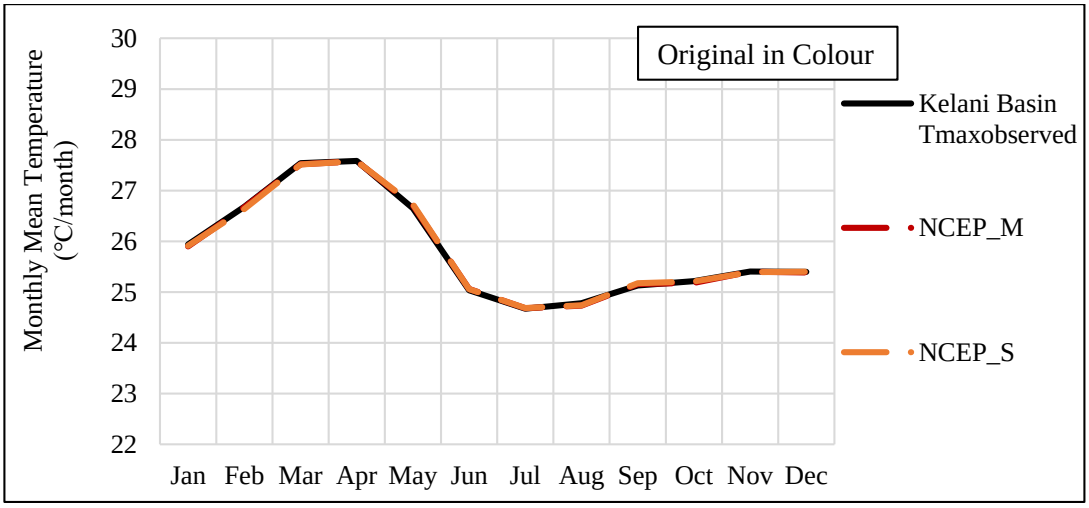

Figure 4-41 Calibration of Temperature Maximum of Kelani River Basin (1970-2000)

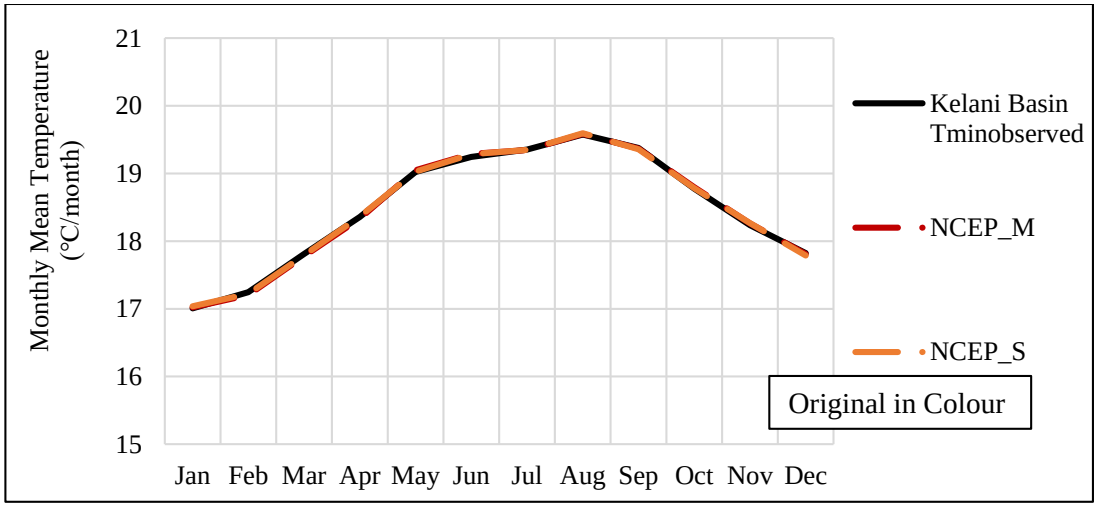

Figure 4-42 Calibration of Temperature Minimum of Kelani River Basin (1970-2000)

Figure 4.43 and Figure 4.44 represent the average model error percentage for the calibration of the temperature of the temperature maximum and temperature minimum for the period of 1970 to 2000 according to monthly and seasonal sub-models.

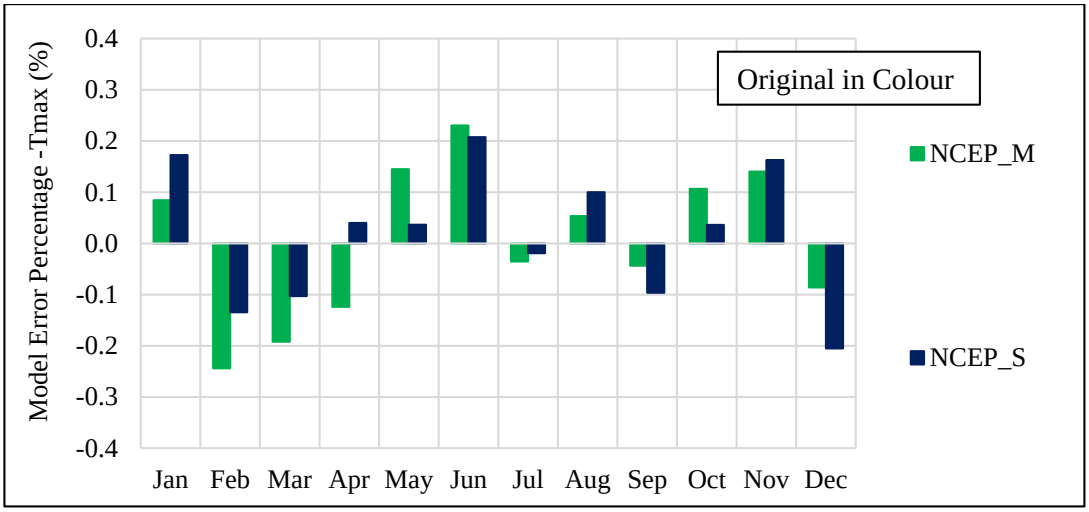

Figure 4-43 Model Error Percentage of Calibration of Temperature Maximum of Kelani River Basin

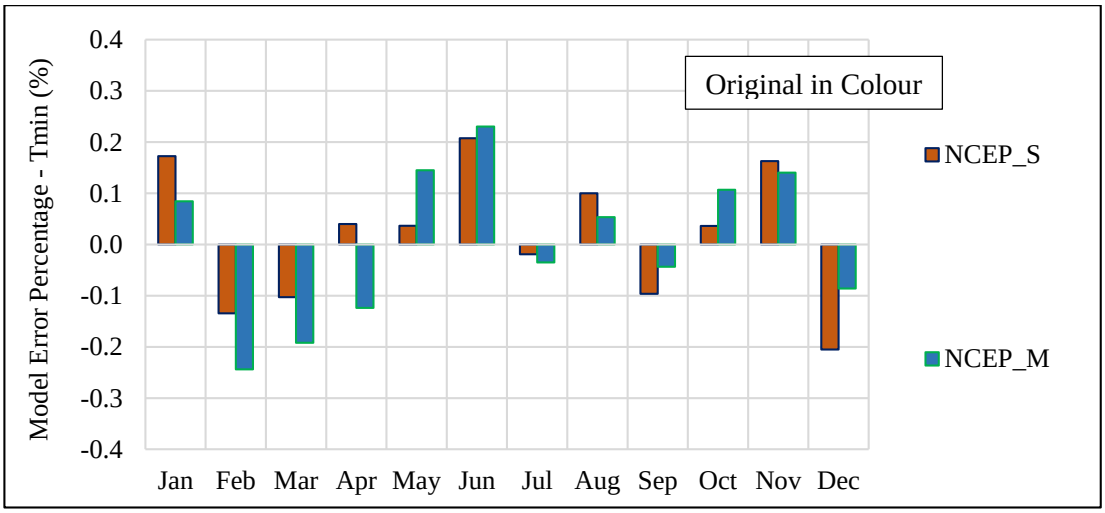

Figure 4-44 Model Error Percentage of Calibration of Temperature Minimum of Kelani River Basin

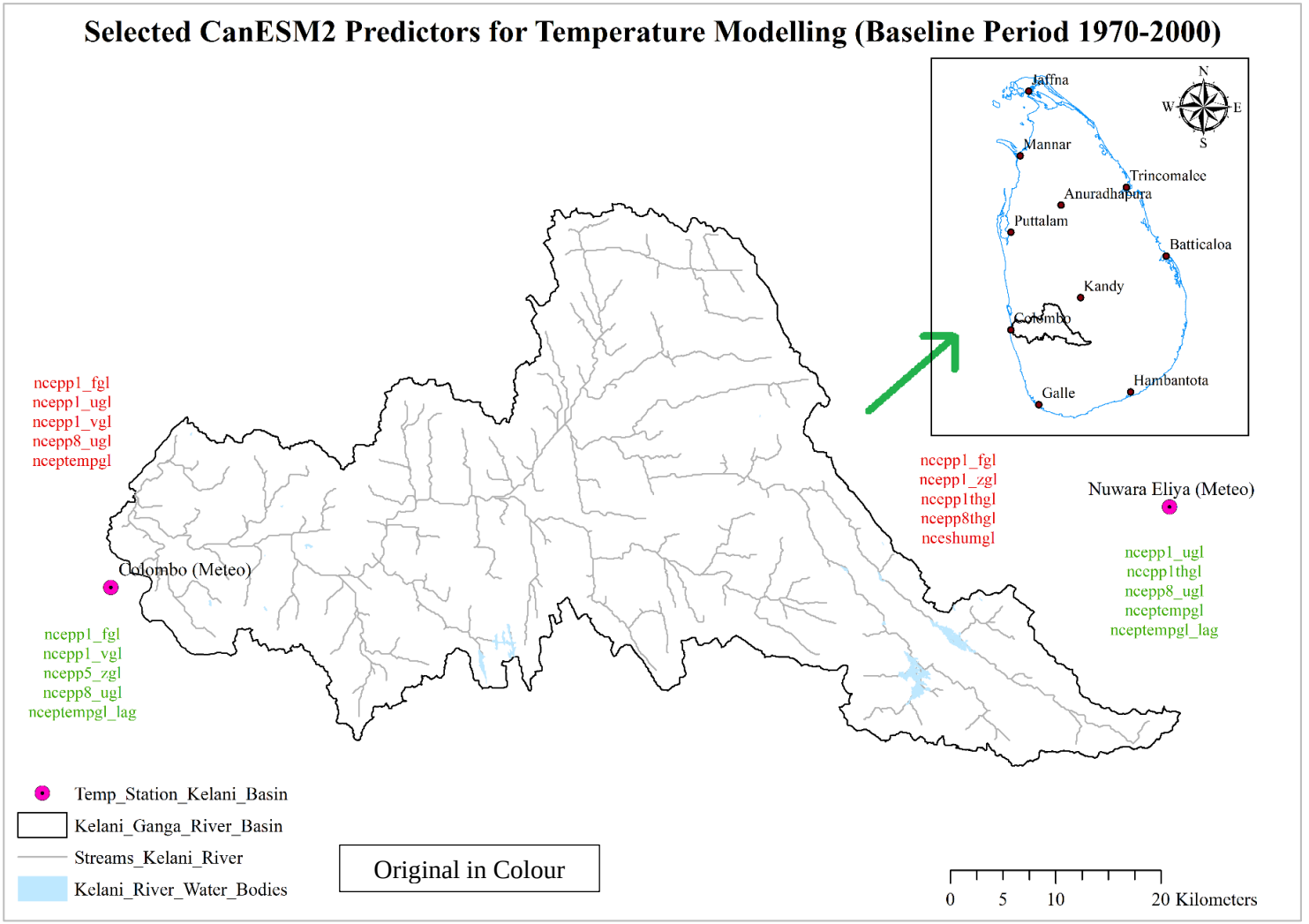

Figure 4-45 Selected Predictors for Calibration of Model of Tmax and Tmix

Table 4.10 summarises the results of the statistical check of temperature calibration in the Kelani River basin.

Table 4-10 Summary Statistics of Kelani River Basin Temperature Calibration Model Outputs

	Precipitation	R^2	RMSE (°C)	μ (°C)	σ (°C)	RE_μ (°C)	RE_σ (°C)
Tmax	Observed			25.830	1.554		
	NCEP_M	0.9991	1.741	25.826	1.620	0.000	-0.042
	NCEP_S	0.9988	1.765	25.830	1.636	0.000	-0.053
Tmin	Observed			18.492	1.513		
	NCEP_M	0.9993	1.864	18.494	1.602	0.000	-0.059
	NCEP_S	0.9958	1.881	18.495	1.649	0.000	-0.090

4.3.5 Validation of Temperature Data of GCM (NCEP/CanESM2) Model (without Bias Correction)

The wo sub models SDSM-M and SDSM-S were validated with four sets of data (two from SDSM-M and SDSM-S) generated from 2001 to 2005. Figure 4.46 and 4.47 shows the temperature maximum and minimum model output for Kelani River basin without application of bias correction. Figure 4.48 and 4.48 show the results of model error percentage without bias correction for both temperature maximum and minimum.

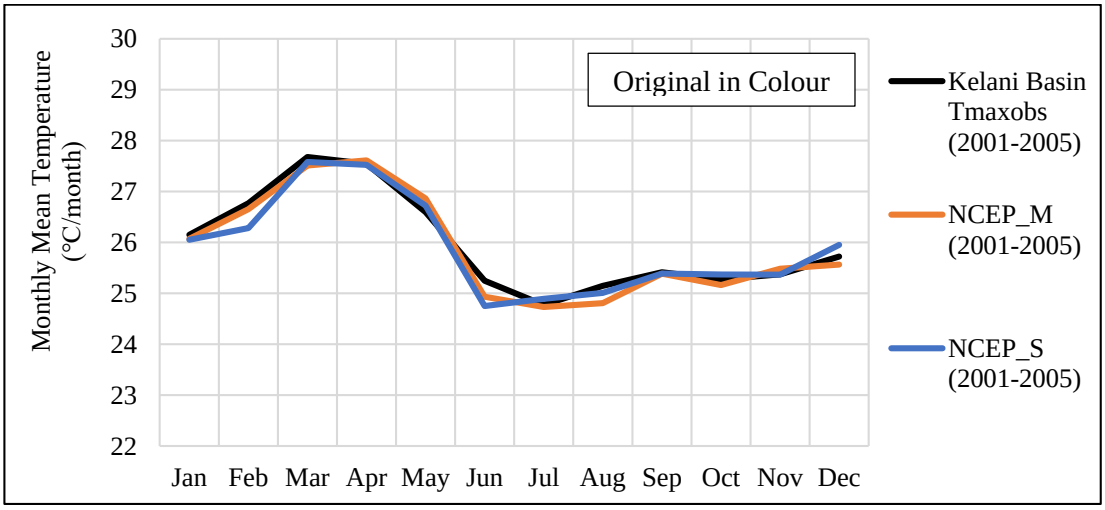

Figure 4-46 Validation of Kelani River Basin Modelled Tmax (2001-2005) without Bias Correction

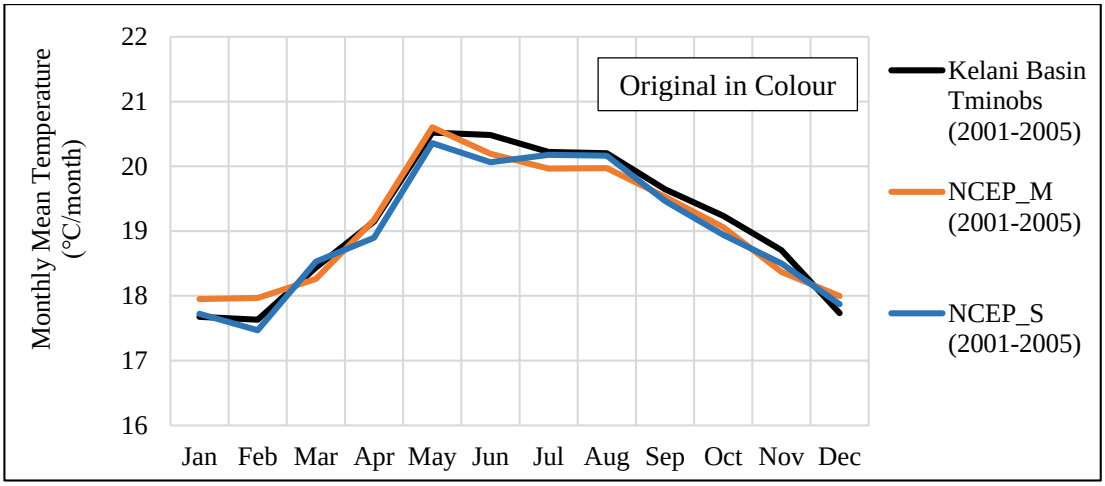

Figure 4-47 Validation of Kelani River Basin Modelled Tmin (2001-2005) without Bias Correction

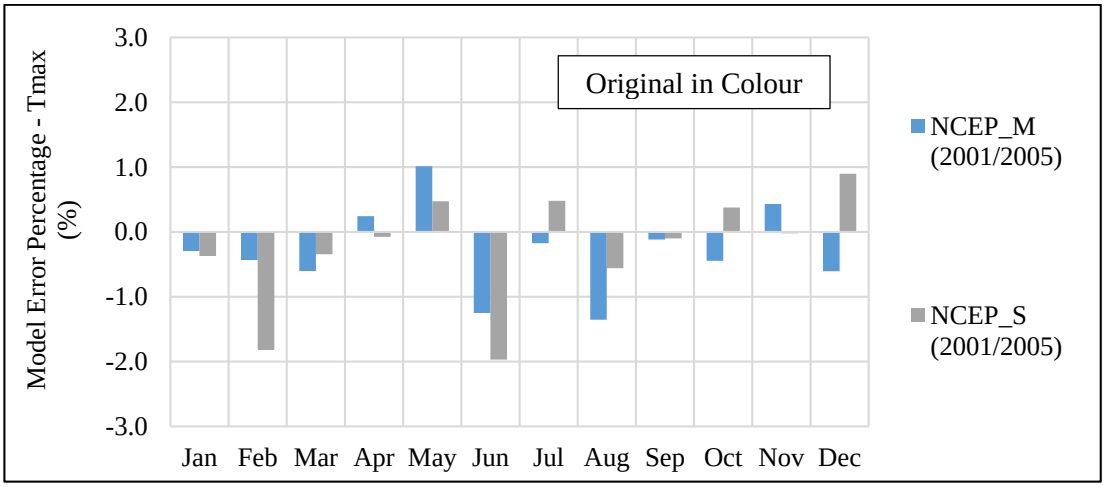

Figure 4-48 Modelled Error Percentage of Temperature Maximum without Bias Correction

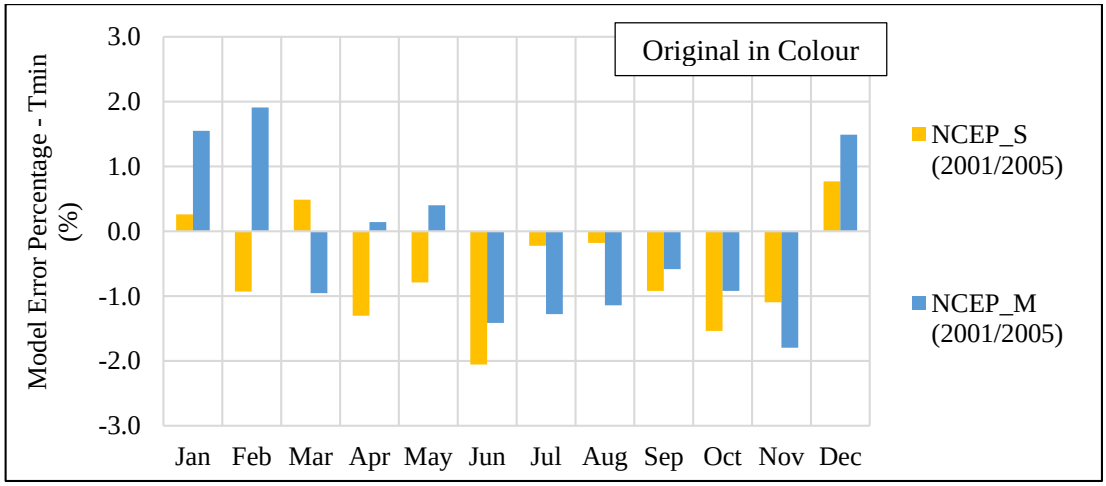

Figure 4-49 Modelled Error Percentage of Temperature Minimum with Bias Correction

Table 4.11 presents the summary statistics of validation of temperature maximum and minimum of Kelani river basin without application of bias correction.

Table 4-11 Summary Statistics of Kelani River Basin Temperature Validation Model Outputs without Bias Correction

	Precipitation	R^2	RMSE (℃)	μ (℃)	σ (℃)	RE_μ (℃)	RE_σ (℃)
Tmax	Observed			25.970	1.406		
	NCEP_M	0.9719	1.713	25.890	1.621	0.003	-0.152
	NCEP_S	0.9405	1.677	25.907	1.605	0.002	-0.142
Tmin	Observed			19.144	1.542		
	NCEP_M	0.9610	1.586	19.093	1.679	0.003	-0.087
	NCEP_S	0.9784	1.600	19.023	1.703	0.006	-0.104

4.3.6 Validation of Temperature Data of GCM (NCEP/CanESM2) Model (with Bias Correction)

The method described in Section 2.8.4.3 was applied to correct the bias of the modelled temperature maximum and minimum of the Kelani river basin. The following Figures of 4.50 and 4.51 represent the bias-corrected temperature maximum and minimum. Also, Figures of 4.52 and 4.53 represent the model error percentage of temperature

maximum and minimum concerning the observed mean for both monthly and seasonal sub-models. Table 4.12 is giving the summary statistics of the validation of Kelani river basin temperature maximum and minimum with the application of bias correction.

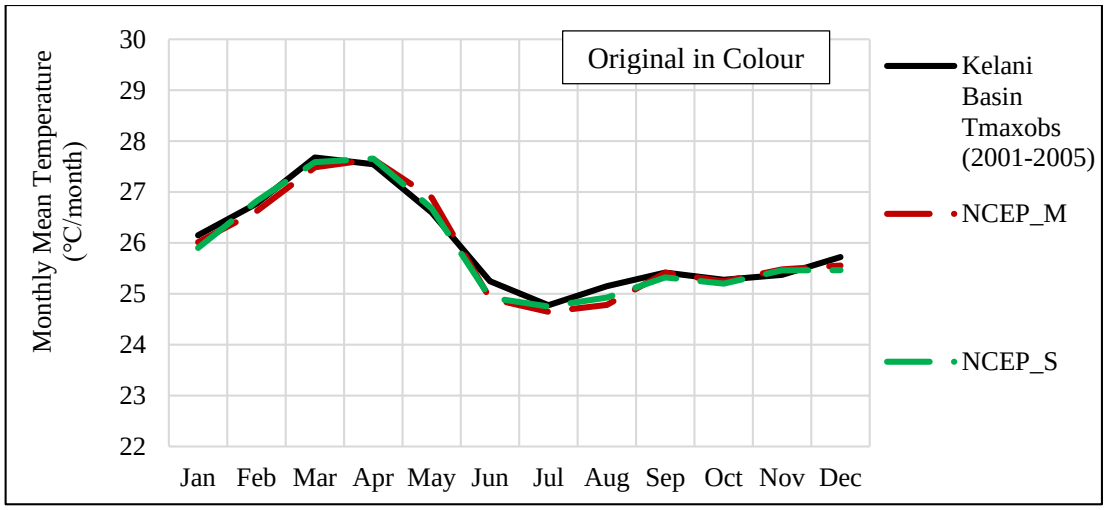

Figure 4-50 Validation of Kelani River Basin Modelled Tmax (2001-2005) with Bias Correction

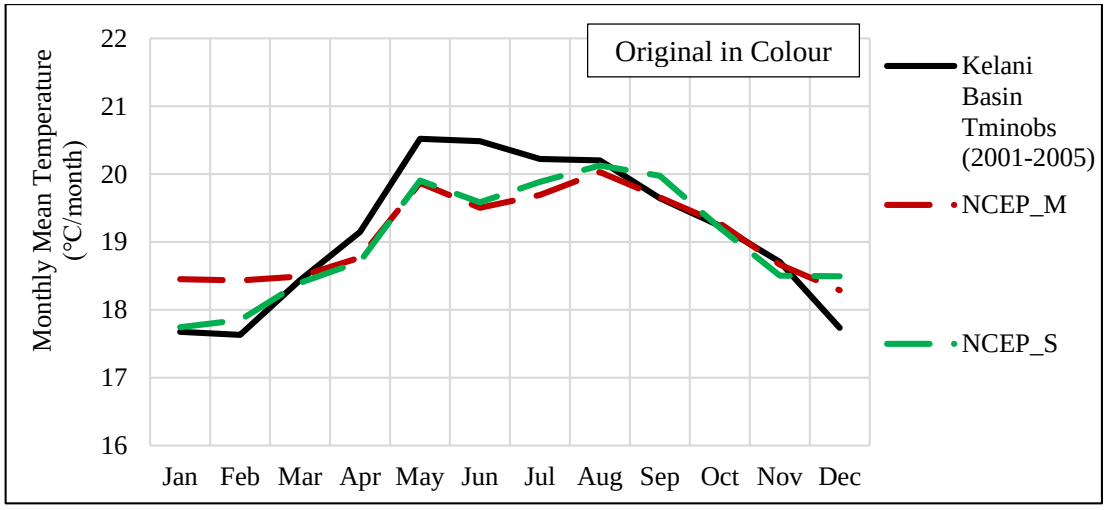

Figure 4-51 Validation of Kelani River Basin Modelled Tmin (2001-2005) with Bias Correction

According to the Figure 4.51, there was an increase in Temperature minimum between January to February and decrease between April to July. That is the temperature minimum would be increased or decreased in the modelled temperature also with respect to the observed.

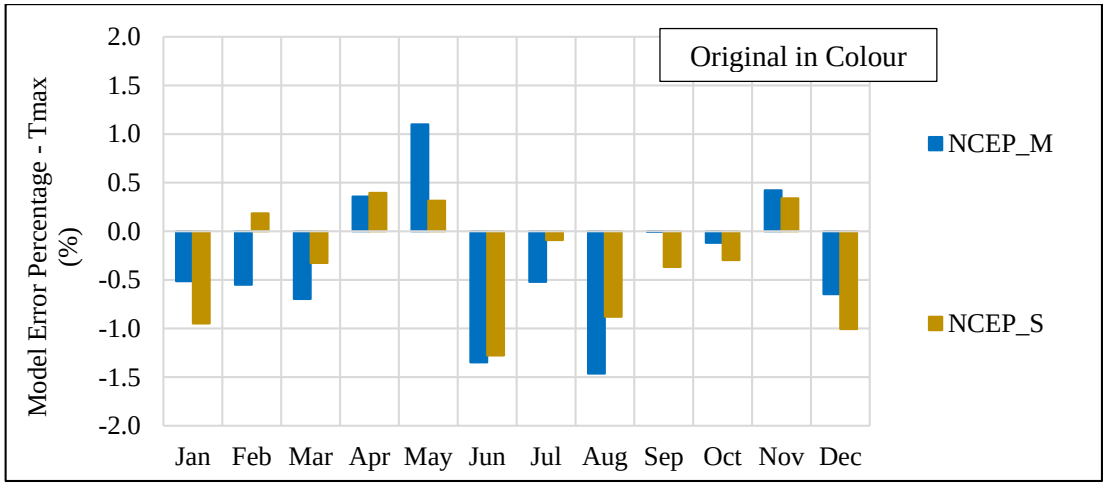

Figure 4-52 Modelled Error Percentage of Temperature Maximum with Bias Correction

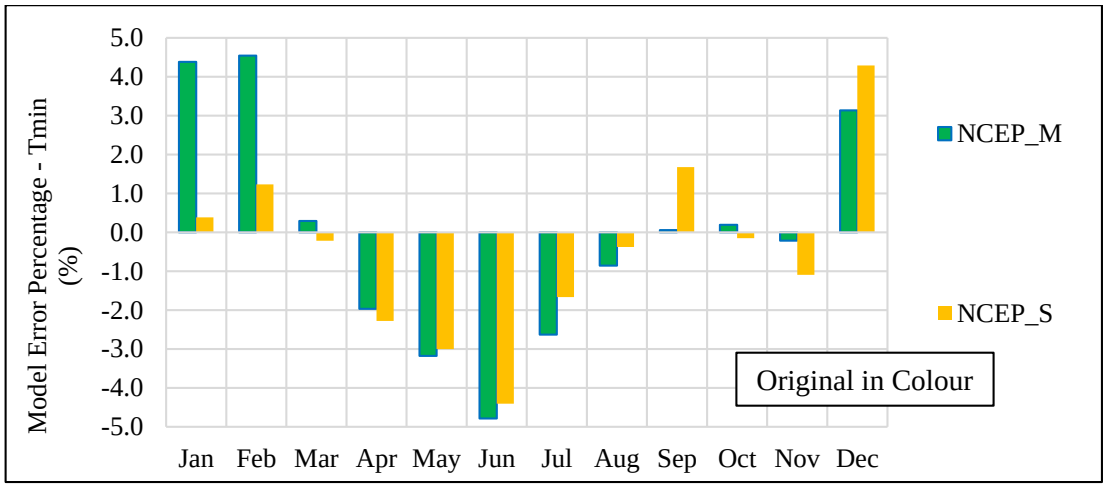

Figure 4-53 Modelled Error Percentage of Temperature Maximum with Bias Correction

As in the Figure 4.53, the model error percentage increased in the modelling of temperature minimum with respect to the temperature maximum. This kind of scenario would happen due to the length of the validation time window with respect to the calibration period.

Table 4-12 Summary Statistics of Kelani River Basin Temperature Validation Model Outputs with Bias Correction

	Precipitation	R^2	RMSE (℃)	μ (℃)	σ (℃)	RE_μ (℃)	RE_σ (℃)
Tmax	Observed			25.970	1.406		
	NCEP_M	0.9693	1.715	25.885	1.620	0.003	-0.155
	NCEP_S	0.9821	1.669	25.884	1.643	0.003	-0.169
Tmin	Observed			19.144	1.542		
	NCEP_M	0.8723	1.656	19.098	1.528	0.002	0.009
	NCEP_S	0.8620	1.649	19.040	1.612	0.005	-0.045

4.3.7 Future Changes of Catchment Rainfall under RCP2.6, RCP4.5 and RCP8.5 Scenarios

The following Table 4.13 presents the future changes in seasonal and annual mean precipitation in the Hanwella sub-watershed for the periods of 2020s (2010-2039), 2050s (2040-2069) and 2080s (2070-2099) with respect to the baseline period of 1970-2000 under the RCP2.6, RCP4.5 and RCP8.5 scenarios obtained from the two sub-models of SDSM-M and SDSM-S. The changes in precipitation predicted by two sub-models are different from each other with respect to the magnitude. Also, these two sub-models show the mean annual increments concerning the baseline period in the 2020s, 2050s and 2080s for three scenarios. The results were tabulated as the changes in catchment rainfall for Hanwella sub-watershed (Table 4-13).

Because of that, the streamflow modelling is done only using Hanwella sub-watershed, and the available calibrated streamflow model was also developed for the Hanwella sub-watershed by De Silva et al. (2014).

According to the monthly sub-model SDSM-M, the south-west monsoon (SWM) increased and the maximum increase is 18.40% for the RCP2.6 scenario for the period of the 2050s. Also, the maximum decrease is -6.01% for northeast monsoon (NEM) for the RCP8.5 scenario for the period of the 2080s.

Table 4-13 Future Changes of Catchment Rainfall (%) of Hanwella Sub-watershed under RCP2.6, RCP4.5 & RCP8.5 scenarios

	Season	SDSM-M (%)			SDSM-S (%)		
		2020s	2050s	2080s	2020s	2050s	2080s
RCP 2.6	SWM	14.33	18.40	16.75	0.60	1.96	2.37
	NEM	-0.26	-6.40	1.21	12.21	9.72	8.56
	1st IM	-0.02	-1.02	-2.50	4.47	-2.86	6.02
	2nd IM	2.73	-1.63	-1.87	13.11	15.38	16.87
	Yala	12.35	16.18	15.13	3.65	3.67	4.13
	Maha	0.79	-3.85	2.09	7.85	7.81	7.67
	Annual	7.93	8.51	9.24	5.25	5.26	6.32
RCP 4.5	SWM	15.65	13.28	14.58	0.88	3.76	2.89
	NEM	-5.94	-3.29	-3.05	14.73	17.54	16.81
	1st IM	-2.13	-1.58	-2.97	1.42	5.29	6.01
	2nd IM	0.48	5.00	4.38	13.37	16.68	13.15
	Yala	13.72	11.88	14.16	3.59	7.37	4.87
	Maha	-2.61	0.76	1.30	8.02	10.06	9.75
	Annual	7.47	7.62	6.89	5.29	8.40	9.12
RCP 8.5	SWM	13.62	13.54	12.33	2.44	5.95	4.01
	NEM	-0.23	-5.35	-6.01	15.31	13.42	16.75
	1st IM	-1.59	0.92	1.05	-0.28	3.20	4.11
	2nd IM	1.48	2.21	1.93	14.36	17.28	17.01
	Yala	12.17	11.91	11.87	4.53	8.13	7.56
	Maha	-0.64	-0.29	1.00	8.80	10.40	9.59
	Annual	7.26	7.24	8.05	6.16	9.00	10.34

* SWM – South West monsoon (May – September), NEM – North East monsoon (December – February), 1st IM – First inter monsoon (March – April), 2nd IM – Second inter monsoon (October – November)

Figure 4.54 to Figure 4.57 represent the future changes in the mean of precipitation in the Kelani river basin and Hanwella sub-watershed, respectively, according to monthly and seasonal sub-models for the 2020s, 2050s and 2080s future periods.

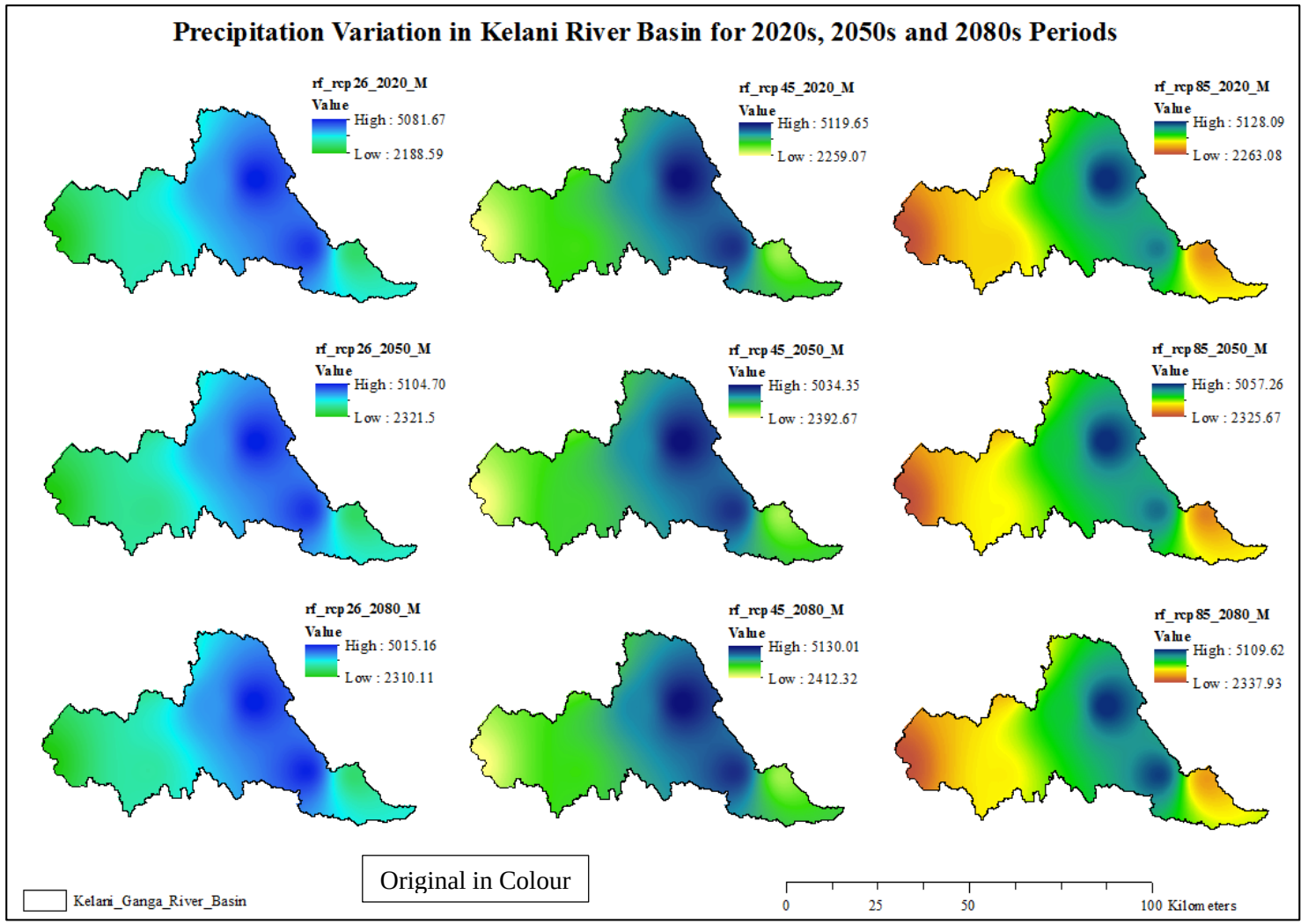

Figure 4-54 Future Change of Average Annual Precipitation in Kelani River Basin for SDSM-M

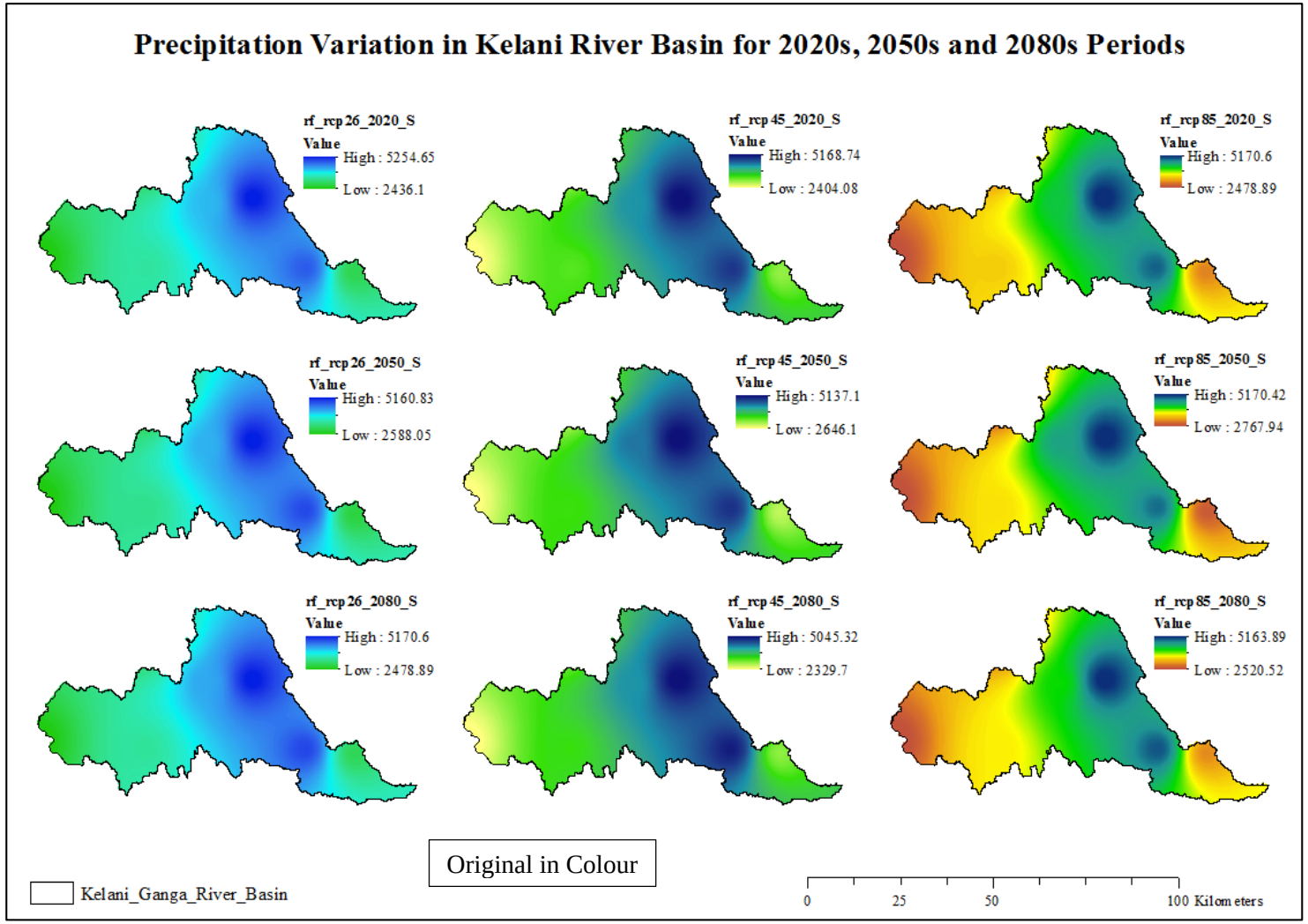

Figure 4-55 Future Change of Average Annual Precipitation in Kelani River Basin for SDSM-S

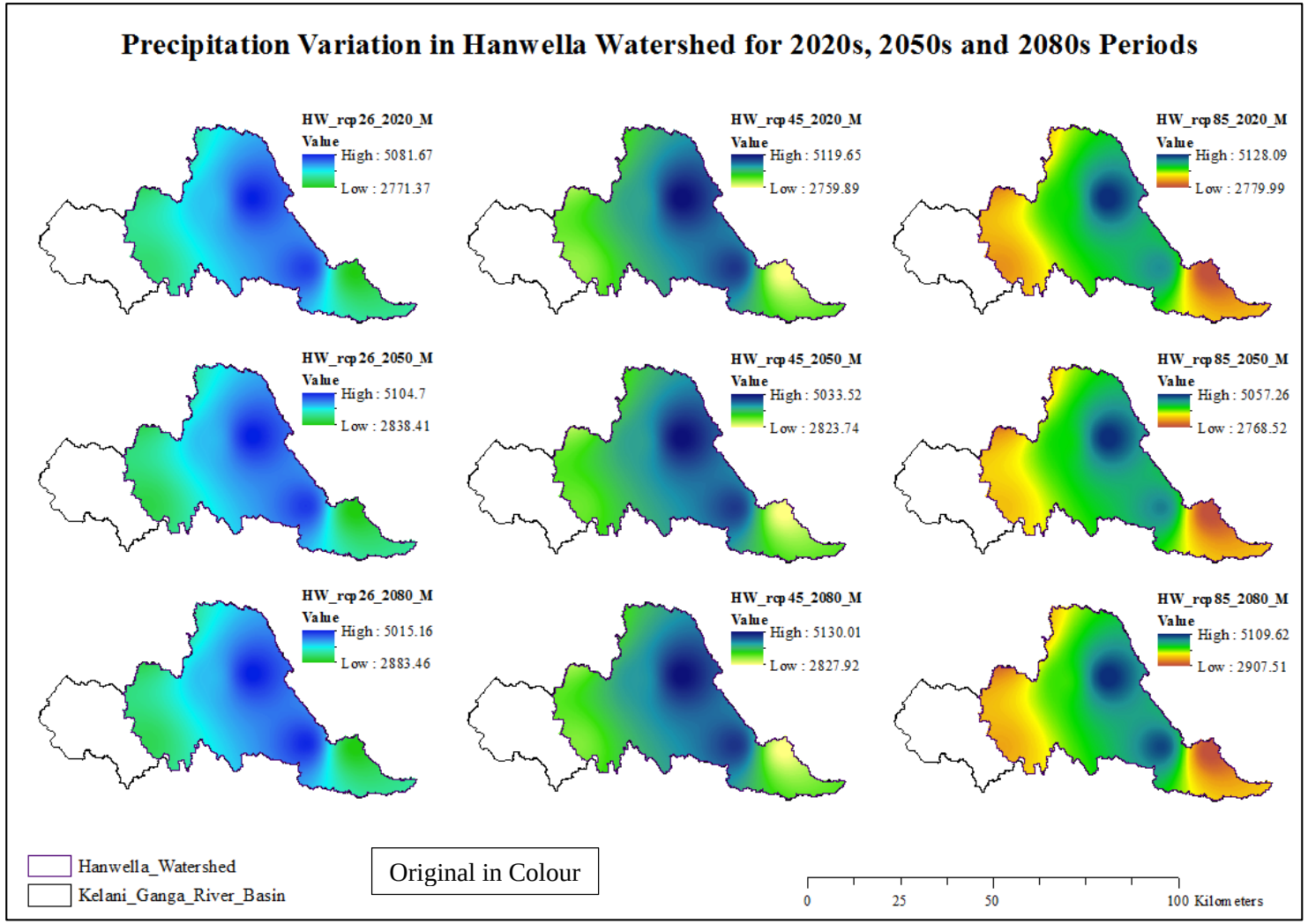

Figure 4-56 Future Change of Average Annual Precipitation in Hanwella Sub-watershed for SDSM-M

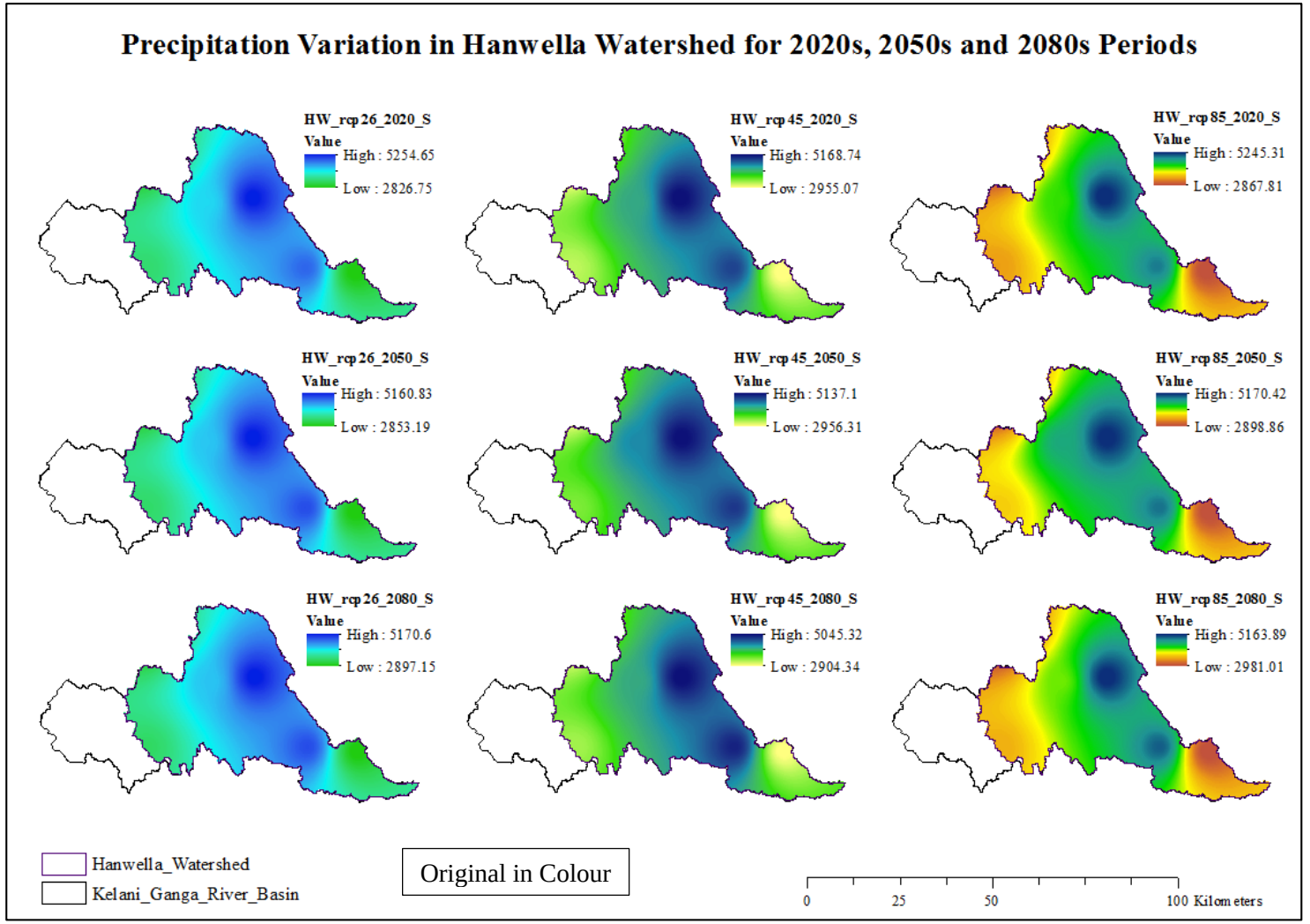

Figure 4-57 Future Change of Average Annual Precipitation Change in Hanwella Sub-watershed for SDSM-S

4.3.8 Future Changes of Temperature (T_{max} and T_{min}) RCP2.6, RCP4.5 and RCP8.5 Scenarios

The temperature trends in observed data are calculated for the Kelani River Basin with respect to the Colombo and Nuwara-Eliya temperature gauge stations. The following two tables of Table 4.14 and 4.15 represent the results of the future changes of the T_{max} and T_{min} for catchment average temperature variation with respect to the SDSM-M and SDSM-S sub-models for the future periods of the 2020s (2010-2039), 2050s (2040-2069) and 2080s (2070-2099) under RCP2.6, RCP4.5 and RCP8.5 scenarios as increment or decrement of the river basin average temperature maximum and minimum with respect to the baseline period of 1970-2000. To calculate the average catchment temperature, Thiessen polygon map was used (Figure 4.28).

According to the Table 4.14, the maximum increase for the maximum of temperature minimum is 2.81℃ for the 2020s period by seasonal sub-model for the RCP2.6 scenario, and minimum decrement of the minimum of temperature minimum is -1.85℃ for 2050s period by monthly sub-model for RCP4.5 scenario.

Table 4-14 Future Change of Temperature Minimum of Kelani River Basin

Kelani River Basin **Tmin**		Observed Maximum (℃)		Observed Minimum (℃)	
		22.77		**10.94**	
		SDSM-M (℃)	SDSM-S (℃)	SDSM-M (℃)	SDSM-S (℃)
2020s	RCP2.6	1.75	2.81	0.02	0.09
	RCP4.5	1.29	2.30	-0.35	-0.19
	RCP8.5	0.86	1.55	-0.74	0.17
2050s	RCP2.6	1.37	1.84	0.10	-0.11
	RCP4.5	1.32	2.38	-1.85	-1.00
	RCP8.5	1.58	1.43	-0.71	-0.37
2080s	RCP2.6	1.41	1.89	-0.65	-0.93
	RCP4.5	1.32	1.96	0.11	-0.79
	RCP8.5	0.71	2.55	0.34	-1.22

According to the Table 4.15, the maximum increase for the maximum of temperature maximum is 1.64℃ for the 2020s period by seasonal sub-model for the RCP2.6 scenario, and minimum decrement of the minimum of temperature maximum is -0.97℃ for 2020s period by seasonal sub-model for RCP4.5 scenario.

Table 4-15 Future Change of Temperature Maximum of Kelani River Basin

Kelani River Basin **Tmax**		Observed Maximum (℃)		Observed Minimum (℃)	
		31.00		**19.60**	
		SDSM-M (℃)	SDSM-S (℃)	SDSM-M (℃)	SDSM-S (℃)
2020s	RCP2.6	0.99	1.64	0.97	0.74
	RCP4.5	0.56	1.03	0.84	-0.97
	RCP8.5	0.77	0.86	0.79	0.11
2050s	RCP2.6	0.87	0.83	0.78	0.24
	RCP4.5	0.52	0.84	0.87	0.07
	RCP8.5	1.09	1.13	0.64	0.03
2080s	RCP2.6	0.55	0.88	0.57	0.52
	RCP4.5	0.25	1.12	0.76	0.04
	RCP8.5	1.03	1.36	0.88	0.91

Table 4.16 and 4.17 represents the model maximum and minimum of the temperature minimum and the maximum of Colombo and Nuwara-Eliya meteorology observations. The maximum increase of temperature maximum for Colombo is 2.18℃ for monthly sub-model in the 2080s period according to the RCP8.5 scenario and for Nuwara-Eliya is 3.29℃ for monthly sub-model in the 2020s period according to the RCP2.6 scenario, respectively. Also, the maximum increase of temperature minimum for Colombo is 3.25℃ for seasonal sub-model in the 2050s period according to the RCP8.5 scenario and for Nuwara-Eliya is 5.95℃for seasonal sub-model in the 2080s period according to the RCP8.5 scenario.

Figure 4.58 shows the future change of the average temperature of the Kelani River Basin according to the monthly sub-model (SDSM-M).

Table 4-16 Future Change of Temperature Minimum at Point Temperature in Kelani River Basin

Tmin		Colombo				Nuwara-Eliya			
		Max (℃)		Min (℃)		Max (℃)		Min (℃)	
		29.60		**16.40**		**17.90**		**0.40**	
		SDSM-M		SDSM-S		SDSM-M		SDSM-S	
		max	min	max	min	max	min	max	min
2020s	RCP2.6	2.12	-0.89	2.38	1.04	3.61	0.55	4.51	0.24
	RCP4.5	2.14	0.08	1.86	1.25	4.88	-0.36	4.42	-0.25
	RCP8.5	2.18	-2.07	2.27	0.94	3.52	0.16	4.47	0.87
2050s	RCP2.6	1.93	-0.50	2.26	1.07	4.58	1.33	3.89	3.53
	RCP4.5	3.08	-1.36	1.75	0.81	3.54	1.58	3.41	2.55
	RCP8.5	2.39	1.15	3.25	0.88	4.01	2.00	3.76	2.78
2080s	RCP2.6	1.86	-0.40	1.74	0.49	5.91	0.24	3.60	0.94
	RCP4.5	1.97	0.90	1.25	0.99	3.67	0.04	4.29	-0.30
	RCP8.5	2.18	0.89	2.16	1.63	3.42	0.17	5.95	0.20

Table 4-17 Future Change of Temperature Maximum at Point Temperature in Kelani River Basin

Tmax		Colombo				Nuwara-Eliya			
		Max (℃)		Min (℃)		Max (℃)		Min (℃)	
		37.00		**21.60**		**27.70**		**13.50**	
		SDSM-M		SDSM-S		SDSM-M		SDSM-S	
		max	min	max	min	max	min	max	Min
2020s	RCP2.6	0.16	0.75	0.10	4.21	1.25	-2.43	2.98	-3.30
	RCP4.5	0.14	3.59	-0.17	2.60	3.29	-2.85	3.49	-2.66
	RCP8.5	0.17	2.79	0.23	2.06	1.11	-3.61	2.09	-4.29
2050s	RCP2.6	0.28	-0.61	1.24	3.97	1.93	-2.96	1.78	-3.62
	RCP4.5	1.13	2.61	0.14	3.54	1.39	-4.66	1.18	-3.47
	RCP8.5	0.21	3.23	0.53	4.01	2.53	-2.82	1.54	-3.01
2080s	RCP2.6	0.03	0.25	-0.16	4.12	1.75	-3.81	2.25	-5.22
	RCP4.5	0.74	3.68	0.14	3.77	1.23	-3.10	2.90	-3.67
	RCP8.5	2.18	3.63	-0.35	4.14	1.68	-2.80	2.75	-1.78

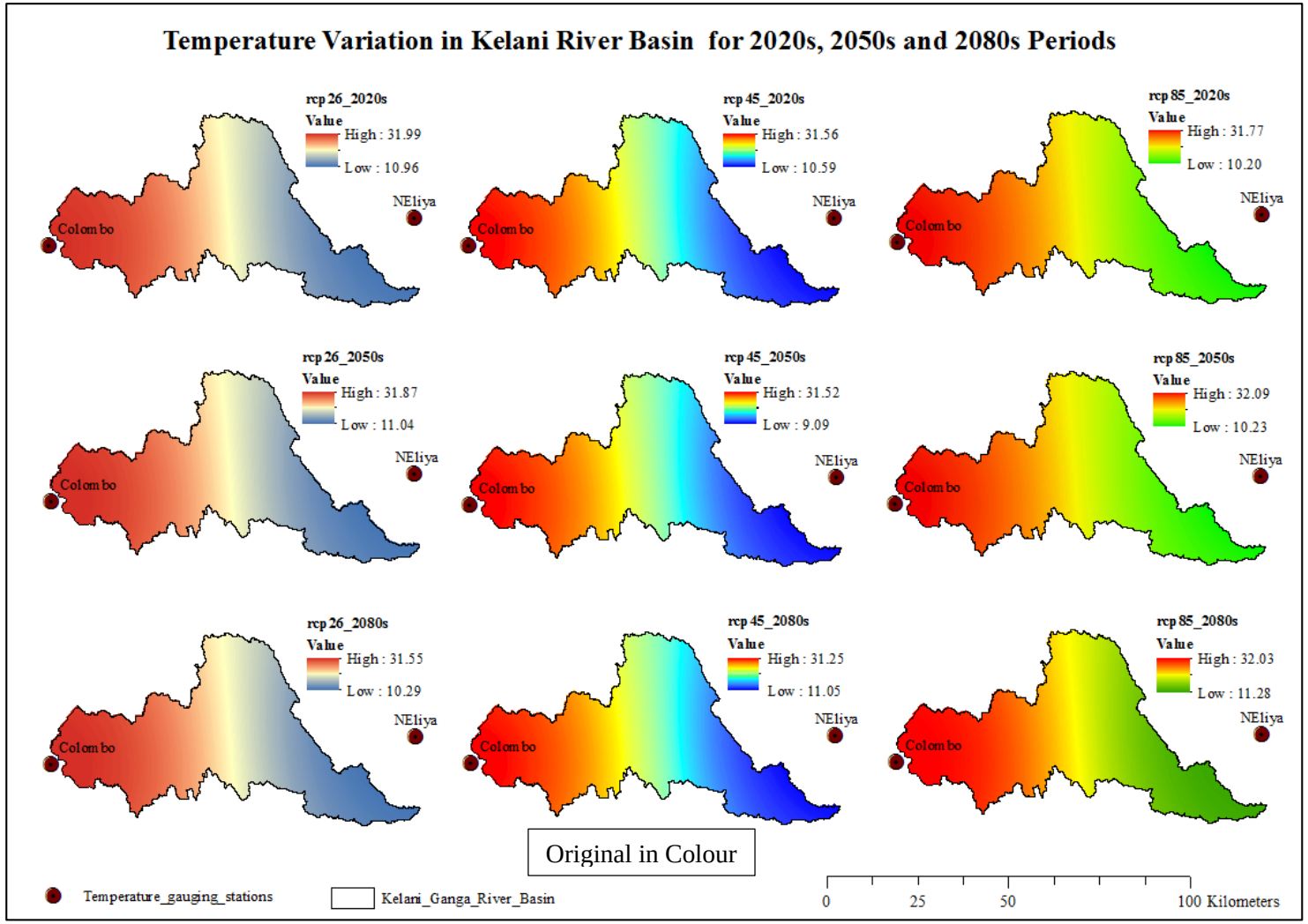

Figure 4-58 Future Change of Average Temperature in Kelani River Basin

4.4 Future Streamflow Variation in Hanwella Sub-watershed

The Hanwella sub-watershed was selected to evaluate the future change of the streamflow in the Kelani River basin and also the existing developed hydrology model was used. Hanwella sub-watershed is the largest upper sub-catchment of the Kelani river basin, and the gauging station of the Hanwella is placed just upstream from sea-fall of the river within 30km distance (De Silva et al., 2014). This model was developed to calculate the event-based and continuous streamflow. For the present study, the continuous based model was used. The Table 4.18 and 4.19 represent the calibrated model parameters of continuous hydrology model of streamflow modelling in Hanwella sub-watershed of Kelani river basin.

In the continuous model, Soil Moisture Accounting method was used as loss method and Recession Baseflow method was used as baseflow extimation method to model streamflow and the baseflow of the Hanwella sub-watershed in Kelani river basin.

Table 4-18 Calibrated Parameters of Hydrograph and Baseflow Methods (De Silva et al., 2014)

Hydrograph	
Parameter	Value
Time of Concentration (Tc)	28 hrs.
Storage Coefficient (R)	40 hrs.
Baseflow	
Parameter	Value
Initial Discharge (m^3/s)	65.0
Recession Constant	0.54
Ratio to Peak	0.40

Table 4-19 Summary of Calibrated Parameters of Soil Moisture Accounting Loss Method (De Silva et al., 2014)

Parameter	**Value**
Canopy (%)	0
Surface (%)	0
Soil (%)	70
Ground water 1 (%)	45
Ground water 2 (%)	82
Canopy storage (mm)	10
Surface storage(mm)	0
Maximum infiltration (mm/h)	10
Imperviousness (%)	40
Soil storage (mm)	125
Tension storage (mm)	75
Soil percolation (mm/h)	1
Ground water 1 storage (mm)	100
Ground water 1 percolation (mm/h)	1
Ground water 1 coefficient (hr)	100
Ground water 2 storage (mm)	150
Ground water 2 percolation (mm/h)	1
Ground water 2 coefficient (hr)	1

Due to the non-stationarity of the precipitation data, there would be a significant change for the result of the streamflow model with respect to the modelled flow at validation. Hence, for the present study, only the change of the baseflow model was considered as a sensitivity analysis. This is because of the non-stationarity condition of the precipitation with respect to the climate change.

4.4.1 Sensitivity Analysis of HEC-HMS Calibrated Model

As discussed in the section 3.1.4, the sensitivity analysis was performed according to the method of local sensitivity analysis. The existing model developed was validated for the period from January 2005 to December 2007. For the present study, also with the different precipitation stations with respect to the existing ones, the model was validated for the same time window from January 2005 to December 2007. Table 4.20, gives the tabulated results of the objective functions selected (Nash-Sutcliffe and

MRAE results) for evaluation of the streamflow model output. The flow duration curve and the model flow and observed flow graphs are also given in Figures 4-59~4-61.

Table 4-20 HEC-HMS Model Performance of Streamflow Modelling from Calibrated Model of Hanwella Sub-watershed (De Silva et al., 2014)

Hanwella Sub-watershed Model	Nash-Sutcliff	MRAE	Mass Balance Error (%)	Flow Comparison					
				High		**Intermediate**		**Low**	
				MRAE	NASH	MRAE	NASH	MRAE	NASH
Jan, 05 – Dec, 07	0.749	0.502	-3.15	0.303	0.340	0.476	-0.142	0.821	-65.515

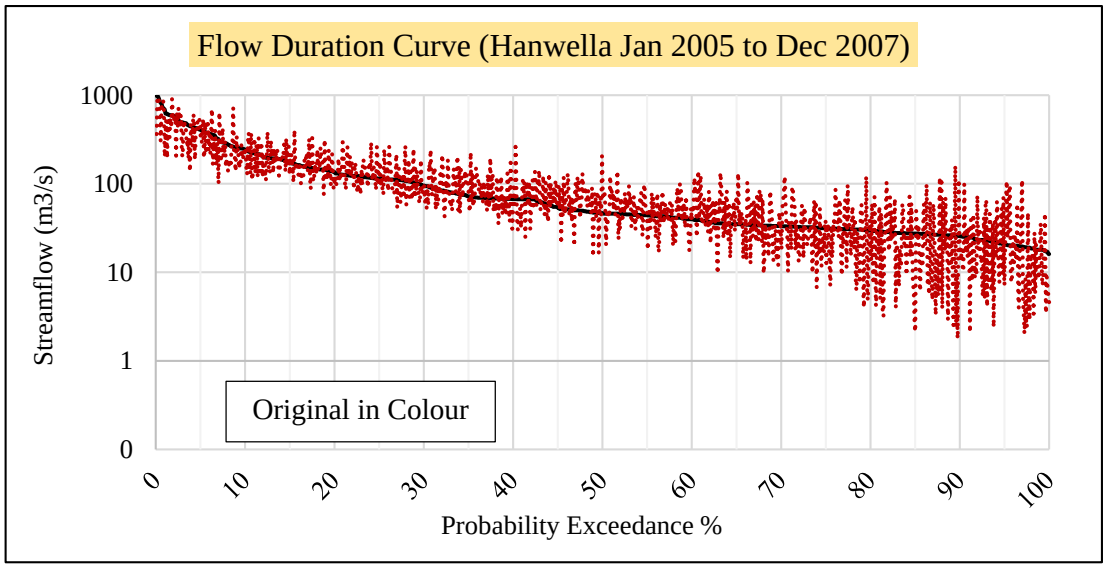

Figure 4-59 Flow Duration Graph of HEC-HMS Model Flow and Observed Flow (Jan, 2005 - Dec, 2007)

According to the Figure 4.59, the model flow slightly underestimated in high flows and somewhat overestimated in low flow (Table 4.20). According to the model sensitivity with respect to the baseflow model, the initial discharge, recession constant and ratio to peak were modified to the following new values tabulated in Table 4.21. Further, the percentage increase and decrease with the existing model are also given in the same table. According to the Table 4.21, the initial discharge was increased by 10%, recession constant was increased by 50% and ratio to peak flow was decreased

by 30% with respect to the existing baseflow parameters to obtain the reliability of the calibrated HEC-HMS model application for Hanwella sub-watershed to evaluate the future streamflow in the Kelani River basin.

Table 4-21 Summary Result of Sensitivity Analysis of Baseflow Model

Parameter	Existing Values	New Value	(%) change
Initial Discharge (m3/s)	65.0	71.5	10.0
Recession Constant	0.54	0.81	50.0
Ratio to Peak	0.40	0.28	-30.0

Figure 4.60 attached below shows the model performance with respect to the goodness of fit value (R^2) which is represents that 75% of the model flow is satisfactory with respect to the observed flow.

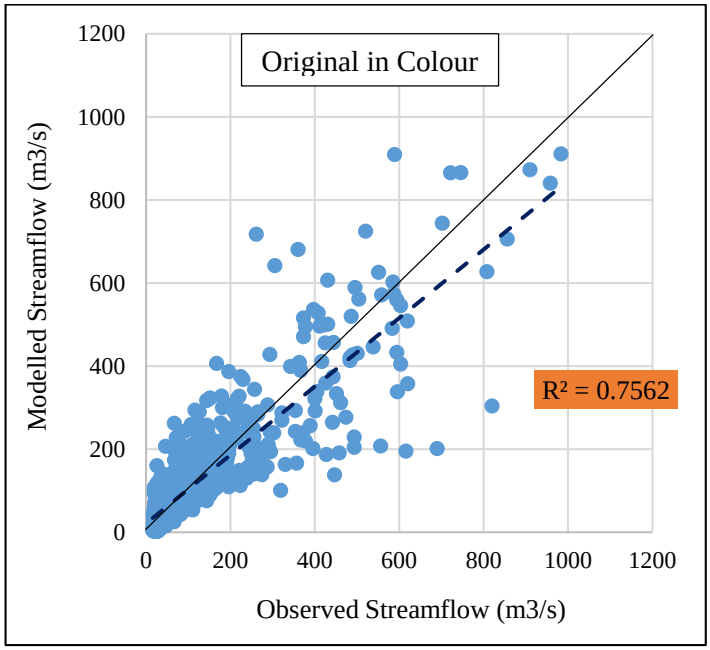

Figure 4-60 Streamflow Model Performance with respect to the Observed Streamflow at Hanwella

The following Figure 4.61, attached is the comparison of model streamflow and observed streamflow for the model application period of January 2005 to December

2007 for Hanwella sub-watershed for the newly changed baseflow parameters tabulated in Table 4.21.

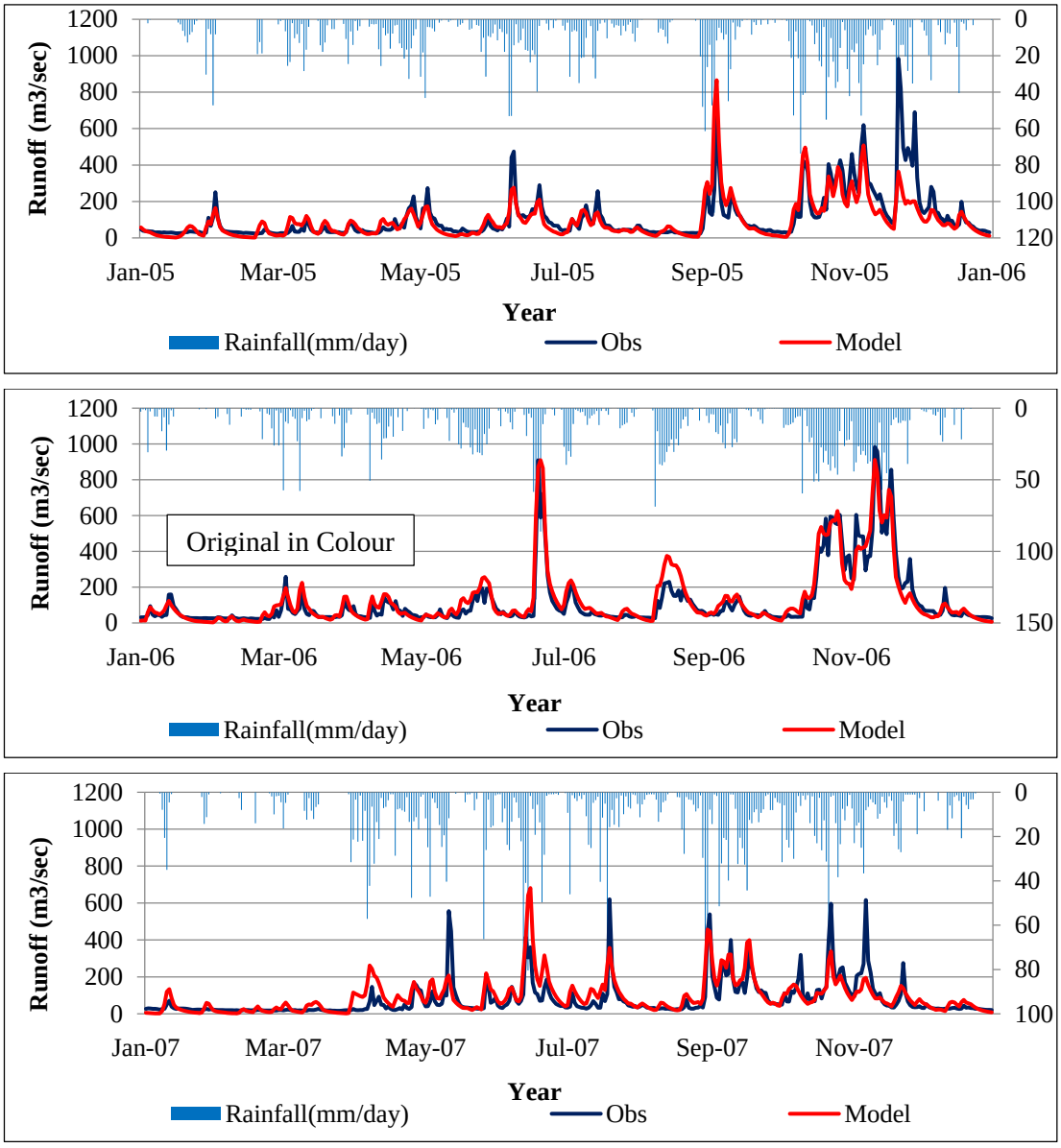

Figure 4-61 Streamflow Comparison of Modelled and Observed Streamflow for 2005-2007

4.4.2 Future Change of Streamflow

Streamflow variation in future is predicted by the validated HEC-HMS model of Hanwella sub-watershed. The streamflow of baseline period and the predicted periods

(the 2020s, 2050s and 2080s) streamflow mean is matched for the future scenarios of RCP2.6, RCP4.5 and RCP8.5 for both sub-models of monthly (SDSM-M) and seasonal (SDSM-S), respectively. Also, the change in water availability wascalculated. The difference in water availability is the variation of the mean of future streamflow to the baseline period streamflow. The following two tables of Table 4.22 represent the summary of the variation of the streamflow in future for Hanwella sub-watershed for seasonal and annual basis.

Following Figure 4.62 and 4.63 attached illustrate the future change of precipitation in Hanwella sub-watershed with respect to the monthly (SDSM-M) and seasonal (SDSM-M) sub-models for the period of the 2020s period. This future change of precipitation is directly linked with the effect of change of the future streamflow variation in the Hanwella sub-watershed.

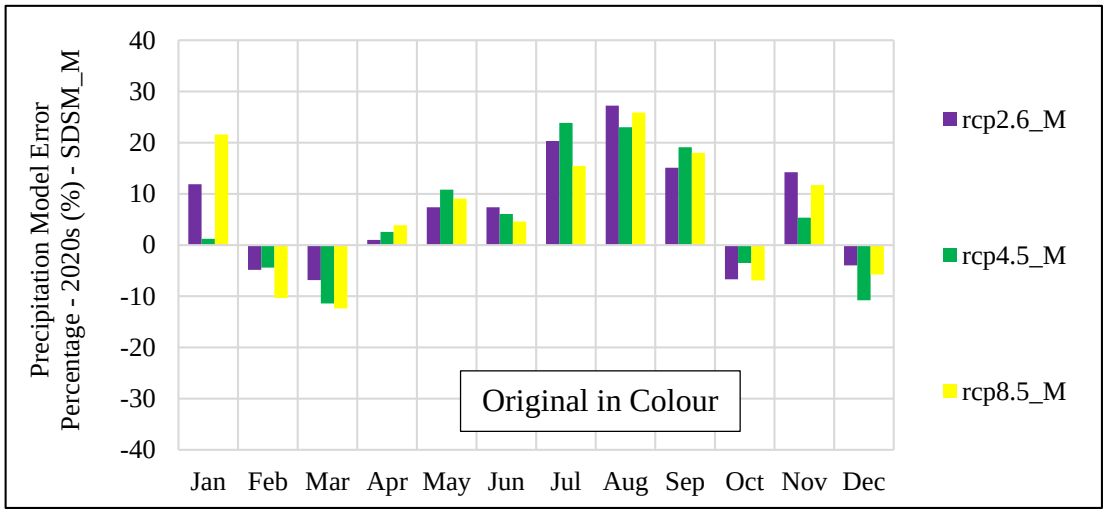

Figure 4-62 Model Error Percentage of Future Rainfall of Hanwella Sub-watershed for 2020s (SDSM_M)

According to the Figure 4.62, the maximum change of catchment precipitation is given for the month of August, and the maximum decrease is shown for the month of March according to the monthly sub-model. The maximum increment is 27.23% for the RCP2.6 scenario for the September, and maximum decrement is -12.39% for March for RCP8.5 scenario.

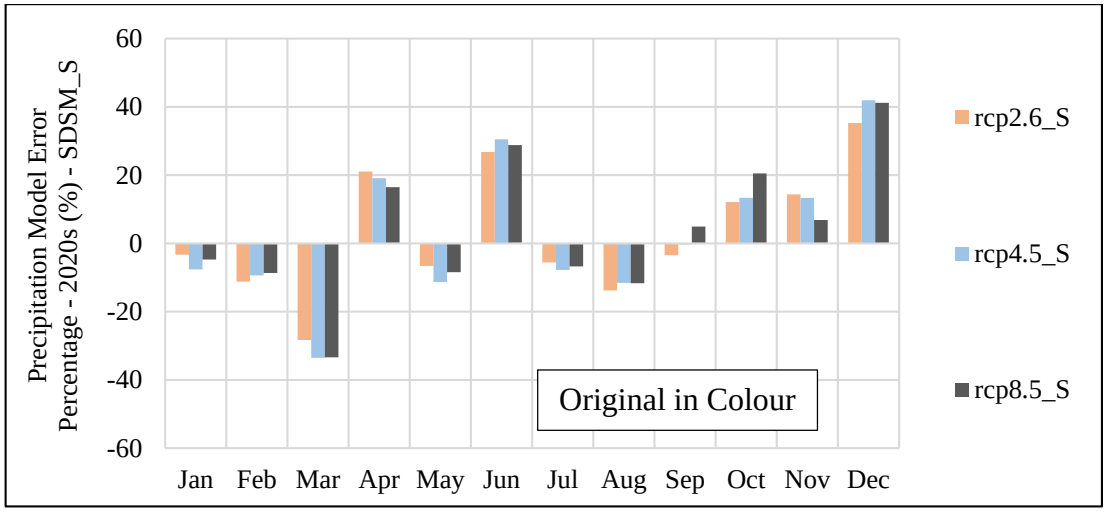

Figure 4-63 Model Error Percentage of Future Rainfall of Hanwella Sub-watershed for 2020s (SDSM_S)

According to the seasonal sub-model (Figure 4.63), the maximum increment is given for the month of December for the three scenarios and the model output of RCP4.5 is giving a 41.18% change for the observed mean and the maximum decrement shown for the month of March for the three scenarios as output of RCP4.5 is given as -33.50% change for the observed mean precipitation.

The future change of streamflow of Hanwella sub-watershed is altogether decreased with respect to the climate forcing criterias (Table 4.22). According to the trend analysis in the Section 4.2.2 and Table 4.1, the annual and seasonal trends of catchment and point precipitation tend to decrease. It was proven in the future streamflow as well with respect to the trend of observed streamflow (1985-2015) of the Hanwella sub-watershed. Figure 4.64 and Figure 4.65 represent the future streamflow variation of the Hanwella sub-watershed with respect to the modelled streamflow of for the period of 1985-2010 with the optimised and calibrated HEC-HMS model developed by De Silva et al. (2014) for Hanwella sub-watershed for the period of the 2020s according to monthly and seasonal sub-models. The figures of future streamflow variations of the 2050s and 2080s were attached to the Appendix 09.

Table 4-22 Percentage of Future Change of Streamflow in Hanwella Sub-watershed for RCP2.6, RCP4.5 and RCP8.5 Scenarios

	Season	RCP 2.6		RCP 4.5		RCP 8.5	
		SDSM_M (%)	SDSM_S (%)	SDSM_M (%)	SDSM_S (%)	SDSM_M (%)	SDSM_S (%)
2020s	SWM	0.67	5.29	-0.31	-3.17	0.80	-1.28
	NEM	1.31	2.69	-7.34	7.24	0.73	4.02
	1st IM	-1.79	5.91	-0.50	0.10	0.19	0.26
	2nd IM	-2.87	-7.32	-11.02	-7.17	-5.83	-5.36
	Yala	-0.45	-4.17	-0.85	-3.01	-.021	-1.34
	Maha	-0.51	-3.01	-8.35	-2.41	-3.14	-2.04
	Annual	-0.47	-3.71	-3.85	-2.77	-1.34	-1.62
2050s	SWM	3.27	-1.91	-3.27	-1.90	1.05	1.82
	NEM	-6.93	3.95	-3.97	12.37	-0.93	8.18
	1st IM	0.88	-1.26	-1.22	4.68	3.23	2.99
	2nd IM	-14.09	-4.08	-2.70	0.59	-7.16	-0.61
	Yala	2.57	-2.04	-340	-0.51	0.72	1.75
	Maha	-10.33	-1.43	-2.31	3.22	-3.70	2.31
	Annual	2.59	-1.80	-2.96	0.98	-1.05	1.98
2080s	SWM	1.01	1.09	0.75	-2.33	-4.05	6.43
	NEM	-5.41	4.60	5.02	3.31	0.58	9.62
	1st IM	0.19	-0.98	-1.06	2.20	7.30	3.67
	2nd IM	-7.95	1.91	6.18	3.65	-9.55	-3.94
	Yala	0.61	0.49	1.29	-1.10	-2.66	5.23
	Maha	-6.13	2.83	5.98	2.40	-5.26	1.49
	Annual	-2.09	1.43	1.62	0.33	-3.70	3.74

* SWM – South West monsoon (May – September), NEM – North East monsoon (December – February), 1st IM – First inter monsoon (March – April), 2nd IM – Second inter monsoon (October – November)

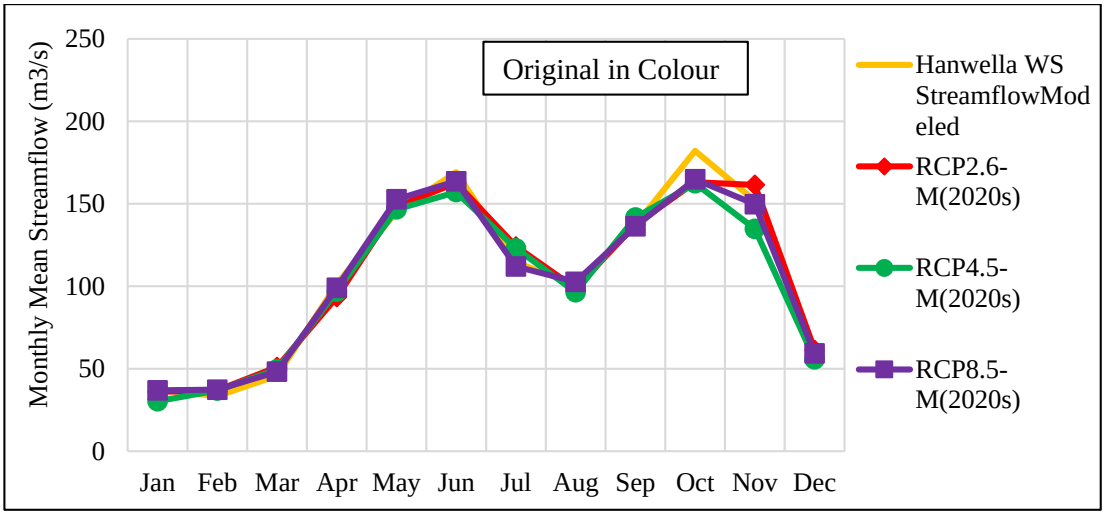

Figure 4-64 Future Streamflow Variation of Hanwella Sub-watershed in 2020s for SDSM_M

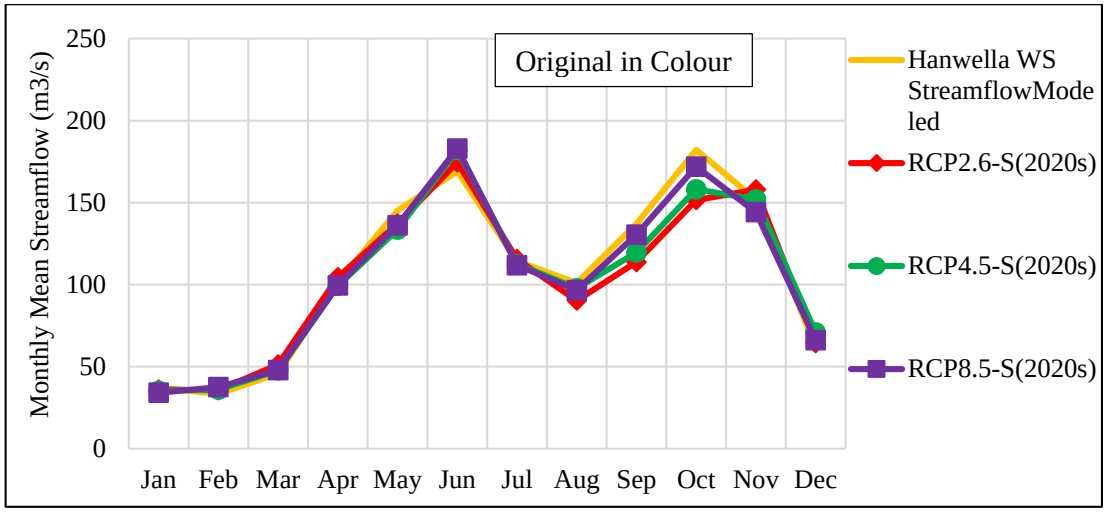

Figure 4-65 Future Streamflow Variation of Hanwella Sub-watershed in 2020s for SDSM_S

Figure 4.66 and Figure 4.67 show the future streamflow availability in the Kelani River Basin with respect to the streamflow model of the Hanwella sub-watershed.

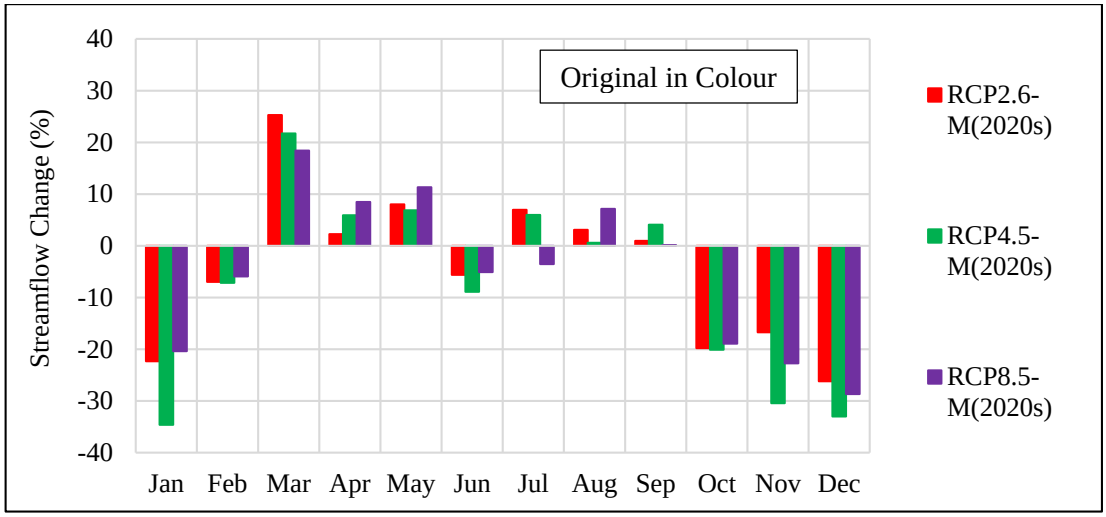

Figure 4-66 Future Streamflow Availability in Hanwella Sub-watershed in 2020s for SDSM_M

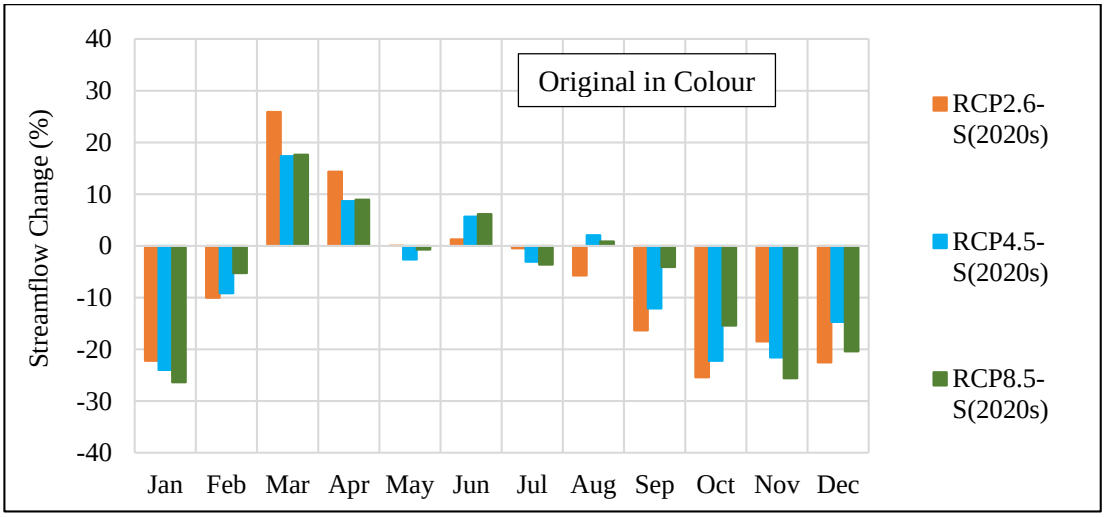

Figure 4-67 Future Streamflow Availability in Hanwella Sub-watershed in 2020s for SDSM_S

5. DISCUSSION

5.1 Data and Data Period

In selecting the data period, first, the data availability of 45-years at the Kelani River basin gauging stations was considered. For the Kelani river basin, chosen seven number of rainfall stations have a longer data record up to 2015 without minor errors from 1970. For climate change studies with related to GCM predictions, WMO and IPCC recommended at least 30-years period data in the daily resolution.

5.2 Identification of Trends and Extremes in Rainfall and Temperature

5.2.1 Identification of Trends in Rainfall

Historical data in rainfall shows that point and catchment rainfall in the Kelani River basin has changed during the period of 1970/1971-2014/2015. However, it was observed that annual point and catchment rainfall in the Kelani river basin shows a cyclic behaviour. As per IPCC (2007), the trend in global average annual rainfall between the periods of 1901-2005 had been statistically insignificant, while a downward trend has been observed in South Asia since 1901. Similarly, Hanwella and Glencourse watersheds in Kelani River basin shows a decreasing trend of -12.16 mm and -14.74 mm per annum, respectively, during the 1970/1971-2014/2015 period, which is less than 1% of average annual rainfall in respective watersheds. Five out of seven gauging stations namely Hanwella, Laxapana, Annfield, Yatiyanthota and Dunedin show a decreasing trend in annual rainfall with the highest annual reduction of -24.28 mm per year in Yatiyanthota. It is noted that, even though the trends do not indicate significant changes, magnitudes of decreasing trends in Kelani river basin has a spatial variability, especially in Colombo and Pasyala rainfall stations showing an increasing trend in annual rainfall. It indicates that the importance of studying the changes in precipitation within the watersheds also.

Seasonal rainfall in Maha and Yala seasons were also showing a downward trend of less than -1% of seasonal rainfall in both seasons for both sub-watersheds indicating that the average reduction in rainfall is not significant in the Kelani River basin. Seasonal rainfall in an individual station reveals the similar pattern too with the annual

rainfall in Yala season but Maha season, two out of seven stations show a downward trend. The IPCC states that as a result of the climate change, dry month would become drier and wet months would become even wetter. However, monthly rainfall in point rainfall and the catchment rainfall does not reveal any significant trends in the Kelani River basin. In conclusion, it can be stated that even though rainfall in the Kelani river basin shows a declining trend, substantial changes which could impact the historical data could not be detected affecting the water resources management. However, there could be a cumulative effect in the Kelani river basin due to the downward trends of the rainfall as well.

5.2.2 Identification of Trends in Temperature (Basin Temperature)

Historical records of temperature data show that average, minimum and maximum temperature has varied during the 1970/1971-2014/2015 period which indicates changes in temperature. Even though the changes in temperature are not continuously rising, increasing trends can be observed in annual and seasonal averages and the rising minimum temperature indicates that the climate warming has taken place in the Kelani river basin during the period of 1970/1971-2014/2015.

The IPCC predicts that the annual global average temperature to be increased by at least an amount of 1.0 ℃ in the year 2100. However, according to the current rate of increase of the average annual temperature of maximum temperature is about 0.0057 ℃ per year between 1970/1971-2014/2015 will result in a rise of 0.485 ℃ by the year 2100 in the Kelani river basin if the rate of increase is linear as shown by historical data. Also, the annual average temperature of temperature minimum is 0.0256 ℃ per year between 1970/1971-2014/2015 and this will result only an increase of 2.176 ℃ by the year 2100 in Kelani river basin if the rate of increase is linear as shown. According to the IPCC (2007), the average annual global temperature relative to the period of 1961-1990 baseline period increased by 0.128 ℃ to 0.177 ℃ per decade in the last 50-years and last 25-years respectively. Also, the air temperature in Sri Lanka has increased by 0.64℃ during over the past 40-years and 0.97 ℃ over the past 72-years of the period, which revealed an inclining trend of 0.14 ℃ temperature per decade (Giorgi et al., 2012). According to the historical trend of the Kelani river basin for the period of 1970/1971-2014/2015, the decadal increase of the temperature is

about 0.1 ℃, which is also proof of the trend of increase of air temperature of Sri Lanka as well. Hence, it can be stated that even though the historical data indicates a temperature rise in the Kelani River basin, unlike the predicted global and regional warming trends, the magnitude of temperature at the Kelani river basin has increased only slightly in the recent years.

5.2.3 Identification of Trends in Streamflow

Interpreting IPCC 2008 documentation on potential trends in river flow in the 20th century, it could be noted that some studies have found significant trends, but most of them have found no trends. The streamflow of the Kelani river basin is gauged at three locations of Hanwella, Glencourse and Kithulgala. For the present study, only Hanwella was considered. The annual trend of the streamflow for the period of 1985/1986-2014/2015 has revealed downward trends as -32.51 mm per annum in Hanwella which is less than 1% of the average annual streamflow. In Hanwella sub-watershed, it showed a downward trend for the both Maha and Yala seasons as well. The amount of decrease is -17.42 mm per season for Maha and -15.09 mm per season for Yala in Hanwella sub-watershed. Similar to temperature and rainfall changes, a significant impact on water resources management could not be identified due to the changes in streamflow. However, given the decreasing trends in river flow, it would be essential to investigate the impacts of moisture conditions and the land use changes in the catchment.

5.2.4 Identification of Extremes

5.2.4.1 Extremes of Precipitation

To identify the extremes of the climate (temperature maximum, temperature minimum and precipitation), the IPCC recommended indices were used for both temperature and precipitation in the Kelani River basin. The selected indices for precipitation is described in Section 4.1.2 and Table 4.1. To identify the behaviour of the extremes of the precipitation, 10 number of indices were used for the present study to check the response of the extreme events in the point rainfall stations. According to the IPCC indices, the extreme rainfall indices as identified as R20 which is daily rainfall greater than 20 mm per day. Most of the stations in this manner have an incremental trend,

while the others have a decremental trend. But in the future predictions, extreme events would be increased with respect to the CO_2 emission to the environment, and it will increase the extreme events of the precipitation with the increase of temperature in the Kelani river basin.

In the previous study of Climate Change study of Kelani River basin done by HadCM3 model by Herath et al. (2012) has revealed a decreasing trend for observed precipitation and increasing trend for future predictions of the precipitation. That reveals the increase of total precipitation due to the increase in the extremely heavy events of rainfall in future (Herath & Ratnayake, 2004).

To identify the extreme events of the rainfall, the return period of the annual daily maximum was calculated. The return period of the maximum daily precipitation for the period of 1970/1971-2000/2005 were obtained for each rainfall station. Because according to the IPCC (2015), it was revealed that the number of extreme events would increase while the frequency of occurrence of extreme events would also increase. From this aspect, it can be evaluated with the same return period of annual daily maximum rainfall of observed with respect to the predicted rainfall for the same period, whether the annul maximum would increase or not after bias correction.

Without the application of the bias correction, the variations in the maximum rainfall events cannot be identified because the SDSM model provides only the mean variation, not the extremes and the dry values for precipitation (Section 2.9).

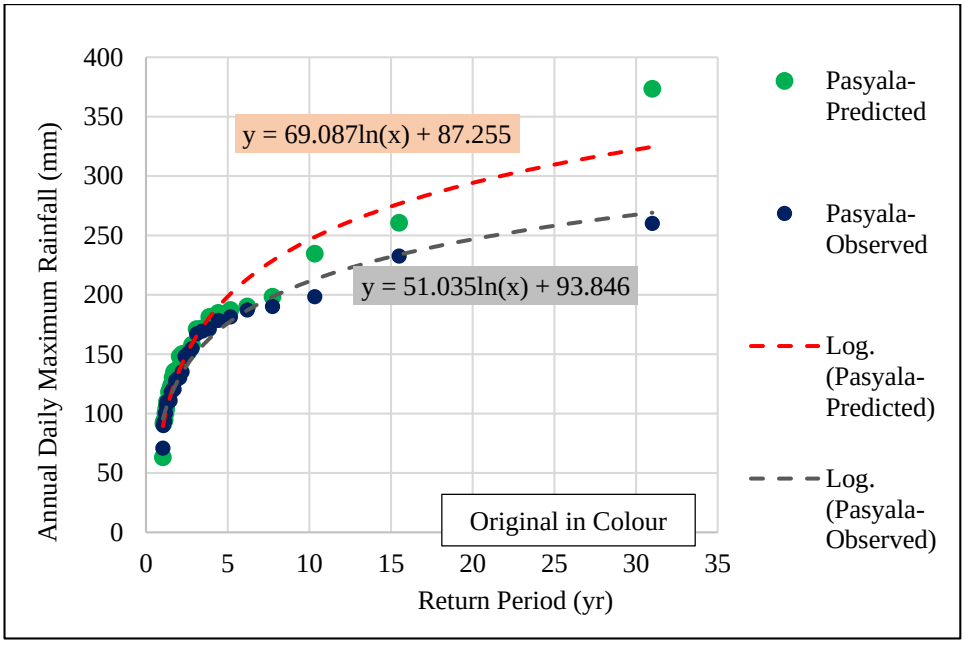

Figure 5-1 Plot of Return Period of Annual Daily Maximum Rainfall for Pasyala

5.2.4.2 Extremes of Temperature

To identify the behaviour of the extremes of the temperature in the Kelani River basin and point temperature, IPCC recommended 12 number of extreme indices were used. It was described in the Section 4.1.3 and summary results of the trends of the extreme indices of temperature maximum, temperature minimum and average temperature in Kelani river basin were tabulated in Table 4.2.

According to the tabulated results of trends of extremes of temperature, the SU25 (maximum temperature > 25 ℃), TXn (annual minimum of Tmax), TNn (annual minimum of Tmin) and TR20 (minimum temperature > 20 ℃ or tropical nights) have increased. These indices are indicating the rising trend of temperature in future due to the change of climatology of temperature in the Kelani river basin. Temperature does not have a direct link with the streamflow, but it would affect the precipitation pattern by increasing the drought periods, extreme events and increasing the evaporation quantity of the surface water as well. Also, the temperature rising in the Kelani River basin in future would be a result of the increased amount of carbon emission in the region.

5.2.5 Identification of the GCM

According to the literature review, the general circulation models (GCMs) are a type of climate models which mathematically represent the general circulation of a planetary atmosphere or ocean. The impact of the climate change in present and future have been widely studied using GCMs, which are considered one of the most effective and useful tools for exploring the process of physical changes of the earth's surface atmospheric system. Also, GCMs can provide very credible information in regards to the events of historical, current and future change of climate system for the selected region. Usually, GCMs are in coarser resolution. The prediction of the basin-scale climate change from the coarser resolution GCMs are challenging in statistical downscaling methods.

But the performance of the models depend on several factors and also-based on the region, the selected GCM would give reliable results about the climate change. That depends on the validity of the use of the GCM for the selected region. Therefore, by considering the extensive use of the GCM, for this study GCM developed by the Canadian Earth System Model Version 2 was selected. The reason for the selection of CanESM2 GCM is, it was used for number of case studies in the region and has produced reliable outputs as a result of the change of climate in history, current and future (Patabandige et al., 2016). The use of Hadley Centre Model Version 3 was previously used to evaluate the climate change of the Kelani River basin with respect to the emission scenarios of A2 & B2 by Herath et al. (2012).

5.2.6 Selection of the Climate Scenario

For the future climate change evaluation in the selected river basin, it was required to identify a future climate scenario which can be incorporated with the GCM model application. In 1996, the IPCC began the development of a new set of emission scenarios, effectively to update and replace the well-known IS92 scenarios (Herath et al., 2015). The approved new set of scenarios is described in the IPCC Special Report on Emission Scenarios (SRES). However, greenhouse gas emissions are directly affected by non-climate change policies designed for a wide range of other purposes. From the four developed storyline scenarios by IPCC in 1996, CanESM2 GCM model

has the facility to access three scenarios namely Representative Concentrative Pathways of RCP2.6, RCP4.5 and RCP8.5 climate change scenarios for the region which are the selected climate change scenarios for the present study.

5.2.7 Downscaling of GCM Outputs

For the present study, the statistical downscaling technique was used to calibrate and validate the GCM model output and as well as to evaluate the future climate change with respect to the baseline period. To downscale the GCM outputs, the Statistical Downscaling Model (SDSM) was used based on the method called multiple linear regression. In the downscaling process of the climate data, observed rainfall and temperature data were used for the model calibration for the period of 30-years from 1970-2000 and then the model was validated for the period of 5-years from 2001 to 2005 under RCP2.6, RCP4.5 and RCP8.5 scenarios with the application of bias correction with mean shifting method as described in Section 2.9.4.3. To check the accuracy of the downscaled output, six statistical indicators of the mean (μ), standard deviation (σ), the relative error of the mean (RE_μ), relative error of standard deviation (RE_σ), root mean square error (RMSE) and goodness of fit (R^2) were used. Further, the downscaling results were evaluated by the monthly, annual and seasonal sub-models with respect to the baseline period.

To downscale the GCM outputs the most suitable predictors out of 26 NCEP predictors given in the model were selected. Therefore, to select the most suitable predictor for each climate station the regression results of correlation of predictand and predictors, correlation of super predictor to other predictors and with the percentage reduction in Partial Correlation (PRP %) were statistically evaluated.

5.2.8 Evaluation of Future Climate Change

From the downscaled results of RCP2.6, RCP4.5 and RCP8.5, the future change of climatology in the Kelani river basin was obtained with respect to the change of temperature and precipitation in future. The maximum increment of catchment average maximum temperature was increased by 1.36°C in the 2080s according to the seasonal sub-model under RCP8.5scenario as annual trend, and the maximum increase of the maximum of average temperature minimum is 2.55°C in the 2080s according to the

seasonal sub-model by RCP8.5 scenario as an annual trend with respect to the baseline period. Section 4.3.8 described how temperature would change in the future with respect to the RCP2.6, RCP4.5 and RCP8.5 scenarios in the Kelani River basin (Herath et al., 2012).

These climate change scenarios were helpful to generate the future climatology data of precipitation and temperature for the three selected periods of the 2020s, 2050s and 2080s. These three representative concentration pathways were described in IPCC SRES, and it was used to evaluate the annual and seasonal runoff coefficient variation of Sri Lankan river basins by Patabandige et al. (2016). In that study, the Kelani river basin runoff coefficient was getting decreased with respect to the future change of rainfall. This was implemented well in the future streamflow evaluation in Section 4.3.10 for the Hanwella sub-watershed. The streamflow in the Kelani River basin was getting decreased with the future climate change and it is tabulated in the Table 4.22, and the maximum decrease of the streamflow is in 2nd Inter monsoonal period of the 2050s is -14.09% according to the monthly sub-model. Further, the annual change of the streamflow will have decremental change for future periods of the 2020s and 2050s, except for 2080s. Because of that, it is presumed that with the trend of representative concentration pathways in the period of the 2080s during which the population will also increase, thus raising the amount of carbon produced. In the meantime, the impervious area would also be raised with the development. Hence, streamflow would be increased in the 2080s period.

Further, Section 4.3.7 describes the future change of the precipitation according to the RCP scenarios. Table 4.13 gives the tabulated summary of the future change of the precipitation in the Hanwella sub-watershed of the Kelani River basin. In that, according to the annual variation of rainfall, there was a slight increase with respect to the observed annual average raifall by both the monthly and seasonal sub-models. This would be possible due to the rise in extreme events of the future precipitation series. But that increment is not more than 10% of the observed value.

5.3 Evaluation of the Streamflow

5.3.1 Use of Hydrology Models for Computation of Streamflow

For streamflow evaluation, the HEC-HMS model was used for the Hanwella sub-watershed. The parameters used in the HEC-HMS model for continuous runoff modelling were according to the previously calibrated and validated model by De Silva et al. (2014) for the same watershed of Hanwella sub-watershed in the Kelani River basin. For the present study, the result of the selected objective functions of NASH and MRAE for the use of the developed model are 0.749 and 0.502, respectively. Further, the goodness of fit value (R^2) is about 0.754 which shows an agreeable correlation. Using the same model, a sensitivity analysis for the baseflow model was performed except for the loss model and the hydrograph model to achieve a better performance of the streamflow modelling. However, the precipitation stations used were different for the present study concerning the stations used by De Silva et al. (2014).

This might haveled to slightly different results due to the non-stationarity of the precipitation series with the change of climate forcing. Hence, following the sensitivity analysis, the baseflow parameters were refined and the newly adjusted parameters of the baseflow are 71.5 m^3/s as Initial Discharge, 0.810 as Recession Constant and 0.28 as Ratio to Peak flow.

5.3.2 Evaluation of Future Streamflow Change

The impact on streamflow and water availability were analysed as seasonal and annual variations. The plots of monthly average flow for the baseline period of streamflow modelling and three future periods show that the hydrograph ordinates for the future periods obey the same pattern with respect to the baseline period but the possible increases and decreases concerning the seasonal and annual basis are given as results of water availability in future. The highest variation of the average streamflow is about 199.3 m^3/s for June for the 2080s period according to the monthly sub-model under RCP8.5 scenario for Hanwella sub-watershed. The monthly average peak of the future streamflow increased with respect to the baseline period. The increase in the peak and the underlying changes in the future streamflow with respect to the baseline period streamflow clearly indicates slight changes in seasonal and annual water availability.

Scenario RCP4.5 and RCP8.5 predicts a very significant increase and decrease in the average monthly flow during the Maha and Yala as well as the seasonal monsoon periods with respect to RCP2.6. The change of streamflow would affect the water availability in the Kelani River basin in future.

5.4 Link between Climate Warming and Changes in Rainfall and Streamflow

The IPCC states that rainfall could increase or decrease because of global warming. In both Hanwella and Glencourse sub-watersheds of the Kelani River basin, rainfall reduces with the increase in temperature. But a clear link between temperature and the precipitation could not be identified. Further, according to the prediction of the future climate, when the temperature increases, the rainfall also increases leading to an increase in the future streamflow. Hence, it can be stated that the increase in the temperature observed and predicted may not be the only reason for the increasing of streamflow in the future. The IPCC says that most of the studies which have found significant trends in river flows have been unable to separate out of the effects of variation in temperature and rainfall from the human interventions in the catchment.

In the Hanwella sub-watershed, reductions in streamflow when the temperature increases were observed. However, according to the future prediction according to the RCP2.6, RCP4.5 and RCP8.5 scenarios, when the temperature increases, the rainfall also increases by increasing the extreme events. Then as result of the change of precipitation, the streamflow will increase in seasonal and annual basis. This would be a result of the identified future variation of GHG emissions and the expected land use changes by the GCM model.

However, for both the sub-watersheds, a clear link between temperature rise and changes in streamflow could not be identified. Therefore, it can be concluded that an increase in the temperature cannot be highlighted as the main reason for the changes in rainfall and streamflow in the Kelani river basin.

6. CONCLUSION

1. According to the historical observations, the Kelani river basin experiences climate warming and changes in rainfall and streamflow as predicted by IPCC and CORDEX South Asia. River basin Temperature maximum is increasing at a rate of 0.0057 ℃/year, and Temperature minimum is increasing at a rate of 0.0256 ℃/year, and Temperature average is rising at a rate of 0.0156 ℃/year, while on average the catchment rainfall is decreasing at a rate of 13.45 mm/year and average streamflow is decreasing at a rate of 37.18 mm/year annually in the Kelani River Basin.
2. In the Kelani river basin, the predicted climate in future shows a decreasing trend in point rainfall and catchment rainfall, but an increasing trend of river basin average temperature. Further, the streamflow has a decreasing trend for sub-watersheds of Hanwella.
3. The increase in temperature in the Kelani river basin in future does not reflect future changes of the rainfall and streamflow directly. But it would affect and reduce the volume of surface water in the Kelani River basin due to increased evaporation while the increasing of temperature is directly related to the extreme events of rainfall in future as well as longer drought periods or extremes of temperature..
4. The GCM used to identify the changes of climate in future well represented the regional scale climate parameters in Kelani river basin with the use of statistical application of downscaling while the calibrated model of streamflow used well defined the changes of streamflow according to the future changes of precipitation with respect to the base period.
5. The future changes of temperature would lead to extended droughts and extensively higher rainfall intensities due to the increased amount of atmosphere according to the IPCC and as confirmed by the present study in Kelani river basin.

7. RECOMMENDATIONS

1. To check the reliability of the output results of future climatology can be applied to reservoir modelling as well.
2. The basin-wide prediction of future climate (i.e. temperature and rainfall) based on RCM/GCM can effectively be used for water resources planning and management as well as for hydroelectric power scheme designs.
3. It is recommended to to carry out further investigation on possible variation of streamflow with respect to other climate warming parameters with the use of same GCM/RCM.
4. Recommended to carry out further investigation on how runoff coefficient will be affected in the river basin with the climate change and possible land use changes in future.
5. The predicted changes of streamflow in the Kelani River basin would lead to reduce the generation of Hydro-electric and the changes of extremes of temperature and rainfall would be a reason for increased flood vulnerability of the downstream of the Kelani river basin due to increasing of flood extremes of flood with respect to the changes of rainfall. These direct and indirect impacts of climate change should be studied in detail for developing sustainable water resources development alternatives.
6. The present study focused only on the change of rainfall and temperature in the future concerning the coarser GCM and by applying the method called statistical downscaling. The statistical downscaling is a relatively good method to evaluate the climate change in the future in the selected watersheds. In the meantime, the application of Dynamical downscaling considers all anthropogenic effects on the climate system, and the reliability of the output is more accurate than statistical downscaling and use of coarser GCMs and it is recommended to further verify the results of the present study with Dynamical downscaling method or a similar approach.

REFERENCES

Alexander, L. V., Zhang, X., Peterson, T. C., Caesar, J., Gleson, B., Kelin, T. A. M. G., & Vazquez-Aguire, J. L. (2006). Global Observed Changes in daily climate extremes of temperature and precipitation. *Journal of Geophysical Research*.

Allen, M. R., & Ingram, W. J. (2002). Review article Constraints on future changes in climate and the hydrologic cycle. *Nature*, *419*, 224–232.

Aziz, A. O. I., & Burn, D. H. (2006). Trends and variability in the hydrological regime of the Mackenzie River. *Journal of Hydrology*, *319*, 282–294.

Benestad, R.E., Chen, D., & Hanssen-Bauer, I. (2008). Empirical – statistical downscaling. *World Scientific, Singapore*.

Benestad, R. E. (2010). Downscaling precipitation extremes Correction of analog models through PDF predictions. *Theoretical and Applied Climatology*, *100*, 1–21.

Brandit, C. J., & Thornes, J. B. (1996). Mediterranean desertification and land use. *Wiley Online Library*, *554*.

Breshears, D. D., Myers, O. B., Meyer, C. W., Barnes, F. J., Zou, C. B., Allen, C. D., Pockman, W. T. (2009). Tree die-off in response to global change-type drought: mortality insights from a decade of plant water-potential measurements. *The Ecological Society of America*.

Burke, M., Hsiang, S. M., & Miguel, E. (2015). Climate and Conflict. *Annual Review of Economics*.

Burn, D. H. (1994). Hydrologic effects of climate change in west - central Canada. *Journal of Hydrology*, *160*, 53–70.

Burn, D. H., & Elnur, H. (2002). Detection of hydrologic trend and variability. *Journal of Hydrology*, *255*, 107–122.

Burn, D. H., & Simonovic, S. P. (1996). Sensitivity of reservoir operations performance to climatic change. *Water Resources Management*, *10*, 463–478.

Burt, T. P., & Weerasinghe, K. D. N. (2014). Rainfall Distributions in Sri Lanka in Time and Space: An Analysis Based on Daily Rainfall Data. *Climate*, *2*(4), 242–263.

Chow, V. T., Maidment, D. R., & Mays, L. W. (1988). *Applied Hydrology*. McGraw Hill.

Chu, X., & Steinman, A. (2009). Event and Continuous Hydrologic Modeling with HEC-HMS. *Journal of Irrigation and Drainage Engineering*, 119–124.

Chunderlik, J. M., & Simonovic, S. P. (2004). Calibration, verification and sensitivity analysis of the HEC-HMS hydrologic model. *Water Resources Research Report No. 048; Facility for Intelligent Decision Support, Department of Civil and Environmental Engineering, London, Ontario, Canada*.

Cruz, R. V., Harasawa, H., Lal, M., Wu, S., Anokhin, Y., Punsalmaa, B., Huu, N. H. (2007). Climate Change 2007: Impacts, Adaptation and Vulnerability. *Cambridge University Press, Cambridge*, 469–506.

Cubasch, U., & Meehl, G. A. (2001). Projections of Future Climate Change.

De Silva, M. M. G. T., Weerakoon, S. B., & Shrikantha, H. (2014). Modeling of Event and Continuous Flow Hydrographs with HEC–HMS: Case Study in the Kelani River Basin, Sri Lanka. *Journal of Hydrology*.

Department of Meteorology. (2009). Reports: Data and Statements of Department of Meteorology, Sri Lanka.

Dharmasena, G. T. (1999). Assessment potential of electrical energy in small catchments. *Hydrological Annual – 1998/1999, Hydrology Division, Irrigatio n Department of Sri Lanka, Colombo*.

Diaz-Nieto, J. (2005a). A comparison of statistical downscaling and climate change factor methods: impacts on low flows in the River Thames, United Kingdom., 245–268.

Diaz-Nieto, J., & Wilby, R. L. (2005). A comparison of statistical downscaling and climate change factor methods: impacts on low flows in the River Thames, United Kingdom. *Climate Change*, *69*(2–3), 245–268.

Easterling, D. R., Meehl, G. A., Parmesan, C., Changnon, S. A., Karl, T. R., & Mearns, L. O. (2000). Climate Extremes: Observations, Modeling, and Impacts. *Atmospheric Science*, *289*.

Eisner, S., Schewe, J., Gerten, D., Heinke, J., Haddeland, I., Anrell, N. W., Kabat, P. (2013). Multimodel assessment of water scarcity under climate change. *Sustainability Science*, *111*(No. 09), 3245–3250.

Fischer, G., Shah, M., & van Velthuizen, H. (2002). Climate Change and Agricultural Vulnerability. *International Institute for Applied System Analysis*.

Fowler, H. J., Kilsby, C. G., & Stunell, J. (2007). Modelling the impacts of projected future climate change on water resources in North-west England. *Hydrology & Earth System Science*, *11*(3), 1115–1126.

Frich, P., Alexander, L. V., Della-Marta, P., Gleason, B., Haylock, M., Klein Tank, A. M. G., & Peterson, T. (2002). Observed coherent changes in climatic extremes during the second half of the twentieth century. *Climate Research*, *19*, 193–212.

Fujihara, Y., Tanaka, K., Watanabe, T., Nagano, T., & Kojiri, T. (2008). Assessing the impacts of climate change on the water resources of the Seyhan River Basin in Turkey: Use of dynamically downscaled data for hydrologic simulations. *Journal of Hydrology*, *353*(1–2), 33–48.

Gan, J. (2004). Risk and damage of southern pine beetle outbreaks under global climate change. *Forest Ecological Management*, *191*, 61–71.

Gangon-Lebrun, F., & Agrawala, S. (2006). Progress on adaptation to climate change in developed countries. Organization for Economic Co-operation and Development.

Gebremeskel, S., & Li, Y. (2005). Analysisng the effect of climate changes on streamflow using statistically downscaled GCM scenarios. *International Journal of River Basin Management*, 271–280.

Giorgi, F. (2006). Climate change hot-spots. *Geophysical Research Letters*, *33*.

Giorgi, F., & Bi, X. (2005). Regional changes in surface climate interannual variability for the 21st century from ensembles of global model simulations. *Geophysical Research Letters*, *32*.

Giorgi, F., Coppola, E., Solmon, F., Mariotti, L., Sylla, M. B., Bi, X., Brankovic, C. (2012). RegCM4: model description and preliminary tests over multiple CORDEX domains. *Climate Research*, *52:* 7–29.

Giorgi, F., Mearns, L. O., Shields, C., & Mc Daniel, L. (1998). Regional nested model simulations of present day and 2xCO2 climate over the Central Plains of the U.S. *Climate Change*, *40*, 457–493.

Giorgi, F., & Shields, C. (1999). Tests of precipitation parameterizations available in the latest version of the NCAR regional climate model (RegCM) over the continental U.S. *Journal of Geophysics*, *104*, 6353–6376.

Gitay, H., Brown, S., Jallow, B., & Easterling, W. (2001). Ecosystems and their goods and services: Climate Change, 2001, Impacts, Adaptation, and Vulnerability, 237–242.

Gleick, P. H. (1986). Methods for evaluating the regional hydrologic impacts of global climatic changes. *Journal of Hydrology*, *88*, 97–116.

Gleick, P. H. (1987). The Development and Testing of a Water Balance Model for Climate Impact Assessment: Modeling the Sacramento Basin. *Water Resources Research*, *10*(2), 137–161.

Gleick, P. H. (1989). Climate change, hydrology, and water resources. *Reviews of Geophysics*, *27*(3), 329–344.

Gonzalez, P., Neilson, R. P., Lenihan, J. M., & Drapek, R. J. (2010). Global patterns in the vulnerability of ecosystems to vegetation shifts due to climate change. *Global Ecology and Biogeography*, *19*, 755–768.

Government of Maharashtra. (2014). Assessing Climate Change Vulnerability and Adaptation Strategies for Maharashtra: Maharashtra State Adaptation Action Plan on Climate Change (MSAAPC).

Green, I. R. A., & Stephenson, D. (2009). Criteria for comparison of single event models. *Journal of Hydrological Sciences*, *31*(3), 395–411.

Hashimi, M. Z., Shamseldin, A. Y., & Melville, B. W. (2009). Statistical downscaling of precipitation: state-of-the-art and application of bayesian multi-model approach for uncertainty assessment. *Hydrology & Earth System Science*, *6*, 6535–6579.

Hassan, R., Scholes, R., & Ash, N. (2005). Ecosystems and Human Well-being: Current State and Trends, Volume 1. *Island Press, Washington*, 917.

Hasson, S., Lucarini, V., & Pascale, S. (2013). Hydrological Cycle over South and Southeast Asian river basin as simulated by PCMDI/CMIP3 experiments. *Earth System Dynamics*.

Hay, L. E., & Clark, M. P. (2003). Use of statistically and dynamically downscaled atmospheric model output for hydrologic simulations in three mountainous basins in the western United States. *Journal of Hydrology*, *282*, 56–75.

Herath, H. M. V. V., Dayananda, R. G. A. B., & Weerakoon, S. B. (2015). Climate change impact prediction in upper Mahaweli Basin. *International Conference on Structural Engineering and Construction Management*, 148–152.

Herath, S., & Ratnayake, U. R. (2004). Monitoring rainfall trends to predict adverse impacts - a case study from Sri Lanka. *Global Environmental Change*, 71–79.

Herath, S., Weerakoon, S. B., Kawasaki, J., Koontanakulvong, S., Thuc, T., Tuan, L. A., Tabios, G. Q. (2012). Comparative studies on development strategies considering impacts of adaptation to climate change. *Report on Climate Change Adaptation Research Funded by Mitsui Corporation*.

Hidalgo, H. G., Amador, J. A., Alfaro, E. J., & Quesada, B. (2013). Hydrological climate change projections for Central America. *Journal of Hydrology*, *495*, 94–112.

Houghton, J. T., Jenkins, G. J., & Ephraums, J. J. (1990). Climate Change. The IPCC Scientific Assessment. *Cambridge University Press, Cambridge*, 365 pp.

Huang, J. (2011). Estimation of future precipitation change in the Yangtze River basin by using statistical downscaling method. *Stoch Env Res Risk, 25(6)*, 781–792.

Huang, J., & Zhang, J. (2011). Estimation of future precipitation change in the Yangtze River basin by using statistical downscaling method. *Springer - Stochastic Environmental Research and Risk Assessment*, *25*(6), 781–792.

Huang, J., Zhang, J., Zhang, Z., Xu, C. Y., Wang, B., & Yao, J. (2010). Estimation of future precipitation change in the Yangtze River basin by using statistical downscaling method. *Springer - Stochastic Environmental Research and Risk Assessment, 25*, 781–792.

Indian Climatology Institute. (2014). India's Progress in Combating Climate Change.

IPCC, (2007). Climate Change 2007: The Physical Science Basis. Contribution of Working Group I to the Fourth Assessment Report of the Intergovernmental

Panel on Climate Change [Solomon, S., Qin, D., Manning, M., Chen, Z., Marquis, M., Averyt, K.B., Tignor, M., & Miller, H.L. (Eds.)]. Cambridge University Press, Cambridge, United Kingdom and New York, NY, USA.

IPCC, (2013). Climate Change 2013: The Physical Science Basis. Contribution of Working Group I to the Fifth Assessment Report of the Intergovernmental Panel on Climate Change [Stocker, T.F., Qin, D., Plattner, G.K., Tignor, M., Allen, S.K., Boschung, J., Nauels, A., Xia, Y., Bex, V., & Midgley, P.M. (Eds.)]. Cambridge University Press, Cambridge, United Kingdom and New York, NY, USA, 1535 pp, doi: 10.1017/CBO9781107415324.

IPCC, (2014). Climate Change 2014: Synthesis Report. Contribution of Working Groups I, II and III to the Fifth Assessment Report of the Intergovernmental Panel on Climate Change [Pachauri, R.K., & Meyer, L.A. (Eds.)]. IPCC, Geneva, Switzerland, 151 pp.

Jayatillake, H. M., Chandrapala, L., Basnayake, B. R. S. B., & Dharmaratne, G. H. (2005). Water resources and climate change. *Proceedings of Workshop on Sri Lanka National Water Development Report. Wijesekera, N. T. S.; Imbulana, K. A. U. S.; Neupane, B. Eds. Paris, France: World Water Assessment Programme (WWAP).*

Jayawardena, H. K. W. I., Sonnadara, D. U. J., & Jayawardena, D. R. (2005). Trends of Rainfall in Sri Lanka over the Last Century. *Sri Lanka Journal of Physics*, *6*, 7–17.

Kahaya, E., & Kalayci, S. (2004). Trend analysis of streamflow in Turkey. *Journal of Hydrology*, *289*, 128–144.

Kelkar, U., & Bhadwal, S. (2007). South Asian Regional Study on Climate Change Impacts and Adaptation: Implications for Human Development. *United Nations Development Program.*

Kite, J. S., & Linton, R. C. (1993). Depositional aspects of the November 1985 flood on Cheat River and Black Fork, West Virginia. U.S. Geological Survey Bulletin.

Knutti, R., Meehl, G. A., Allen, M. R., & Stainforth, D. A. (2006). Constraining Climate Sensitivity from the Seasonal Cycle in Surface Temperature. *Journal of Climate*, *19*, 4224–4233.

Kostopoulou, E., & Jones, P. D. (2005). Assessment of Climate Extremes in the Eastern Mediterranean. *Meteorological and Atmospheric Physics*, *89*, 69–85.

Krol, M., Bronstert, A., Jaeger, A., Gunter, A., Hauschild, M., & Doll, P. (2000). Integrated modelling of water availability and water use in the semi-arid Northeast of Brazil. *Science Direct*, *25*(3), 227–232.

Kumar, K. S. K., & Parikh, J. (2001). Indian Agriculture and Climate Sensitivity. *Global Environmental Change*, *11*, 147–154.

Lal, M. (2003). Global climate change: India's monsoon and its variability. *Journal of Environmental Studies and Policy*, *6*(1), 1–34.

Lal, R., Delgoda, J. A., Groffman, P. M., Milar, N., Dell, C., & Rotz, A. (2011). Management to Mitigate and Adapt to Climate Change. *Journal of Soil and Water Conservation*, *66*(No. 04).

Lambert, S. J., & Boer, G. J. (2000). CMIP1 evaluation and intercomparison of coupled climate models. *Climate Dynamics*.

Lenton, R. (2004). Water and climate variability: development impacts and coping strategies. *Water Science & Technology*, *49*(7), 17–24.

Lettenmaier, D. P., & Gan, T. Y. (1990). Hydrologic sensitivities of the Sacramento – San Joaquin River Basin, California, to global warming. *Water Resources Research*.

Li, G., Zhang, F., Jing, Y., Liu, Y., & Sun, G. (2017). Response of evapotranspiration to changes in land use and land cover and climate in China during 2001 – 2013. *Science of the Total Environment*, 256–265.

Liu, C. Z. (2002). Suggestion on water resources in China corresponding with global climate change. *China Water Resource*, *2*, 36–37.

Liu, D. L., Timbal, B., Mo, J., & Fairweather, H. (2011). A GIS-based climate change adaptation strategy tool. *International Journal of Climate Change Strategies and Management*, *3*, 140–155.

Lorenz, E. N. (1969). The predictability of a flow which possesses many scales of motion. *Tellus*, *21*, 19.

Lorenz, E. N. (1975). Climatic predictability. GARP Publication Series.

Mahmood, R., & Babel, M. S. (2012). Evaluation of SDSM developed by annual and monthly sub-models for downscaling temperature and precipitation in the

Jhelum basin, Pakistan and India. *Theoretical and Applied Climatology - Springer*, *113*(1–2), 27–44.

Mahmood, R., Babel, M. S., & Shaofeng, J. A. (2015). Assessment of temporal and spatial changes of future climate in the Jhelum river basin, Pakistan and India. *Elsevier*, *10*, 40–55.

Manawadu, L. (2008). Climate Change in Sri Lanka. *Science Direct – Regional Environmental Change*.

Manawadu, L., & Fernando, N. (2008). Climate Change in Sri Lanka. *Journal of Hydrology*.

McGregor, J. L. (2005). Geostrophic Adjustment for Reversibly Staggered Grids. *CSIRO Atmospheric Research, Aspendale, Victoria, Australia*.

Mirza, M. Q. (2002). Global warming and changes in the probability of occurrence of floods in Bangladesh and implications. *Global Environmental Change*, *12*, 127–138.

Mishra, V., & Lilhare, R. (2016). Hydrologic sensitivity of Indian sub - continental river basins to climate change. *Global and Planetary Change*.

Murphy, J. M., Sexton, D. M. H., Barnett, D. N., Jones, G. S., Webb, M. J., Collins, M., & Stainforth, D. A. (2004). Quantification of modelling uncertainties in a large ensemble of climate change simulations. *Nature*, *430*, 768–772.

Narisma, G. T., Foley, J. A., Licker, R., & Ramankutty, N. (2007). Abrupt changes in rainfall during the twentieth century. *Geophysical Research Letters*, *34*(L06710, doi: 10.1029/2006GL028628).

Nemec, J., & Schaake, J. (1982). Sensitivity of water resource systems to climate variation, *27*(3), 327–343.

Paparrizos, S., Maris, F., Weiler, M., & Matzarakis, A. (2016). Analysis and mapping of present and future drought conditions over Greek areas with different climate conditions. *Theoretical and Applied Climatology - Springer*.

Patabandige, C. S., Kazama, S., & Komori, D. (2016). Near future climatic impact on seasonal runoff in Sri Lanka. *Research Gate*.

Patel, M. M., Gandhi, H. M., & Shrimali, N. J. (2014). Literature Study on Application of HEC-HMS for Event and Continuous Based Hydrological Modeling. *IJSRD - International Journal for Scientific Research & Development*, *1*(11).

Paul, B., & Rashid, H. (1993). Flood damage to rice crop in Bangladesh. *Geographical Review*, *83*(2), 151–159.

Peng, S., Huang, J., Sheehy, J. E., Laza, R. C., Visperas, R. M., Zhong, X., Cassman, K. G. (2007). Rice yields decline with higher night temperature from global warming. *National Academy of Science of the USA*, *101*(27), 9991–9975.

Randall, D. A., Wood, R. A., Bony, S., Colman, R., Fichefet, F., Fyfe, J., Taylor, K. (2007). Climate model and their evaluation, In, Climate change 2007: The Physical science basis. Contribution of working group I to the fourth assessment report of the Intergovernmental Panel on Climate Change [Solomon, S, et al., (eds)]. *Cambridge University Press, Cambridge*.

Raut, A. (2006). Climate impacts on Nepal. *Tiempo*, *60*, 3–5.

Reshma, T., Kumar, P., Babu, M., & Kumar, K. (2010). Simulation of runoff in watersheds using SCS-CN and Muskingum-Cunge methods using remote sensing and geographical information systems. *International Journal of Advanced Science and Technology*, *25*, 31–42.

Revadekar, J. V., & Kulkarni, A. (2008). The El Nino-Southern Oscillation and winter precipitation extremes over India. *International Journal of Climatology, 28,* 1445–1452.

Riebsame, W. E., Strzepek, K. M., Wescoat, L. J., Perrit, R., Graile, G. L., Jacobs, J., Yates, D. (1995). Complex river basins. In: Strzepek KM, Smith JB (eds) As climate changes, international impacts and implications. *Cambridge University Press, Cambridge*, 57–91.

Sachindra, D. A. (2014). Statistical downscaling of general circulation model outputs t precipitation - part 1: calibration and validation. *International Journal of Climatology*.

Sachindra, D. A., & Perera, B. J. C. (2016). Statistical Downscaling of General Circulation Model Outputs to Precipitation Accounting for Non-Stationarities in Predictor-Predictand Relationships. *Public Library of Science*, (DOI: 10.137 1/journal.po ne.0168 701).

Salzmann, N., Frei, C., Vidale, P., & Hoelzle, M. (2007). The application of Regional Climate Model output for the simulation of high-mountain permafrost scenarios. *Global and Planetary Change - Elsivier*, *56*, 188–202.

Sanjay, R., Ramarao, M.V.S., Kim, J., Sabin, T.P., Nikulin, G., Asharaf, S., Krishnan, R., Jones, C., Ahrens, B., Mujumdar, M., Giorgi, F., Waliser, D.E., & Rixen, M. (2013). CORDEX Regional Climate Models Performance in Present-day Climate for South Asia. *Climate Change*.

Schoof, J., & Pryor, S. (2001). Downscaling temperature and precipitation: a comparison of regression-based methods and artificial neural networks. *International Journal of Climatology*, *21*, 773–790.

Schwierz, C., Appenzeller, C., Davies, H. C., Liniger, M. A., Muller, W., Stocker, T. F., & Yoshimori, M. (2006). Challenges posed by and approaches to the study of seasonal-to-decadal climate variability. *Climate Change*, *79*, 31–63.

Shivakumar, M. V. K., & Stefanski, R. (2011). Climate change in South Asia. *Springer Science*, 13–30.

Stem, N. (2007). The economics of climate change: the stern review. *Cambridge University Press, Cambridge*, 692.

Stewart, I. T., Cayan, D. R., & Dettinger, M. D. (2004). Changes in snowmelt runoff timing in Western North America under a 'Business as Usual' climate change scenario. *Climate Change*, *62*, 217–232.

Stige, L. C., Stave, J., Chan, K. S., Ciannelli, L., Pettorelli, N., Glantz, M., Stenseth, N. C. (2006). The effect of climate variation on agro-pastoral production in Africa. *National Academy of Science of the USA*, *103*, 3049–3053.

Sultana, H., Ali, N., Iqbal, M. M., & Khan, A. M. (2009). Vulnerability and adaptability of wheat production in different climatic zones of Pakistan under climate change scenarios. *Climate Change*, *94*(1–2), 123–142.

Tol, R. S. J. (2001). Equitable cost-benefit analysis of climate change policies. *Ecological Economics - Elsevier*, *36*(1), 71–85.

Tripathi, S., Srinivas, V. V., & Nanjundiah, R. S. (2006). Downscaling of precipitation for climate change scenarios: a support vector machine approach. *Journal of Hydrology*, *330*, 621–640.

Tubiello, F. N. (2005). Climate variability and agriculture: perspectives on current and future challenges. In: Knight B (ed) Impact of climate change, variability and weather fluctuations on crops and their produce markets. *Impact Reports, Cambridge*, 45–63.

UNDP. (2015). “Integrated Results and Resources Framework.” Annex II in Report of the Administrator on the Strategic Plan: Performance and Results for 2014. United Nations Development Program. Presented in Annual Session, June. www.undp.org/content/dam/undp/library/corporate/Executive%20_Board/2015/Annual-session/English/dp2015-11_Annexes%20I%20II%20and%20III.docx. Accessed 03 October 2016.

UNEP. (2007), ‘Insuring for Sustainability: Why and How the Leaders are Doing it’, United Nations Environmental Program. Financial Initiative, UNEP, Geneva.

UNFCCC. (1992). United Nations Framework Convention on Climate Change. http://www.unfccc.int/. Accessed on 25 May 2015.

UNFCCC. (2000). Mechanisms Pursuant to Articles 6, 12 and 16 of the Kyoto Protocol. Principles, Modalities, Rules and Guidelines for the Mechanisms under Articles, 6, 12 and 17 of the Kyoto Protocol: Submissions from Parties, Note by the Secretariat, Addendum, FCCC/SB/2000/MISC.1/Add.2, United Nations Framework Convention on Climate Change Secretariat, Bonn, Germany.

UNFCCC. (2013). Reporting and accounting of LULUCF activities under the Kyoto Pro-tocol. United Nations Framework Convention on Climatic Change, Bonn, Germany. Available at: http://unfccc.int/methods/lulucf/items/4129.php. Accessed 25 May 2015.

Urrutia, R., & Vuille, M. (2009). Climate change projections for the tropical Andes using a regional climate model: Temperature and precipitation simulations for the end of the 21st century. *Journal of Geophysical Research*, *114*.

Vogel, C. (2005). Seven fat years and seven lean years? Climate change and agriculture in Africa. *IDS Bulettin*, *36*, 30–35.

Wetherald, R. T., & Manabe, S. (2002). Simulation of hydrologic changes associated with global warming. *Journal of Geophysical Research*, *107*(D19), 4379.

Wijeratne, M. A. (1996). Tea: plucking strategies. *Planters Chronicle*, 443.

Wijesekera, N. T. S. (1998). Surface water resources and climate change. *National Science Foundation*.

Wijesekera, N. T. S. (2010). Surface Water Resources and Climate Change. *National Science Foundation*, (Ministry of Irrigation and water resources management, Sri Lanka).

Wijesekera, N. T. S., & Abeynayake, J. C. (2003). Watershed similarity conditions for peak flow transition. A study of river basins in the wet zone of Sri Lanka. *Engineer, Journal of the Institution of Engineers Sri Lanka*.

Wijesekera, N. T. S., & Musiake, K. (1990). Streamflow Modelling of Sri Lankan Catchments (1) – Mahaweli River Catchment at Peradeniya, Seisan Kenkyu. *Journal of the Institute of Industrial Science*.

Wilby, R. L., Dawson, C. W., & Barrow, E. M. (2002). SDSM - A decision support tool for the assessment of regional climate change impacts. *Elsevier*, *17*, 147–159.

Wilby, R. L., & Dessai, S. (2010). Robust adaptation to climate change. *Royal Meteorological Society*, (DOI: 10.1002/wea.543).

Wilby, R. L., Whitehead, P. G., Wade, A. J., Butterfield, D., Davis, R. J., & Watts, G. (2006). Integrated modelling of climate change impacts on water resources and quality in a lowland catchment: River Kennet, UK. *Elsevier*, *330*, 204–220.

Wilby, R. L., & Wigley, T. M. L. (2000). Precipitation predictors for downscaling: observed and General Circulation Model relationship. *International Journal of Climatology*, *20*, 641–661.

Xiao, G., Liu, W., Xu, Q., Sun, Z., & Wang, J. (2005). Effects of temperature increase and elevated CO2 concentration, with supplemental irrigation, on the yield of rain-fed spring wheat in a semiarid region of China. *Agricultural Water Management*, *74*(3), 243–255.

Xiaofeng, G., & Richman, M. B. (1995). On the Application of Cluster Analysis to Growing Season Precipitation Data in North America East of the Rockies. *American Meteorological Scociety*, 897–937.

Xuefeng, C., Steinman, A., & ASCE, A. M. (2009). Event and Continous Hydrologic modeling with HEC HMS. *Journal of Irrigation and Drainage Engineering*.

Zhang, Y., Su, F., Hao, Z., Xu, C., Yu, Z., Wang, L., & Tong, K. (2015). Impact of projected climate change on the hydrology in the headwaters of the Yellow River Basin. *Hydrological Process*, *29*, 4379–4397.

Zorita, E., & von Storch, H. (1999). The analog method as a simple statistical downscaling technique: comparison with more complicated methods. *Journal of Climate*, *12*, 2474–2489.

Zubair, L. (2003). Sensitivity of Kelani streamflow in Sri Lanka to ENSO. *Hydrological Process*.

APPENDICES

APPENDIX 01: - Available Climate Models and Climate Extremes over South Asia

Table A1-1 Climate Models and Their Resolutions

Model ID, Vintage	Sponsor(s), Country	Atmosphere Top Resolution[a] References	Ocean Resolution[b] Z Coord., Top BC References	Sea Ice Dynamics, Leads References	Coupling Flux Adjustments References	Land Soil, Plants, Routing References
1: BCC-CM1, 2005	Beijing Climate Center, China	top = 25 hPa T63 (1.9° x 1.9°) L16 Dong et al., 2000; CSMD, 2005; Xu et al., 2005	1.9° x 1.9° L30 depth, free surface Jin et al., 1999	no rheology or leads Xu et al., 2005	heat, momentum Yu and Zhang, 2000; CSMD, 2005	layers, canopy, routing CSMD, 2005
2: BCCR-BCM2.0, 2005	Bjerknes Centre for Climate Research, Norway	top = 10 hPa T63 (1.9° x 1.9°) L31 Déqué et al., 1994	0.5°–1.5° x 1.5° L35 density, free surface Bleck et al., 1992	rheology, leads Hibler, 1979; Harder, 1996	no adjustments Furevik et al., 2003	Layers, canopy, routing Mahfouf et al., 1995; Douville et al., 1995; Oki and Sud, 1998
3: CCSM3, 2005	National Center for Atmospheric Research, USA	top = 2.2 hPa T85 (1.4° x 1.4°) L26 Collins et al., 2004	0.3°–1° x 1° L40 depth, free surface Smith and Gent, 2002	rheology, leads Briegleb et al., 2004	no adjustments Collins et al., 2006	layers, canopy, routing Oleson et al., 2004; Branstetter, 2001
4: CGCM3.1(T47), 2005	Canadian Centre for Climate Modelling and Analysis, Canada	top = 1 hPa T47 (~2.8° x 2.8°) L31 McFarlane et al., 1992; Flato, 2005	1.9° x 1.9° L29 depth, rigid lid Pacanowski et al., 1993	rheology, leads Hibler, 1979; Flato and Hibler, 1992	heat, freshwater Flato, 2005	layers, canopy, routing Verseghy et al., 1993
5: CGCM3.1(T63), 2005		top = 1 hPa T63 (~1.9° x 1.9°) L31 McFarlane et al., 1992; Flato 2005	0.9° x 1.4° L29 depth, rigid lid Flato and Boer, 2001; Kim et al., 2002	rheology, leads Hibler, 1979; Flato and Hibler, 1992	heat, freshwater Flato, 2005	layers, canopy, routing Verseghy et al., 1993
6: CNRM-CM3, 2004	Météo-France/Centre National de Recherches Météorologiques, France	top = 0.05 hPa T63 (~1.9° x 1.9°) L45 Déqué et al., 1994	0.5°–2° x 2° L31 depth, rigid lid Madec et al., 1998	rheology, leads Hunke-Dukowicz, 1997; Salas-Mélia, 2002	no adjustments Terray et al., 1998	layers, canopy,routing Mahfouf et al., 1995; Douville et al., 1995; Oki and Sud, 1998
7: CSIRO-MK3.0, 2001	Commonwealth Scientific and Industrial Research Organisation (CSIRO) Atmospheric Research, Australia	top = 4.5 hPa T63 (~1.9° x 1.9°) L18 Gordon et al., 2002	0.8° x 1.9° L31 depth, rigid lid Gordon et al., 2002	rheology, leads O'Farrell, 1998	no adjustments Gordon et al., 2002	layers, canopy Gordon et al., 2002
8: ECHAM5/MPI-OM, 2005	Max Planck Institute for Meteorology, Germany	top = 10 hPa T63 (~1.9° x 1.9°) L31 Roeckner et al., 2003	1.5° x 1.5° L40 depth, free surface Marsland et al., 2003	rheology, leads Hibler, 1979; Semtner, 1976	no adjustments Jungclaus et al., 2005	bucket, canopy, routing Hagemann, 2002; Hagemann and Dümenil-Gates, 2001
9: ECHO-G, 1999	Meteorological Institute of the University of Bonn, Meteorological Research Institute of the Korea Meteorological Administration (KMA), and Model and Data Group, Germany/Korea	top = 10 hPa T30 (~3.9° x 3.9°) L19 Roeckner et al., 1996	0.5°–2.8° x 2.8° L20 depth, free surface Wolff et al., 1997	rheology, leads Wolff et al., 1997	heat, freshwater Min et al., 2005	bucket, canopy, routing Roeckner et al., 1996; Dümenil and Todini, 1992

Model ID, Vintage	Sponsor(s), Country	Atmosphere Top Resolution[a] References	Ocean Resolution[b] Z Coord., Top BC References	Sea Ice Dynamics, Leads References	Coupling Flux Adjustments References	Land Soil, Plants, Routing References
10: FGOALS-g1.0, 2004	National Key Laboratory of Numerical Modeling for Atmospheric Sciences and Geophysical Fluid Dynamics (LASG)/Institute of Atmospheric Physics, China	top = 2.2 hPa T42 (~2.8° x 2.8°) L26 Wang et al., 2004	1.0° x 1.0° L16 eta, free surface Jin et al., 1999; Liu et al., 2004	rheology, leads Briegleb et al., 2004	no adjustments Yu et al., 2002, 2004	layers, canopy, routing Bonan et al., 2002
11: GFDL-CM2.0, 2005	U.S. Department of Commerce/ National Oceanic and Atmospheric Administration (NOAA)/Geophysical Fluid Dynamics Laboratory (GFDL), USA	top = 3 hPa 2.0° x 2.5° L24 GFDL GAMDT, 2004	0.3°–1.0° x 1.0° depth, free surface Gnanadesikan et al., 2004	rheology, leads Winton, 2000; Delworth et al., 2006	no adjustments Delworth et al., 2006	bucket, canopy, routing Milly and Shmakin, 2002; GFDL GAMDT, 2004
12: GFDL-CM2.1, 2005		top = 3 hPa 2.0° x 2.5° L24 GFDL GAMDT, 2004 with semi-Lagrangian transports	0.3°–1.0° x 1.0° depth, free surface Gnanadesikan et al., 2004	rheology, leads Winton, 2000; Delworth et al., 2006	no adjustments Delworth et al., 2006	bucket, canopy, routing Milly and Shmakin, 2002; GFDL GAMDT, 2004
13: GISS-AOM, 2004	National Aeronautics and Space Administration (NASA)/ Goddard Institute for Space Studies (GISS), USA	top = 10 hPa 3° x 4° L12 Russell et al., 1995; Russell, 2005	3° x 4° L16 mass/area, free surface Russell et al., 1995; Russell, 2005	rheology, leads Flato and Hibler, 1992; Russell, 2005	no adjustments Russell, 2005	layers, canopy, routing Abramopoulos et al., 1988; Miller et al., 1994
14: GISS-EH, 2004		top = 0.1 hPa 4° x 5° L20 Schmidt et al., 2006	2° x 2° L16 density, free surface Bleck, 2002	rheology, leads Liu et al., 2003; Schmidt et al., 2004	no adjustments Schmidt et al., 2006	layers, canopy, routing Friend and Kiang, 2005
15: GISS-ER, 2004	NASA/GISS, USA	top = 0.1 hPa 4° x 5° L20 Schmidt et al., 2006	4° x 5° L13 mass/area, free surface Russell et al., 1995	rheology, leads Liu et al., 2003; Schmidt et al., 2004	no adjustments Schmidt et al., 2006	layers, canopy, routing Friend and Kiang, 2005
16: INM-CM3.0, 2004	Institute for Numerical Mathematics, Russia	top = 10 hPa 4° x 5° L21 Alekseev et al., 1998; Galin et al., 2003	2° x 2.5° L33 sigma, rigid lid Diansky et al., 2002	no rheology or leads Diansky et al., 2002	regional freshwater Diansky and Volodin, 2002; Volodin and Diansky, 2004	layers, canopy, no routing Alekseev et al., 1998; Volodin and Lykosoff, 1998
17: IPSL-CM4, 2005	Institut Pierre Simon Laplace, France	top = 4 hPa 2.5° x 3.75° L19 Hourdin et al., 2006	2° x 2° L31 depth, free surface Madec et al., 1998	rheology, leads Fichefet and Morales Maqueda, 1997; Goosse and Fichefet, 1999	no adjustments Marti et al., 2005	layers, canopy, routing Krinner et al., 2005
18: MIROC3.2(hires), 2004	Center for Climate System Research (University of Tokyo), National Institute for Environmental Studies, and Frontier Research Center for Global Change (JAMSTEC), Japan	top = 40 km T106 (~1.1° x 1.1°) L56 K-1 Developers, 2004	0.2° x 0.3° L47 sigma/depth, free surface K-1 Developers, 2004	rheology, leads K-1 Developers, 2004	no adjustments K-1 Developers, 2004	layers, canopy, routing K-1 Developers, 2004; Oki and Sud, 1998
19: MIROC3.2(medres), 2004		top = 30 km T42 (~2.8° x 2.8°) L20 K-1 Developers, 2004	0.5°–1.4° x 1.4° L43 sigma/depth, free surface K-1 Developers, 2004	rheology, leads K-1 Developers, 2004	no adjustments K-1 Developers, 2004	layers, canopy, routing K-1 Developers, 2004; Oki and Sud, 1998

Model ID, Vintage	Sponsor(s), Country	Atmosphere Top Resolution[a] References	Ocean Resolution[b] Z Coord., Top BC References	Sea Ice Dynamics, Leads References	Coupling Flux Adjustments References	Land Soil, Plants, Routing References
20: MRI-CGCM2.3.2, 2003	Meteorological Research Institute, Japan	top = 0.4 hPa T42 (~2.8° x 2.8°) L30 Shibata et al., 1999	0.5°–2.0° x 2.5° L23 depth, rigid lid Yukimoto et al., 2001	free drift, leads Mellor and Kantha, 1989	heat, freshwater, momentum (12°S–12°N) Yukimoto et al., 2001; Yukimoto and Noda, 2003	layers, canopy, routing Sellers et al., 1986; Sato et al., 1989
21: PCM, 1998	National Center for Atmospheric Research, USA	top = 2.2 hPa T42 (~2.8° x 2.8°) L26 Kiehl et al., 1998	0.5°–0.7° x 1.1° L40 depth, free surface Maltrud et al., 1998	rheology, leads Hunke and Dukowicz 1997, 2003; Zhang et al., 1999	no adjustments Washington et al., 2000	layers, canopy, no routing Bonan, 1998
22: UKMO-HadCM3, 1997	Hadley Centre for Climate Prediction and Research/Met Office, UK	top = 5 hPa 2.5° x 3.75° L19 Pope et al., 2000	1.25° x 1.25° L20 depth, rigid lid Gordon et al., 2000	free drift, leads Cattle and Crossley, 1995	no adjustments Gordon et al., 2000	layers, canopy, routing Cox et al., 1999
23: UKMO-HadGEM1, 2004		top = 39.2 km ~1.3° x 1.9° L38 Martin et al., 2004	0.3°–1.0° x 1.0° L40 depth, free surface Roberts, 2004	rheology, leads Hunke and Dukowicz, 1997; Semtner, 1976; Lipscomb, 2001	no adjustments Johns et al., 2006	layers, canopy, routing Essery et al., 2001; Oki and Sud, 1998

Table A1-2 Extreme Climate Indices used for Extreme Analysis over South Asia

Code	Indicator Name	Definition	Units
FD0	Frost days	Annual count when TN (daily minimum temperature < 25°C	Days
SU25	Summer Days	Annual count when TN (daily maximum temperature > 25°C	Days
TR20	Tropical Nights	Annual count when TN (daily minimum temperature > 20°C	Days
GSL	Growing season length	Annual count between first span of at least 6 days with TG > 5°C and first span after 1st July of 6 days with TG < 5°C, where TG is daily mean temperature	Days
TXx	Max Tmax	Annual maximum value of daily maximum temperature	°C
TNx	Max Tmin	Annual maximum of daily minimum temperature	°C
TXn	Min Tmax	Annual minimum value of daily maximum temperature	°C
TNn	Min Tmin	Annual minimum value of daily minimum temperature	°C
TN10p	Cool nights	Percentage of days when TN < 10th percentile	Days
TX10p	Cool days	Percentage of days when TX < 10th percentile	Days
TN90p	Warm nights	Percentage of days when TN > 90th percentile	Days
TX90p	Warm days	Percentage of days when TX > 90th percentile	Days
WSDI	Warm spell duration indicator	Annual count of days with at least 6 consecutive days when TX > 90th percentile	Days
CSDI	Cold spell duration indicator	Annual count of days with at least 6 consecutive days when TN < 10th percentile	Days
DTR	Diurnal temperature range	Annual mean difference between TX and TN	°C
ETR	Extreme temperature range	Annual difference between highest TX and lowest TN	°C
R10	Number of heavy precipitation days	Annual count of days when rainfall ≥ 10mm	Days
R20	Number of very heavy precipitation days	Annual count of days when rainfall ≥ 20mm	Days
RX1day	Maximum 1-day precipitation amount	Annual maximum 1-day precipitation	mm
RX5day	Maximum 1-day precipitation amount	Annual maximum consecutive 1-day precipitation	mm
R95p	Very wet days	Annual total PRCP when daily rainfall > 95th percentile	mm
R99p	Extremely wet days	Annual total PRCP when daily rainfall > 99th percentile	mm
PRCPTOT	Annual total wet-day precipitation	Annual total PRCP in wet days (daily rainfall ≥ 1mm)	mm
SDII	Simple daily intensity index	Annual total precipitation divided by the number of wet days (defined as daily rainfall ≥ 1mm) in the year	mm/day
R95PT	Annual contribution from very wet days	(R95p/PRCPTOT) x 100%	%
CDD	Consecutive dry days	Maximum number of consecutive days with rainfall < 1mm	Days
CWD	Consecutive wet days	Maximum number of consecutive days with rainfall ≥ 1mm	Days

Table A1-3 Trends of Temperature Indices for Specific Regions over South Asia (Asterisks * denote significant trends at 95% level)

Index	Overall	Sri Lanka	Tropical Region (excluding Sri Lanka)	Greater Himalayan Region	Eastern Himalayan Region	Thar/ Rajasthan desert region
CSDI	-0.17*	-0.08*	-0.16*	0.11	-0.38	-0.33*
WSDI	.010	0.42*	0.05	0.14	0.41*	0.09
DTR	-0.00	-0.01	-0.01	0.08*	0.02*	-0.02
ETR	0.01	-0.03	0.01	0.09	-0.08	0.05
SU25	0.20*	0.19	0.11	0.40	1.10*	0.39*
TN10p	-0.19*	-0.25*	-0.20*	0.15*	-0.29*	-0.29*
TN90p	0.12*	0.33*	0.11	-0.13	0.14	0.17*
TNn	0.01	0.04*	0.00	-0.01	0.02	0.05*
TNx	-0.01	0.01*	0.00	-0.01*	0.02	0.02
TR20	0.04	0.26	0.10	-0.43*	0.70*	0.17
TX10p	-0.14*	-0.24*	-0.14*	-0.03	-0.22*	-0.02
TX90p	0.16*	0.44*	0.14*	0.17*	0.41*	0.10
TXn	-0.02*	0.02	-0.01	-0.03	-0.04*	-0.01
TXx	0.01	0.04*	0.00	0.08	0.06*	0.05*

Table A1-3 Trends of Precipitation Indices for Specific Regions over South Asia (Asterisks * denote significant trends at 95% level)

Index	Overall	Sri Lanka	Tropical Region (excluding Sri Lanka)	Greater Himalayan Region	Eastern Himalayan Region	Thar/ Rajasthan desert region
CDD	-0.52*	0.23*	-0.60*	-0.09	-0.25	-0.67*
CWD	.01	-0.03	-0.00	0.01	0.01	-0.02
PRCPTOT	2.97*	-3.82	4.27*	6.05*	1.05	0.13
R10mm	0.09*	-0.12	0.10*	0.18*	0.04	0.01
R20mm	0.05*	-0.04	0.07*	0.10*	0.01	0.00
R95p	0.63	-0.66	1.02	2.06	-0.16	0.69
R99p	0.20	-0.60	0.34	1.09*	-0.31	0.09
RX1day	0.08	0.02	0.25*	0.34	-0.12	0.08
RX5day	0.07	-0.23	0.35	0.96	-0.28	0.04
SDII	-0.02*	0.02*	-0.02	0.02	-0.01	0.01

APPENDIX 02: - Thiessen Weighted Rainfall and Streamflow Comparison (Visual Checking – Hanwella Watersheds)

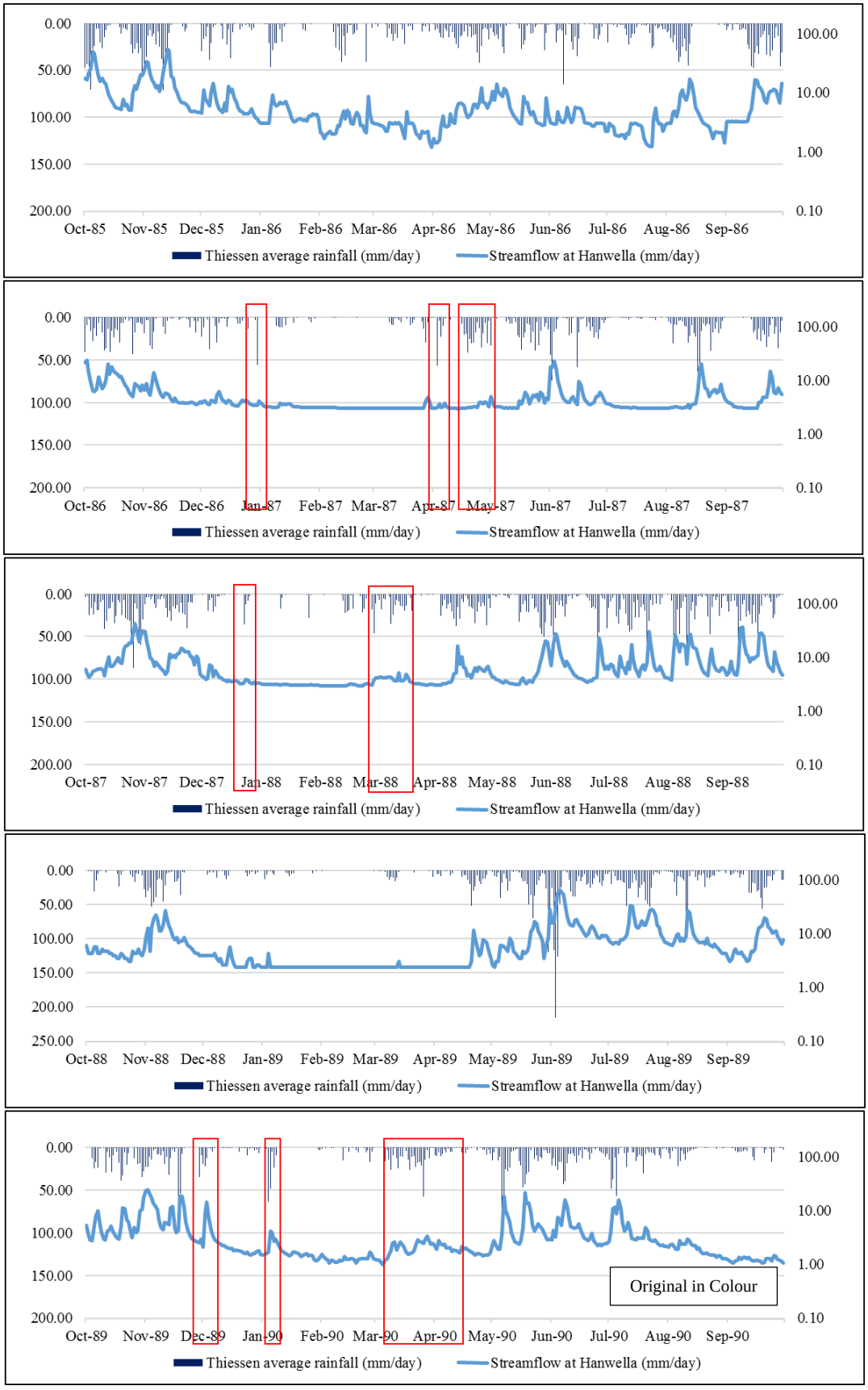

Appendix 02 - 1 Streamflow response for Thiessen average rainfall of Hanwella (85-90)

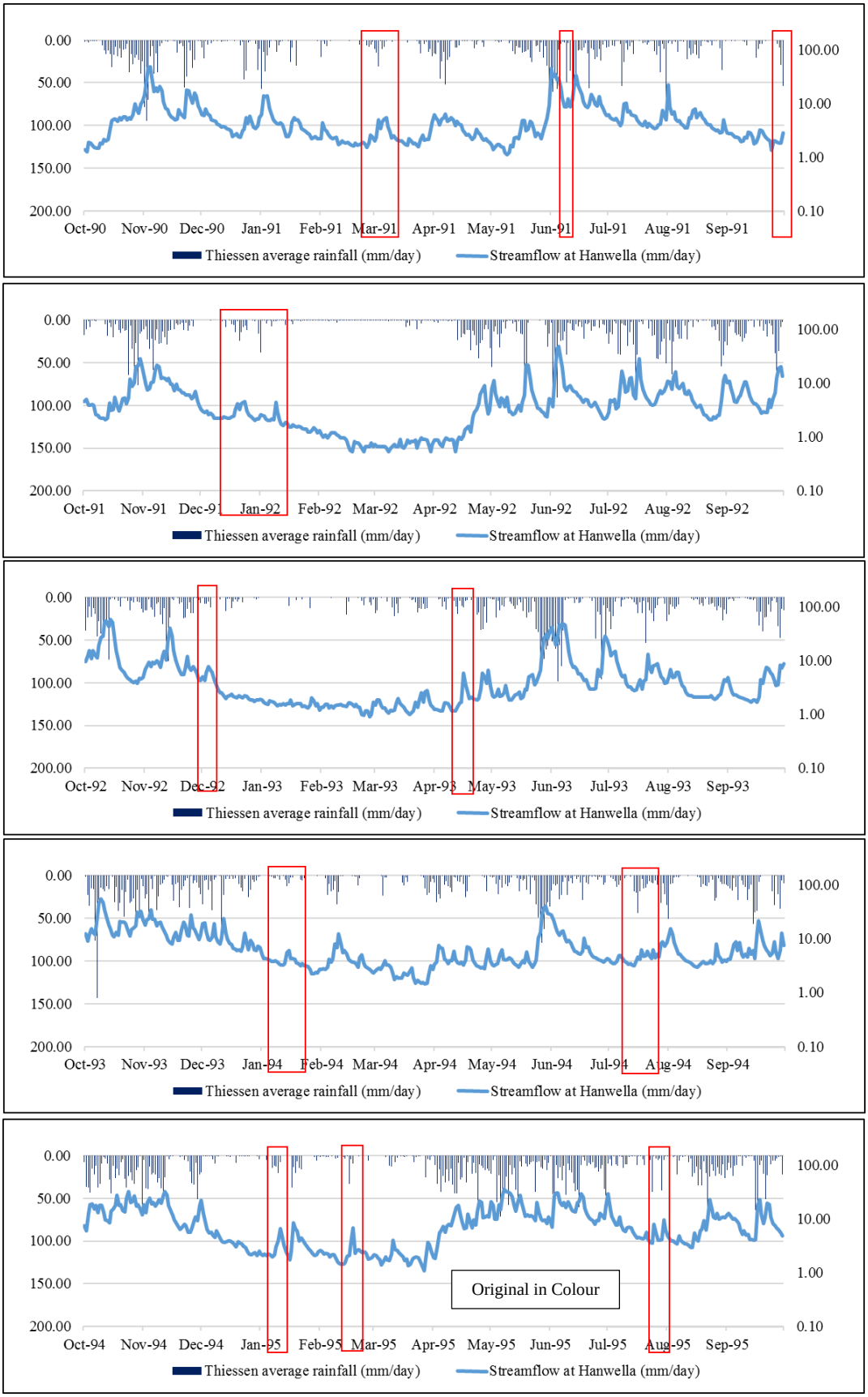

Appendix 02 – 2 Streamflow response for Thiessen average rainfall of Hanwella (90-95)

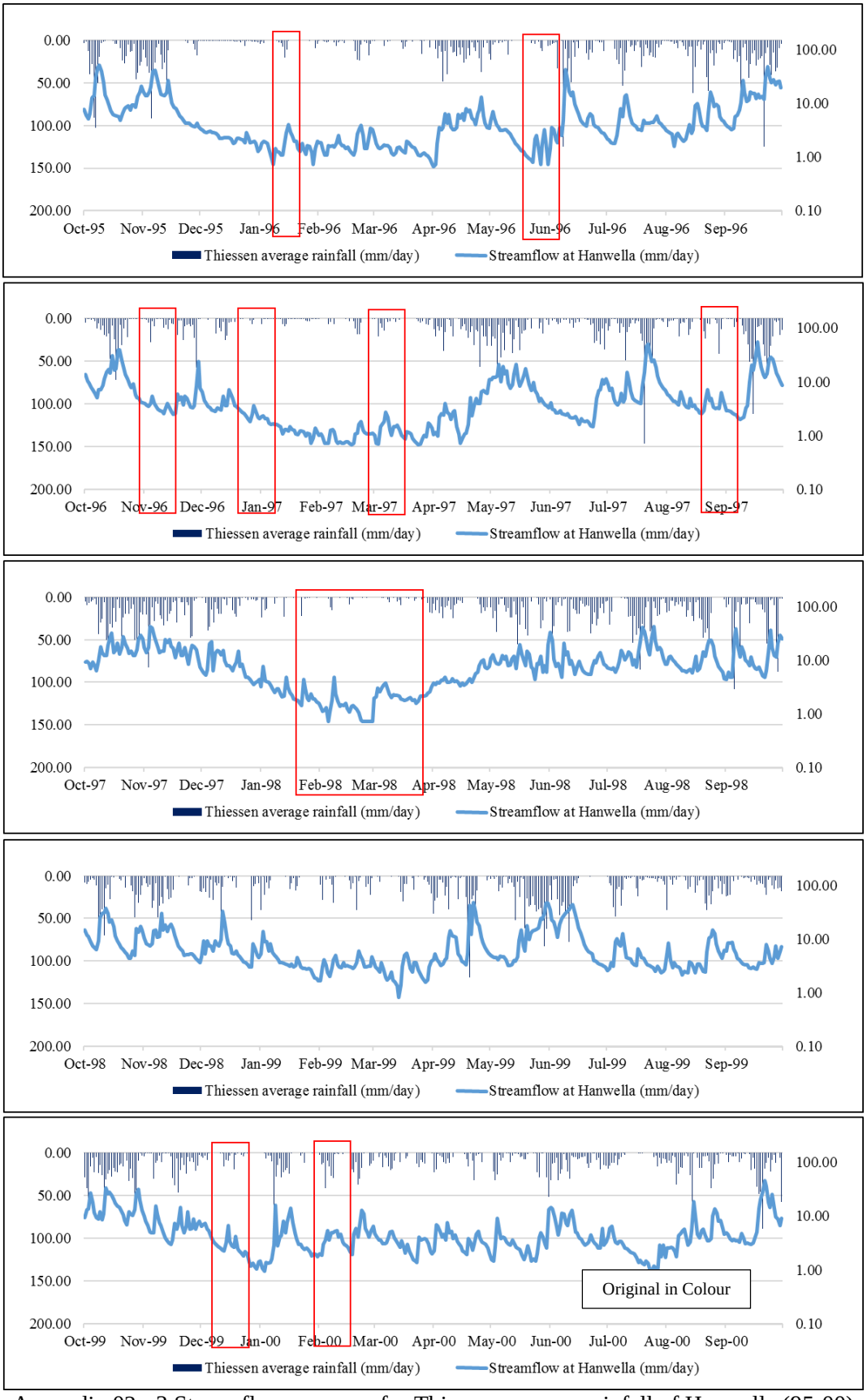

Appendix 02 - 3 Streamflow response for Thiessen average rainfall of Hanwella (95-00)

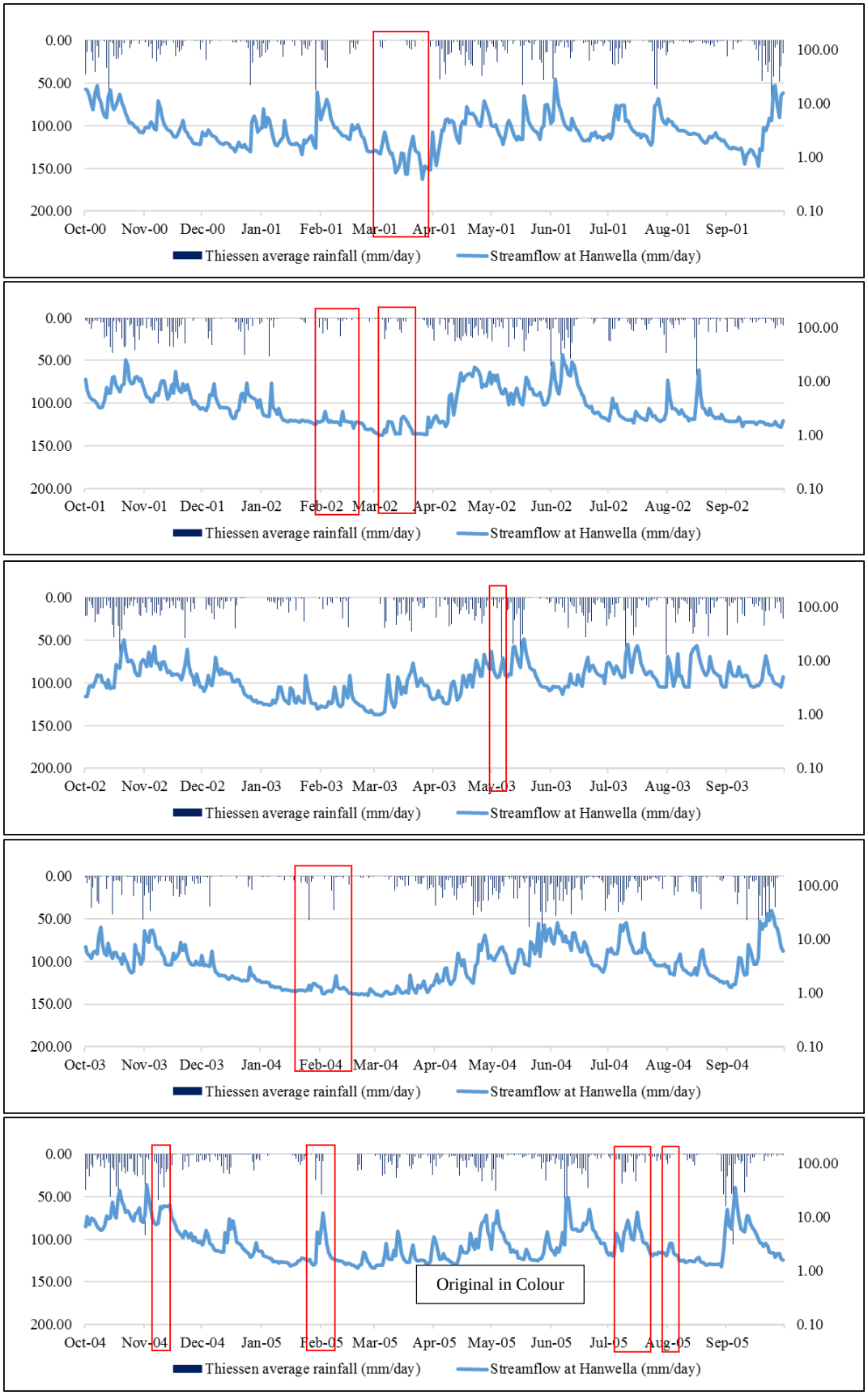

Appendix 02 - 4 Streamflow response for Thiessen average rainfall of Hanwella (00-05)

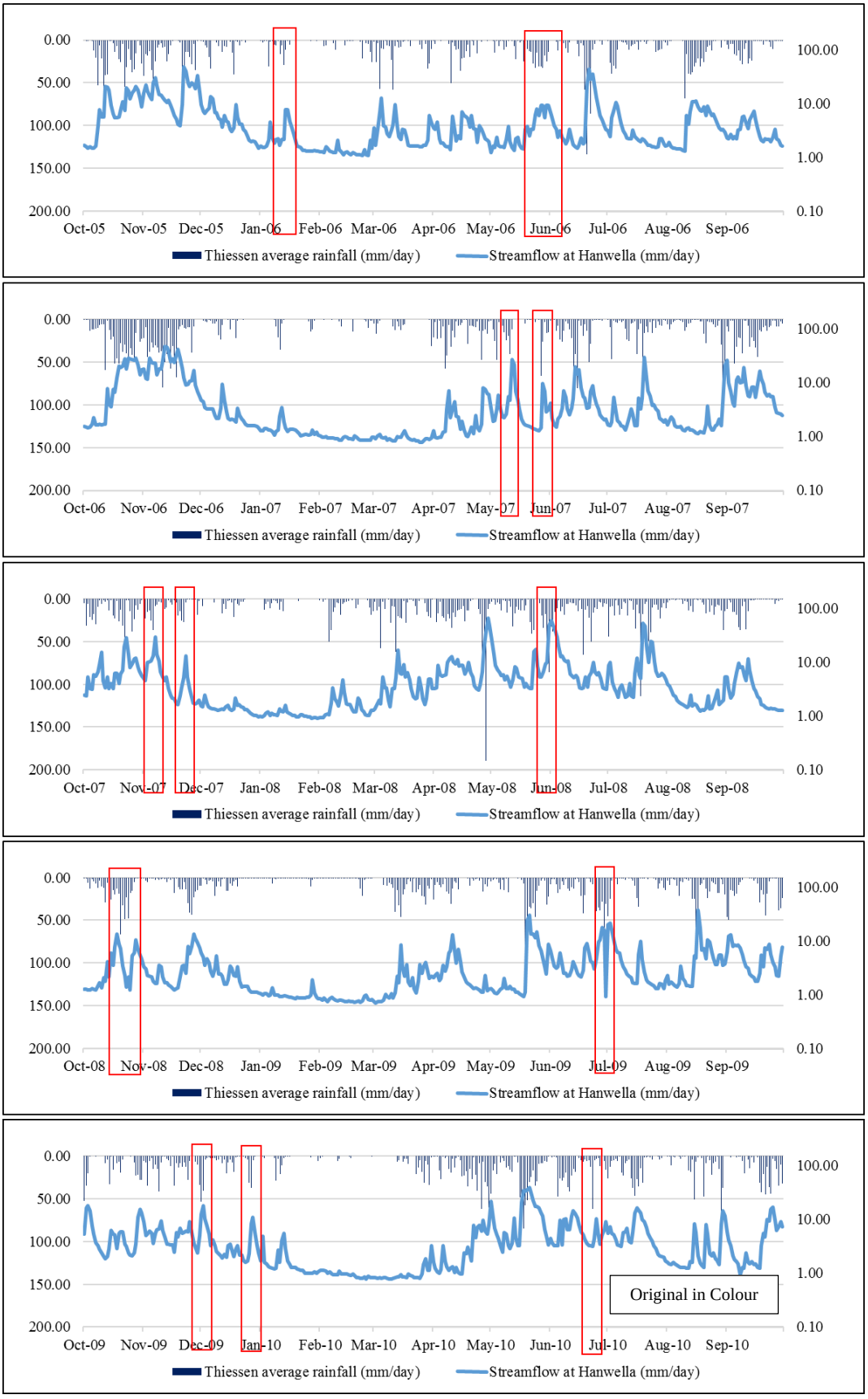

Appendix 02 - 5 Streamflow response for Thiessen average rainfall of Hanwella (05-10)

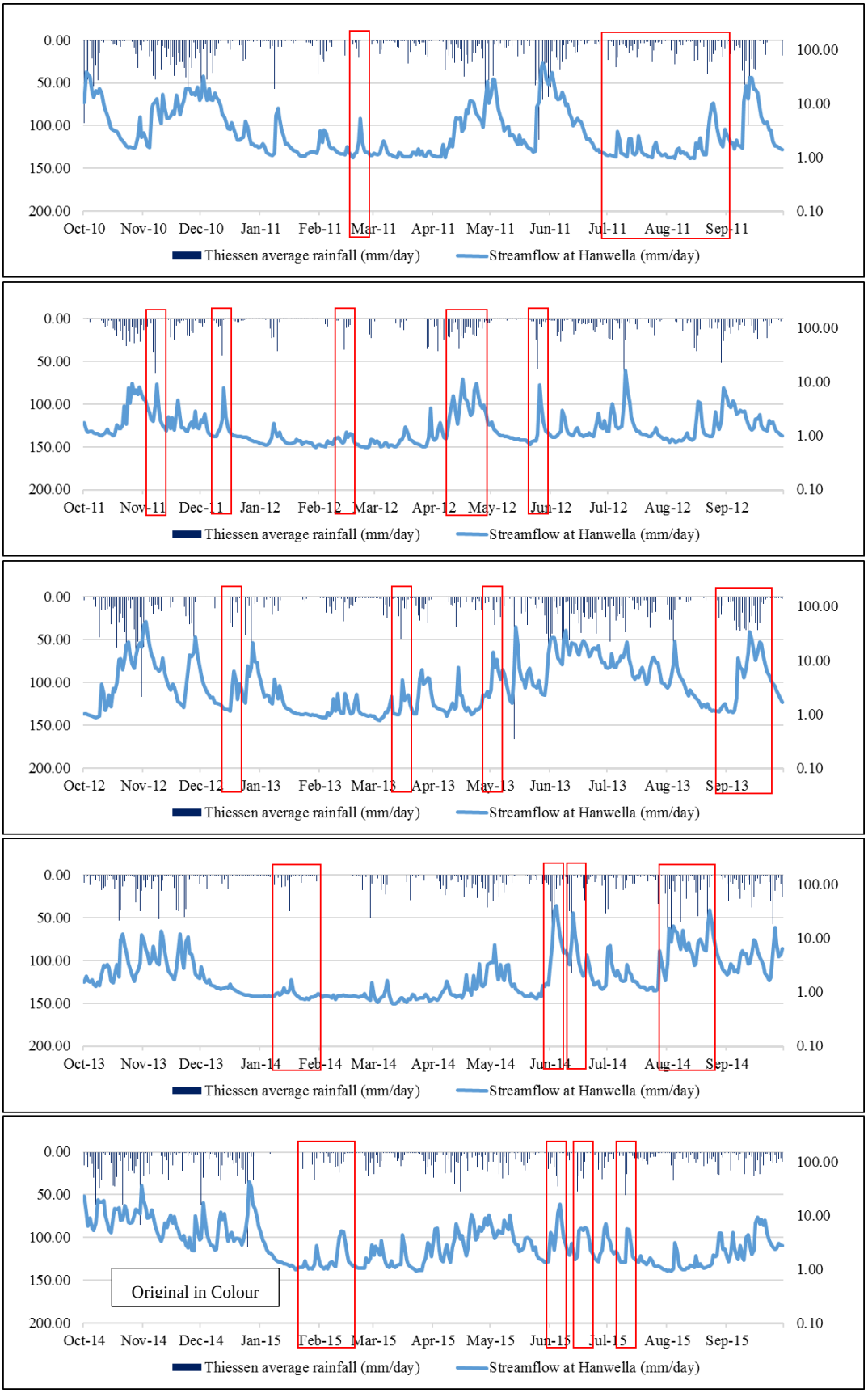

Appendix 02 - 6 Streamflow response for Thiessen average rainfall of Hanwella (10-15)

APPENDIX 03: - Monthly Rainfall Comparison (1970-2015)

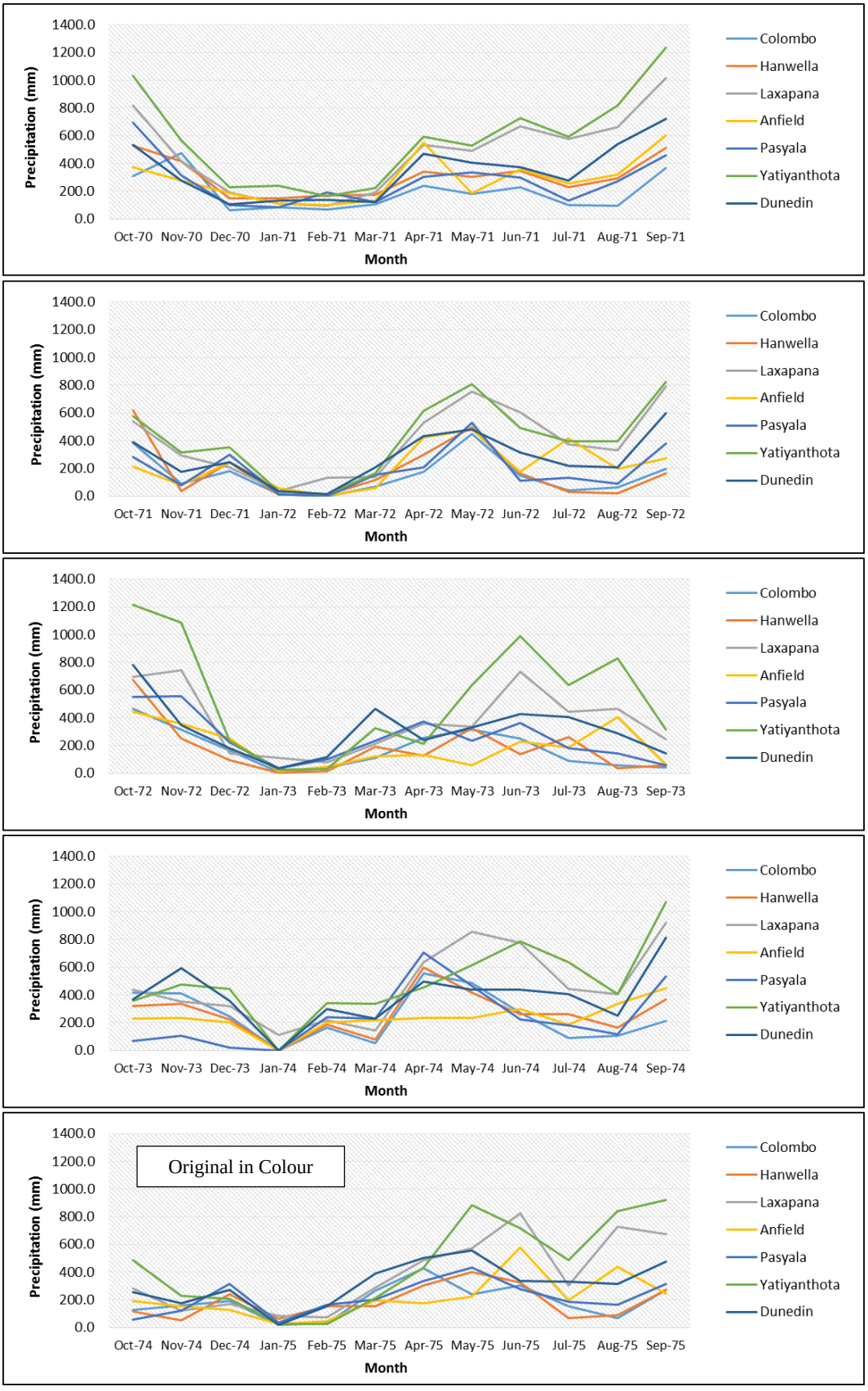

Appendix 03 - 1 Monthly cumulative precipitation variation from 1970-1975

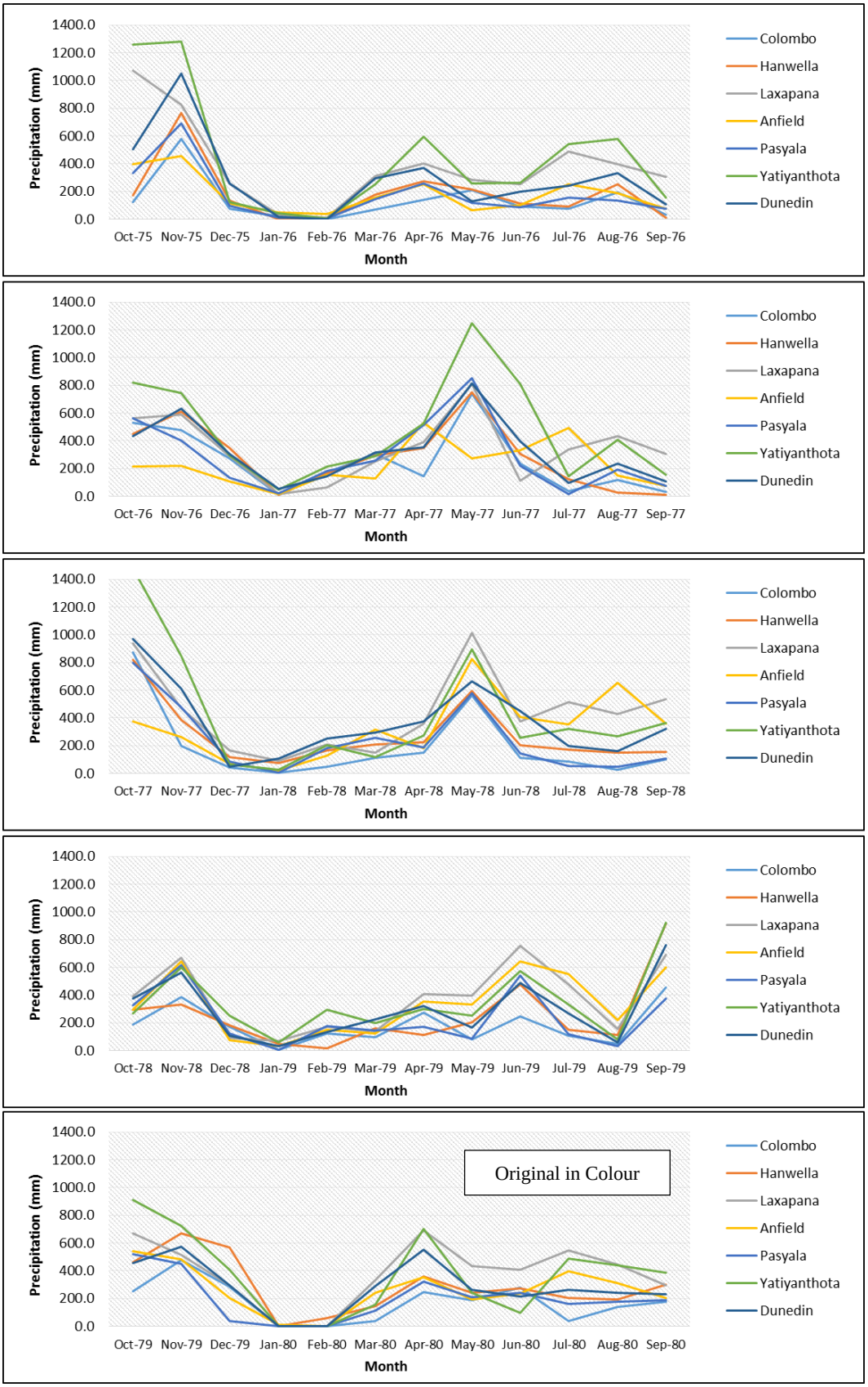

Appendix 03 - 2 Monthly cumulative precipitation variation from 1975-1980

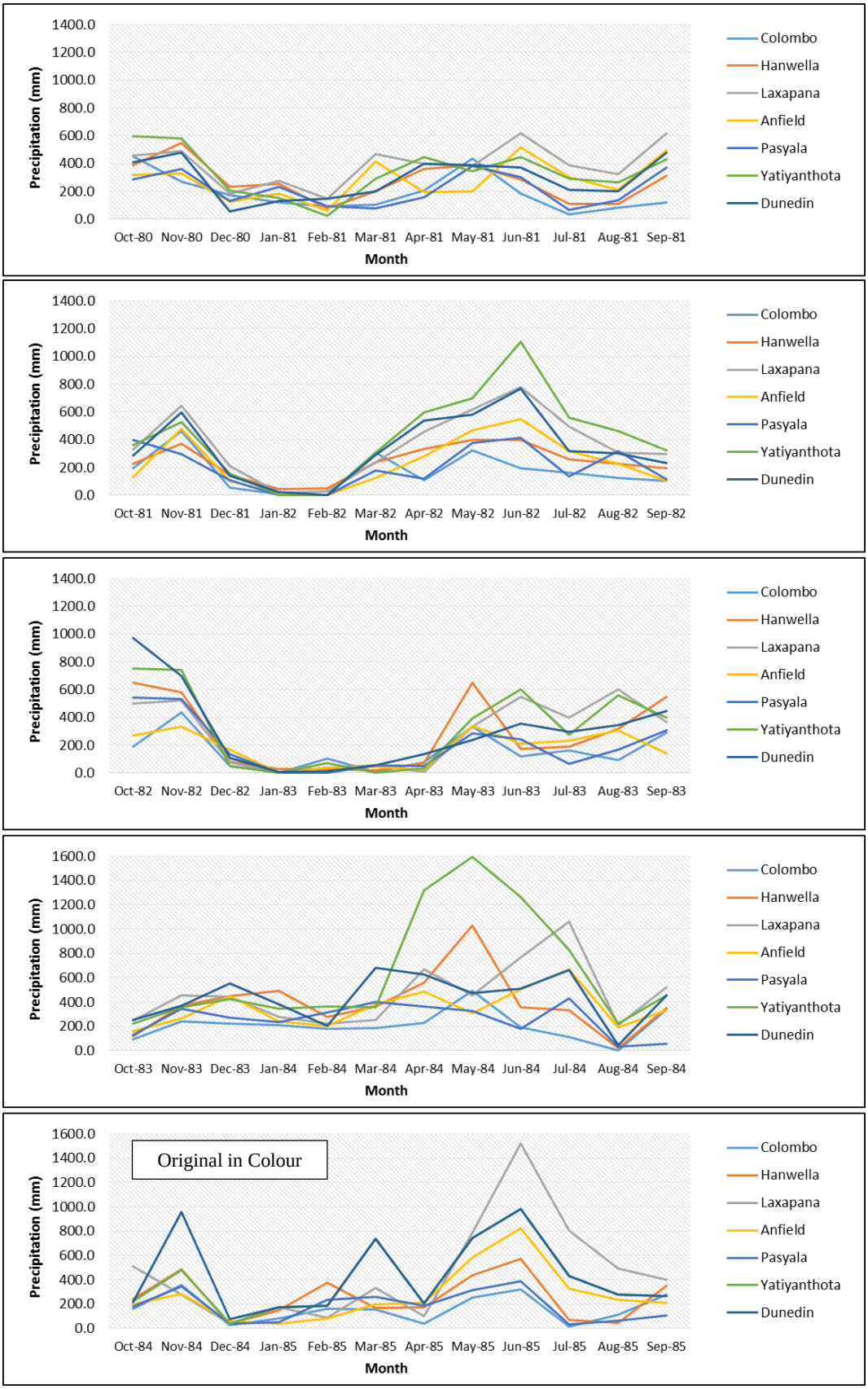

Appendix 03 - 3 Monthly cumulative precipitation variation from 1980-1985

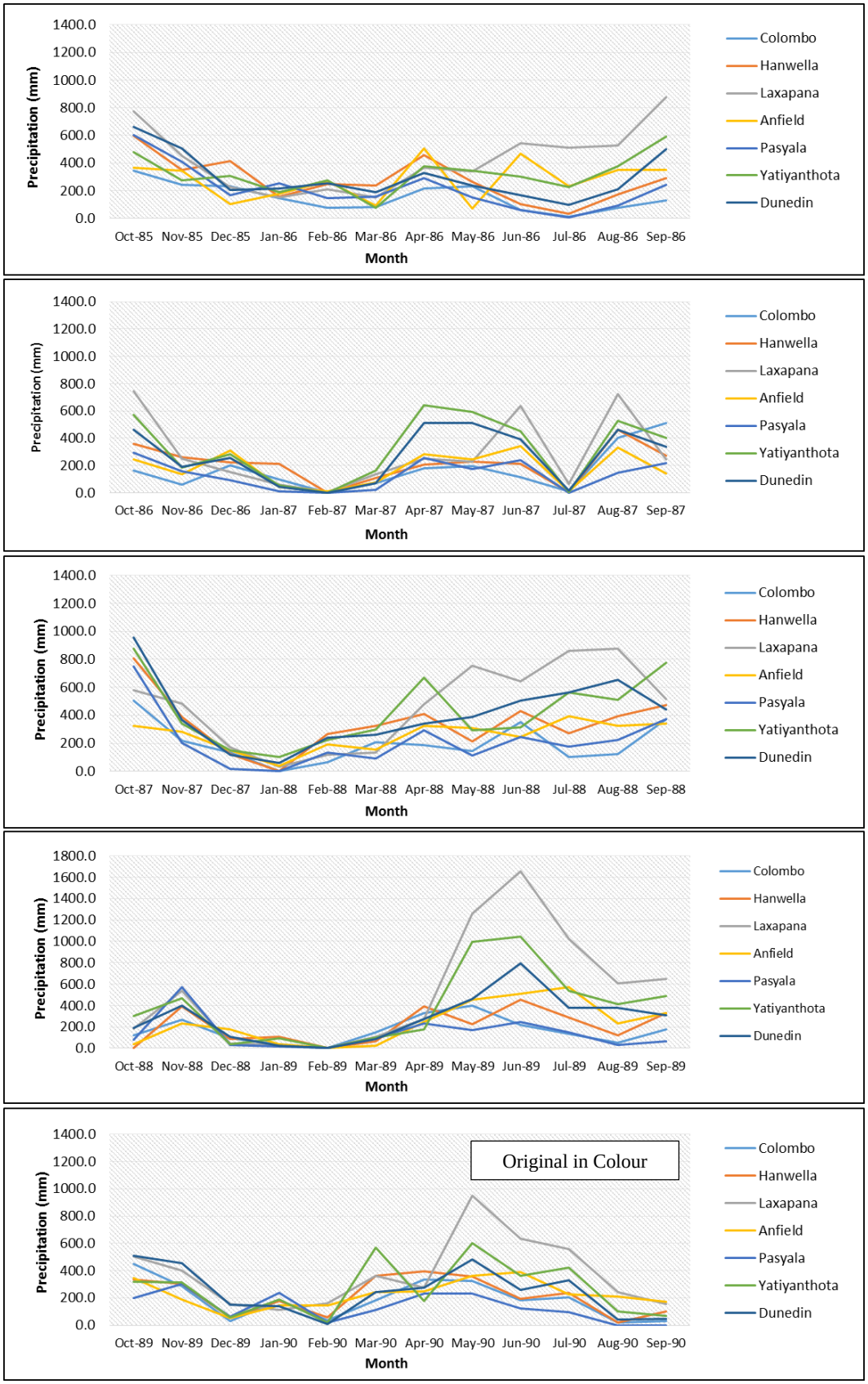

Appendix 03 - 4 Monthly cumulative precipitation variation from 1985-1990

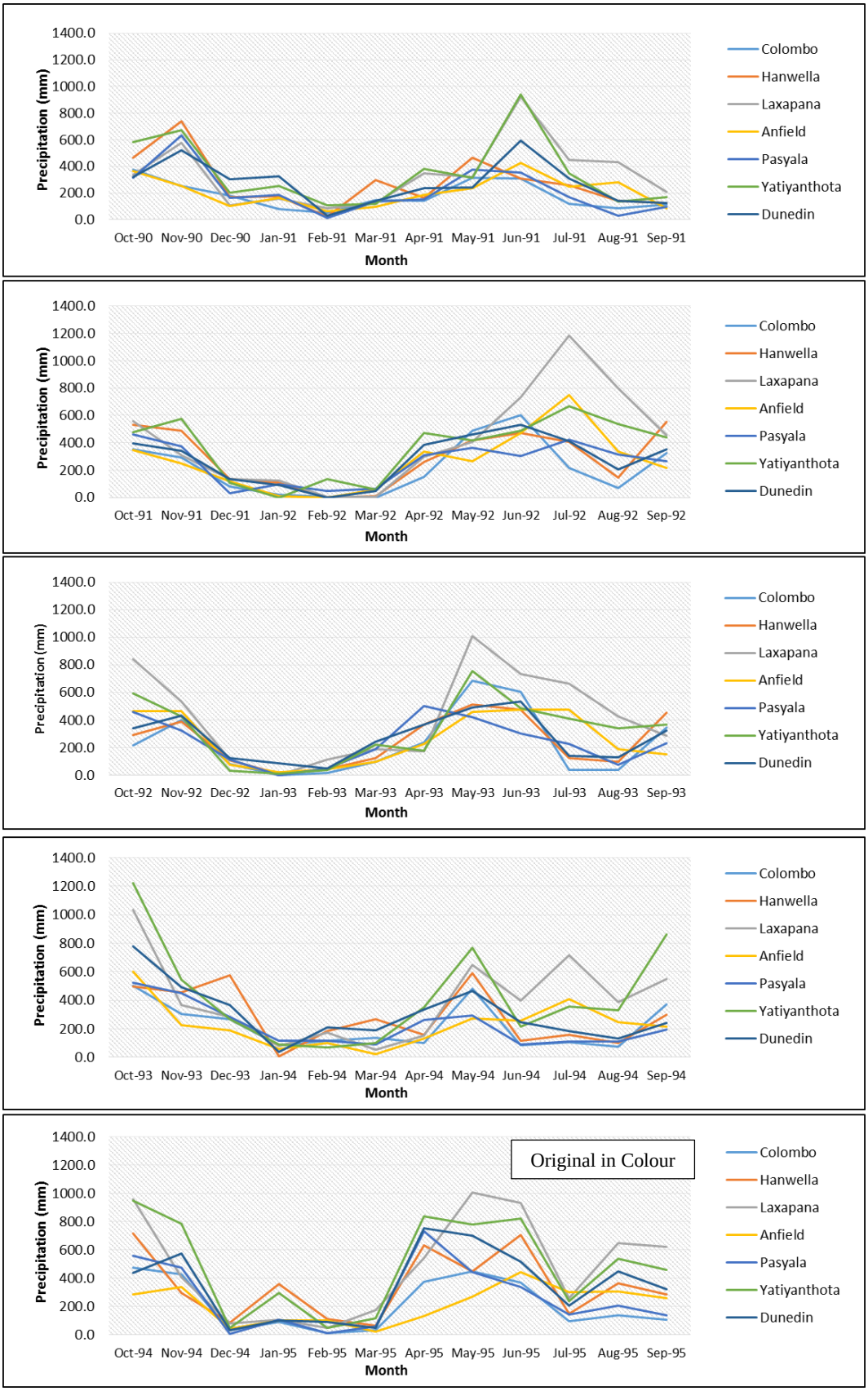

Appendix 03 - 5 Monthly cumulative precipitation variation from 1990-1995

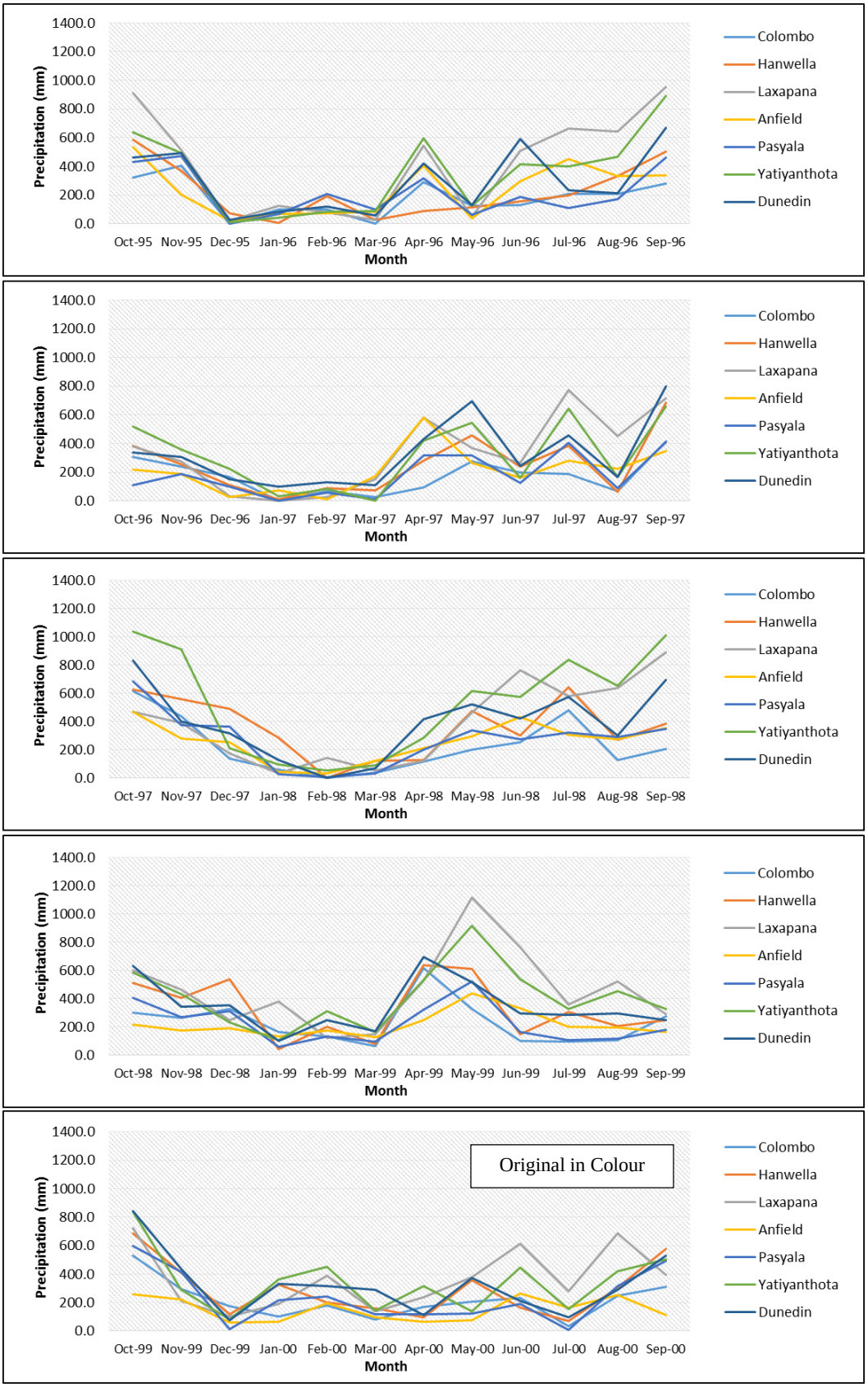

Appendix 03 – 6 Monthly cumulative precipitation variation from 1995-2000

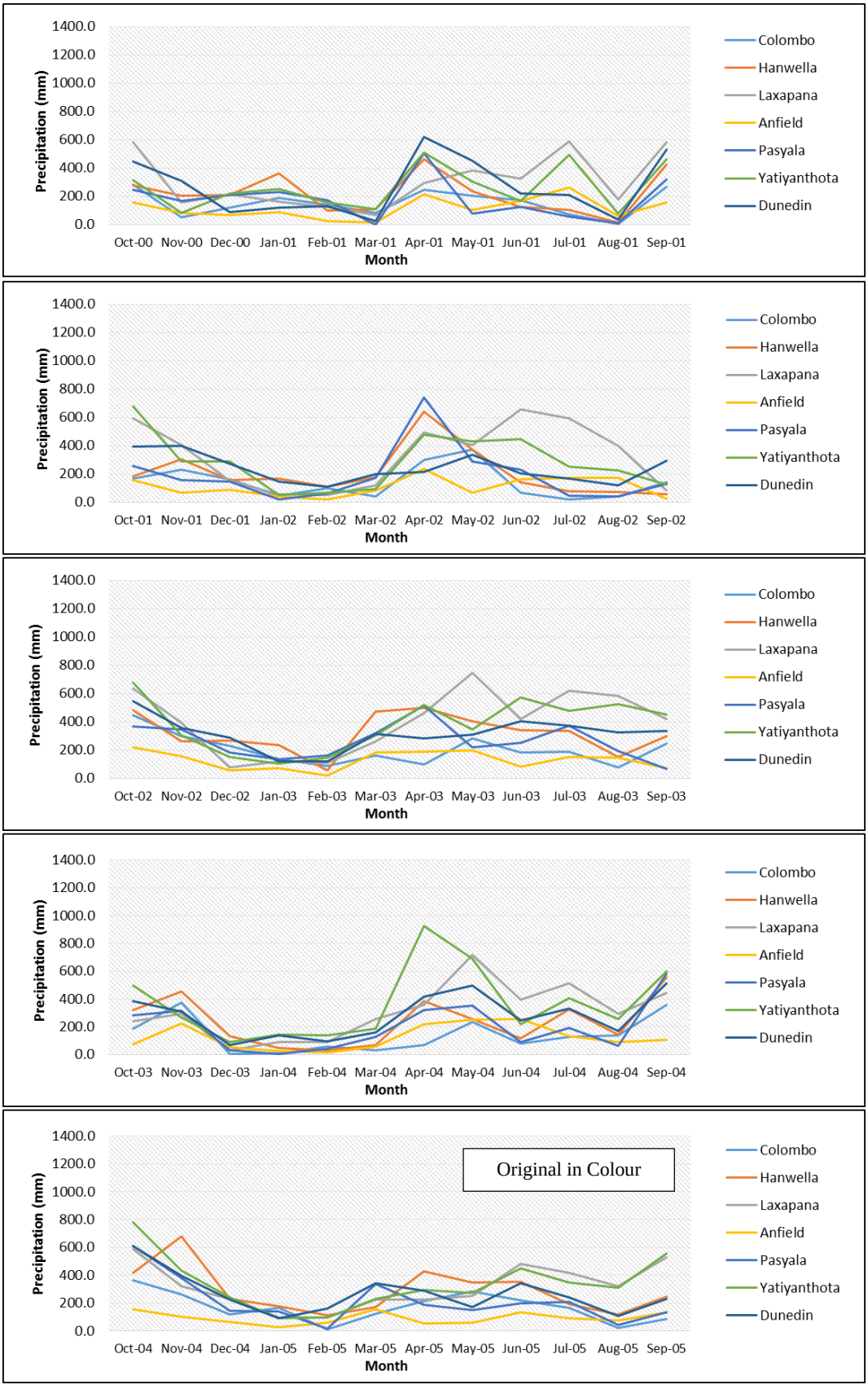

Appendix 03 - 7 Monthly cumulative precipitation variation from 2000-2005

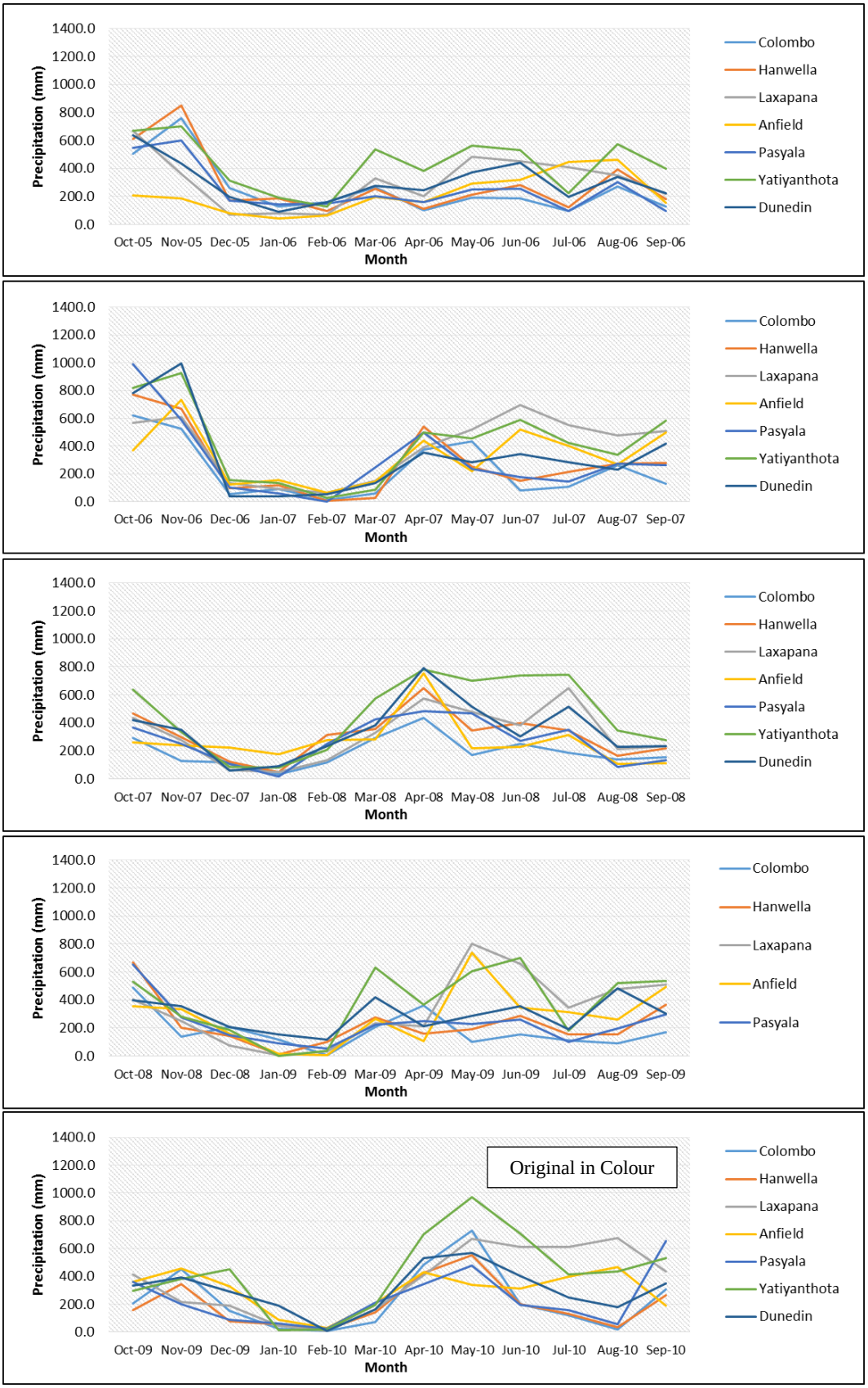

Appendix 03 - 8 Monthly cumulative precipitation variation from 2005-2010

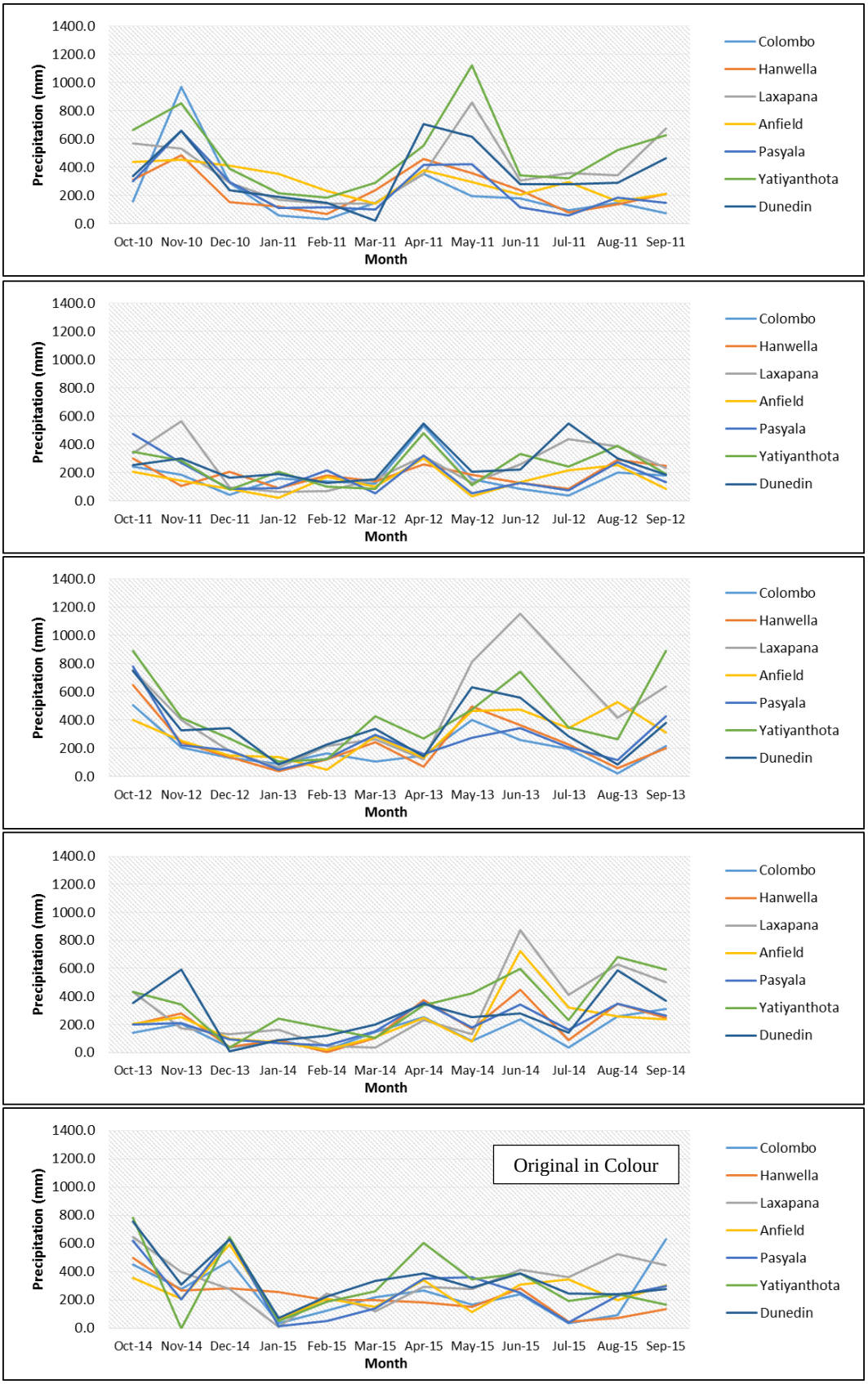

Appendix 03 - 9 Monthly cumulative precipitation variation from 2010-2015

APPENDIX 04: - Replacing of Missing Values of Evaporation (Colombo)

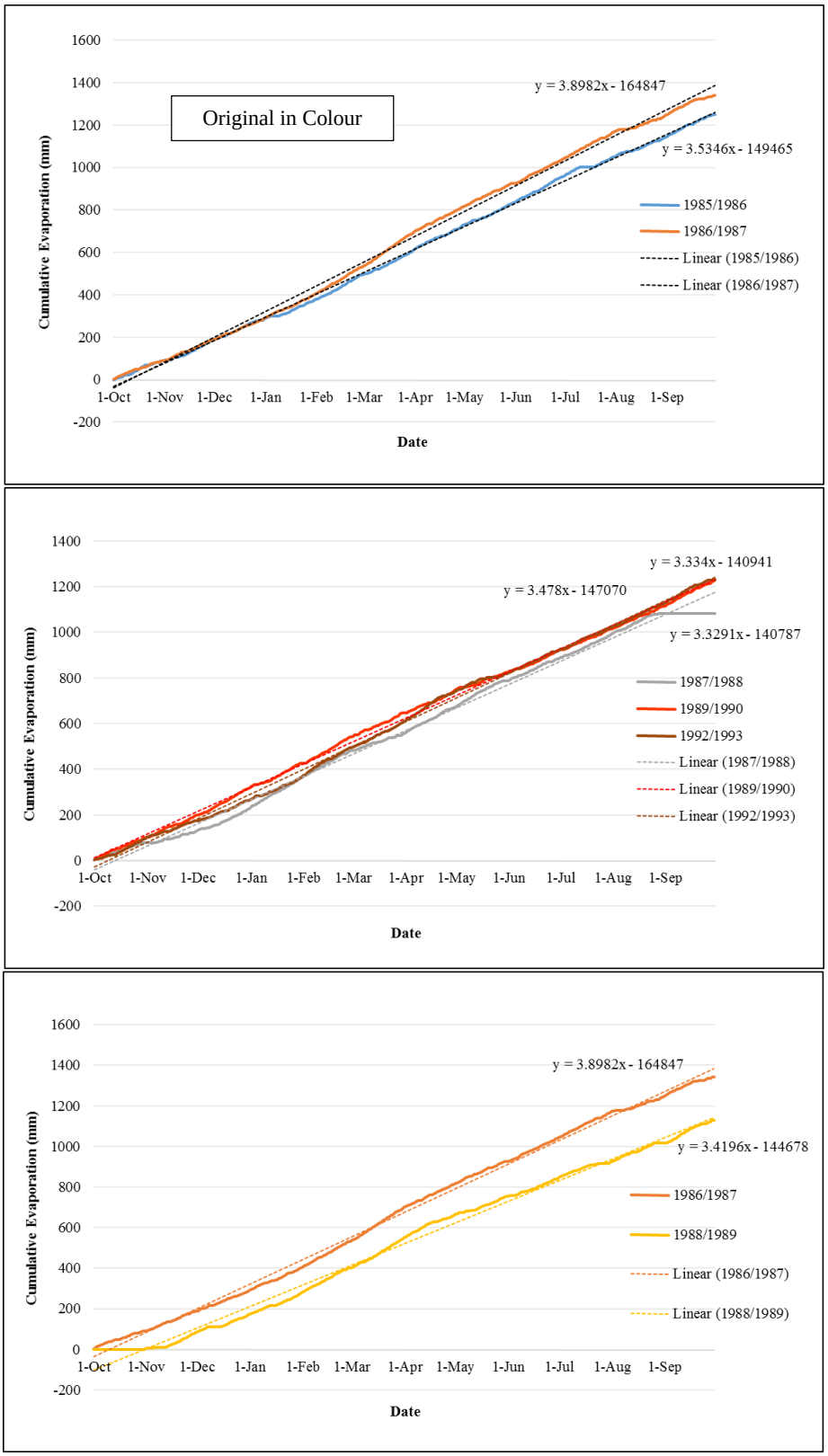

Appendix 04 - 1 Replacing missing data of evaporation of Colombo Meteorology observation from 1985-1992

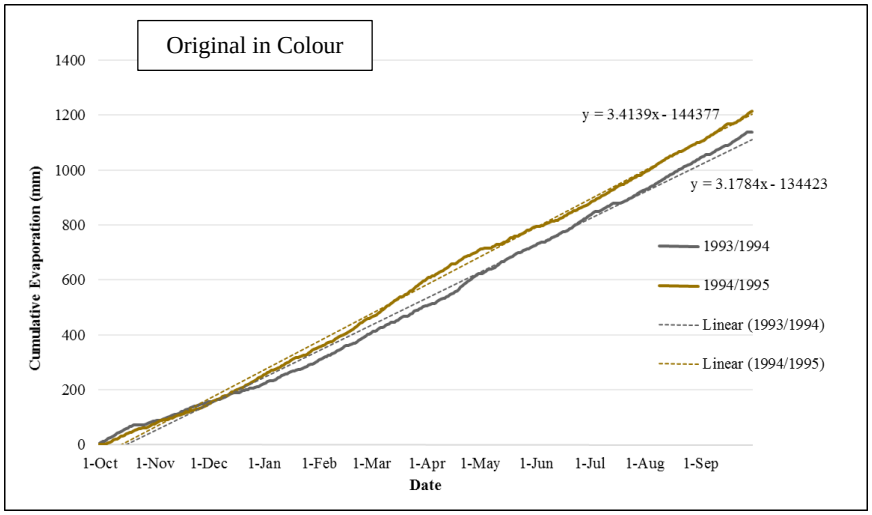

Appendix 04 - 2 Replacing missing data of evaporation of Colombo Meteorology observation from 1993-1995

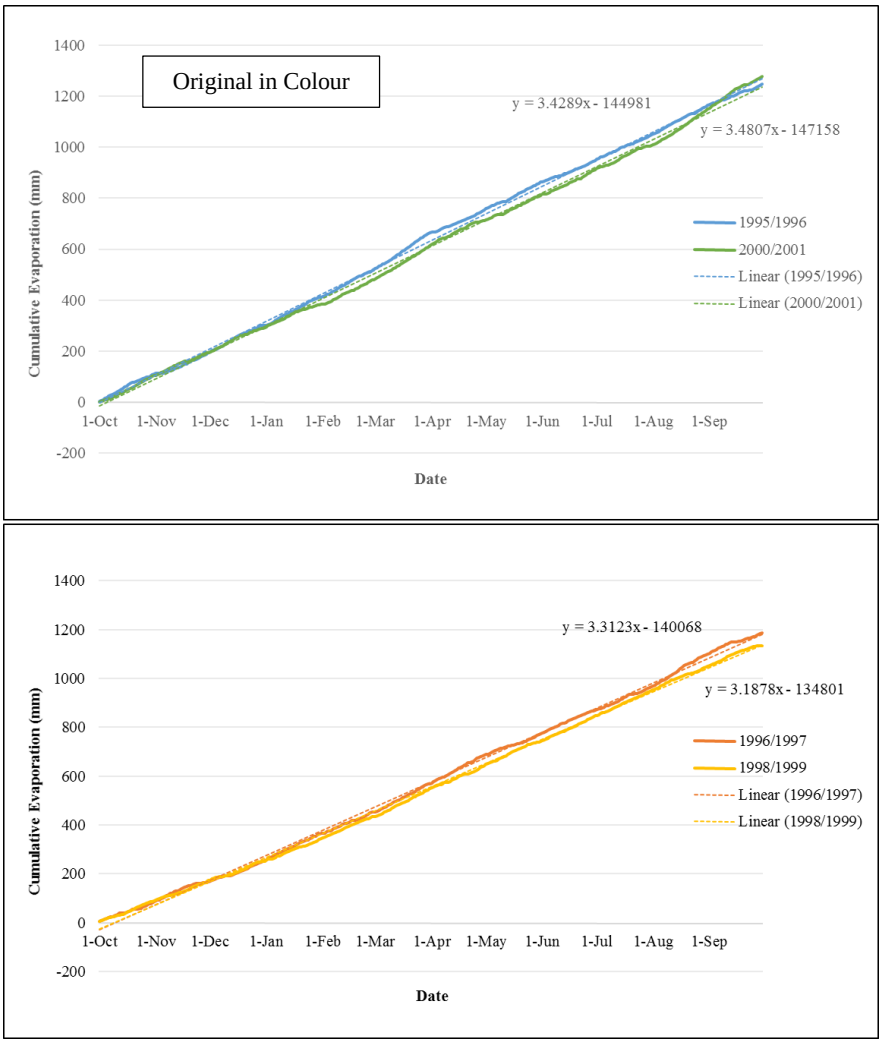

Appendix 04 - 3 Replacing missing data of evaporation of Colombo Meteorology observation from 1995/1996, 2000/2001, 1996/1997 & 1998/1999

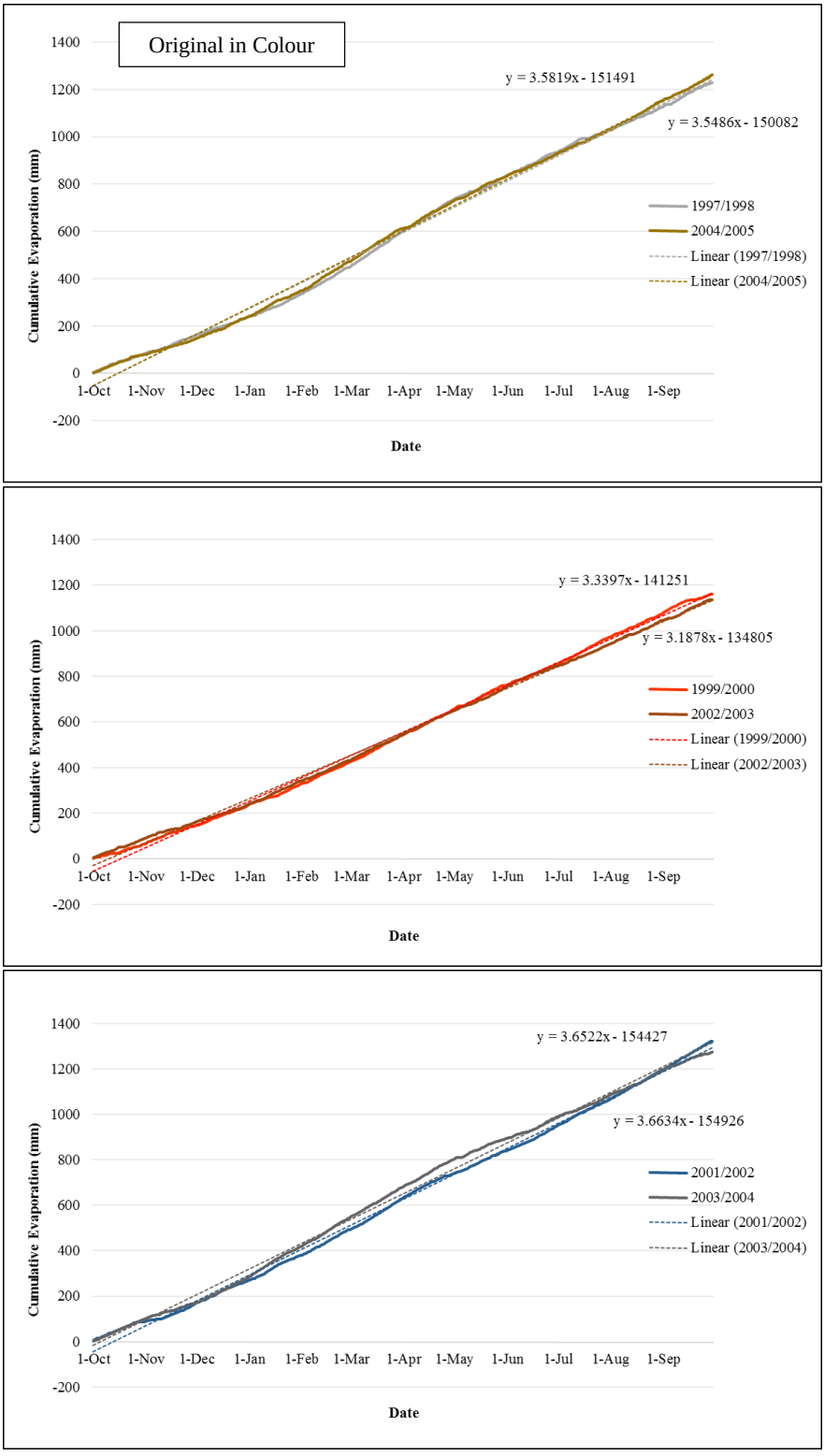

Appendix 04 - 4 Replacing missing data of evaporation of Colombo Meteorology observation from 1997/1998 & 2004/2005, 1999/2000 & 2002/2003, 2001/2002 & 2003/2004

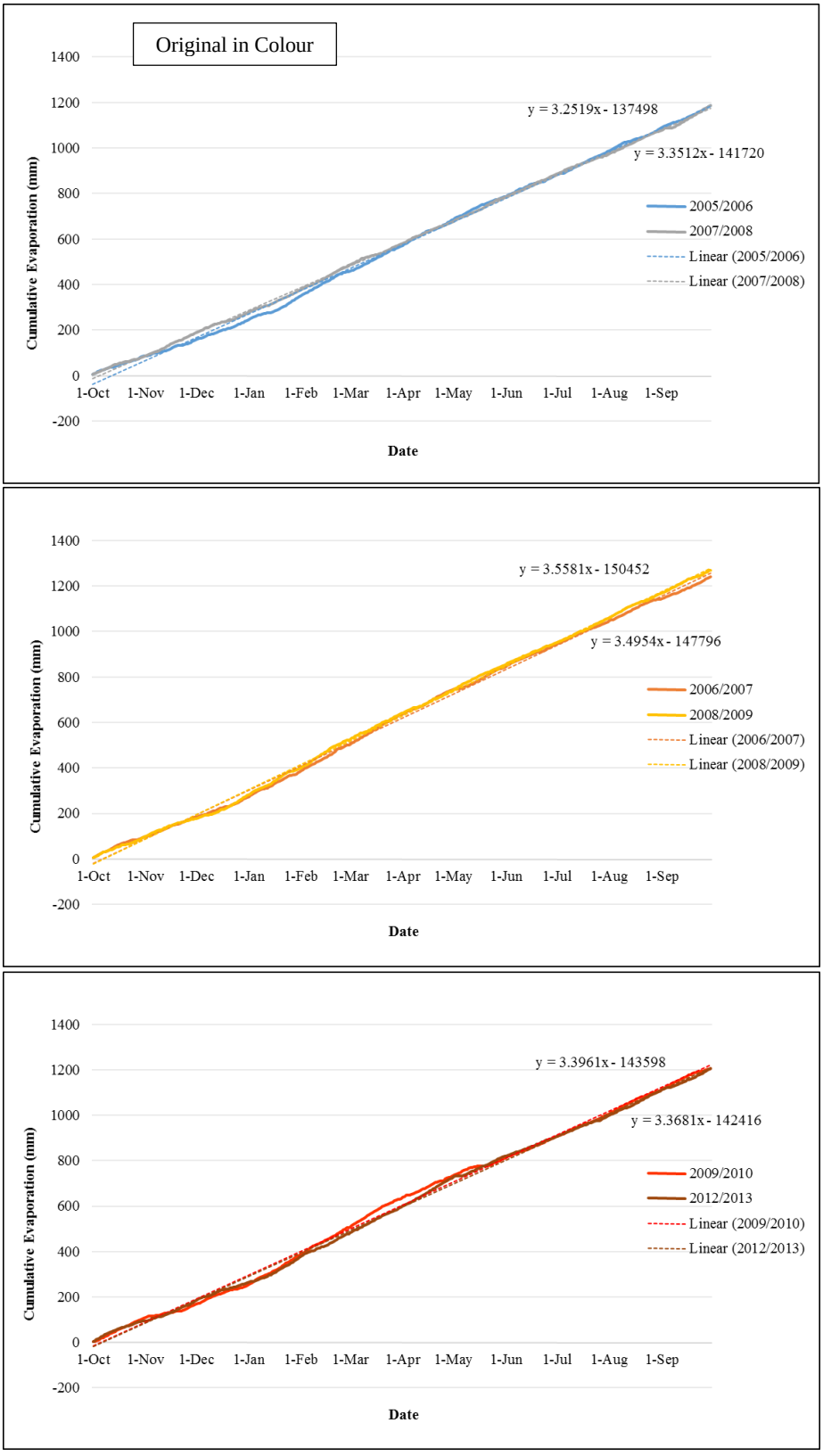

Appendix 04 - 5 Replacing missing data of evaporation of Colombo Meteorology observation from 2005/2006 & 2007/2008, 2006/2007 & 2008/2009, 2009/2010 & 2012/2013

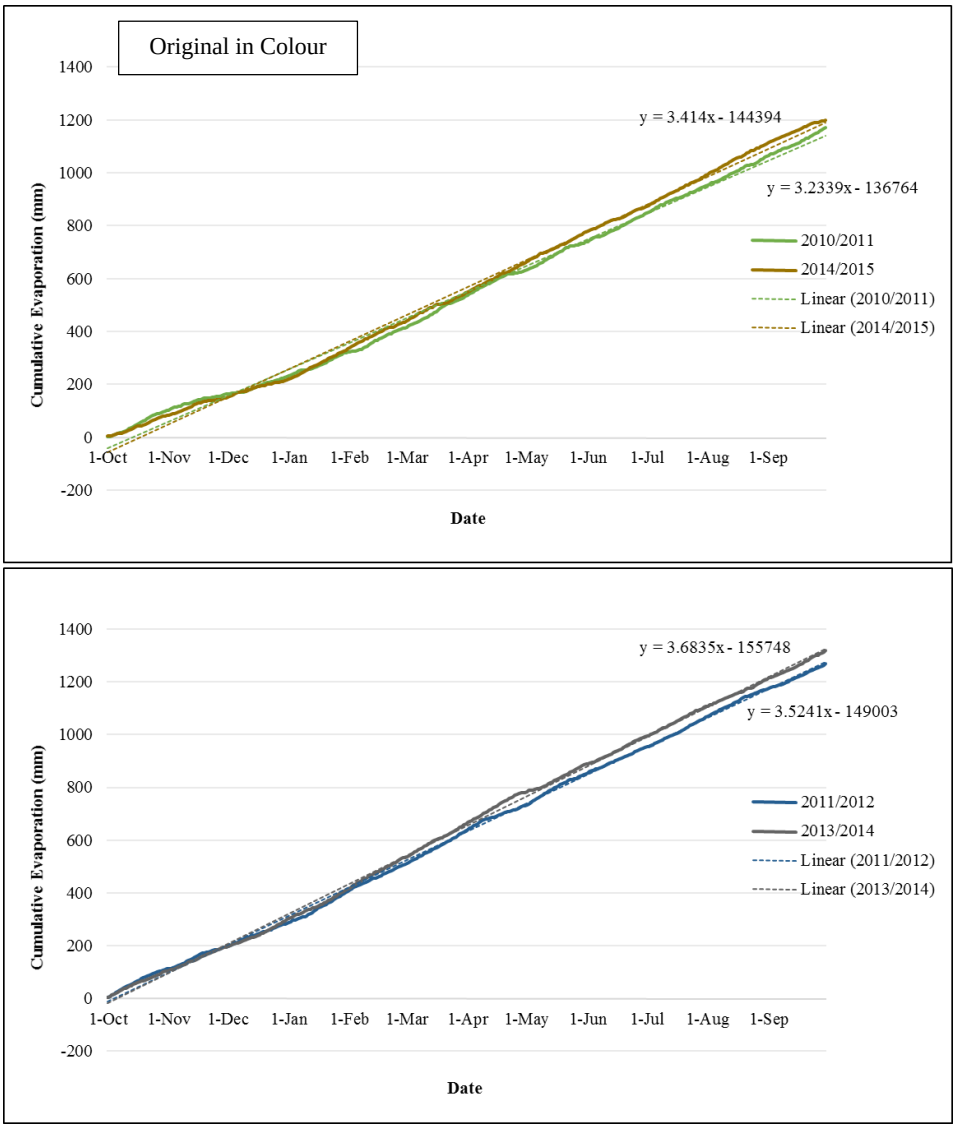

Appendix 04 - 6 Replacing missing data of evaporation of Colombo Meteorology observation from 2010/2011 & 2014/2015, 2011/2012 & 2013/2014

APPENDIX 05: - Trend Analysis of Point Rainfall

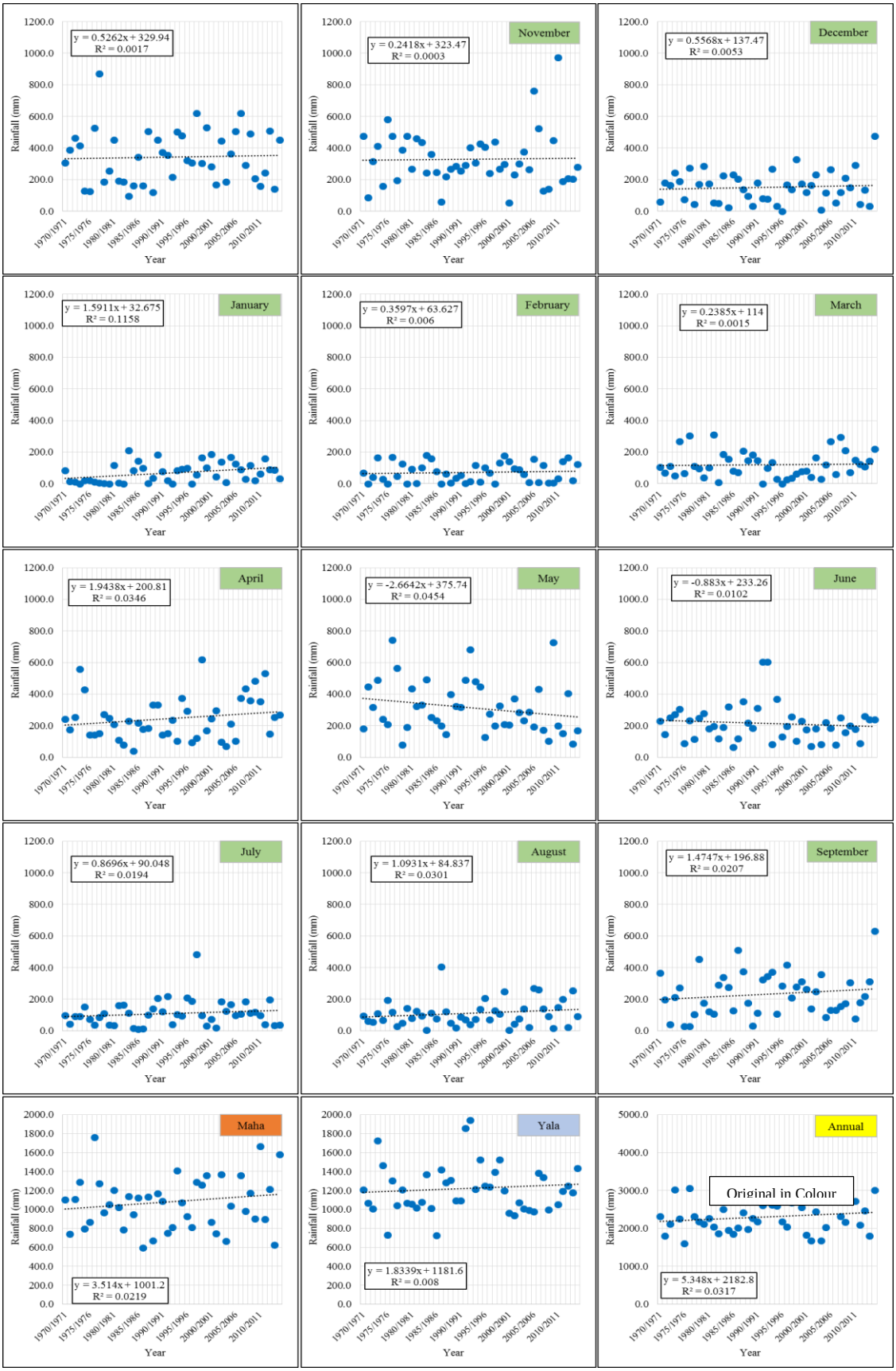

Appendix 05 - 1 Trends of Rainfall at Colombo (1970-2015)

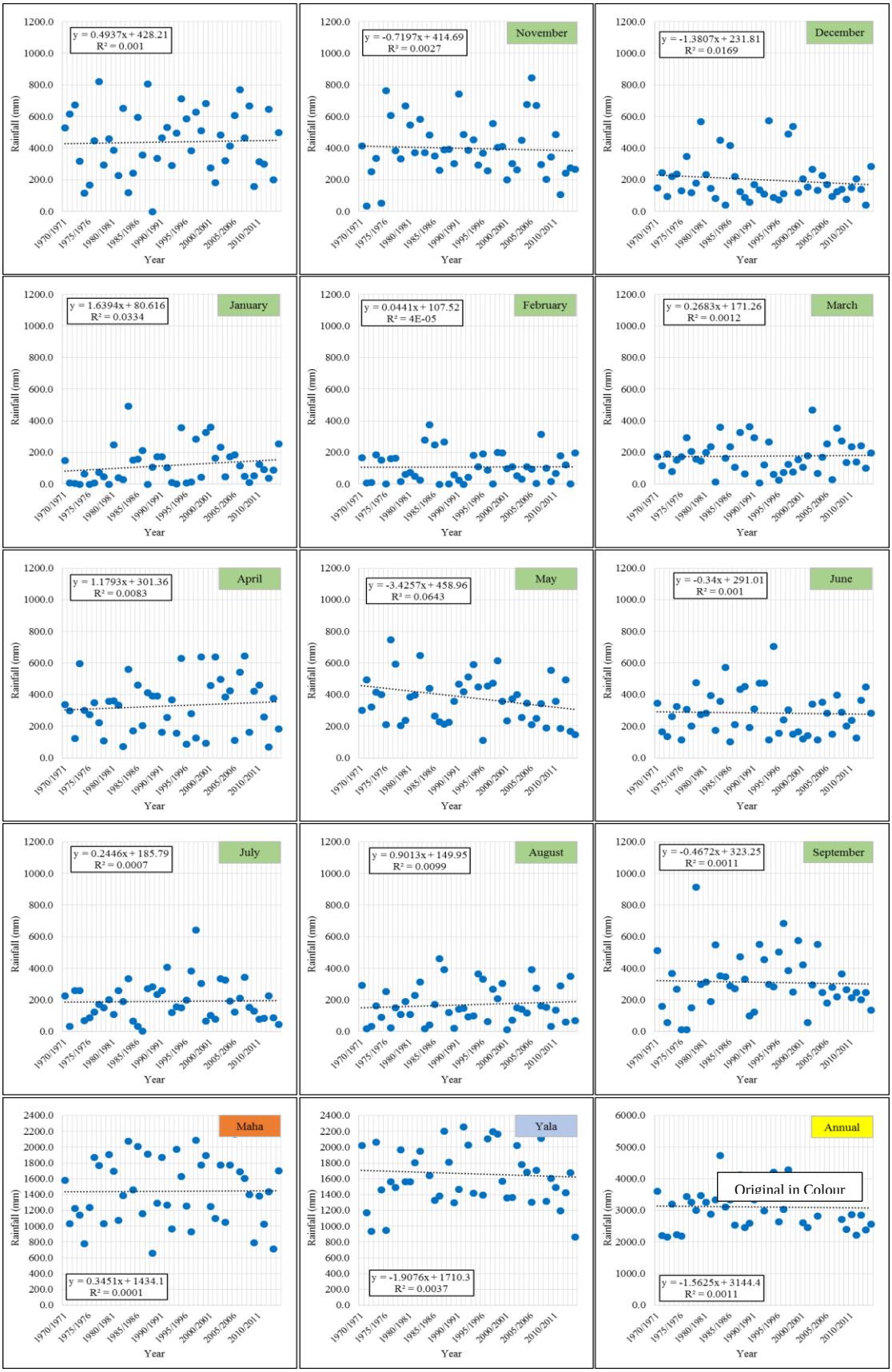

Appendix 05 - 2 Trends of Rainfall at Hanwella (1970-2015)

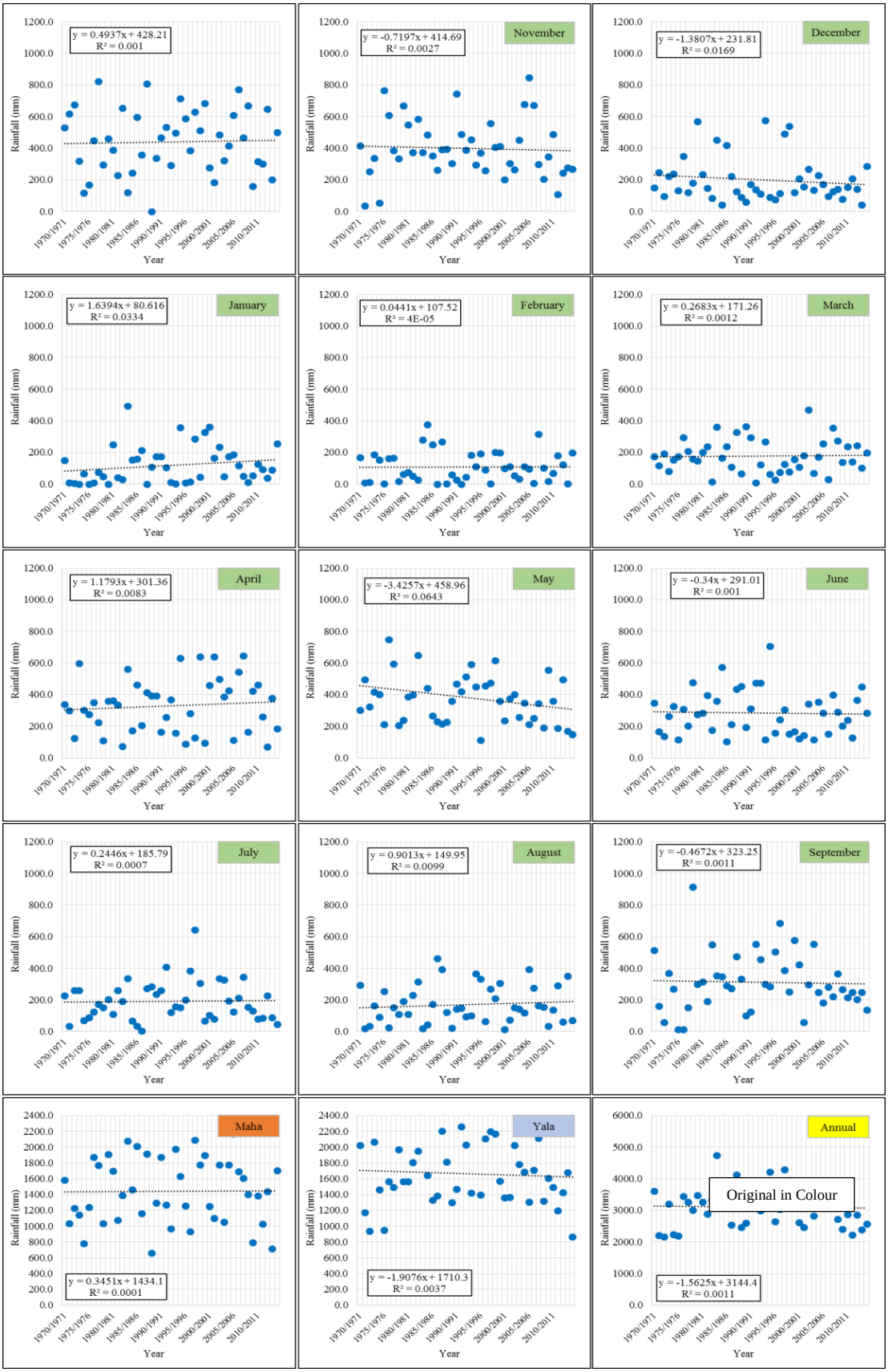

Appendix 05 - 3 Trends of Rainfall at Laxapana (1970-2015)

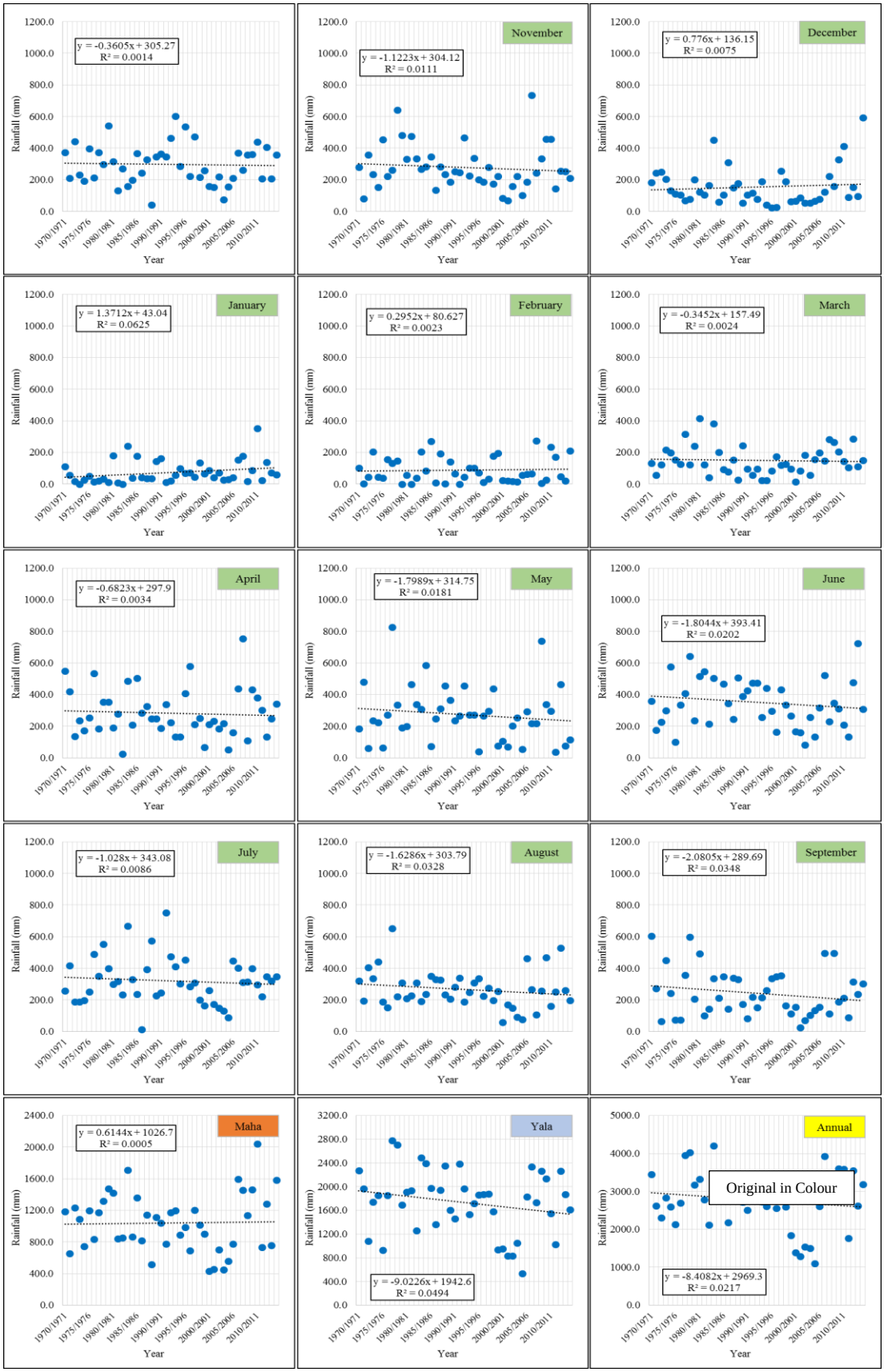

Appendix 05 - 4 Trends in Rainfall at Annfield (1970-2015)

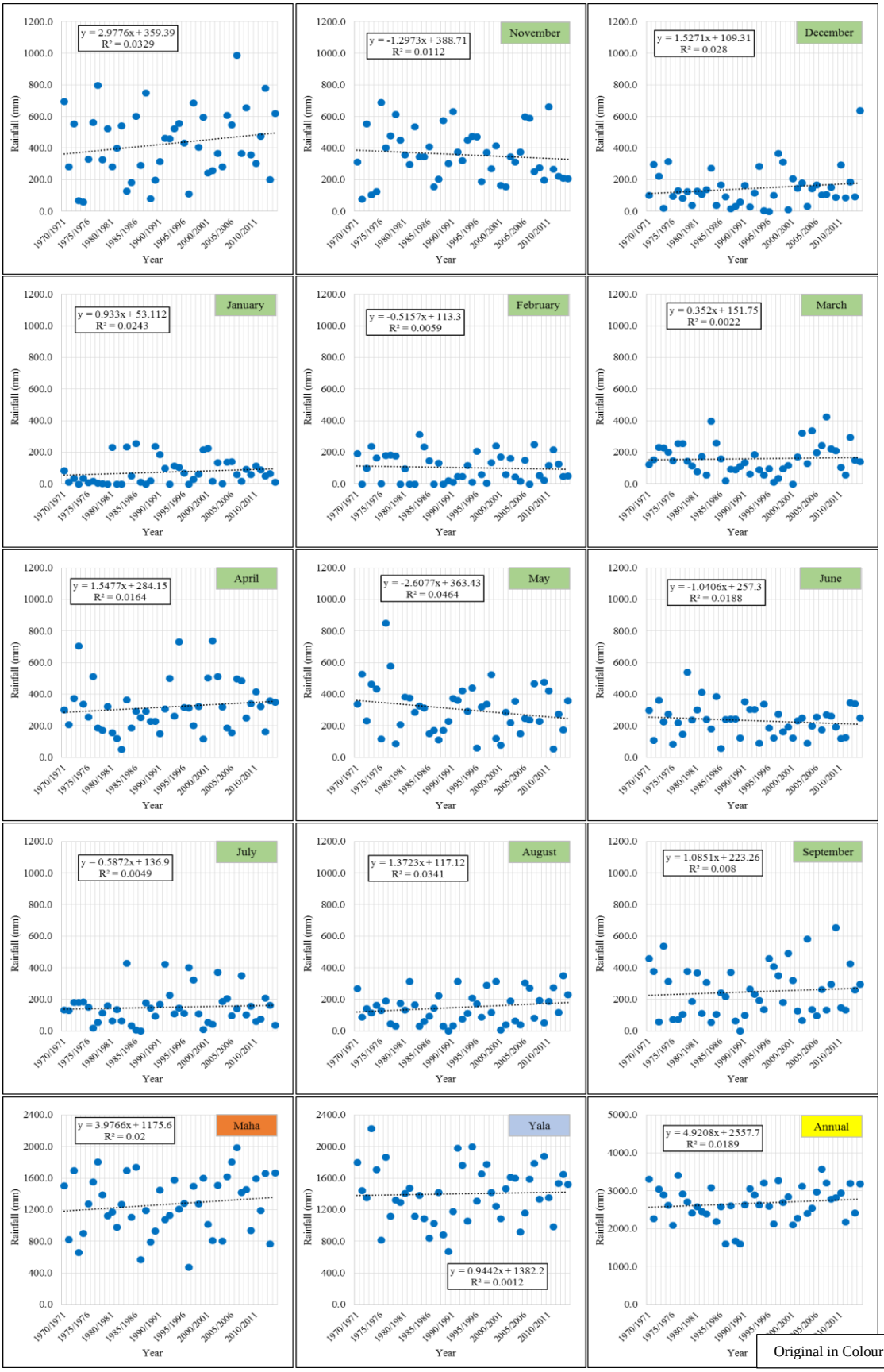

Original in Colour

Appendix 05 – 5 Trends in Rainfall at Pasyala (1970-2015)

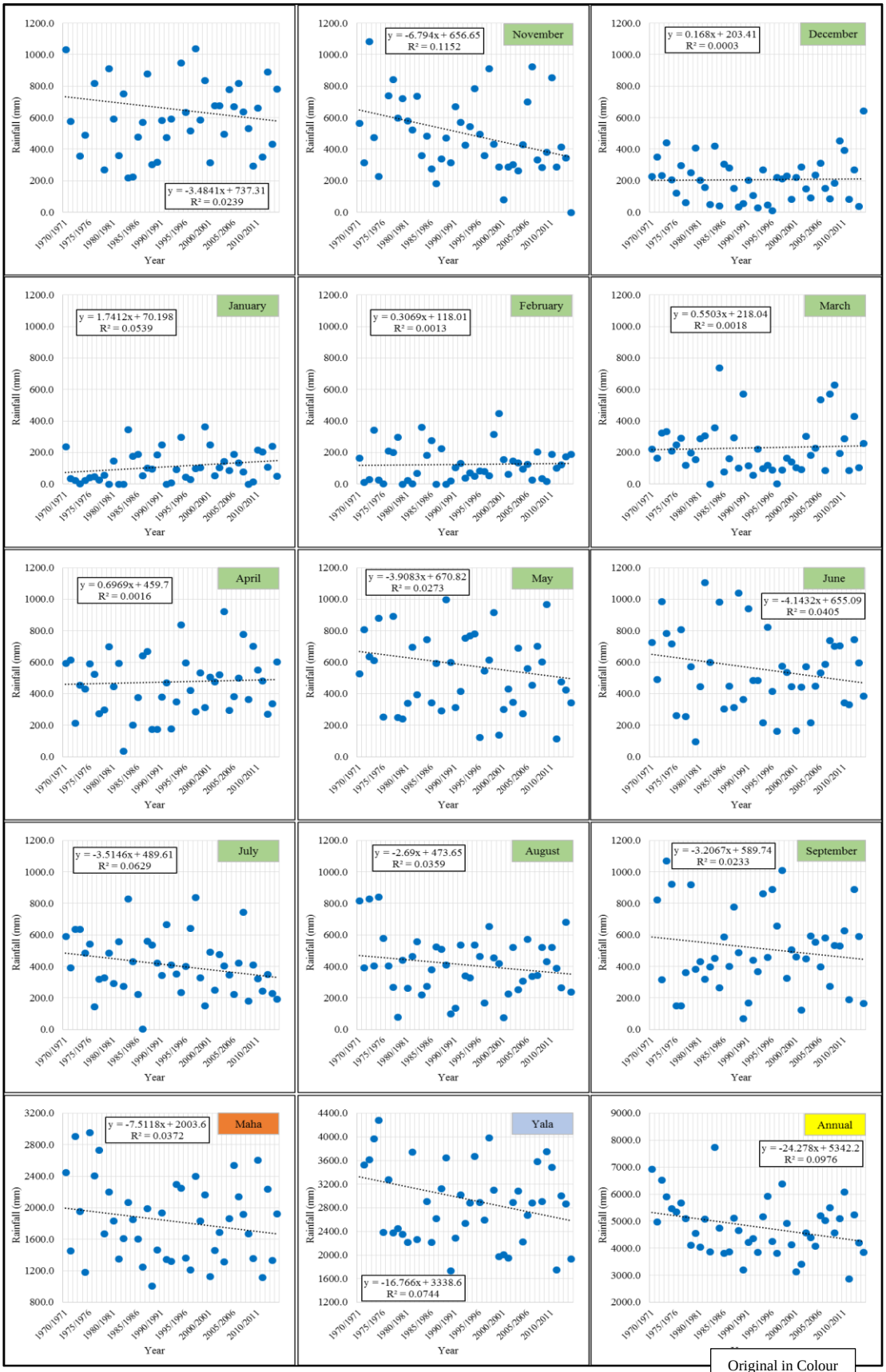

Original in Colour

Appendix 05 - 6 Trends in Rainfall at Yatiyanthota-Wewalthalawa (1970-2015)

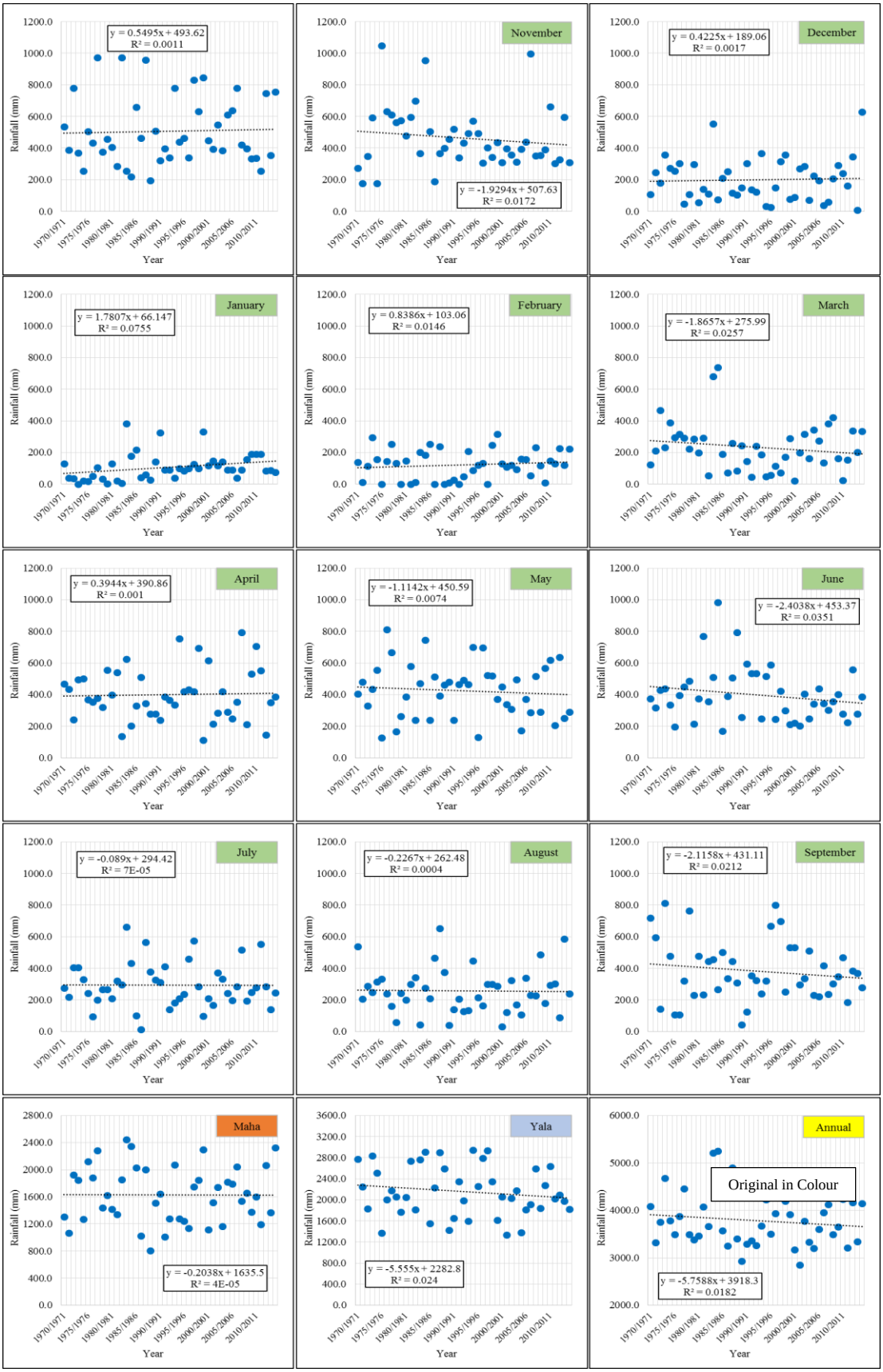

Appendix 05 - 7 Trends in Rainfall at Dunedin-Chesterford (1970-2015)

APPENDIX 06: - Trend Analysis of Catchment Rainfall

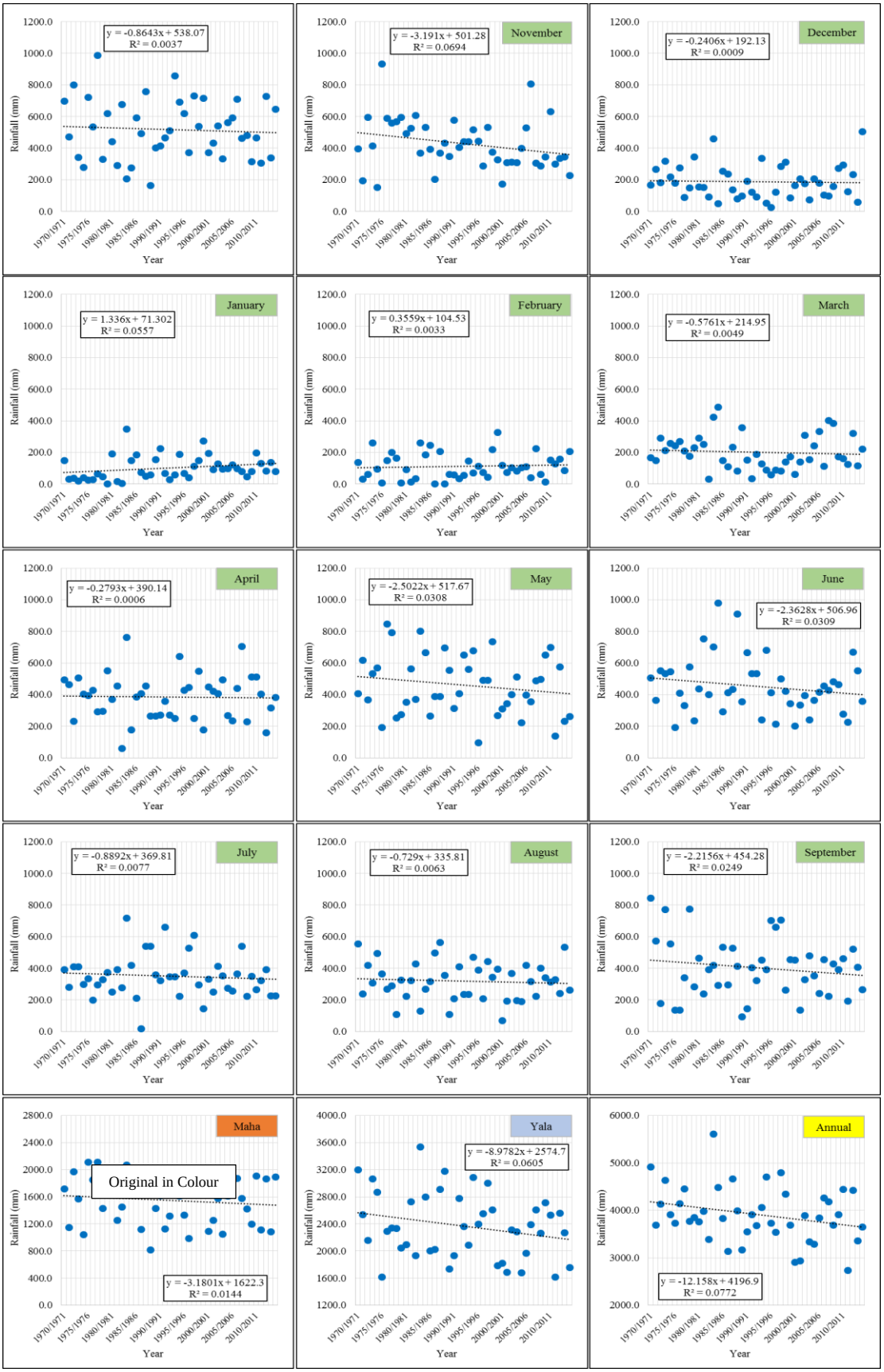

Appendix 06 - 1 Trends in Catchment Rainfall at Hanwella Watershed (1970-2015)

APPENDIX 07: - Trends Analysis of Point Temperature

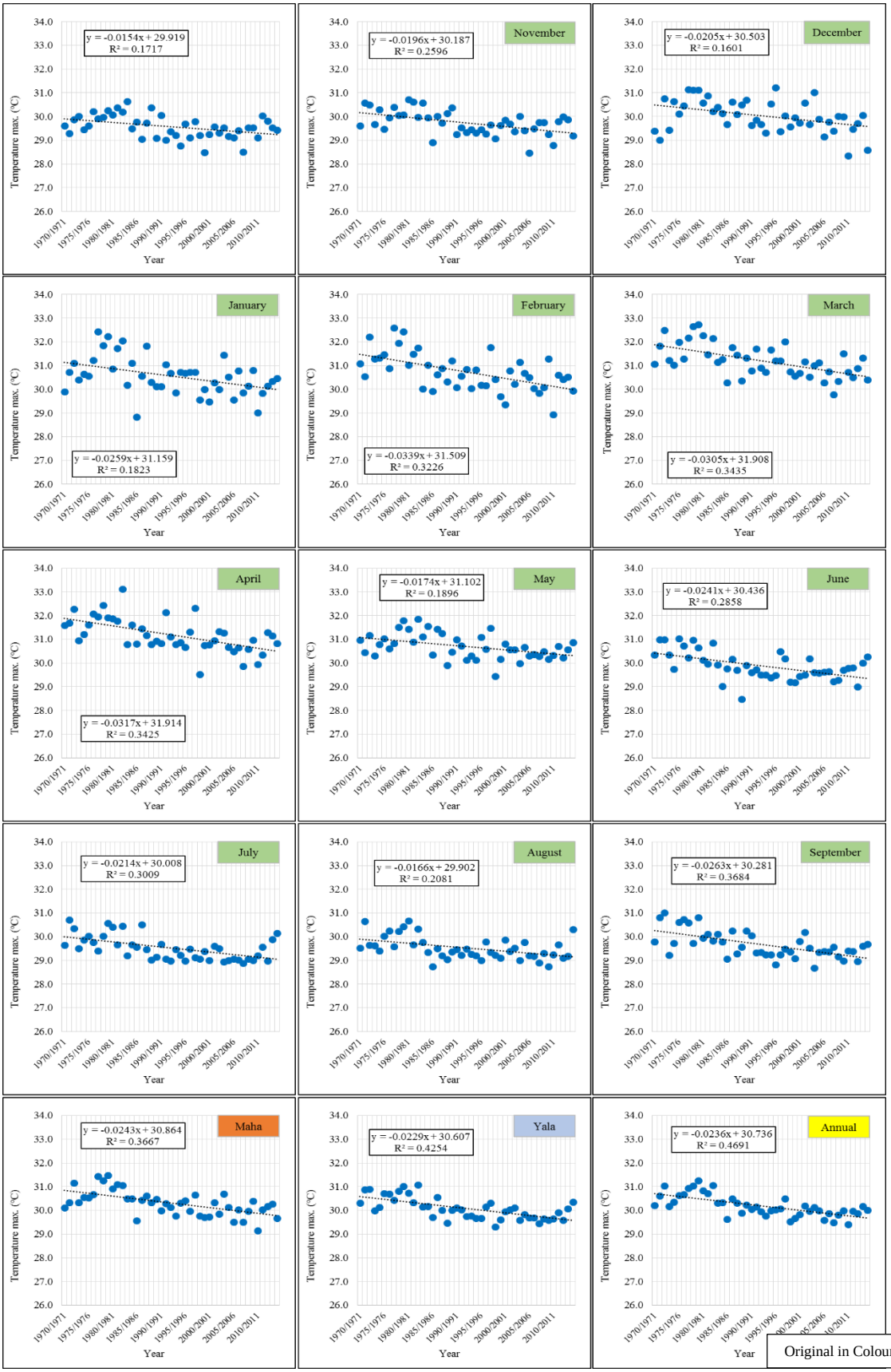

Appendix 07 - 1 Trends of Colombo T_{max} (1970-2015)

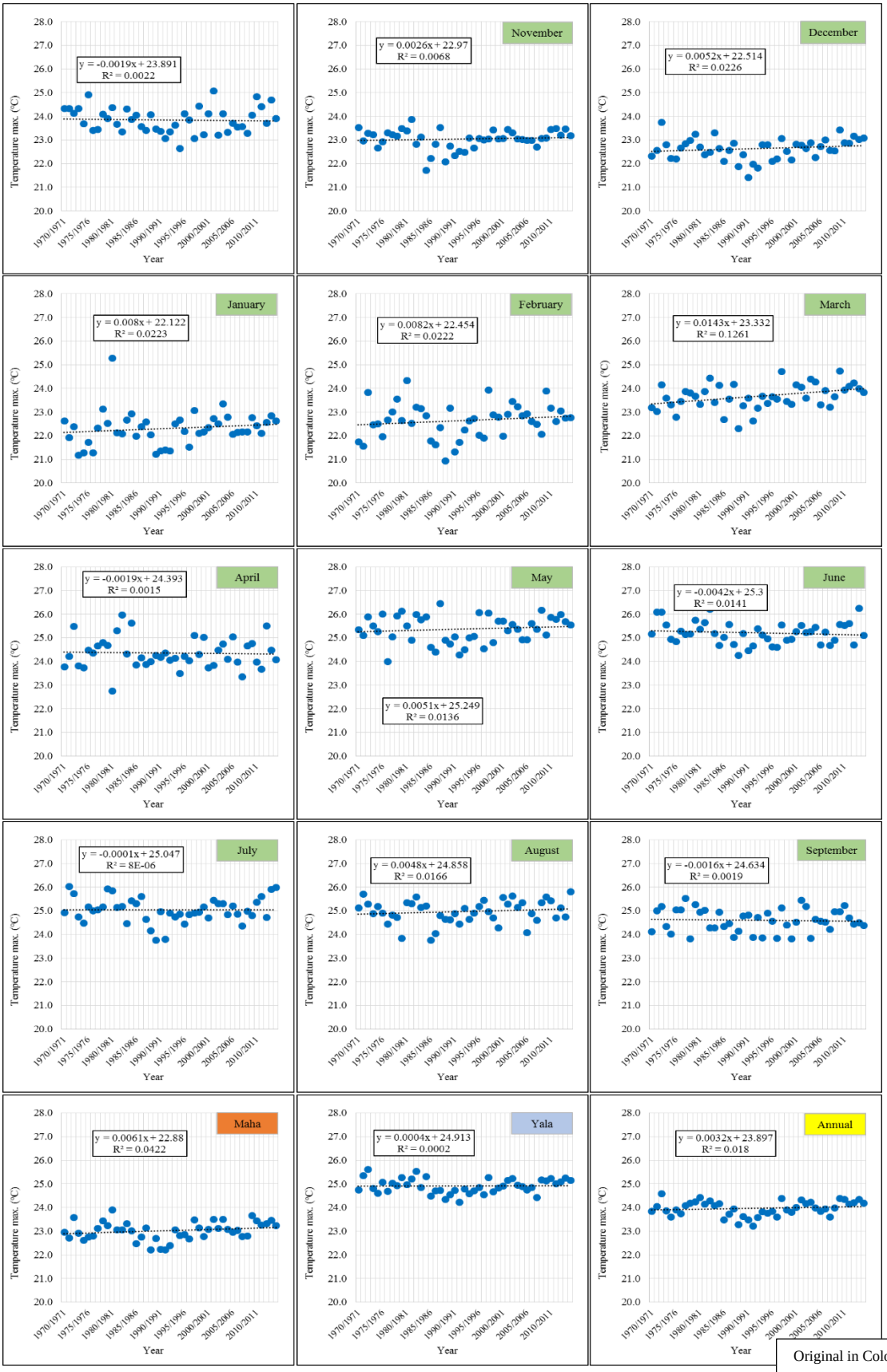

Original in Colour

Appendix 07 - 2 Trends of Colombo T_{min} (1970-2015)

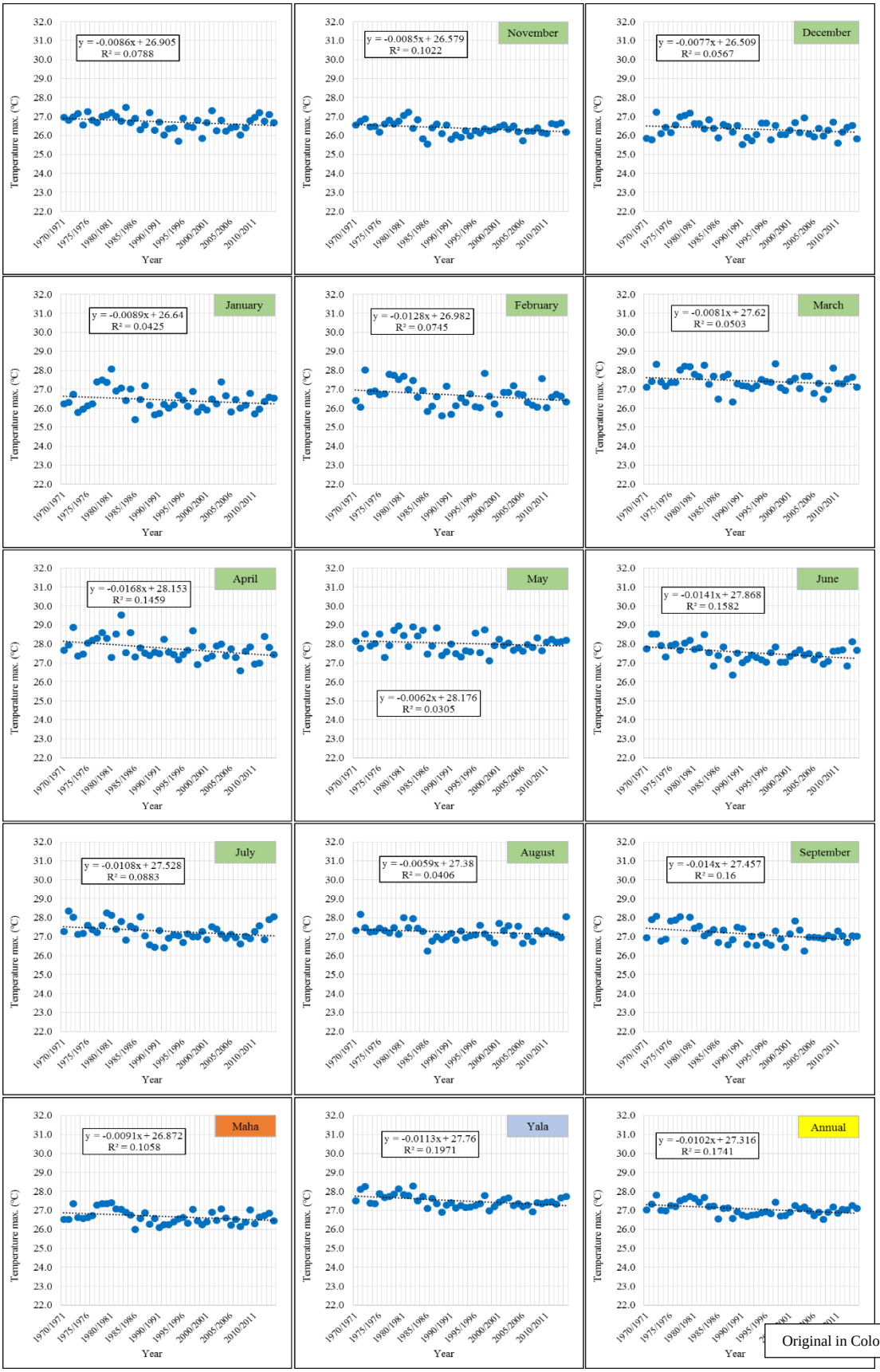

Appendix 07 - 3 Trends of Colombo T_{avg} (1970-2015)

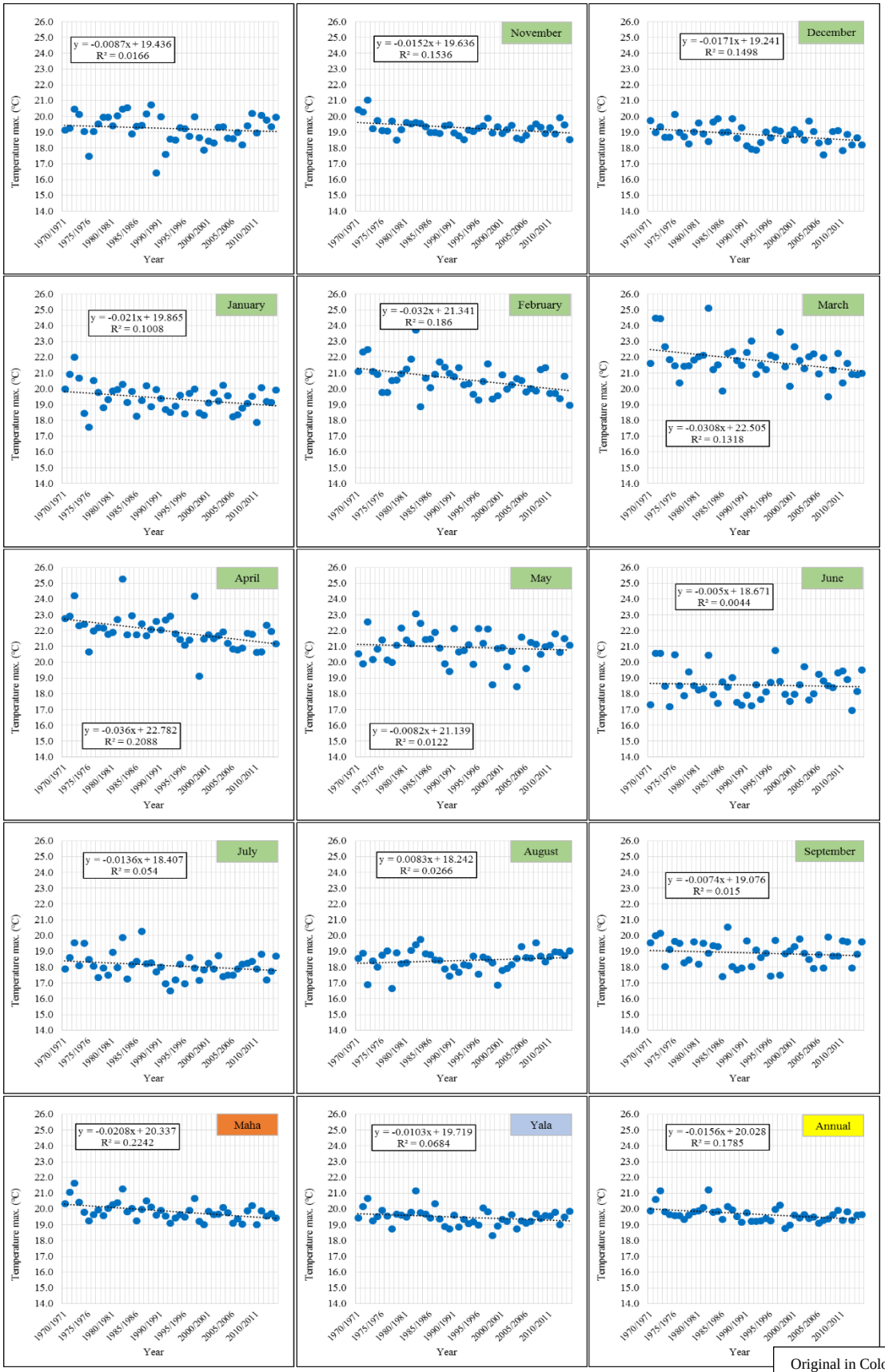

Original in Colour

Appendix 07 - 4 Trends of Nuwara-Eliya T_{max} (1970-2015)

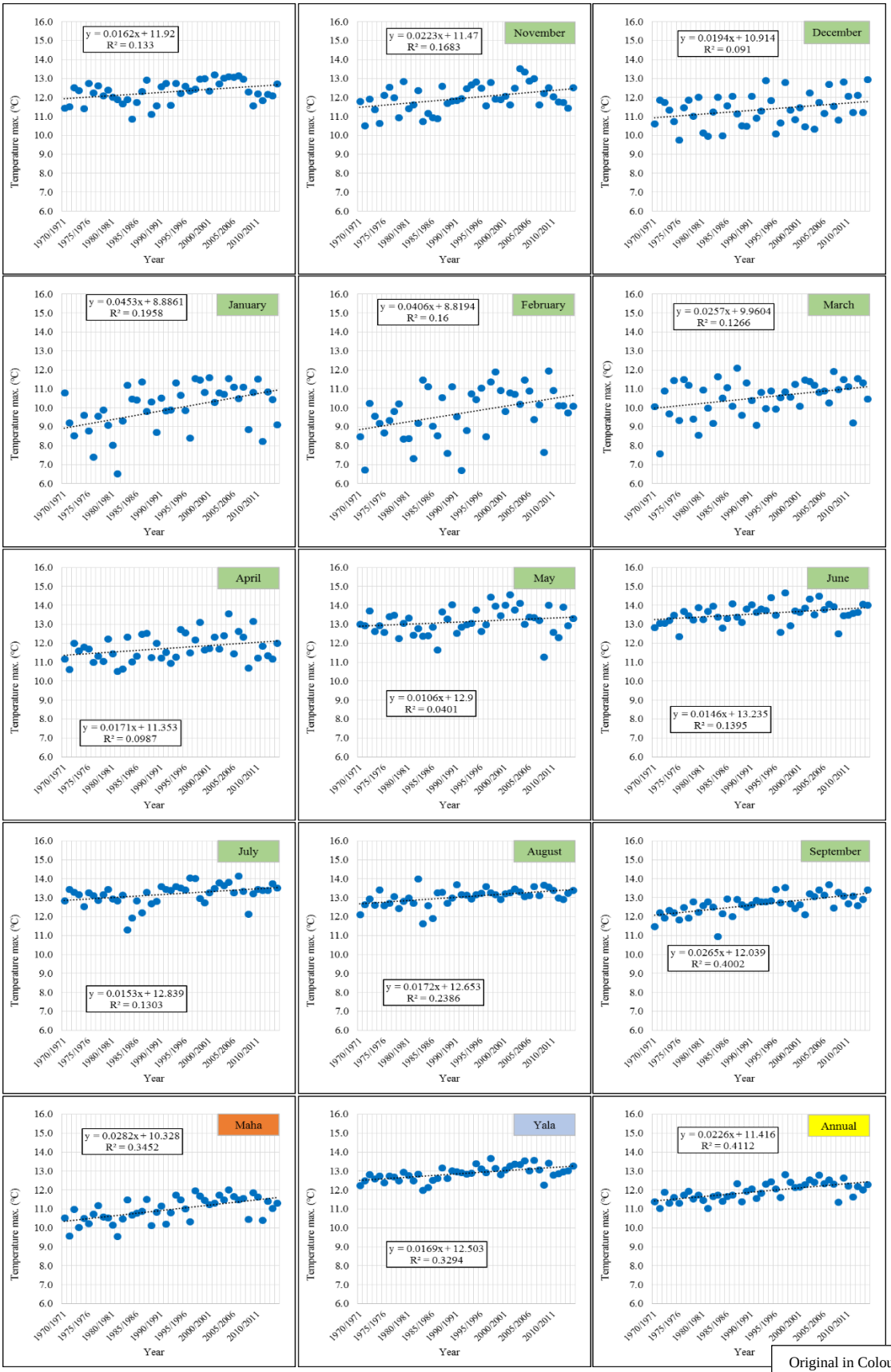

Original in Colour

Appendix 07 - 5 Trends of Nuwara-Eliya T_{min} (1970-2015)

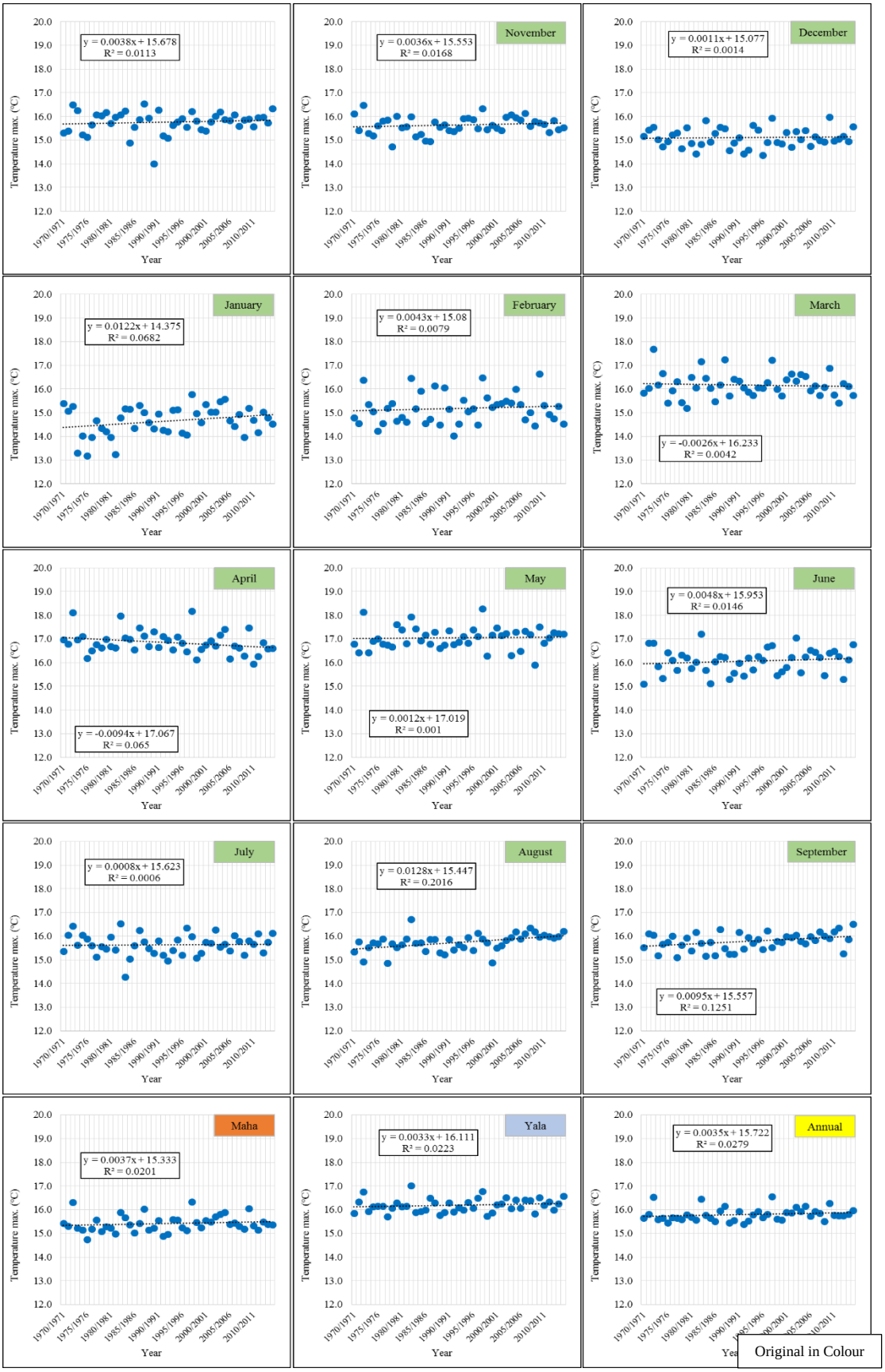

Original in Colour

Appendix 07 - 6 Trends of Nuwara-Eliya T_{avg} (1970-2015)

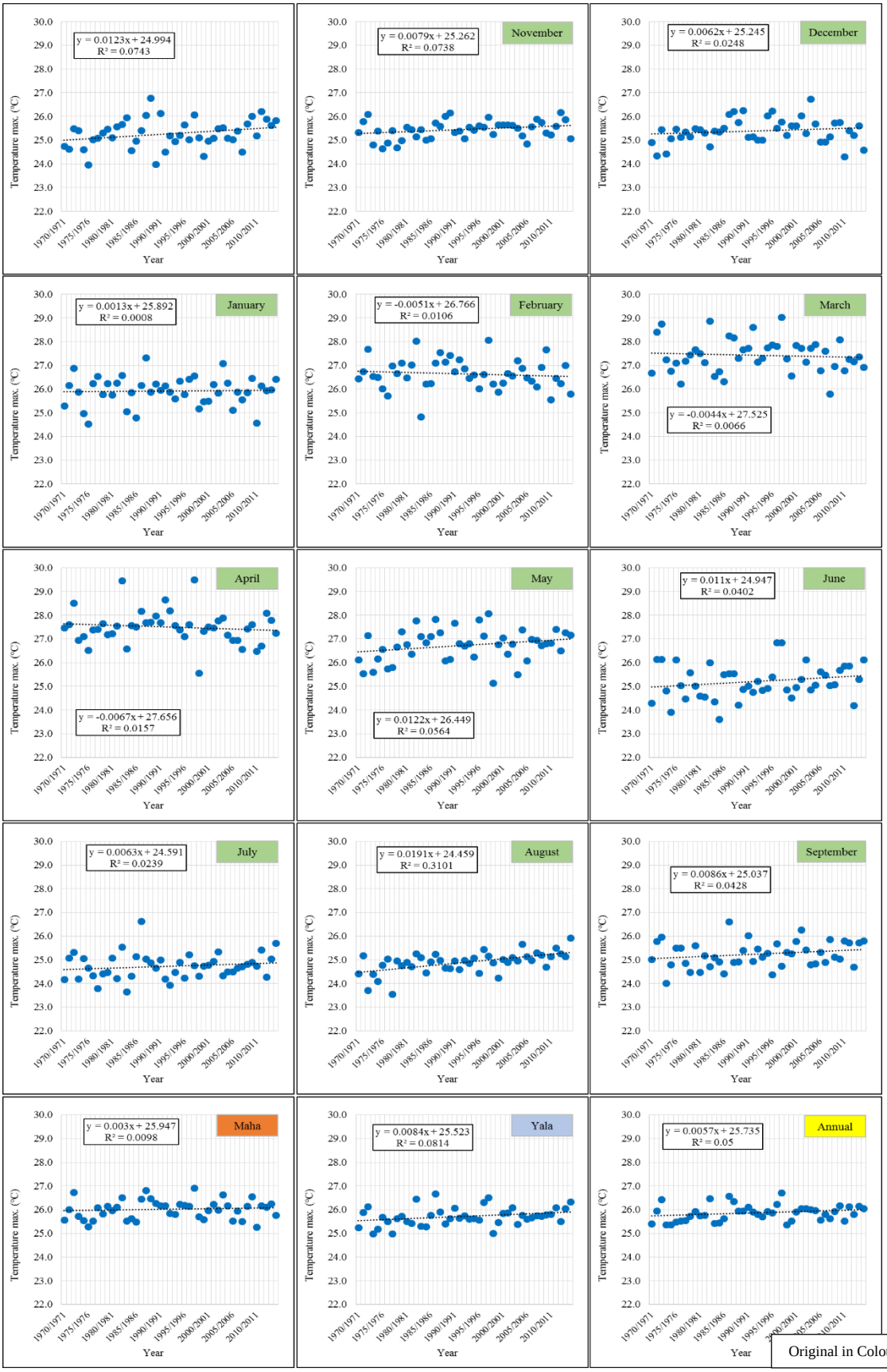

Original in Colour

Appendix 07 - 7 Trends of River Basin T_{max} (1970-2015)

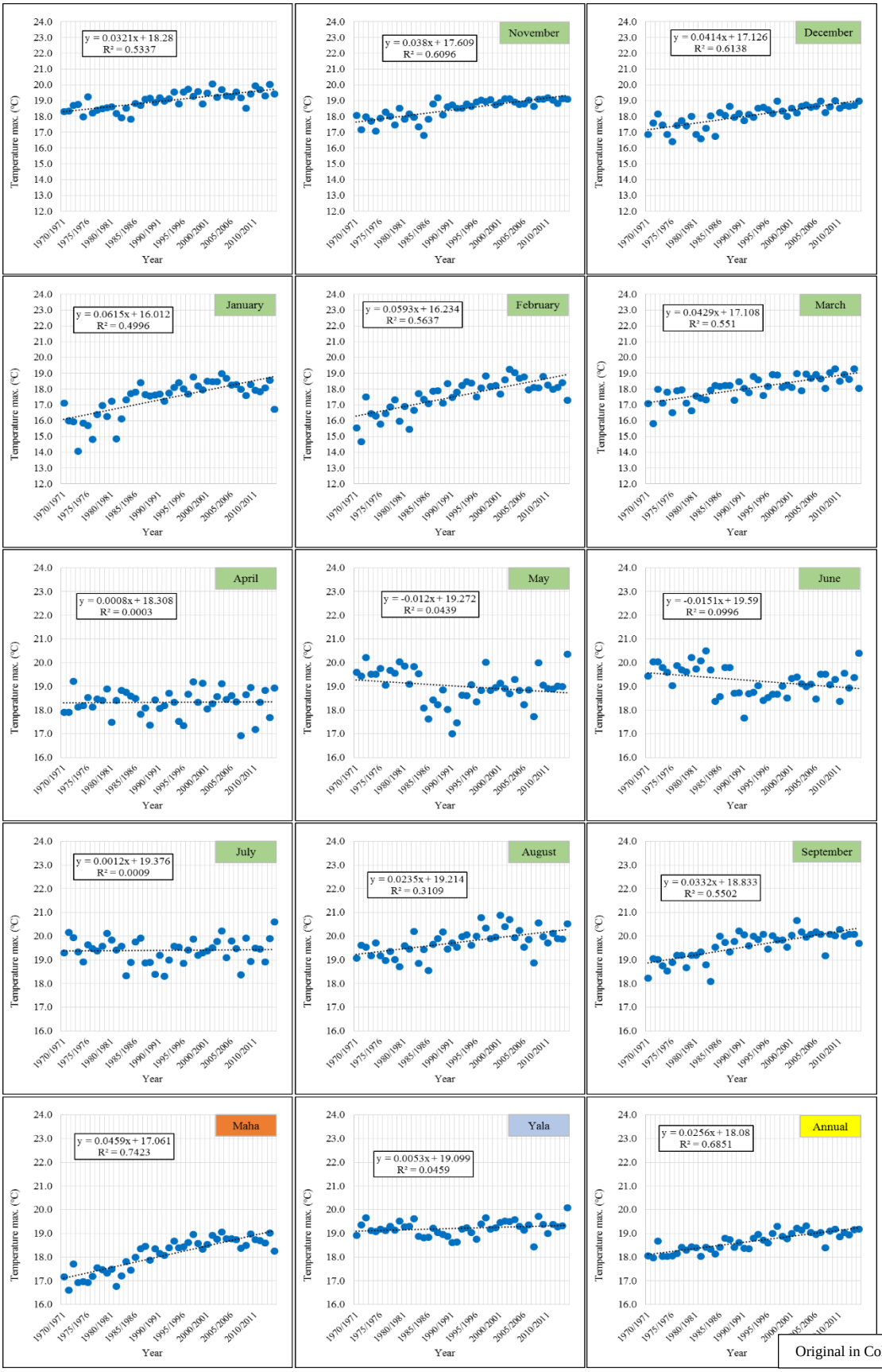

Original in Colour

Appendix 07 - 8 Trends of River Basin T_{min} (1970-2015)

APPENDIX 08: - Trends Analysis of Streamflow (Hanwella Sub-watershed)

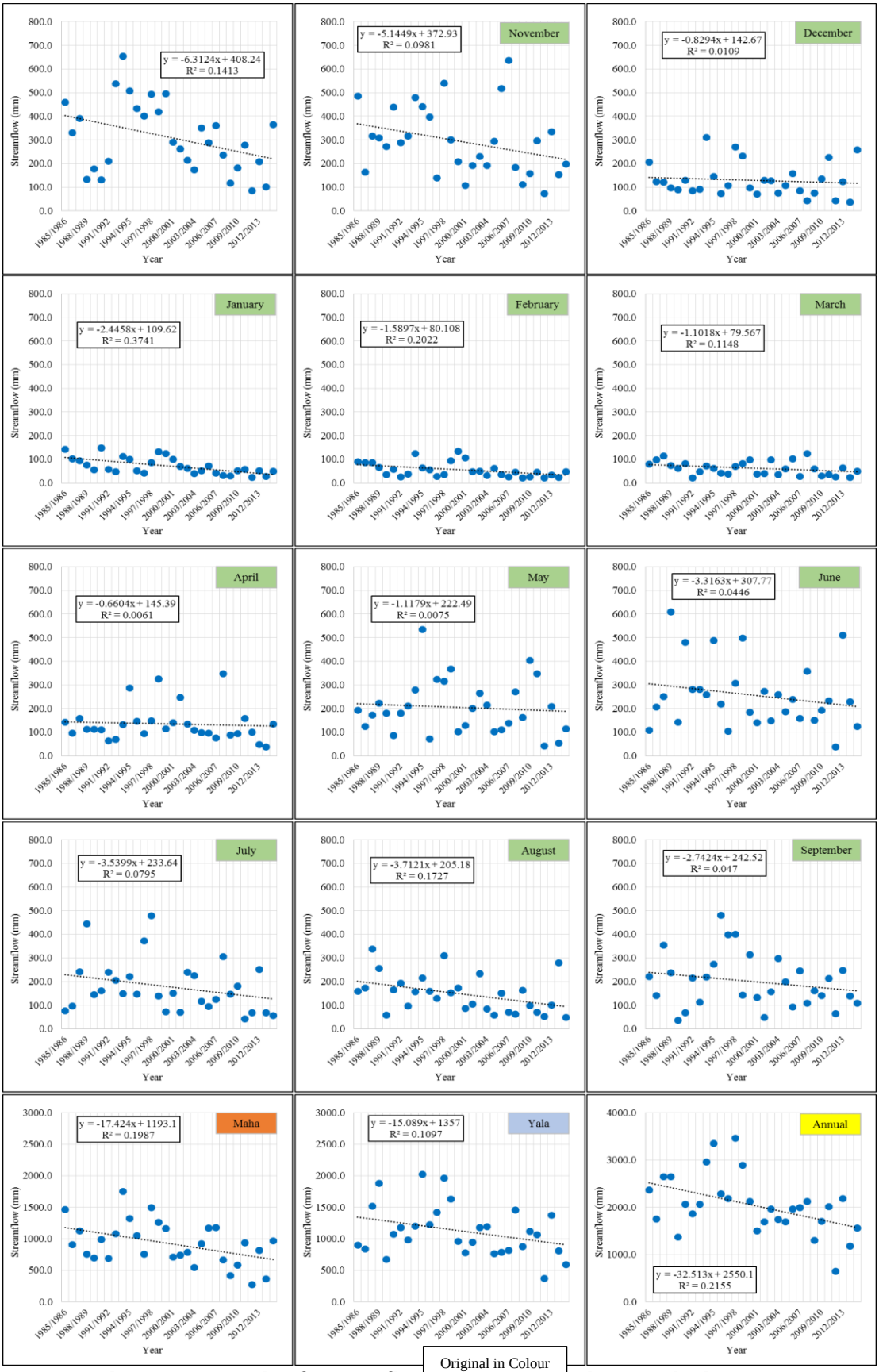

Original in Colour

Appendix 08 - 1 Trends of Streamflow at Hanwella sub watershed (1985-2015)

APPENDIX 09: - Future Streamflow Variations

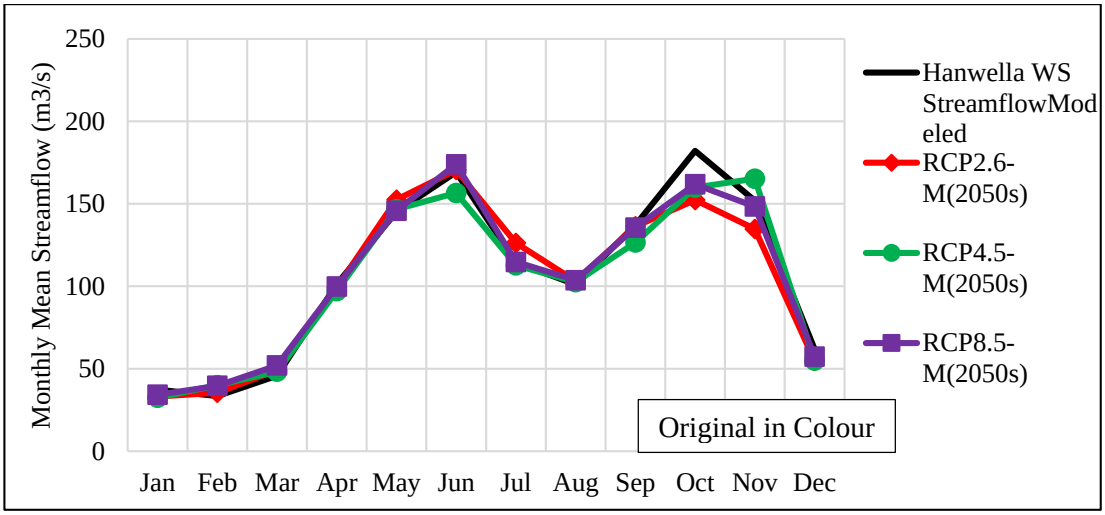

Appendix 09 - 1 Future Streamflow Variation of Hanwella Sub-watershed in 2050s for SDSM_M

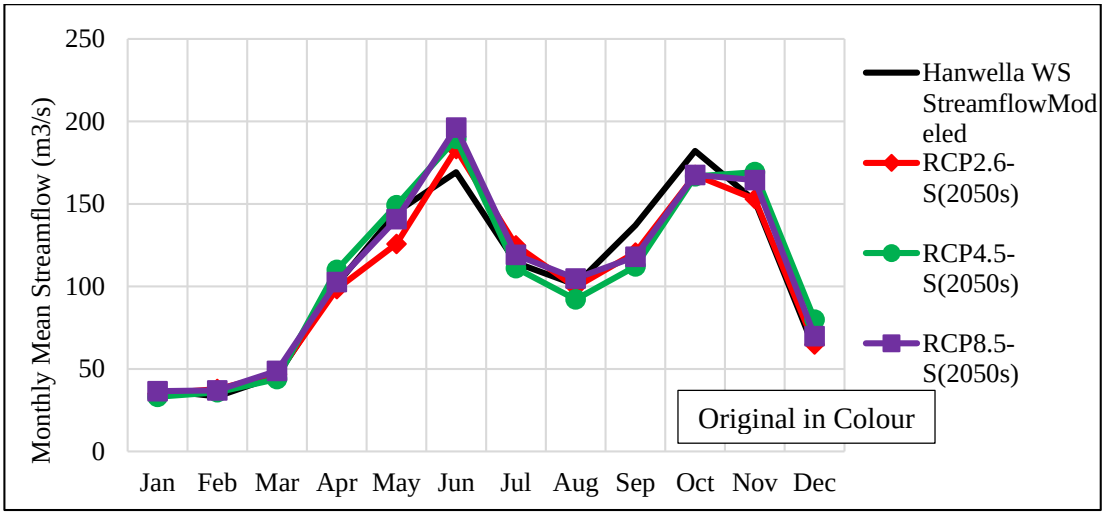

Appendix 09 - 2 Future Streamflow Variation of Hanwella Sub-watershed in 2050s for SDSM_S

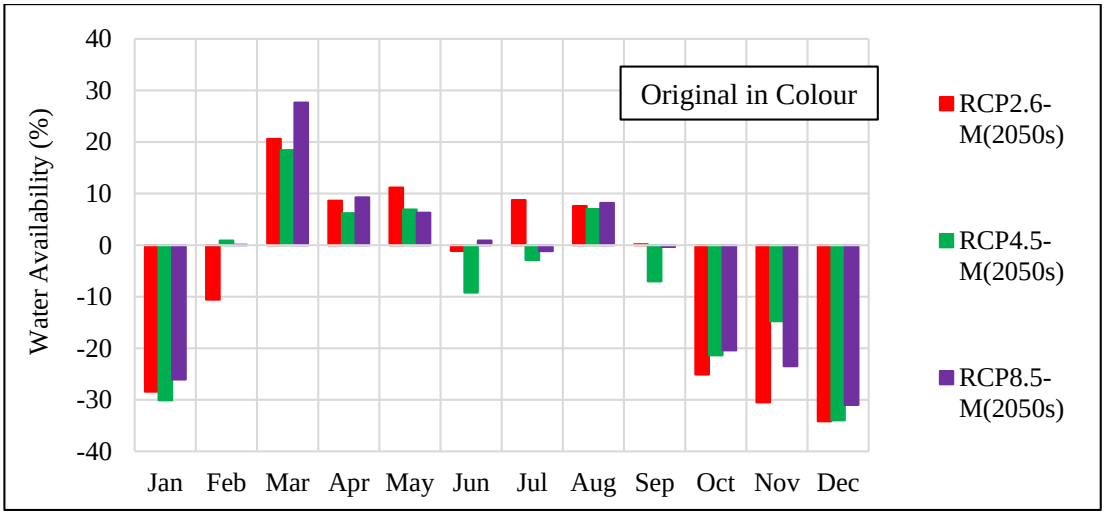

Appendix 09 - 3 Future Streamflow Availability in Hanwella Sub-watershed in 2050s for SDSM_M

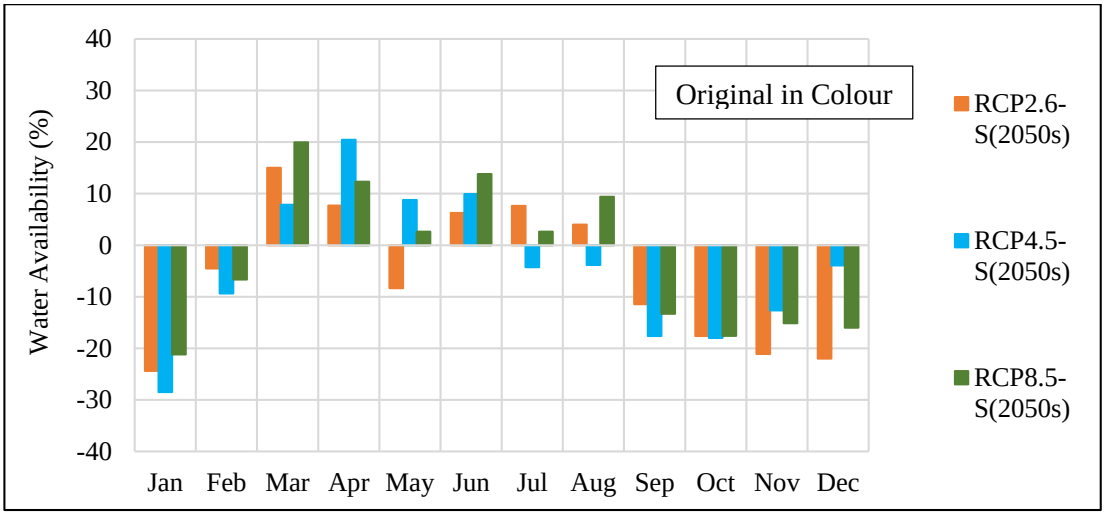

Appendix 09 - 4 Future Streamflow Availability in Hanwella Sub-watershed in 2050s for SDSM_S

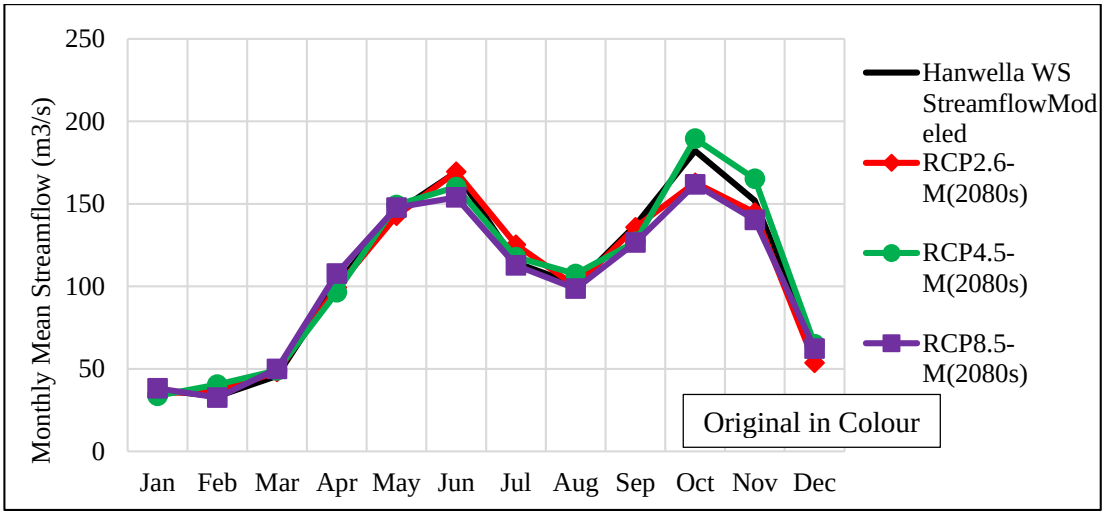

Appendix 09 - 5 Future Streamflow Variation of Hanwella Sub-watershed in 2080s for SDSM_M

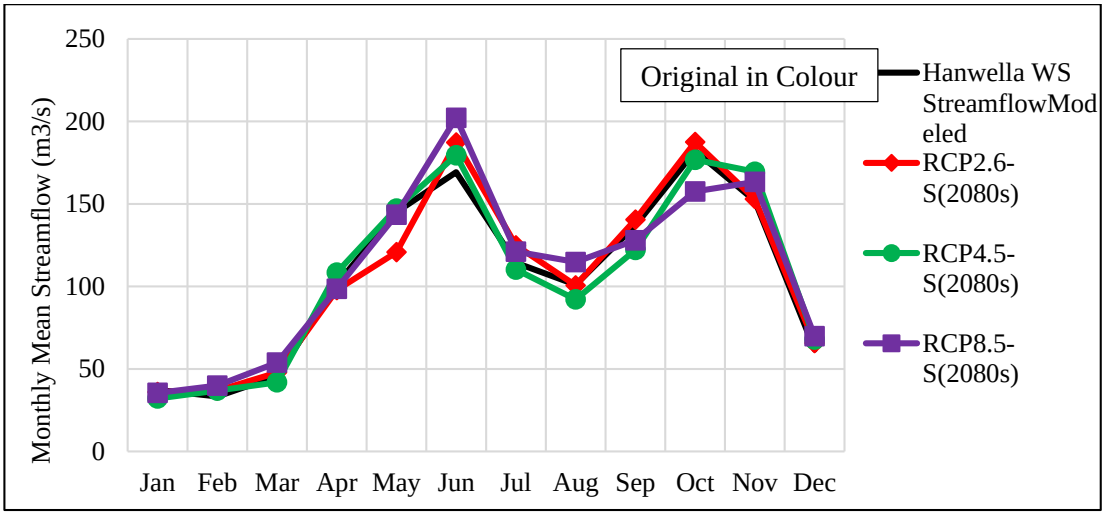

Appendix 09 - 6 Future Streamflow Variation of Hanwella Sub-watershed in 2080s for SDSM_S

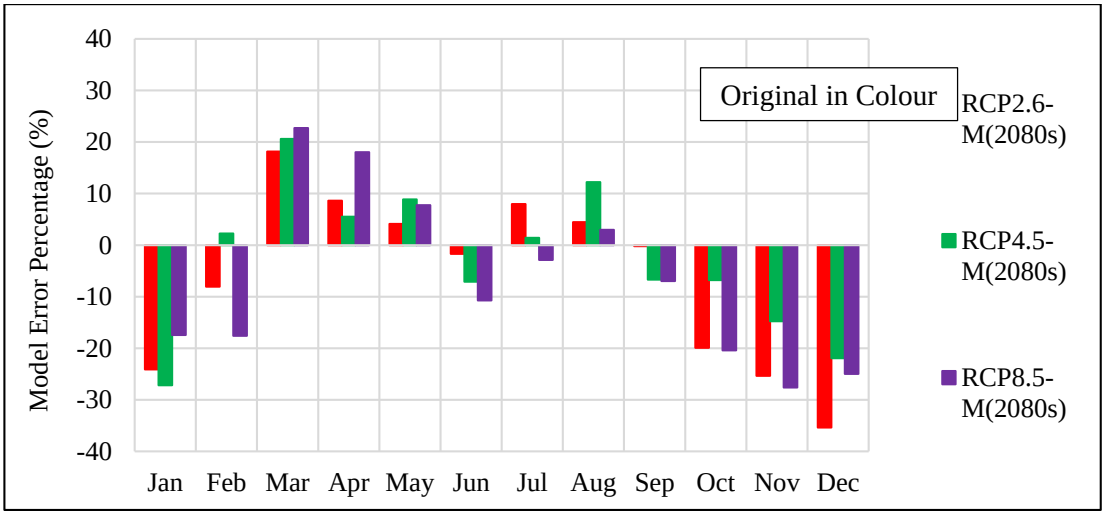

Appendix 09 - 7 Future Streamflow Availability in Hanwella Sub-watershed in 2080s for SDSM_M

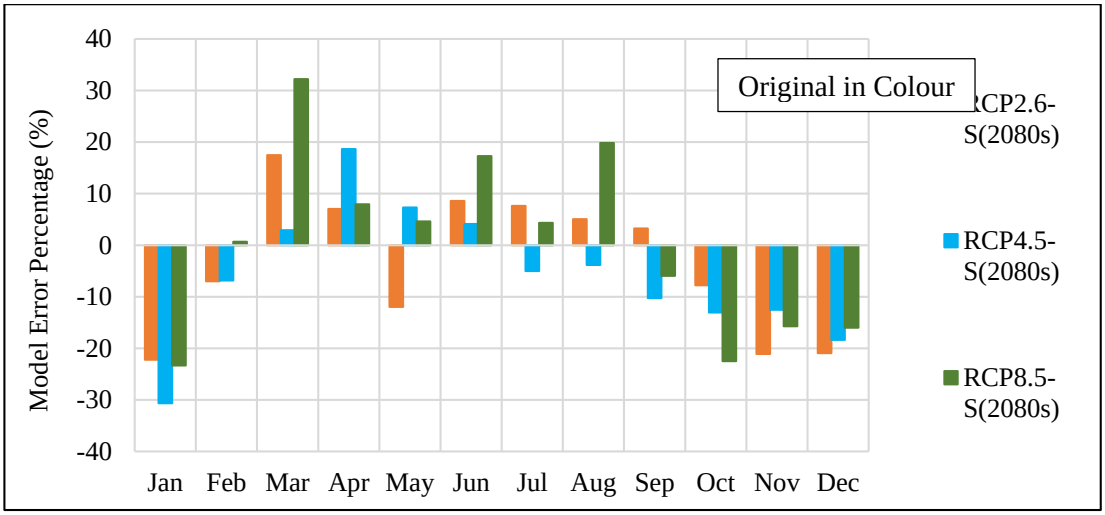

Appendix 09 - 8 Future Streamflow Availability in Hanwella Sub-watershed in 2080s for SDSM_S